Enzymatic reactions and coordination complexes of steroids

Rizwana Sadiq

M.Sc. (Botany), M.Sc. (Analytical Bioscience)

A thesis submitted to the University of Huddersfield in partial fulfilment of the requirement for the degree of Doctor of Philosophy

Department of Chemical and Biological Sciences

University of Huddersfield

August 2015

Declaration

The work described herein was carried out between October 2010 and November 2014 at the School of Applied Sciences, University of Huddersfield.

Declaration

I declare that this is my own work and the use of all the materials from other sources has been properly and fully acknowledged.

Name: Rizwana Sadiq August 2015

This thesis is dedicated to my family and friends, past and present, without their love, support and encouragement, getting this far would have not been possible

Acknowledgements

First, I would like to say my humble gratitude and appreciation to almighty ***Allah*** *for His blessings to accomplish my work.*

I would like to take this opportunity to sincerely express my deepest appreciation and greatest thanks to my supervisor, ***Dr. Lindsay P. Harding****, for the unconditional support, patience, expertise and time she has given me throughout my PhD which has made possible to accomplish this work. Without her guidance and persistent help throughout my thesis and all the directions that led to its end. She has provided a pleasant working atmosphere. It was an exciting experience working here – full of fun, challenge, and inspiration.*

Finally my biggest thanks, goes to my ***Mum*** *and* ***Dad*** *without the guidance, love, support and sacrifice of them I would not have come this far in my life. With their love and continual support during both the good and bad times I have grown a lot. For all they have given me, I am eternally grateful. It is to them I owe my deepest gratitude. Thank you for everything.*

Also I would like to express my gratitude to my brother ***Dr. Sohaib Sadiq,*** *Who spent his valuable time and shared his knowledge and suggestions to complete my work. Without his insight, support, patience and guidance this study would not have been completed. He always stood by my side whether it was a good time or the stressful one.* ***Thank You*** *for keeping me going when things were down and making everyday research in the lab tolerable when nothing ever worked!*

My brother's lovely wife ***Najma,*** *whose kindness, understanding help and support on home front has been monumental in completing my work.*

And my three gorgeous, lovely and noisy nephews ***Haris, Hamza and Hashir*** *have kept me going towards my target throughout my PhD venture. They enriched my life with their hugs, laughter, crying, and shopping. Thank you for being there to take all my stress off my mind.*

Completion of the laboratory work would not have been possible without the help of some special friends who have taught me so much and helped develop my

scientific skills. My kindest gratitude goes to ***Mr. Jim Rooney*** *and* ***Dr. Richard Hughes*** *for continuous help, smiles and support in chromatography throughout my journey. I would like to thank* ***Dr. Neil Mclay*** *(NMR) and* ***Prof. Craig Rice*** *(X-Ray crystallography) for their priceless help. They spent their valuable time and shared their knowledge and suggestions to complete my work.*

I would like to thank all the faculty members, technicians and administrative staff in the research office and School of Applied Sciences for giving me their wonderful support. A massive thank you to all of them who made my doctoral experience so enjoyable;
Lastly, I would like to thank the University of Huddersfield for their fee-waiver scholarship.

Rizwana Sadiq

Abstract

Research in this thesis investigates a simple, rapid, reproducible and specific liquid chromatography-mass spectroscopy (LC-MS) method for the simultaneous detection, confirmation and quantitation of beclomethasone dipropionate (BDP) and its metabolites beclomethasone monopropionate (BMP) and beclomethasone (BOH) which has been developed and validated. The method was validated over a concentration range from 0.001-100 mg/L for BDP and 0.01-10 mg/L for BOH. The calibration graphs exhibited excellent linearity with typical R^2 values for BDP of 0.997 and for BOH of 0.999. The analytes stability was investigated and they were found to be stable for many weeks. BDP was introduced as the first inhaled glucocorticoid for the treatment of asthma in the 1970s and is still a major treatment for asthma nowadays. BDP is an inactive prodrug; for BDP to be effective, it needs to be activated to its active form, beclomethasone-17-monopropionate (17-BMP) and beclomethasone-21-monopropionate (21-BMP). The method involved *in vitro* metabolism of the BDP, incubated with esterase enzyme at 37° C for 2 hrs. The product was analysed by LC-MS. A liquid-liquid extraction procedure was used to purify the products, with four different solvents and five sequential extractions, for initial extraction steps. The extracts were analysed by LC-MS. Extraction with ether gave very good results with 99 % extraction of the required products.

For the first time new methods of labelling steroids, including progesterone and testosterone, with rhenium-containing luminescent labels. For this purpose rhenium complex with 3,3'-diamino-2,2'-bipyridine (complex 1) was used as a fluorescent label for various biomolecules. Preparative HPLC, LC-MS, NMR spectroscopy and X-ray crystallography have been used to identify and characterize the products formed.

The timed reaction of complex 1 with progesterone was run using the newly developed chromatographic method (55 % MeCN, 0.5 mL/min). A solution of complex 1 and progesterone in acetonitrile was heated in the dark for 3 hrs followed by a timed NMR experiment for 6 hours, collecting data at regular intervals. The sample was separated using the preparative HPLC which showed some side

products and two overlapping peaks for the product isomers. The single-crystal X-ray structure of the Re-progesterone product was obtained and measurements of selected bond lengths showed a rearrangement of the double bond between C4 and C5 had occurred at the conjugated end of the progesterone. The refined structure further confirmed the shifting of the double bond. For the analagous product of complex 1 and testosterone attempts were made to crystallise the product both by slow evaporation and by refrigeration of an acetonitrile solution of fraction 2. To date these attempts have been unsuccessful.

Finally, the research work was conducted to combine the work presented above by using enzymatic reactions to modify a biomolecule for reaction with the rhenium-containing complex 1. Galactose oxidase catalyses the oxidations of primary alcohols to the corresponding aldehyde with the reduction of dioxygen to hydrogen peroxide. Research presented in this part of the thesis investigates different methodologies for the oxidation of methyl α-D-galactopyranoside with the help of galactose oxidase to form an aldehyde-containing sugar which will react with the diamino moieties of complex 1. The best method to work with was found to be method 2 using catalase suspension, galactose oxidase and HRP in deionised water. The reaction mixture gave a fairly pure product in good yields.

Abbreviations

AO	Alcohol Oxidase
AUFS	Absorbance Units Full Scale
BDP	Beclomethasone Dipropionate
17-BMP	Beclomethasone-17-monopropionate
21-BMP	Beclomethasone-21-monopropionate
BOH	Beclomethasone
BUD	Budesonide
℃	Degree Celsius (Temperature)
C	Carbon
C_{18} Column	Octadecyl carbon chain-bonded silica column
CD_3CN	Acetonitrile-d_3
CIC	Ciclesonide
CNS	Central Nervous System
COPD	Chronic Obstructive Pulmonary Disease
CO_2	Carbon dioxide
COSY	Correlation Spectroscopy
CSA	Camphor Sulfonic Acid
DCM	Dichloromethane
DERA	Deoxyribose-5-phosphate aldolase
DET	Direct electron transfer
DHT	Dihydrotestosterone
DIPE	Diisopropyl ether
DMSO	Dimethyl sulfoxide
DNA	Deoxyribose nucleic acid
DNP	2,4-Dinitrophenol
D_2O	Deuterium oxide (heavy water)
EIC	Extracted Ion Chromatogram
ELISA	Enzyme-Linked Immuno Sorbent Assay
ESI	Electrospray Ionization
FID	Flame ionization detector
FLIM	Fluorescence Lifetime Imaging Microscopy
FP	Fluticasone Propionate
Gal-GalNAc	D-galactose-β-(1-3)-*N*-acetyl-D-galactosamine
GC-MS	Gas Chromatography coupled with Mass Spectrometry
GO	Galactose oxidase
HCl	Hydrochloric Acid
HMBC	Heteronuclear Multiple Bond Correlation
^{1}H NMR	Proton nuclear magnetic resonance
HP	Human Plasma
HPLC-MS	High Performance Liquid Chromatography coupled with Mass Spectroscopy
HPLC-UV	High Performance Liquid Chromatography with Ultra violet spectroscopy
HPPA	Hydroxyphenylpropionic acid
hr/hrs	Hour (s)
HRP	Horse radish peroxidase
ICH	International Conference on Harmonisation of Technical Requirements for Registration of Pharmaceuticals for Human Use (ICH)
ICS	Inhaled Corticosteroids
ICP-MS	Inductively coupled plasma mass spectroscopy
IS	Internal Standard
IUPAC	International Union of Pure and Applied Chemistry

kDa	KiloDalton
LC-ESI-MS-MS	Liquid chromatography electrospray ionisation tandem mass spectroscopy
LC-MS	Liquid Chromatography coupled with Mass Spectroscopy
LC-MS-MS	Liquid Chromatography coupled with tandem Mass Spectroscopy
LC-UV	Liquid Chromatography with Ultra Violet Spectroscopy
LLE	Liquid/Liquid Extraction
LOD	Limit of Detection
MALDI–MS	Matrix-assisted laser desorption/ionization coupled with mass spectroscopy
MALDI-TOF–MS	Matrix assisted laser desorption ionization-Time of Flight mass spectroscopy
MDI	Metered-Dose Inhaler
MeCN	Acetonitrile
MeOH	Methanol
mg	Milligram
$MgCl_2$	Magnesium Chloride
mg/L	Milligrams per litre
$MgSO_4$	Magnesium Sulphate
MicrOTOF-Q	Micro Time-of-Flight Quadrupole mass spectrometer
min	Minute (s)
mm	Millimeters
MRI	Magnetic Resonance Imaging
MWCO	Molecular Weight Cut Off
m/z	Mass to Charge ratio
N_2	Nitrogen
nm	Nano meter
NMR	Nuclear Magnetic Resonance
pg mL^{-1}	Picogram per millilitre
ppm	Parts Per Million
prep-HPLC	Preparative High Performance Liquid Chromatography
RIA	Radioimmunoassay
Re(I)	Rhenium (I)
RSD	Relative Standard Deviation
RT	Retention Time
Ru(II)	Ruthenium (II)
SD	Standard Deviation
SiO_2	Silicon Dioxide (silica)
SPE	Solid Phase Extraction
SPME-LC-MS	Solid-phase microextraction coupled with liquid chromatography mass spectrophotometry
SRM	Selected Reaction Monitoring Mode
T/t	Time
TBME/MTBE	*Tert*-butyl-methyl ether
Tc	Technetium
TLC	Thin Layer Chromatography
TRH	Thyrotropin Releasing Hormone
µL	Microlitres
UFLC	Ultra Fast Liquid Chromatography
UV-VIS Detector	Ultraviolet/Visible Spectroscopic Detector

Table of Contents

List of Figures

List of Tables

Chapter 1

In-vitro metabolism of a corticosteroid

Chapter 1: In-vitro metabolism of a corticosteroid

1.1 Introduction

Hormones are groups of powerful chemicals that have a wide range of effects on the body and a range of vital hormonal functions. When a hormone reaches a target cell, it binds to a receptor to initiate a response.[1] They can be divided into naturally-occurring and synthetic groups. The latter are important as therapeutic agents.

1.1.1 Classification of hormones / chemical classes of hormones:

Hormones are classified according to their structure and function.[1] Hormones can be classified by their structure, which divides them as water or fat soluble, which determines:

- how they move in the blood, alone or attached to a protein;
- how they bind to receptor sites outside or inside of the target cell (fat soluble can bind both whereas water soluble hormones usually bind on the outside) and;
- how they will be metabolized.[2]

Vertebrate hormones fall into three chemical classes:

Amino acid derivatives: Some single amino acid derivatives can be classed as hormones. These are derived from the amino acid, phenylalanine.[3] Examples include catecholamines and thyroid hormones. These hormones are stored in endocrine cells until needed.[1,2,4]

Peptide hormones: They are made up of chains of amino acids. Examples of small peptide hormones are thyrotropin releasing hormones (TRH) and vasopressin. These vary from small peptides to long chain proteins, for example, insulin and growth hormone. Glycoprotein hormones have long carbohydrate side chains. Luteinizing hormone, follicle-stimulating hormone and thyroid-stimulating hormone are glycoprotein hormones[1]. They are stored in endocrine cells until needed for processes like metabolism, lactation, growth and reproduction.[2,3,4]

Lipid and phospholipid-derived hormones: They are derived from lipids such as linoleic acid, arachidonic acid and phospholipids. The main classes are the steroid hormones that are derived from cholesterol. These are fat soluble hormones. Examples of steroid hormones are testosterone and cortisol. Among these are the three major sex hormones groups: estrogens, androgens and progesterones.[1,2,3,4]

Glucocorticoids are hormones synthesized in the adrenal cortex and secreted into the blood, where the levels of glucocorticoids fluctuate in a circadian mode. In humans, the naturally occurring glucocorticoid is hydrocortisone (cortisol), which is synthesized from its precursor cortisone. The beneficial effects of glucocorticoids in asthmatic patients were first described in 1950.[5] Since then, many studies have focused on the therapeutic potential of glucocorticoids. Several synthetic glucocorticoids[6] are now available and are powerful agents in the treatment of inflammatory diseases and are by far the most effective anti-inflammatory drugs used in the treatment of asthma.[7]

1.1.2 History of corticosteroids

Glucocorticoids (also known as glucocorticosteroids or corticosteroids) are among the most widely used drugs in the world and are effective against many inflammatory and immune diseases. The most common use of corticosteroids is in the treatment of asthma, where inhaled corticosteroids have become first-line therapy and by far the most effective anti-inflammatory treatment. The treatment of chronic inflammatory diseases was revolutionized by the discovery of the therapeutic utility of glucocorticosteroids in the 1950s. Since this time they have been the mainstay of treatment for chronic inflammatory diseases.[5]

All major chronic inflammatory diseases (including inflammatory bowel disease, psoriasis, rheumatoid arthritis and asthma) can be treated with glucocorticoids. They are the most effective anti-inflammatory agents currently available. However, since the elucidation of their clinical effectiveness in 1948 for the treatment of rheumatoid arthritis by Kendall and Hench, who were awarded the Nobel Prize for Medicine for this work in 1950, it has become clear that the beneficial effects of ever increasing doses of glucocorticosteroids are countered by the onset of severe side-effects. Moreover, the recent developments in our understanding of the action of

glucocorticosteroids have suggested that it may be possible to develop new glucocorticosteroids with different pharmacology which lack the ability to induce many of the pathways involved in the manifestation of side-effects.

Enormous progress has been made in improving glucocorticosteroid treatment since the introduction of hydrocortisone as the first clinically used corticosteroid. Extensive drug development has resulted in highly potent molecules, the pharmacokinetic profiles of which have been optimized to minimize systemic exposure and to target activity to the lung.[8]

1.1.3 Types of corticosteroids

Corticosteroids exist in two groups; endogenous (naturally produced) and exogenous (originally outside the body). Endogenous corticosteroids, such as cortisol, are important for physiological processes, including immune response, stress response, and growth.

Exogenous corticosteroids, including

a) systemic (*e.g.* prednisolone)

b) inhaled (*e.g.* ciclesonide) and

c) topical corticosteroids (*e.g.* hydrocortisone), are widely used for various indications, such as asthma, rheumatoid arthritis, eczema, and Crohn's disease, due to their anti-inflammatory and immunosuppressive effects. However, both short-term and chronic exposure to corticosteroids could result in a variety of adverse effects, including growth retardation in pediatric patients, oropharyngeal candidiasis, skin atrophy, adrenal suppression, risk of cataracts, and osteoporosis.[9,10,11]

1.1.4 Inhaled corticosteroids (ICS)

Inhaled corticosteroids (ICS) are currently the standard first-line therapy for the treatment of airway diseases, for example asthma. They reduce bronchial hyper-responsiveness by reducing the underlying inflammation in the airways through the inhibition of inflammatory cell migration and infiltration and the release of pro-inflammatory cytokines. The pharmacokinetic and pharmacodynamic properties of ICS determine their therapeutic efficacy as well as their propensity for local and systemic side effects.[12,13,14] All corticosteroids are 21-carbon atom steroids, with a basic four-ring structure, as shown in Fig. 1.

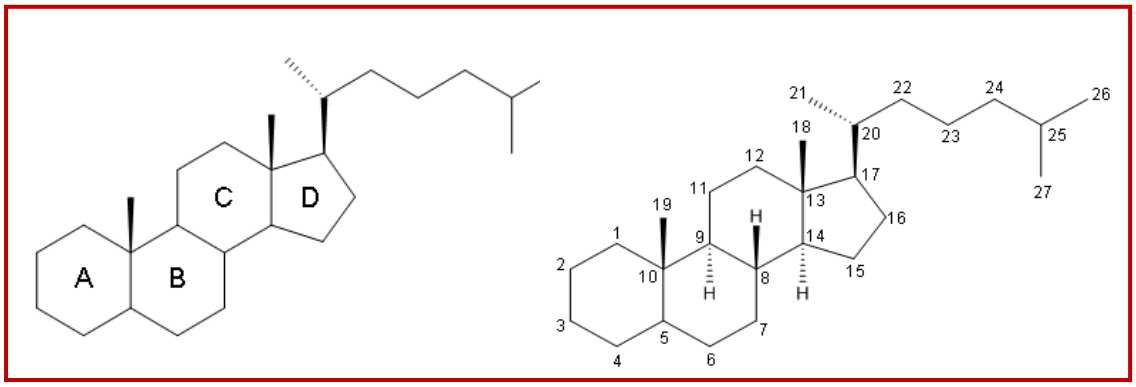

Figure 1: The basic skeleton of a steroid showing the IUPAC numbering system.[15,16,17]

1.1.5 Functions

Corticosteroid medicines are derivatives of the natural corticosteroid hormones that are produced by the adrenal glands.[18] Corticosteroids are widely used as:

I. Anti-inflammatory and immunosuppressive agents in a variety of chronic conditions.
II. Replacement therapy (to replace hormones due to an underlying health condition).
III. To the skin for the localised treatment of various inflammatory skin disorders.[6,18]
IV. As a regulator of a number of physiological processes, including development, stress responses, and homeostasis. These activities have important therapeutic consequences, and today corticosteroids are indispensable for the treatment of a wide variety of inflammatory diseases.[19]

Corticosteroids should not be confused with anabolic steroids, which are sometimes used (illegally) by body builders and athletes. Unlike anabolic steroids, corticosteroids do not affect muscle strength.[6]

1.1.6 Side Effects

The efficacy of ICS is now established in short and long-term studies in adults and children, but there are still concerns about side effects, particularly in children and when high inhaled doses are used. Several side effects have been recognized including systemic side effects. In the treatment of airway diseases side-effects can

be limited by targeted delivery to the airway and lung and significant progress has been made through the use of a variety of lung-targeting strategies.[8]

General side effects may include, cough, pneumonia in chronic obstructive pulmonary disease (COPD) patients and oropharyngeal candidiasis. Systemic side effects including adrenal and growth suppression, bruising, osteoporosis, cataracts and metabolic abnormalities (insulin, glucose) limit their systemic use; however, inhaled corticosteroids play a pivotal role in the treatment of asthma and chronic obstructive pulmonary disease.[19,20]

1.1.7 *Mechanism of action*

Although glucocorticoids have been known for a long period of time, their precise mechanism of action is still not completely understood. However, recent studies have increased our understanding of their complex mechanisms of action.[7] A general outline is shown in Fig. 2:

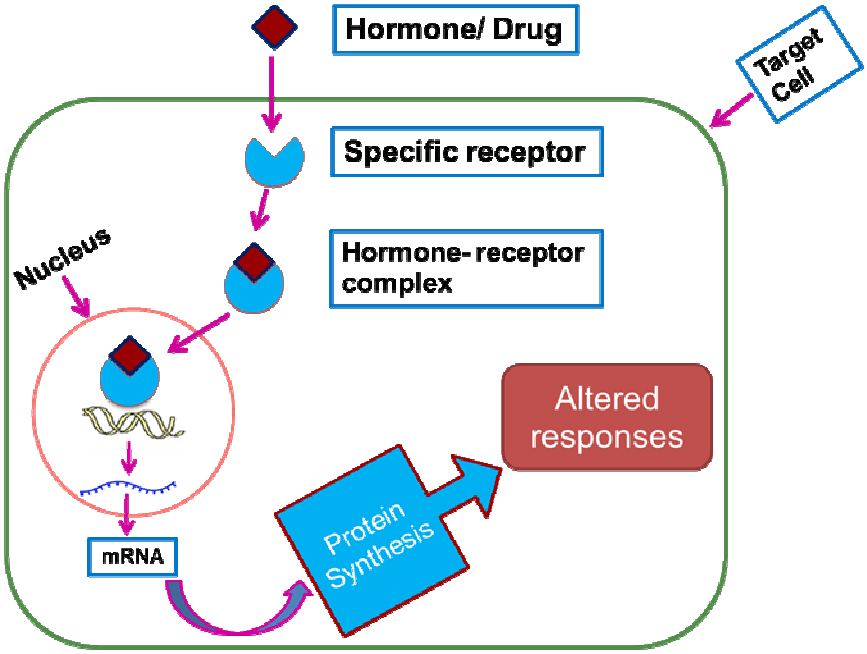

Figure 2: A general mechanism of action of ICS.[21]

As described in Fig. 2, the diverse actions of steroids are mediated through a single receptor, which is present in most cell types. Steroids are lipophilic and unbound glucocorticoids thus rapidly cross the cell membrane and enter the cytoplasm, where they combine with the glucocorticosteroid receptor.[21] Protein molecules that hold the receptor in an inactive state (heat shock proteins) then

dissociate, and the glucocorticosteroid-receptor complex translocates to the nucleus. In the nucleus, the glucocorticosteroid-receptor complex acts as a transcription factor, binding to specific recognition sequences of steroid-sensitive genes resulting in gene activation or suppression. The results can include inhibition of leukocyte infiltration at the site of inflammation, interference in the function of mediators of inflammatory response, and suppression of humoral immune responses (*i.e.* upregulation of certain anti-inflammatory mediators, such as lipocortin-1 and neutral endopeptidases, and down regulation of pro-inflammatory mediators such as cytokines and chemokines). This is believed to be a major mechanism contributing to the anti-inflammatory effects of inhaled steroids in asthma.[22,23] The use of ICS has represented a major breakthrough in the treatment of asthma since their introduction in the 1970s. Among the various ICS available in the market, beclomethasone dipropionate (BDP) was the first, introduced in 1972 in a pressurized metered-dose inhaler (MDI) and later in a dry powder inhaler and an aqueous nasal spray.

1.1.8 Pharmacokinetics

The science of pharmacokinetics aims to quantify the ways in which the body absorbs, distributes, metabolizes, and eliminates drugs. The knowledge of the pharmacokinetic behaviour of drugs is essential not only for understanding the basis of their safety, efficacy, and therapeutic ratios, but also for predicting their behaviour and secondary effects when administered.[24]

The pharmacokinetic behaviour of ICS is important in relation to systemic effects. The fraction of steroid which is inhaled into the lungs acts locally on the airway mucosa, but may be absorbed from the airway and alveolar surface. This fraction therefore reaches the systemic circulation. The fraction of ICS which is deposited in the oropharynx is swallowed and absorbed from the gut. This absorbed fraction may be metabolized in the liver before reaching the systemic circulation (first-pass metabolism). A high level of first-pass metabolism will decrease the risk of unwanted systemic effects from the GI fraction of the dose (Fig. 3). The ideal ICS should have high lung bioavailability, negligible oral bioavailability, low systemic absorption, high systemic clearance and high protein binding.[19,20]

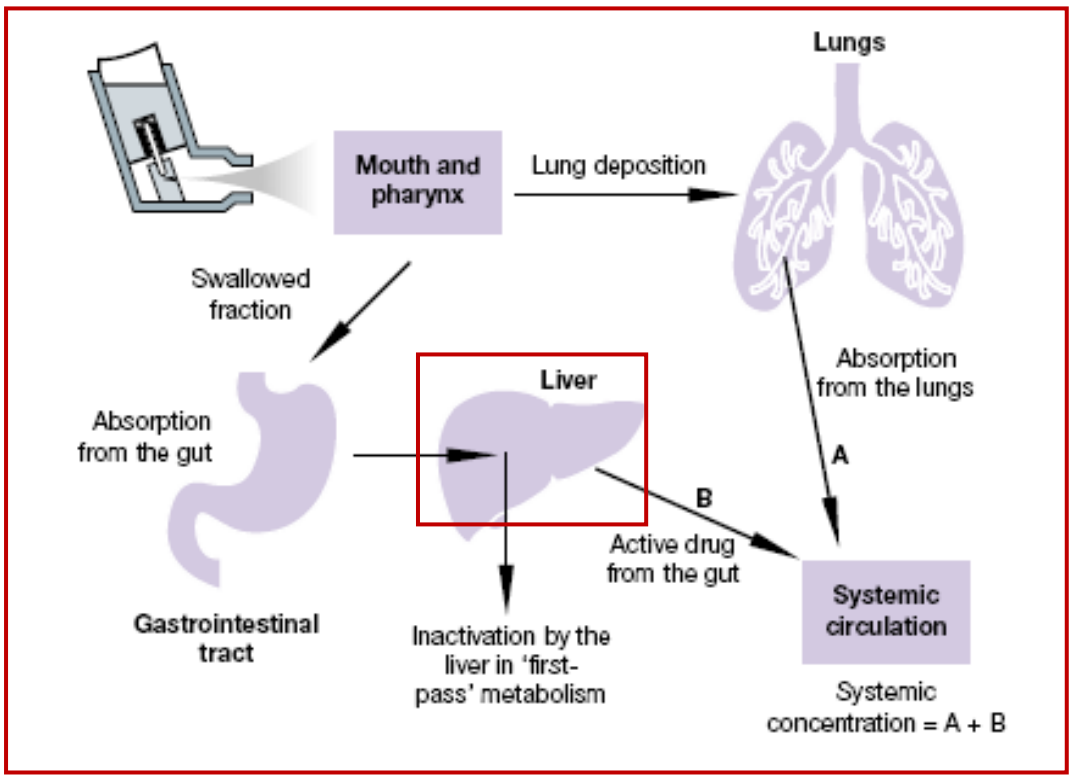

Figure 3: In vivo pharmacokinetics of inhaled steroids.[25]

1.1.9 Beclomethasone Dipropionate (BDP)

Beclomethasone dipropionate, (9-chloro-11β,17,21trihydroxy-16β- methylpregna-1,4-diene-3,20-dione-17,21-dipropionate, BDP), the active component of Beconase AQ nasal spray, is a commonly-used anti-inflammatory steroid and a pro-drug with weak glucocorticoid receptor binding activity.[26] BDP is an important glucocorticoid diester in the inhalation therapy of lung diseases such as asthma.[27] BDP is a white to creamy-white, odourless powder, which is very slightly soluble in water, very soluble in chloroform, and freely soluble in acetone and in ethanol.[26] The structure is shown in Fig. 4(a)(b). BDP is structurally complex since it has two side chains, as well as methyl groups at positions 18 and 19 and a chlorine atom at C9. It has four carbonyl and carboxyl groups available for hydrogen bonding.[28]

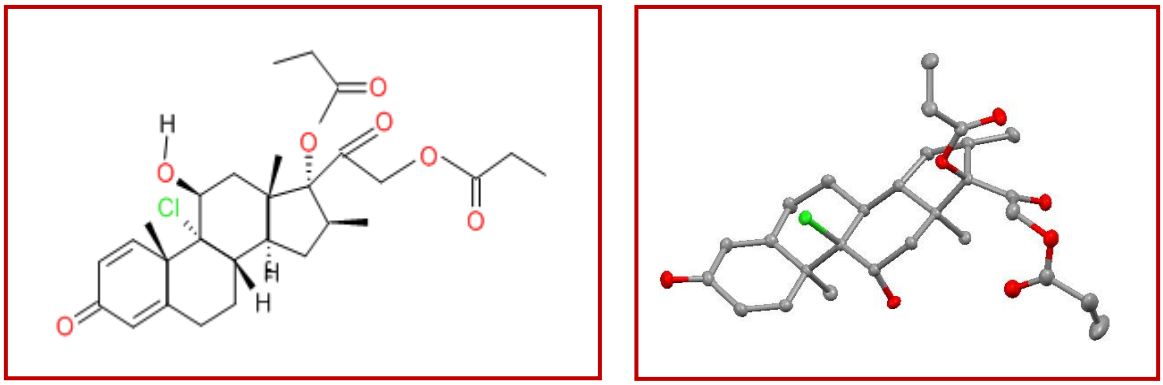

Figure 4 (a): 2D structure of BDP **(b):** 3D structure of BDP

Beclomethasone dipropionate is used in the treatment of bronchial asthma and allergic (seasonal) and vasomotor rhinitis.[29,30] It is marketed, variously, as a solution or powder under the brand names Beclovent, Beconase, Qvar, Clenil, Modulite, Pulvinal and Vancenase. The actuated doses are usually in the range 0.04 – 0.08 mg per actuation.[31,32]

1.1.10 Metabolism of Beclomethasone dipropionate (BDP)

For several decades it has been recognised that the lungs contain non-specific esterases and as such a potential site for the hydrolysis of ester drugs and it is desirable to modify the physicochemical characteristics of a drug by the production of ester prodrugs. It has been reported that ester prodrugs of xenobiotics whose site of action is in the lungs were synthesised.[23,33] Despite this history, there are surprisingly few reports in the literature in which the pulmonary hydrolysis of esters has been investigated *in vitro*. As a preliminary investigation into pulmonary esterase activity, prior to the *in vivo* investigation of pulmonary first-pass ester metabolism, the hydrolysis of four aliphatic esters of biphenylacetic acid was studied.[23]

The aims of this study were to investigate whether the kinetic parameters of ester hydrolysis are dependent on the physicochemical nature of the esters; and whether enzyme kinetics derived in blood can be used to predict the pulmonary situation. It appeared that kinetic parameters for non-specific esterase catalysed hydrolysis are predictable from the ester's physicochemical nature. The pulmonary enzyme kinetics for hydrolysis can be directed from the kinetics measured in blood.[34]

And three major metabolites of BDP, beclomethasone-17-monopropionate (17-BMP), beclomethasone-21-monopropionate (21-BMP), and beclomethasone (BOH) are formed *via* hepatic cytochrome P450 3A-family catalyzed biotransformation (Fig. 5).[11,21,34,35,36,37] More than 90% of inhaled beclomethasone is found as its active metabolite in the systemic circulation.[22,36,38] In order to be effective, BDP needs to be converted to 17-BMP *via* hydrolysis, which is largely enzyme-catalysed *in vivo*.[30]

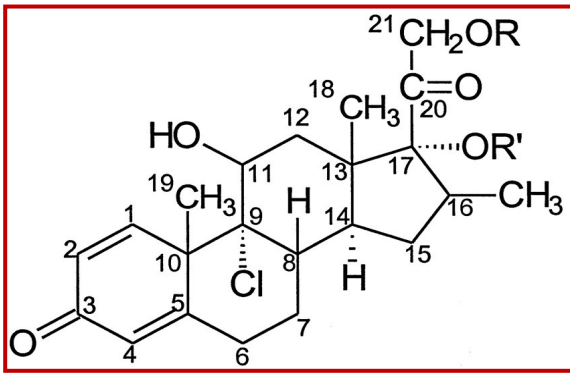

	R	R'
BDP	COC_2H_5	COC_2H_5
17-BMP	H	COC_2H_5
21-BMP	COC_2H_5	H
BOH	H	H

Figure 5: BDP and its primary metabolites.[39]

The proposed degradation pathway of BDP in human plasma is presented in Fig. 6. Essentially, three reactions are involved: ester hydrolysis, transesterification, and loss of hydrochloric acid (HCl) to form an epoxide. In plasma, the hindered 17α-propionate group of BDP is more resistant to ester hydrolysis than that at the 21-position, giving rise to 17-BMP as the major product (Fig. 6).[30]

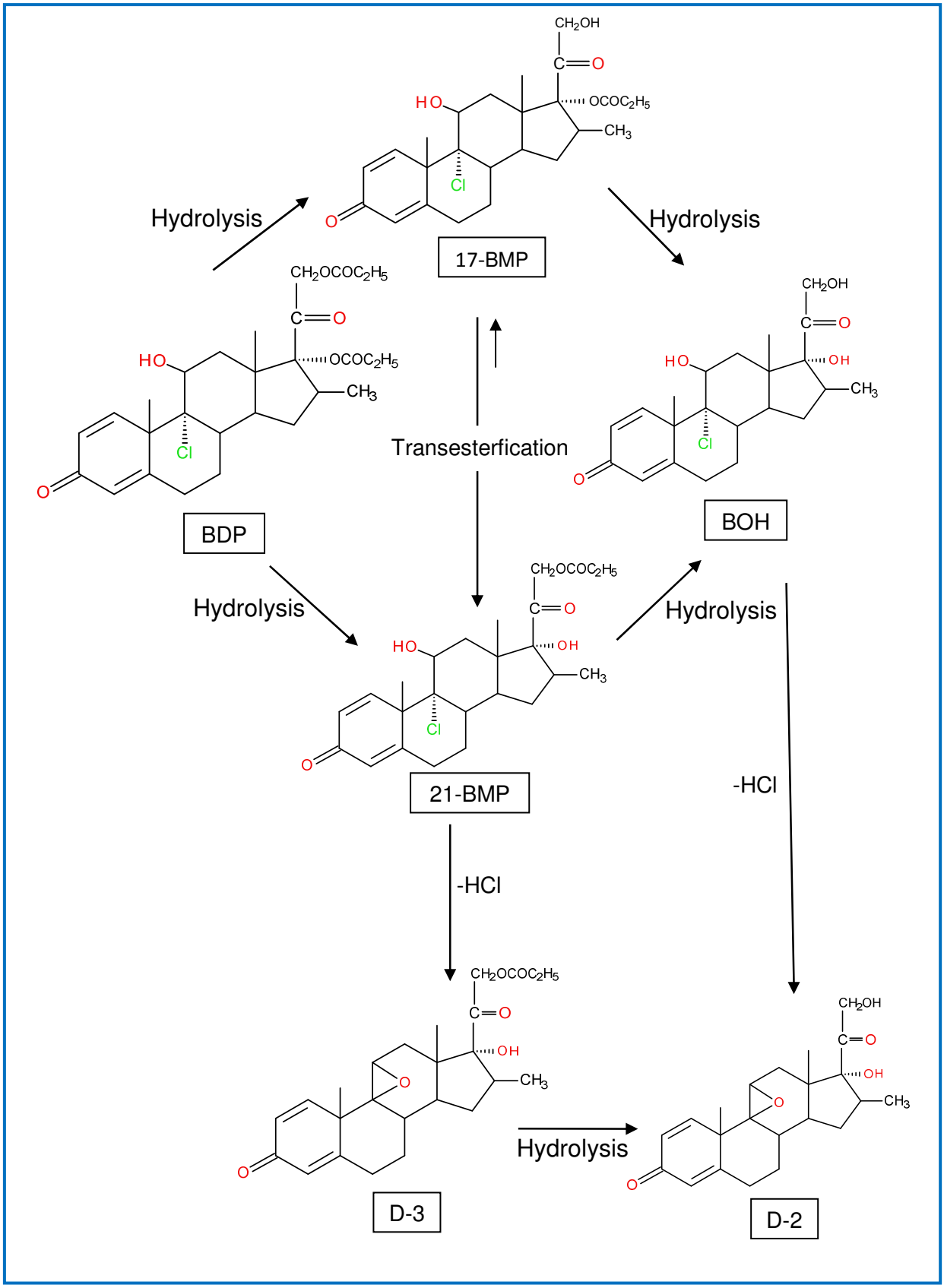

Figure 6: A proposed degradation pathway of BDP in human plasma.[30]

The rapid formation of 17-BMP, a potent and more hydrophilic degradation product, may lead to extensive absorption of the drug from the lower respiratory tract because it may be cleared more rapidly into the systemic circulation which results in substantial systemic effects, such as adrenal suppression, osteoporosis, reduced total bone mass and mineral density, as well as the inhibition of body growth in children. The metabolic biotransformation of BDP has been studied and reviewed by many authors.[37,40] For the oral inhalation route, some metabolism occurs in the lungs before entering the systemic circulation; the lung tissues metabolize Beclomethasone dipropionate rapidly to 17-BMP and more slowly to BOH. The mean elimination half-life of 17-BMP is 2.8 hrs; the biological half-life of beclomethasone is roughly 15 hrs. Irrespective of the route of administration (injection, oral or inhalation), beclomethasone and its metabolites are excreted predominantly in the faeces. Less than 10% of the drug and its metabolites are excreted in the urine.[22,38]

The decomposition kinetics of BDP have been studied extensively. For example, Foe, Brown and Seale proposed a method to monitor the kinetics of decomposition of BDP, 17-BMP, and BOH which were characterized in whole human plasma (HP). A reverse-phase HPLC assay was used for simultaneous separation and quantification of beclomethasone propionate esters and six degradation products, three of which were previously unidentified. Following incubation of BDP, a number of products were formed and a new metabolic pathway for BDP was proposed in an article in 1998.[31]

Daley-Yates, Price *et al*.[32] worked to assess the absolute bioavailability, pharmacokinetics and metabolism of BDP in humans following intravenous, oral, intranasal and inhaled administration.[32] Twelve healthy subjects participated in this study where BDP was administered *via* the following routes: intravenous infusion (1000 mg), oral (4000 mg, aqueous suspension), intranasal (1344 mg, aqueous nasal spray) and inhaled (1000 mg ex-valve, metered dose inhaler). Blood samples were collected for 24 hrs post dose for the measurement of BDP, 17-BMP and BOH in plasma by LC-MS. The chemical structures and relative receptor affinities for BDP and its main metabolites are shown in Fig. 7 below.

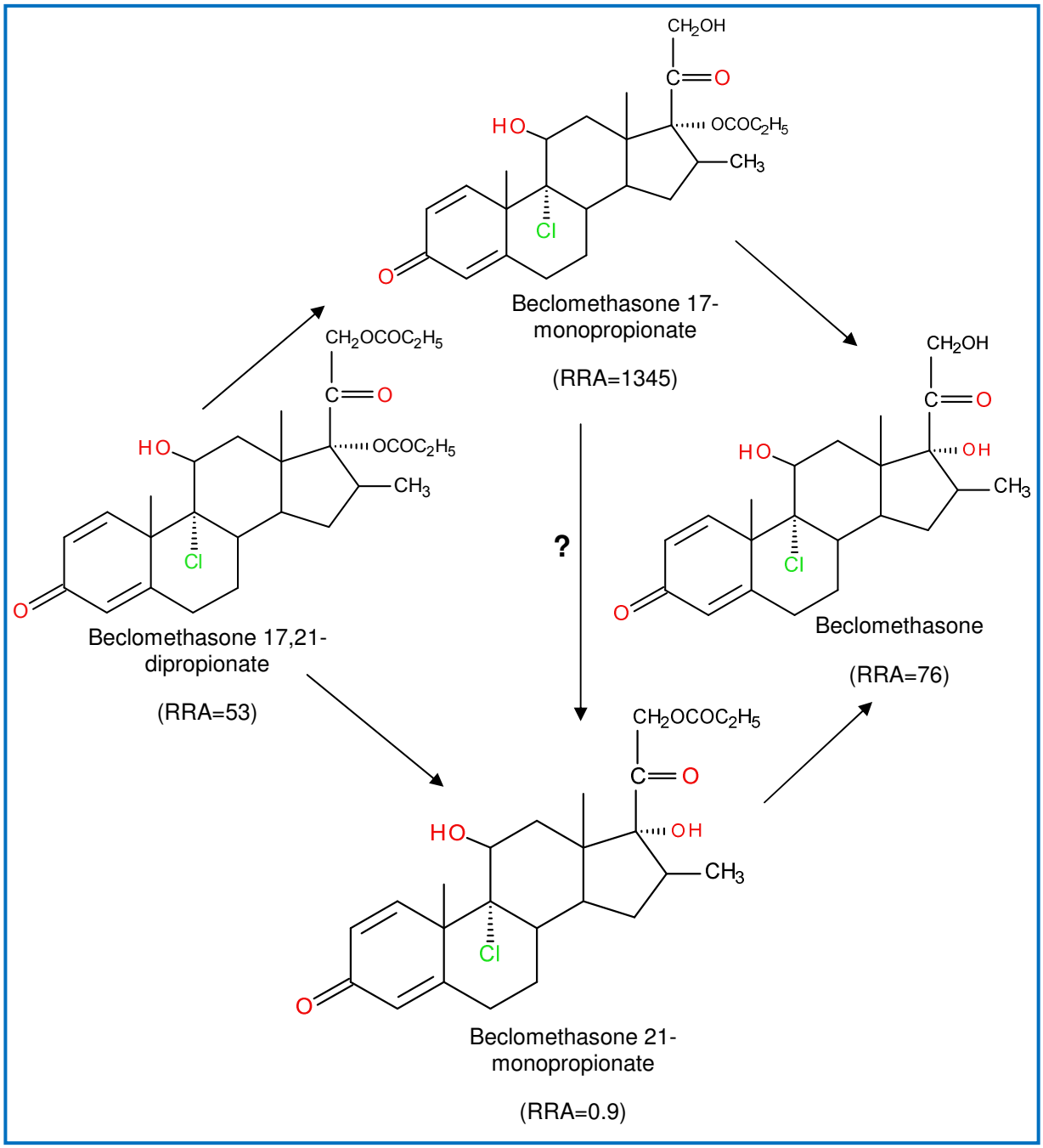

Figure 7: The chemical structures and relative receptor affinities for BDP and its main metabolites.[32]

BDP was not extensively distributed to the tissues but was eliminated rapidly with a high clearance and short half-life (0.5 hr). The disappearance of BDP was accompanied by the appearance of 17-BMP after a delay of approximately 1.5 hrs, which was in agreement with the fact that it was converted by esterases. Unchanged BDP has negligible oral and intranasal bioavailability with limited absorption following inhaled dosing. The oral and intranasal bioavailabilities of the active metabolite 17-

BMP were high, but direct absorption in the nose was insignificant. The total inhaled bioavailability of 17-BMP (lung + oral) was also high (62%) of which approximately 36% was due to pulmonary absorption.[32,39]

Nave and McCracken investigated the *in vitro* metabolism of BDP, budesonide (BUD), ciclesonide (CIC), and fluticasone propionate (FP) in human lung precision-cut tissue slices. In this study, differences in an *in vitro* metabolism of currently available ICS in human lung tissue slices were evaluated with respect to their local effect on pulmonary residence time. Lung tissue slices were incubated with BDP, BUD, CIC, and FP (initial target concentration of 25μM) for 2, 6, and 24 hrs. Metabolites and remaining parent compounds in the tissue samples were analyzed by HPLC with UV detection. It was shown that BDP was hydrolyzed to active 17-BMP and to pharmacologically inactive BOH and 21-BMP. BMP was the major metabolite at 2 hrs and 6 hrs, whereas BOH was the major metabolite at 24 hrs. At 24 hr, BMP accounted for 26.6% and BOH for 64.9% of BDP-related material. These authors observed clear differences between the investigated ICS regarding the time of the drugs within the lung tissue slices.[40]

1.1.11 Methods of detection and quantitation of corticosteroids

Steroid detection has been critical for the diagnosis of disorders of steroid hormone synthesis and metabolism since the 1960s. In addition, analytical methods are necessary since the therapeutic and doping use of corticosteroids has been widespread for several decades. A range of methodologies for detecting corticosteroids in biological fluids has previously been investigated. Unfortunately detection of corticosteroids in biological matrices has been problematic; traditional analytical techniques including gas chromatography coupled with mass spectroscopy (GC-MS), enzyme-linked immune sorbent assay (ELISA) or HPLC-UV show poor sensitivity or selectivity. Other analytical methods widely used to determine corticosteroids are based on radioimmunoassay (RIA) procedures; these are characterised by their high sensitivity. However, RIA is hazardous due to the use of radioactive materials. Also, modification of an assay procedure is difficult and time consuming. RIA requires approval and training to work with radioactive materials.[41]

Methods for the detection and quantification of synthetic corticosteroids by GC-MS have been reported. Although providing good sensitivity, these methods are not easy to use. The Atlanta Olympic Games in 1996 marked the first time every specimen was screened by GC-MS.[42] Today, liquid chromatography coupled with mass spectroscopy (LC-MS) represents a powerful alternative combining rapidity, specificity and sensitivity. Several publications have proposed the detection of corticosteroids using LC with tandem mass spectroscopy (LC–MS–MS).[42,45,48]

1.1.12 Specific methods for detection and quantitation of Beclomethasone dipropionate (BDP)

Investigation of a drug's pharmacokinetic behaviour is a vital part of its development. Therefore, there are many methods in the literature for extraction and quantitation of BDP and its metabolites from a variety of sample types. In pharmaceutical preparations and biological matrices, multiple analytical procedures have been reported for the analysis of BDP using HPLC[42,43,44,45,46,47], GC or capillary electrophoresis.[30,43,48,49]. Perhaps surprisingly, spectrophotometric techniques have scarcely been used.[23,43]

Jian-Jun Zou and colleagues developed a method for determining the pharmacokinetic profiles of BDP.[33] It is believed that this paper is the first report of a simple and sensitive method to determine the two main active metabolites, BOH and 17-BMP, in human plasma by liquid chromatography electrospray ionization tandem mass spectroscopy (LC–ESI (+/–)–MS–MS) using BDP as internal standard (IS) and to study the pharmacokinetics after intramuscular injection in healthy Chinese volunteers. Extraction was carried out on plasma with an ether-cyclohexane mixture and both metabolites were separated by HPLC on a Hanbon Lichrospher C_{18} column with a mobile phase of methanol–water (85:15, v/v) at a flow rate of 0.7 mL/min. Calibration curves were linear. The mean plasma extraction recoveries for BOH and 17-BMP were in the ranges of 82.7–85.9% and 83.6–85.3%, respectively. The method was successfully applied to study the pharmacokinetics of a new formulation of BDP injection in healthy Chinese volunteers. The method achieved good sensitivity and specificity for the determination of BOH and 17-BMP in human plasma. No significant interference caused by endogenous compounds was observed. The alternate acquisitions of positive and negative ions in selected

reaction monitoring mode (SRM) also offered lower background and higher response. Plasma was not assayed for the minor and inactive metabolite 21-BMP. The method is simpler and faster than any other described in the literature. This method is suitable for pharmacokinetic studies in human subjects.

Guan, Uboh and colleagues presented a sensitive LC-MS-MS method for the detection, confirmation and quantification of BDP, 17-BMP, 21-BMP and BOH in equine plasma and urine. BDP contains two ester groups and 17-BMP and 21-BMP might be further hydrolyzed by plasma esterases to BOH. Therefore, it was necessary to evaluate the stability or decomposition of BDP, 17-BMP and 21-BMP in equine plasma at ambient temperature (25 ℃). The concentration of BDP decreased by 36% over 2 hrs and that of 21-BMP by 86%, but the concentration of 17-BMP did not change over the 2 hrs period. The results showed that 17-BMP was stable in equine plasma at ambient temperature during the time period (2 hrs.). The method was evaluated with regard to the limit of detection, quantification range, precision and accuracy. The extraction efficiency was >89% for BDP and 17-BDP.[36]

The correlation coefficients of the calibration curves were >0.99. The limit of confirmation was 25 pg mL^{-1} for BDP and 17-BMP and 50 pg mL^{-1} for BOH in plasma. The quantification accuracy was within the range 78–116% for all the analytes in plasma and urine, which was satisfactory for quantification at very low concentrations. The intra-day relative standard deviation (RSD) was <16% for all the analytes and the inter-day RSD was <24%. The method was successfully applied to the analysis of equine plasma and urine samples for the analytes given to horses by inhalation. 17-BMP was the major analyte detected so it is the target analyte to detect the use of BDP in race horses.[36]

1.2 Aim of the study

17-BMP is usually prepared using human lung homogenates. It is very difficult, both ethically and medically, to obtain a lung. Therefore, this project aims to develop a newer, rapid, ethically acceptable, robust method for conversion of BDP to its active metabolite, 17-BMP, *in vitro*, using pure esterase enzyme and hence removing the need to obtain lung tissue. The isolation and purification of 17-BMP should also be facilitated by this approach.

1.3 Experimental

1.3.1 Materials

Beclomethasone dipropionate (BDP, IUPAC: 9-chloro-11β,17,21trihydroxy-16β-methylpregna-1,4-diene-3,20-dione-17,21-dipropionate), was purchased from Fluka chemicals (purity 99 %).

Beclomethasone (BOH, IUPAC: 9α-chloro-16β-methyl-1,4-pregnadiene-11β,17α,21-triol-3,20-dione) was purchased from Sigma Aldrich, U.K.

Standard solutions (1 mg/mL) of beclomethasone dipropionate (BDP) and beclomethasone (BOH) were prepared in methanol. Working solutions were prepared by successive dilution with methanol and stored in the fridge at 4 °C.

Esterase from porcine liver was purchased from Sigma Aldrich UK.

Acetonitrile (MeCN), methanol (MeOH), ethanol (certified HPLC grade), cyclohexane dichloromethane (DCM) and *tert*-butyl methyl ether (TBME/MTBE) were purchased from Fisher Scientific (UK).

Diethyl ether was purchased from Sigma Aldrich, U.K.

A Mettler AT 261 Delta Range ® Fact analytical balance was used for weighing the solid forms of BDP and BOH.
Eppendorf research-grade micropipettors were used for measuring out the required amount of solution (Fisher Scientific, UK).

1.3.2 Instrumentation

1.3.2.1 Liquid chromatography mass spectroscopy (LC-MS)

Chromatographic separation was developed on a Shimadzu Prominence UFLC system and Lab Solutions v. 5 software was used for the processing of the data (Schimadzu Corporation UK). It is an ultra-high-speed prominence LC-20AD XR that achieves both ultra-high-speed analysis and ultra-high separation, based on high analysis precision and reliability comprising of prominence System Controller, schimadzu Solvent Delivery Unit, prominence AutoSampler (SIL-20A XR), prominence Column Oven (CTO-20A), Schimadzu Fluorescence Detector (RF-10A

XL, prominence Diode Array Detector (SPD-M20A) and prominence Degasser (DGU-$20A_3$.

The column used was a Lichrospher 100, RP-18 (250 mm x 4.6 mm, 5 µm), column purchased from VWR (Merck, Germany). The mobile phase (A) was HPLC grade water and mobile phase (B) was acetonitrile. The flow rate was kept constant at 1.00 mL/min. The injection volume was 20 µL. The eluent UV absorbance was monitored using a diode array detector and monitored at a wavelength of 240 nm for the steroids.

The samples were analysed by a Bruker MicrOTOF-Q mass spectrometer coupled to the UFLC system to facilitate the study of BDP standards and metabolite formation. The mass spectrometer was a hybrid quadrupole/orthogonal accelerated Time-of-Flight equipped with an electrospray ionization (ESI) ion source. Positive ion ESI was chosen. Data acquisition and processing was carried out using Bruker's proprietary DataAnalysis software.

1.3.2.2 Chromatographic conditions

Table 1 below briefly describes the instrumental parameters used for the analysis of BDP, BMP and BOH.

HPLC	Shimadzu UFLC
Mode	Isocratic
Analytical Column	Lichrospher 100, RP-18 (250 mm x 4.6 mm, 5 µm), column no. 026023, Lot No. 497017
Injection Port Type	Manual
Syringe Volume	50 µL
Injection Volume	20 µL
Column Flow	1.0 mL/min
Detector	Diode array, monitored at 240 nm
Run Time	20 min

Table 1: Instrumental parameters for the analysis of BDP, BMP and BOH

The analytical column (C18) was selected on the basis of previous methodology which gave the required results. BDP and its metabolites were absorbed best at 240 nm.

1.4 Methodology

1.4.1 Method development for the analysis of BDP

The challenge encountered in steroid analysis is to develop a specific technique for the analysis of an individual steroid in the presence of many structurally similar compounds. Often steroids and their metabolites differ by only the presence or absence of two hydrogen atoms or in the structure of the rings.

1.4.1.1 Detection methods of BDP Analyte

To optimize the HPLC parameters, several mobile phase compositions were evaluated for the detection of BDP. Table 2 below summarises the methods used.

Sample No.	Conc. of solution [mg/L]	Mobile Phase	
		A %	B %
		[HPLC H_2O]	[MeCN]
1	1000	40	60
2	100	40	60
3	100	25	75
4	100	20	80
5	100	50	50

Table 2: Method development for the analysis of BDP

1.4.1.2 Identification of BDP Analytes

To detect the peak of BDP, a 100 ppm solution was run in duplicate to determine the retention time. For this purpose 100 ppm, 10ppm and 1 ppm working solutions were prepared by serial dilution. The retention time was confirmed and it was decided to use the same method for further analysis.

1.4.2 Method optimization and validation

Method optimization and validation was done according to the International Conference on Harmonisation of Technical Requirements for Registration of Pharmaceuticals for Human Use (ICH) guidelines.

1.4.2.1 Experimental Protocol for Beclomethasone dipropionate (BDP)

1.4.2.1.1 Stock solutions

Standards

A stock solution of BDP was prepared in methanol at a concentration of 1000 ppm. BDP (1.0 mg) was weighed and put into an eppendorf tube. The stock solution was made by dissolving the weighed amount in 1.0 mL of MeOH to achieve a clear solution with the final concentration of 1000 ppm (1.0 mg/1.0 mL). After preparation the stock solutions were labelled and stored in a fridge at 4 °C and allowed to equilibrate at room temperature for at least 15 min before use. The same method was used to prepare separate solutions of the metabolites.

Mixed standards of BDP and BOH

A stock solution of BDP and BOH was prepared as follows: BDP (1 mg) and BOH (1 mg) were weighed separately and dissolved in methanol separately. Working standard solutions were prepared by serial dilution of mixed aliquots of the stock solutions.

1.4.2.1.2 Calibration standard solutions

BDP

Standards were prepared by serial dilution of the stock solution with methanol to give concentrations of 100, 50, 25, 10, 5, 2.5, 1, 0.1 and 0.01 ppm. In order to get a calibration graph for BDP, the samples were run twice for each concentration. The calibration curves were constructed by plotting the average peak area of each analyte against the concentration.

BOH

Standards were prepared by serial dilution of the stock solution with MeOH to give a concentration range from 0.01 - 10 ppm.

Mixed solution of BDP and BOH

A working solution (100 ppm) was made prior to preparation of the calibration solutions of the mixed BDP and BOH sample. From the stock solution, an aliquot (0.1 mL) was pipetted out from both the stock solutions and 0.8 mL of MeOH was added to make a total volume of 1 mL. The working standards were made by serial dilution of the 100 ppm mixed solution within the concentration range from 0.01 - 1 ppm, as depicted in Table 3 below. The standard solutions were prepared daily.

Conc. (ppm)	Analyte Solution (ml)	MeOH (ml)	Total Volume(ml)
100	0.1 + 0.1 from 1000 ppm solution	0.8	1
10	0.1 from 100 ppm mix. solution	0.9	1
1	0.1 from 10 ppm mix. solution	0.9	1
0.75	0.75 from 1 ppm mix. solution	0.25	1
0.5	0.5 from 1 ppm mix. solution	0.5	1
0.25	0.5 from 0.5 ppm mix. solution	0.5	1
0.1	0.1 from 10 ppm mix. solution	0.9	1
0.01	0.1 from 0.1 ppm mix. solution	0.9	1

Table 3: Preparation of working solutions for calibration

Calibration graphs for mixed runs of BDP and BOH were plotted by taking the average of two replicate values for 0.01, 0.1, 0.25, 0.5, 0.75, 1 and 10 ppm, as the samples were run twice for each concentration. In the MS experiments extracted ion chromatograms (EICs) were obtained for two ions, *i.e. m/z* 521 and 543 for BDP and *m/z* 409 and 431 for BOH corresponding to $[M+H]^+$ and $[M+Na]^+$ respectively. Graphs were plotted using the peak areas of the EICs.

1.4.2.1.3 Standard solutions for Limit Of Detection (LOD) determination

For determination of the LOD, a previously prepared mixed standard solution of BDP and BOH was used. The solution was serially diluted each time *i.e.* 100 to 10 ppm, 1.0, 0.5, 0.1, 0.01 and 0.001 ppm. Solutions were run in the HPLC system until no peak was observed. According to ICH guidelines, the limit of detection (LOD) is defined as the lowest concentration of an analyte in a sample that can be detected but not quantified. The limit of detection (LOD) was determined as the lowest concentration where the chromatographic peak had a signal-to-noise ratio of ≥ 3:1.

1.4.2.1.4 Standard solutions for stability studies

To check the stability of the analytes, BDP (0.31 mg) was dissolved in ethanol (0.5 mL) and deionized water (4.5 mL). The solution was divided into two parts. One aliquot was stored in the freezer and the other under laboratory conditions (~ 20 °C). For the next four days, these solutions were run in the HPLC, in duplicate, at various time intervals.

1.4.2.1.5 Standard solutions for Repeatability (Intra/ Same Day)

For the intra-day (same day) quality checks, working solutions of 2.5 ppm and 80 ppm were analysed by HPLC at regular time intervals during the day, in duplicate.

1.4.2.1.6 Standard solutions for Reproducibility (Inter/Different Day)

For inter-day (different days) quality checks, working solutions of 2.5 ppm and 80 ppm were analysed by HPLC for the next 4 days, at specific times, in duplicate.

1.4.3 Enzyme hydrolysis of Beclomethasone dipropionate (BDP) using porcine esterase

The qualitative and quantitative analysis of synthetic corticosteroids is a major challenge. BDP contains two ester groups in its molecule and is a good candidate for hydrolysis to the monoesters 17-BMP and 21-BMP by plasma esterases, and 17-BMP and 21-BMP might be further hydrolyzed by plasma esterases to BOH. So, enzyme hydrolysis of BDP was carried out to prepare 17-BMP as selectively as possible.

1.4.3.1 Instrumentation

The hydrolysis reaction was carried out in a stirred thermostatic bath and circulator (Model GD100-S5) fitted with Optima™ digital thermostat (GD100) for precise temperature control from 0-100° C.

Removal of the enzyme from reaction mixtures was performed on an MSE Microcentaur centrifuge at 13,000 rpm.

1.4.3.2 Reaction solution for enzyme hydrolysis of BDP using porcine esterase

BDP was hydrolysed enzymatically to prepare 17-BMP in *in vitro* conditions. BDP (0.31 mg) was dissolved in ethanol/water (1:4 v/v) and porcine liver esterase (2.0 mg) was added. The solution was incubated at 37 °C for 20 hrs in the dark. After incubation of BDP with esterase the enzyme was removed from the solution. The reaction mixture was placed into an Amicon cartridge (10,000 MWCO, Millipore, UK) which was placed into an ultra-centrifuge and spun at 13,000 rpm for 30 mins for the removal of the enzyme from the sample. The particles bigger than 10,000 MWCO are retained in the upper portion of the filter. The small molecules (including solvent) are collected in the lower portion. The liquid fraction containing the small molecules was diluted with deionised water to the desired concentration prior to analysis.

1.4.3.3 Enzyme hydrolysis protocol using porcine esterase

In the first timed experiment, several small aliquots equal to 0.5 mL were removed from the reaction mixture at t = 0 min, 30 min, 1 hr, 2 hr, 17.4 hr and 20 hr. The enzyme was removed from the solution as detailed in 1.4.3.2. Deionized water (0.5 mL) was added to each tube and the samples were analysed using LC-MS. The hydrolysis reaction was repeated and the method followed was the same as above except that the time for the collection of fractions was decreased from 20 hrs to 6 hrs. The main purpose was to obtain more data points in fewer hrs.

Sample Aliquots – 0 min, 30 min, 1 hr, 2 hr and 6 hr

Next the aliquots were collected for 2 hrs only:

Sample Aliquots – 0 min, 5, 10, 20, 30, 45, 60, 75, 90 and 120 min

Enzyme hydrolysis was carried out using ethanol instead of methanol for 2 hrs. All the sample aliquots were analysed using LC-MS in the same way as before; extracted ion chromatograms of *m/z* 465 were used for data analysis.

1.4.3.4 Enzyme hydrolysis of BDP (large scale) using porcine esterase

The results from the small scale experiments were very encouraging, so it was decided to try the reaction on a bigger (preparative) scale. For this purpose BDP (1.77 mg) was dissolved in ethanol (0.1 mL) to make a clear solution. Then, deionized water (9.9 mL) and esterase enzyme (1 mg) were added to make a 10 mL reaction solution. The reaction solution was incubated in a water bath at 37 °C in the dark for 20 hrs with subsequent analysis using LC-MS.

1.5 Nuclear Magnetic Resonance (NMR)

1.5.1 Instrumentation

All the hydrolysis reaction was carried out using either a Bruker Avance 500 AV500 500.13 MHz NMR spectrum with Ultra Shield^{TM} magnet, at room temperature with 11.7 Tesla superconducting magnet or on a Bruker DPx400 400.13 MHZ unshielded magnet. NMR samples were prepared in deuterium oxide (D_2O), d_6-DMSO, d_6-ethanol and d_3-CD_3CN. The computer software used was Topspin 1.3.

1.5.2 Reaction solution to prepare 17-BMP using NMR

Firstly, enzyme hydrolysis was performed to prepare 17-BMP in *in vitro* conditions, using BDP (10.0 mg), dissolved in ethanol/water (1:4 v/v). The drug was incubated with porcine liver esterase (2.0 mg, 0.182 mL, 35.6 mg protein/mL, 154 units/mg protein) at 37 °C for 2 hrs in the dark. An aliquot (0.5 mL) was removed from the reaction solution and the enzyme removed using an Amicon cartridge as before. The sample was then analysed using LC-MS to check that the reaction had proceeded to completion. The solution was then evaporated under N_2 (to reduce the volume) and the remaining volume of the solution was transferred to a 250 mL round bottom flask, frozen under liquid nitrogen and freeze dried overnight using a Modulyo Edward's Model RV 3 freeze dryer. The parameters used are tabulated below:

Temperature	-45^0 C
Pressure	10^{-3} Torr
Capacity of round-bottom flask	250 ml
Sample volume	3-4 ml

Table 4: Instrumental parameters used for freeze dryer

The dried product was dissolved in d_6-ethanol (650 µL) and its ^{1}H NMR spectrum was recorded using a Bruker Avance 500 MHz NMR spectrometer at room temperature with an 11.7 Tesla superconducting Ultra Shield^{TM} magnet. The computer software used for acquisition and processing was Topspin 1.3.

1.6 Liquid-Liquid Extraction (LLE) of BDP and its metabolites from the reaction solution

A liquid-liquid extraction (LLE) procedure was developed to recover both BDP and its metabolites from the reaction solution. BDP and its metabolites are polar molecules and are extractable from acidic, neutral and basic solutions. In preliminary experiments, ether-cyclohexane, DCM, ether and TBME were compared for extraction of BDP and its metabolites using 5 mL of reaction mixture. Sequential

extractions were carried out from the same water layer with the organic solvent (5 x 5 mL), using the four different solvents as described above.

1.6.1 Preparation of a reaction solution with porcine esterase enzyme and BDP [50:1]

The reaction solution was prepared and incubated with esterase enzyme as before for 2 hrs. The enzyme was removed from the reaction solution using an Amicon cartridge and the reaction solution was divided into two equal aliquots (2.5 mL + 2.5 mL).

1.6.2 Preparation of a reaction solution with porcine esterase enzyme and BDP [300:1]

In this method, a 300:1 ratio of BDP to enzyme was used. For this purpose, BDP (10 mg) and esterase enzyme (10 mg) were required in order to prepare and isolate a usable amount of product. Before trying this amount, it was decided to carry out a small trial run with the smallest concentration of BDP but using a lower ratio of esterase (300:1) in order to reduce the amount of enzyme used. BDP (0.31 mg) and esterase enzyme (0.31 mg) were dissolved in ethanol (0.5 mL) and deionized water (4.5 mL). Keeping the first steps the same as other methods, the reaction mixture was incubated for two hours. An aliquot (0.5 mL) was removed and analysed using LC-MS to check that the reaction had been successful. Cyclohexane (1 mL) and ether (4 mL) were added to the remaining reaction mixture of 4.5 mL. The organic layer was separated and set aside. To the same water layer, the same amounts of cyclohexane and ether mixture were added again. The organic layer was separated for the second time and set aside. The extraction was repeated for the third time and the fractions were combined and evaporated under nitrogen. MeCN (1 mL) was added to the sample which was then analysed using LC-MS in duplicate.

1.6.3 Liquid liquid extraction of BDP and its metabolites (single extraction)

A water-immiscible organic solvent was added to the reaction solution in a 10 mL conical flask. The addition was carried out in a fume cupboard. The mixture was swirled and then allowed to settle and the upper organic layer was separated by a

glass pipette and stored in a small labelled vial. Solvents used (in separate experiments) are listed below:

- Cyclohexane/ether (1:4)
- Ether
- Dichloromethane
- TBME

The organic layer was dried under nitrogen gas and acetonitrile (1 mL) was added prior to analysis using LC-MS, in duplicate. A further experiment was carried out to determine whether removal of the enzyme was necessary prior to LLE. After incubation for two hrs, the reaction mixture was divided into two parts. One aliquot was spun through a size-exclusion cartridge in order to remove enzyme and the other aliquot was extracted without further preparation. To both aliquots, a mixture of cyclohexane (0.5 mL) and ether (2.0 mL) was introduced, in separate 10 mL conical flasks. The addition was done in a fume cupboard. The mixture was swirled and then allowed to settle. It formed two layers, an upper organic layer and a lower aqueous layer. The upper organic layer was separated by a glass pipette for both portions. Both were stored in small labelled vials. The organic layers were evaporated under nitrogen, reconstituted with 1 mL of acetonitrile and analysed in duplicate using LC-MS.

1.6.4 Liquid liquid extraction of BDP and its metabolites (Multiple Extraction)

The hydrolysis reaction was carried out as before and the extracting solvent was added in a 10 mL conical flask. Extraction was repeated several times (n=5). The main aim was to extract all of the product from the solution. Solvents used (in separate experiments) are listed below:

- Cyclohexane/ether (1:4)
- Ether
- Dichloromethane
- TBME

After removal of the organic layer, the aqueous layer was extracted four more times and the organic layers were collected separately. The water layer was retained and

stored at -18 °C. All five organic fractions were evaporated separately under nitrogen then reconstituted in MeCN (1 mL) and the samples were analysed using LC-MS.

1.7 Results and Discussion

1.7.1 Method development for the analysis of BDP

Beclomethasone dipropionate is a potent pro-drug generating 17-BMP and is used in the treatment of chronic and acute respiratory disorders in humans. The therapeutic dose of BDP by inhalation results in very low plasma and urinary concentrations of BDP and its metabolites that pose a challenge to detection and confirmation by laboratories. To solve this problem, a method involving the use of LC-MS was developed for the detection, confirmation and quantification of the analytes. Different methods for identification of BDP were tried. The best method for elution of BDP compound was with 80 % MeCN with a low retention time and a sharp peak.

However, the research will be conducted on the metabolites of BDP, it is important to find a retention time with enough time lapse in between to be able to detect the metabolites which would elute before the parent drug due to their increased polarity. So, for this purpose method with 60 % MeCN as depicted in Table 5 below, was selected.

Conc. [mg/L]	Mobile Phase		RT/Min	Peak area [AU]
	A % [HPLC H_2O]	B % [MeCN]		
0.1	40	60	8.948	2038
0.5	40	60	8.937	13845
1	40	60	8.985	28101
10	40	60	8.933	272393
100	40	60	9.263	3325540

Table 5: Retention times and peak areas for BDP with the selected method

1.7.2 Method optimization and validation

Method validation was, according to the guidelines given by ICH, performed by evaluating the calibration and linearity, LOD, stability, reproducibility and repeatability of the method.

1.7.2.1 Calibration and Linearity

Calibration is the process of determining the relationship between response and known concentrations of an analyte under set conditions. The average of two values for 0.1, 1, 5, 10, 25, 50 and 100 ppm were used to plot the calibration curves as the samples were run in duplicate for each concentration. The calibration curve exhibited good linearity, as determined by linear regression analysis, with average correlation coefficients 0.9976 for UV data and 0.8847 for MS data.

1.7.2.2 Calibration graphs for BDP

A typical chromatogram for a BDP standard is shown in Fig. 8, below. The analysis time was less than 20 min with BDP eluted at 9.29 min.

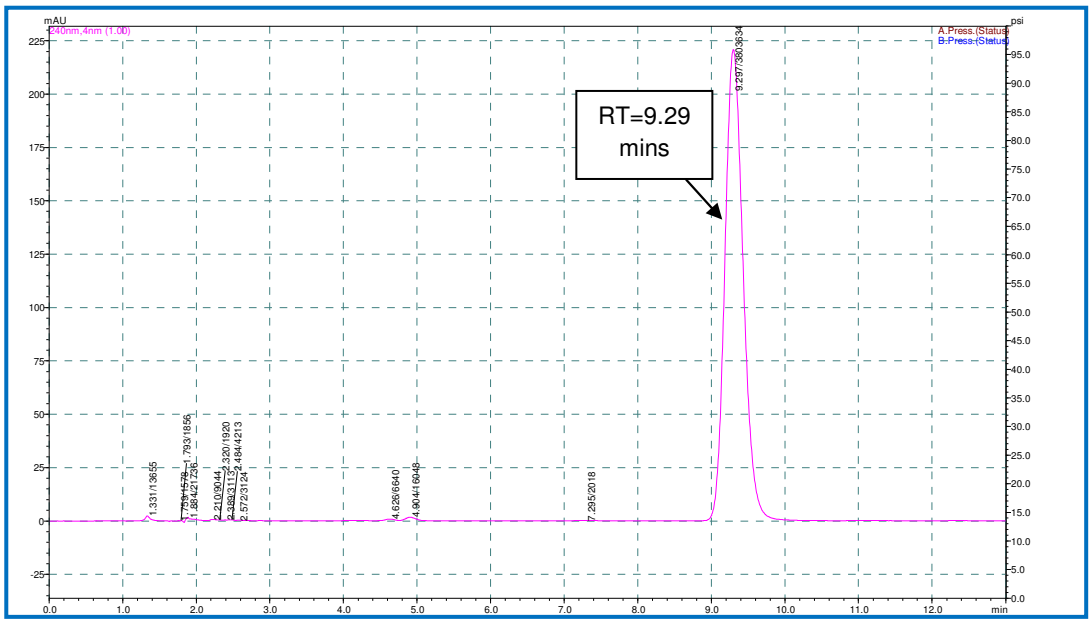

Figure 8: Chromatogram of a BDP standard (100 ppm) obtained at 240 nm (n=3)

A nine-point calibration graph was constructed. A straight line was fitted to the data using linear regression. A representative plot describing the calibration data for BDP (UV detection) is shown in Fig. 9, with the data tabulated in Table 6 and for BDP (MS detection) in Table 6 and Fig. 10.

BDP Calibration [LC]		
Conc. [mg/L]	**Average Peak Area [AU]**	**Standard Deviation [S.D]**
0.01	926.35	88.6
0.1	3079.6	878.22
1	31368.2	473.19
2.5	92174.45	1279.65
5	186434.2	1012.43
10	337386.95	2973.87
25	848969.15	11613.59
50	2076176.5	41401.38
100	3867942.4	90946

Table 6: A typical set of calibration data for BDP with UV detection

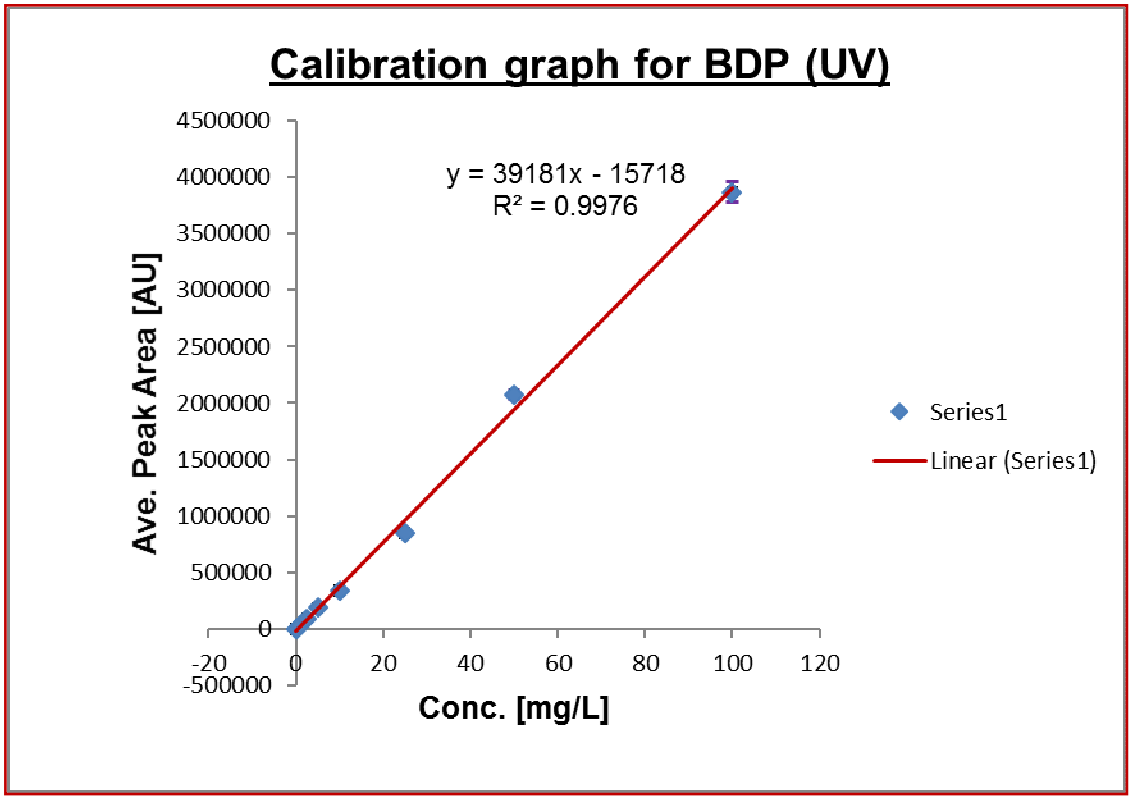

Figure 9: Calibration graph for BDP (UV) (n=9)

A sample representative for BDP (MS) is shown in table 7 and Fig. 10. A straight line was fitted to the data using linear regression over the studied range of concentrations is shown by the equation y = 8981.4x+106102. It is clear from the calibration graph that the linearity was poor since the R^2 value is 0.8847.

BDP Calibration [MS]		
Conc. [mg/L]	**Average Peak Area [AU]**	**Standard Deviation [S.D]**
0.01	578.16	203.73
0.1	7029.34	317.28
1	56617	3719.38
2.5	116701	7710.29
5	177318	3517.15
10	257107	10834.29
25	478052	59389.89
50	723735.5	4171.22
100	876658.5	11202.69

Table 7: Typical calibration data for BDP with MS detection

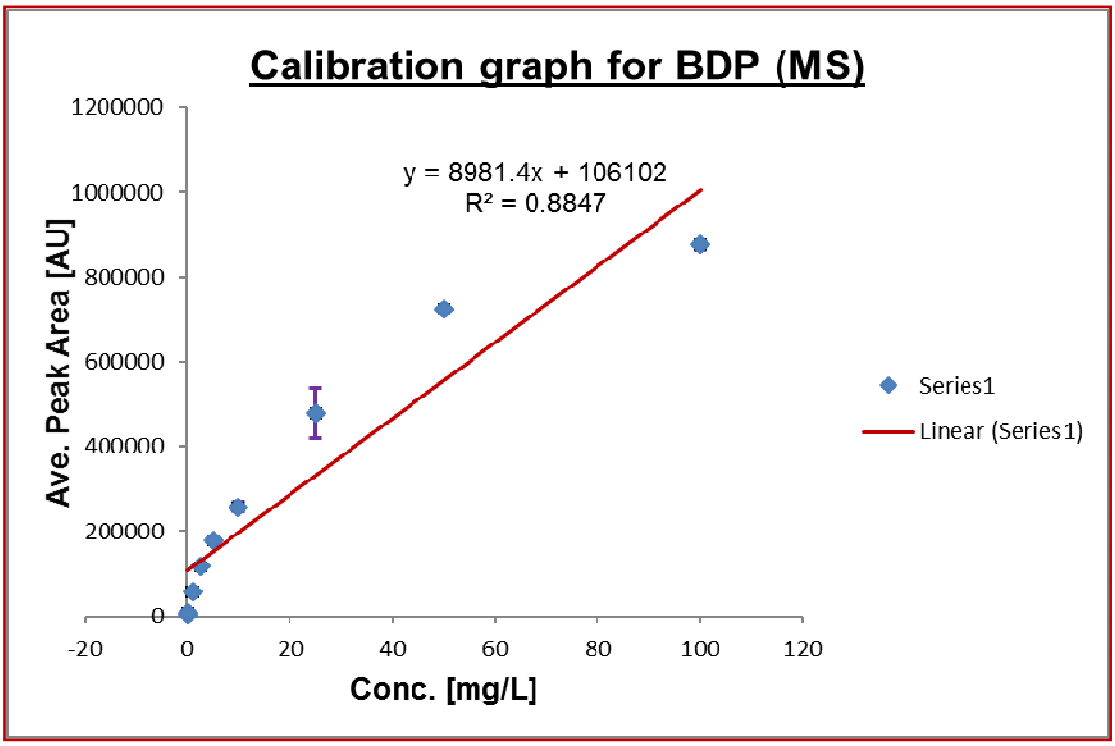

Figure 10: Calibration graph for BDP-MS at known concentration and peak areas (n=9)

1.7.2.3 Calibration graphs for BOH

The graphs were plotted by taking the average of two peak area values for 0.01, 0.1, 1, 2.5, 5 and 10 ppm standards, as the samples were run twice for each concentration. Each calibration curve exhibited good linearity, as determined by linear regression analysis, with correlation coefficients 0.9995 for LC data and 0.9985 for MS data. Table 8 and Fig. 11 represent the calibration data and graph for BOH, below.

BOH Calibration [LC]		
Conc. [mg/L]	**Average Peak Area [AU]**	**Standard Deviation [S.D]**
0.01	170.7	62.08
0.1	2666.4	56
1	36280.3	66.39
2.5	105125.75	593.05
5	213749.3	2834.5
10	413868.3	4011.84

Table 8: Typical calibration data for BOH-UV

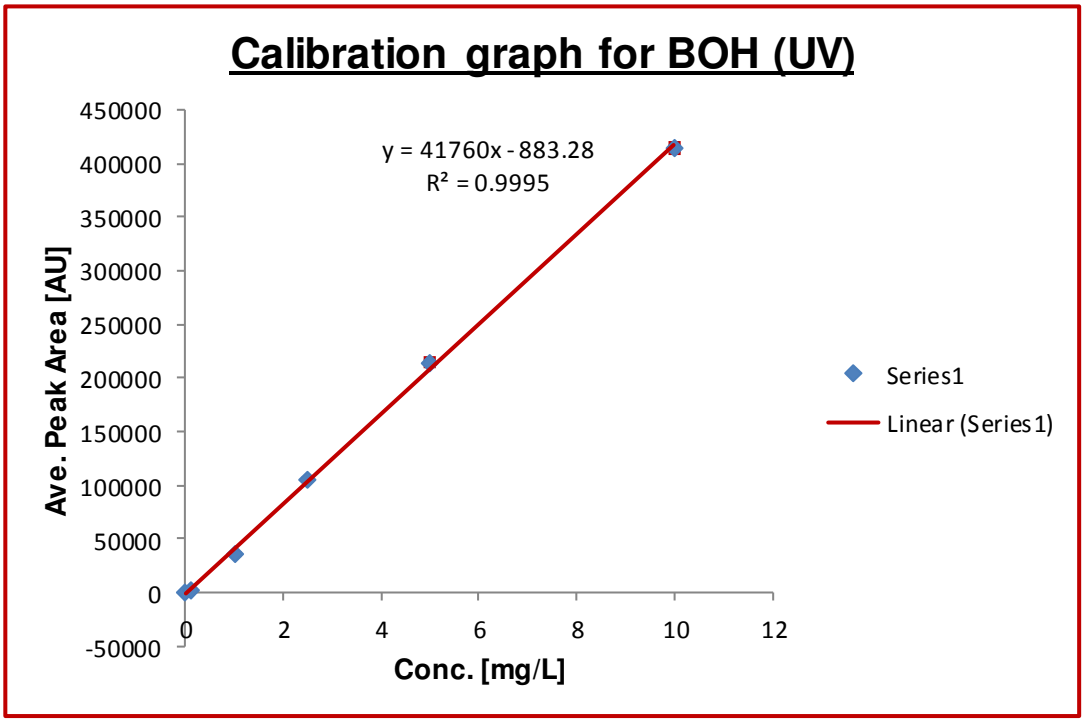

Figure 11: Calibration graph for BOH-UV with known concentration and peak areas (n=2)

The above graph showed excellent linearity with R^2 value 0.9995. Fig. 12 shows a typical chromatogram for BOH at 100 ppm.

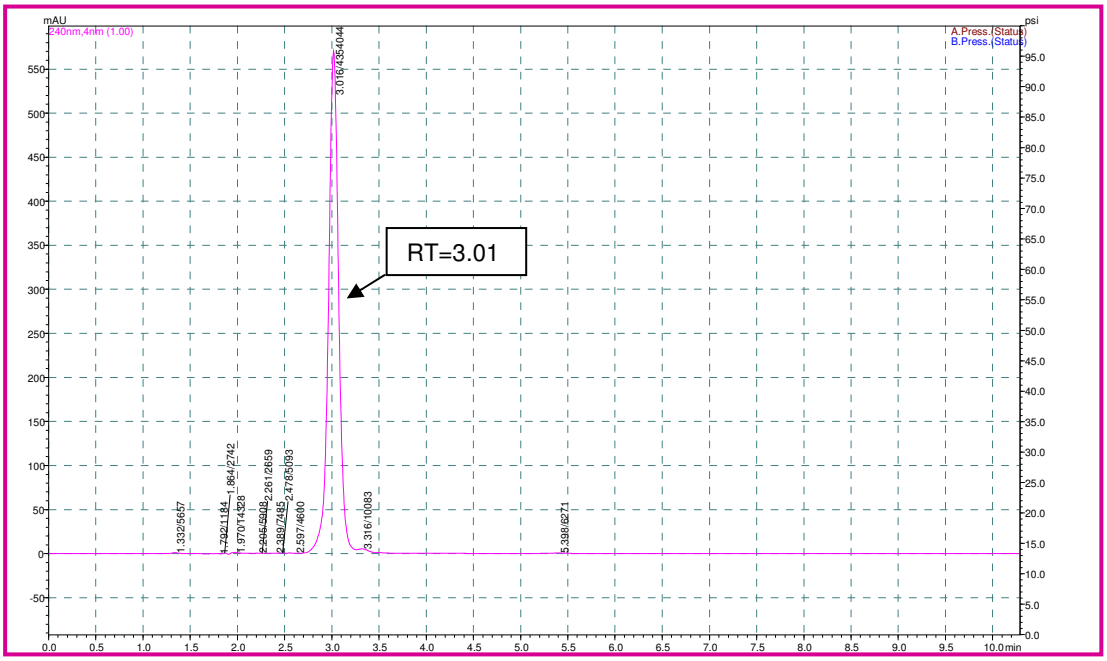

Figure 12: Typical chromatogram for analysis of BOH (n=2)

BOH Calibration [MS]		
Conc. [mg/L]	**Average Peak Area [AU]**	**Standard Deviation [S.D]**
0.01	767.59	271.67
0.1	1374.26	520.12
1	3222.29	613.25
2.5	8241.65	453.64
5	13631.5	1952.32
10	22168.5	891.66

Table 9: A typical set of calibration data for BOH (MS)

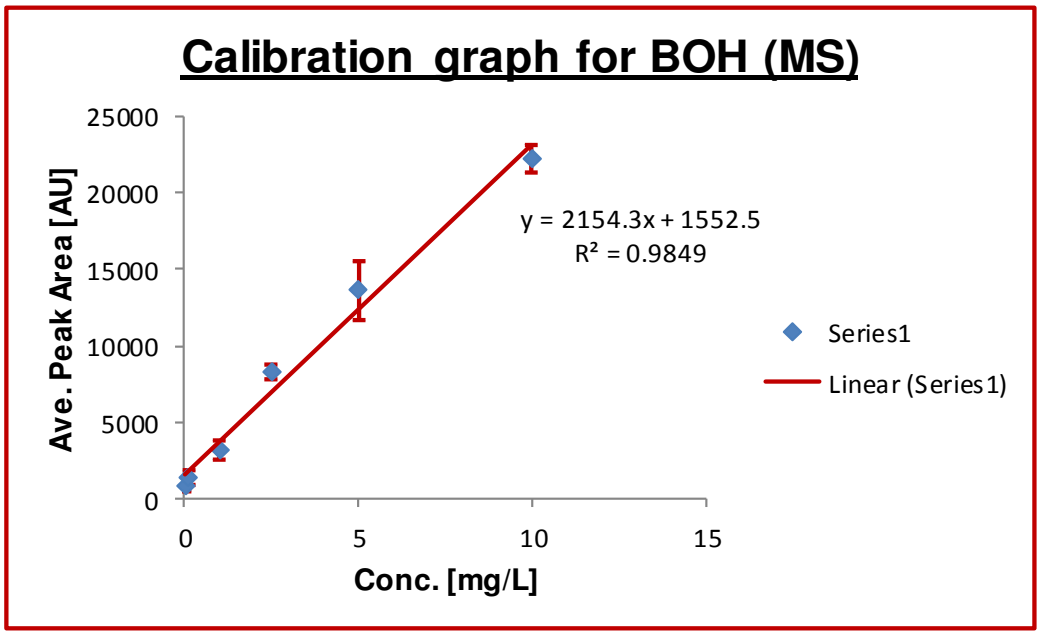

Figure 13: Calibration graph for BOH-MS

The above MS graph for BOH showed good linearity with a R^2 value of 0.9849 (n=2)

1.7.2.4 Calibration graphs for mixture run of BOH and BDP

Calibration graphs were plotted by taking the average of two values for 0.01, 0.1, 0.25, 0.5, 0.75 and 1 ppm standards. A sample of the calibration data for a mixed run of BOH and BDP is shown in Table 10 and Fig. 14 and 15. Fig. 16 shows a typical chromatogram.

BOH Calibration [LC]			BDP Calibration [LC]	
Conc. [mg/L]	**Ave. Peak Area [AU]**	**Standard Deviation [S.D]**	**Ave. Peak Area [AU]**	**Standard Deviation [S.D]**
0.01	4582.1	957.28	3571.4	476.87
0.1	40619.65	3860.31	32199.75	248.55
0.25	8620.3	72.12	8106.75	31.61
0.5	19622.35	253.21	16335.5	146.37
0.75	30945.3	388.2	26839.1	322.16
1	40270.35	123.96	34089.1	155.28

Table 10: Typical calibration data for a mixed run of BDP and BOH

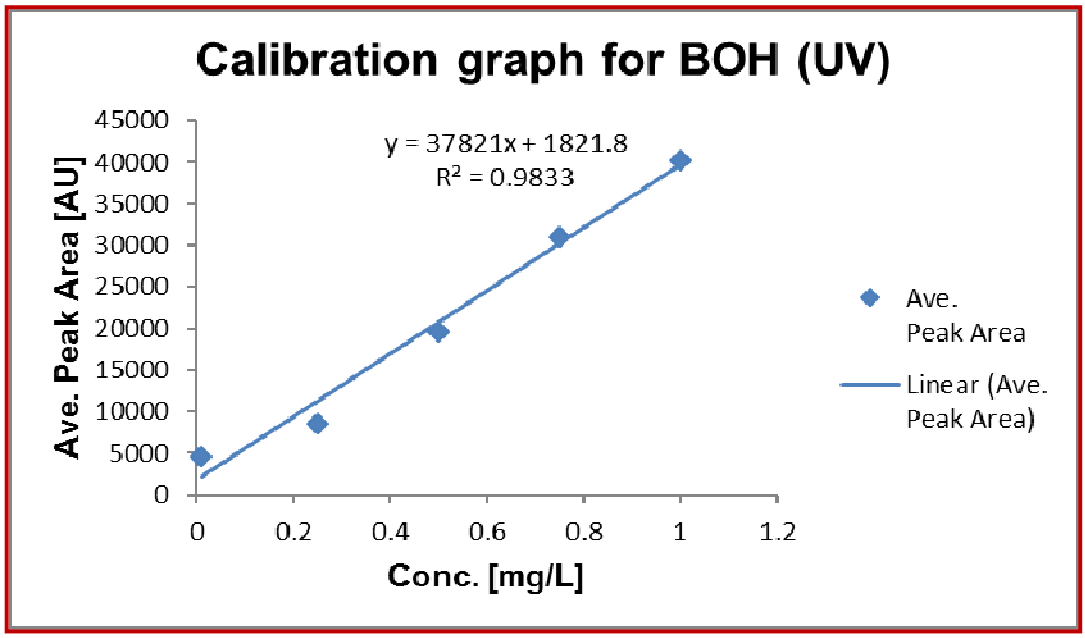

Figure 14: Calibration graph for mixture run for BOH-UV (n=2)

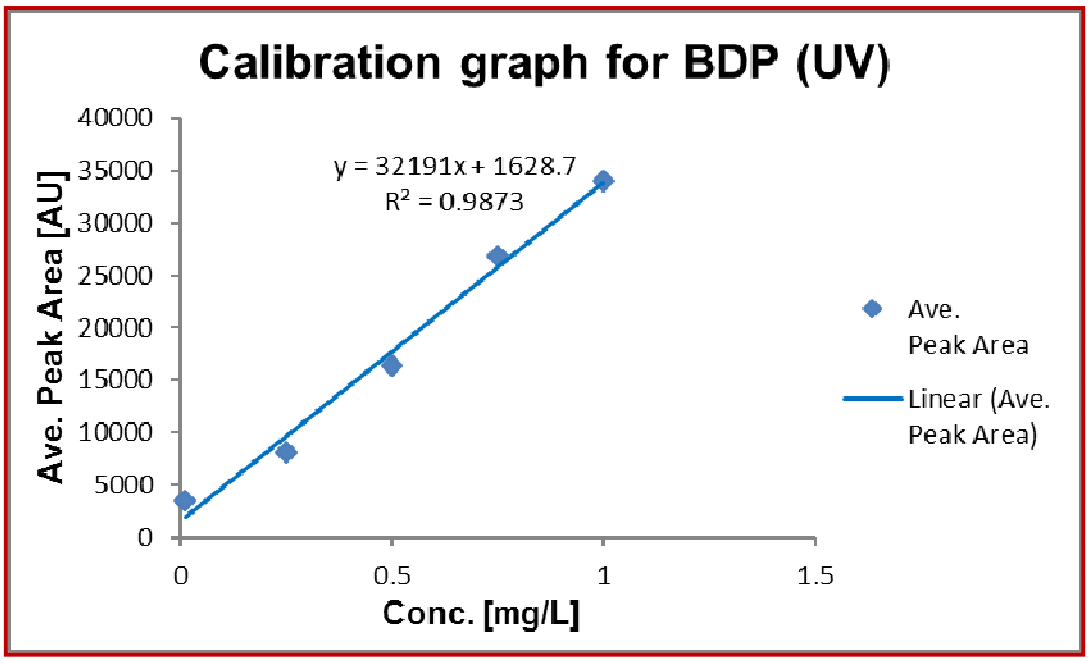

Figure 15: Calibration graph for a mixture run for BDP-UV (n=2)

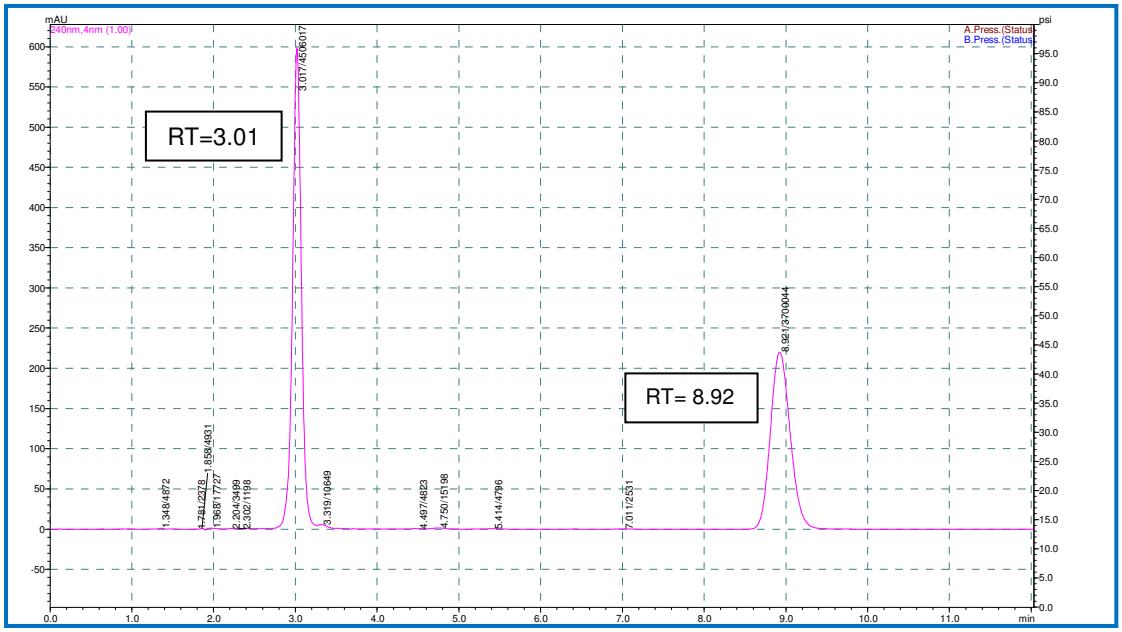

Figure 16: A typical chromatogram showing the mixed run of BDP and BOH at 100 ppm concentration (n=2)

Each calibration curve, as determined by linear regression analysis, exhibited linearity for LC data with correlation coefficients of 0.9833 for BOH and 0.9873 for BDP. For MS data correlation coefficients for BOH and BDP were 0.9233 and 0.9899. A curve was observed in the graphs for BOH and BDP, possibly because BDP and BOH existed as multiple adducts with different masses. EICs were used to plot graphs for BOH (Table 11, Fig. 17) and for BDP (Table 15, Fig. 19) below.

BOH Calibration [MS(409+431)]		
Conc. [mg/L]	**Average Peak Area [AU]**	**Standard Deviation [S.D]**
0.01	737.61	189.19
0.1	4038.13	715.68
0.25	1955.27	300.87
0.5	2550.56	859.27
0.75	2722.49	145.48
1	4460.86	378.97

Table 11: A sample calibration data for BOH with m/z 409+431

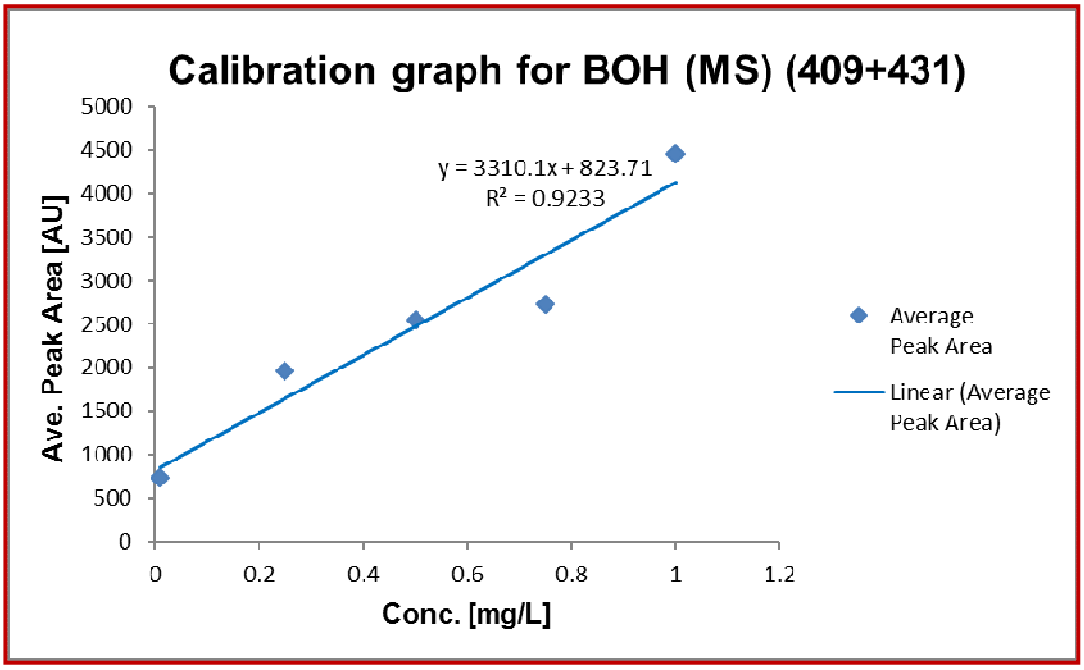

Figure 17: Calibration graph for BOH (MS) (409+431) (n=2)

The above graphs showed that by plotting graphs with two adducts with different masses (409 and 431), R^2 was improved. So, it was decided to perform calibration by considering six possible adducts with different masses, summarized in Tables 12 and 13 for BOH. Again, EICs were used to plot graphs for BOH (Table 14, Fig. 18) below.

Masses	Mol. Wt. BOH (408)
$[M+H]^+$	409
$[M+Na]^+$	431
$[2M+H]^+$	817
$[2M+Na]^+$	839
$[3M+H]^+$	1225
$[3M+Na]^+$	1247

Table 12: Adducts of BOH used to plot revised calibration curves

.

		BOH-409		BOH-431		BOH-817		BOH-839		BOH-1225		BOH-1247	
Conc.	Injection	Reten. Time	Peak Area	Reten. Time	Peak Area	Reten. Time	Peak Area	Reten. Time	Peak Area	Reten. Time	Peak Area	Reten. Time	Peak Area
0.01	**1**	3.6	807.2	3.5	869.26	3.6	497.14	3.6	756.85	3.5	253.92	3.6	238.13
	2	3.7	400.46	3.6	873.52	3.4	262.54	3.6	789.71	3.8	225.5	3.6	268.31
	Ave	**3.65**	**603.83**	**3.55**	**871.39**	**3.5**	**379.84**	**3.6**	**773.28**	**3.65**	**239.71**	**3.6**	**253.22**
	S.D	**0.07**	**287.61**	**0.07**	**3.01**	**0.14**	**165.89**	**0**	**23.24**	**0.21**	**20.10**	**0**	**21.34**
	Preci	**1.94**	**47.63**	**1.99**	**0.35**	**4.04**	**43.67**	**0**	**3.00**	**5.81**	**8.38**	**0**	**8.43**
0.1	**1**	3.6	3207.59	3.6	4746.05	3.6	349.39	3.6	441.82	3.7	219.56	3.6	113.81
	2	3.6	3856.53	3.7	4342.32	3.6	150.19	3.7	682.42	3.6	268.03	3.8	139.76
	Ave	**3.60**	**3532.06**	**3.65**	**4544.19**	**3.6**	**249.79**	**3.65**	**562.12**	**3.65**	**243.80**	**3.7**	**126.79**
	S.D	**0.00**	**458.87**	**0.07**	**285.48**	**0**	**140.86**	**0.07**	**170.13**	**0.07**	**34.27**	**0.14**	**18.35**
	Preci	**0.00**	**12.99**	**1.94**	**6.28**	**0**	**56.39**	**1.94**	**30.27**	**1.94**	**14.06**	**3.82**	**14.47**
0.25	**1**	3.5	2779.8	3.7	2090.34	3.7	210.46	3.3	175.74	3.6	180.08	3.6	142.75
	2	3.6	1556.23	3.7	1394.7	3.8	372.59	3.5	375.36	3.5	133.37	3.6	129.58
	Ave	**3.55**	**2168.02**	**3.70**	**1742.52**	**3.75**	**291.53**	**3.4**	**275.55**	**3.55**	**156.73**	**3.6**	**136.17**
	S.D	**0.07**	**865.19**	**0.00**	**491.89**	**0.07**	**114.64**	**0.14**	**141.15**	**0.07**	**33.03**	**0**	**9.31**
	Preci	**1.99**	**39.91**	**0.00**	**28.23**	**1.89**	**39.33**	**4.16**	**51.23**	**1.99**	**21.07**	**0**	**6.84**
0.5	**1**	3.6	3960.46	3.6	2436.79	3.6	398.42	3.7	892.71	3.6	86.75	3.7	322.63
	2	3.7	2355.83	3.7	1449.13	3.5	185.87	3.7	780.9	3.6	267.04	3.9	316.96
	Ave	**3.65**	**3158.15**	**3.65**	**1942.96**	**3.55**	**292.15**	**3.7**	**836.81**	**3.6**	**176.90**	**3.8**	**319.80**
	S.D	**0.07**	**1134.64**	**0.07**	**698.38**	**0.07**	**150.30**	**0**	**79.06**	**0**	**127.48**	**0.14**	**4.01**
	Preci	**1.94**	**35.93**	**1.94**	**35.94**	**1.99**	**51.45**	**0**	**9.45**	**0**	**72.07**	**3.72**	**1.25**
0.75	**1**	3.6	3095.54	3.6	2446.06	3.6	1315.53	3.6	200.39	3.7	215.82	3.6	418.44
	2	3.6	2555.17	3.6	2793.18	3.5	1563.41	3.6	695.09	3.6	78.291	3.7	746.63
	Ave	**3.60**	**2825.36**	**3.60**	**2619.62**	**3.55**	**1439.47**	**3.6**	**447.74**	**3.65**	**147.06**	**3.65**	**582.54**
	S.D	**0.00**	**382.10**	**0.00**	**245.45**	**0.07**	**175.28**	**0**	**349.81**	**0.07**	**97.25**	**0.07**	**232.07**
	Preci	**0.00**	**13.52**	**0.00**	**9.37**	**1.99**	**12.18**	**0**	**78.13**	**1.94**	**66.13**	**1.94**	**39.84**
1	**1**	3.6	3958.13	3.6	4559.99	3.8	268.25	3.6	472.93	3.6	268.55	3.5	175.21
	2	3.5	4427.65	3.6	4897.66	3.8	716.47	3.6	550.39	3.6	277.64	3.6	159.92
	Ave	**3.55**	**4192.89**	**3.60**	**4728.83**	**3.8**	**492.36**	**3.6**	**511.66**	**3.6**	**273.10**	**3.55**	**167.57**
	S.D	**0.07**	**332.00**	**0.00**	**238.77**	**0**	**316.94**	**0**	**54.77**	**0**	**6.43**	**0.07**	**10.81**
	Preci	**1.99**	**7.92**	**0.00**	**5.05**	**0**	**64.37**	**0**	**10.70**	**0**	**2.35**	**1.99**	**6.45**

Table 13: m/z Data for BOH

Conc. [mg/L]	Ave. Peak Area [AU]	Standard Deviation [S.D]
0.01	520.212	269.83
0.25	795.09	910.8
0.5	1121.13	1193.87
0.75	1343.63	1152.95
1	1727.74	2127.85

Table 14: A typical set of calibration data for BOH (MS) (overall)

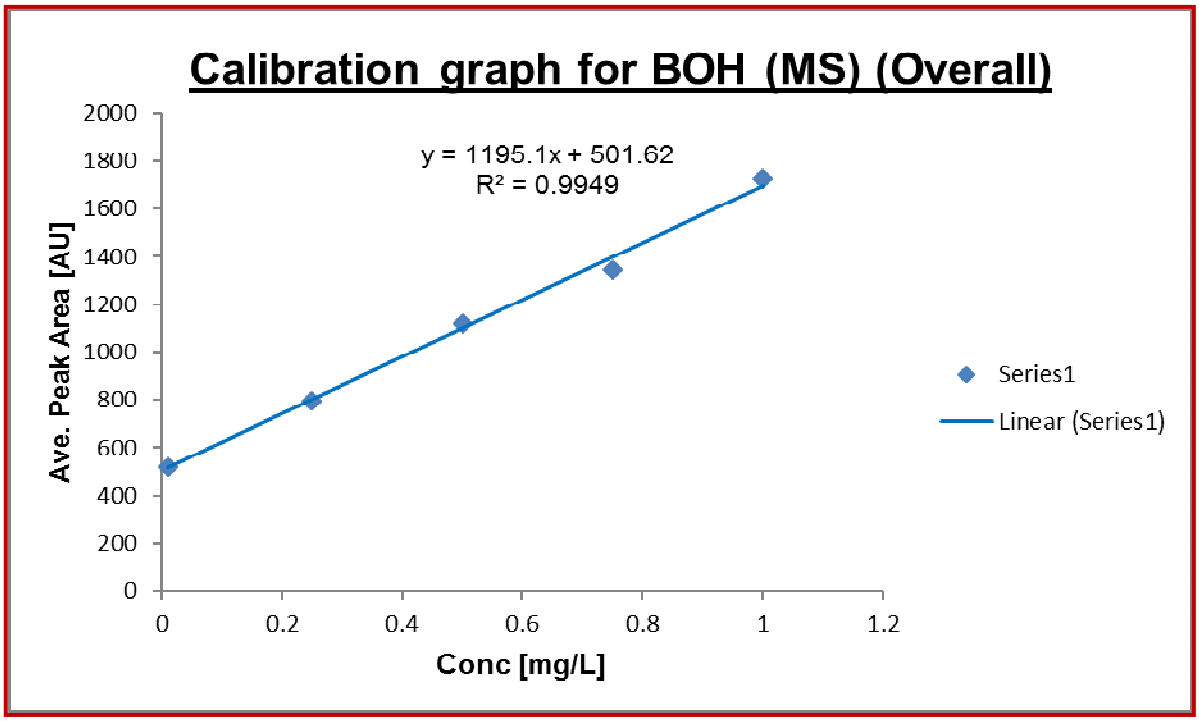

Figure 18: Calibration graph for BOH-MS (overall) (n=2)

After plotting peak areas for all adducts with different masses, an excellent linearity was achieved *i.e.* R^2 = 0.9949 which confirms that BOH existed as multiple adducts with different masses, especially at higher concentrations.

For BDP graphs were plotted with two adducts (+Na) (521+543) (Table 15 and Fig. 19) and then with all the possible adducts with different masses, summarized in Tables 16 and 17. Again, EICs were used to plot the graph for BDP (Table 18, Fig. 20). In the calibration graphs it was observed that the intercepts were not at zero. It is possibly due to the response of the mobile phase from both LC as well as the mass spectrometer.

BDP Calibration [MS(521+543)]		
Conc. [mg/L]	**Average Peak Area [AU]**	**Standard Deviation [S.D]**
0.01	3141.38	4023.85
0.1	21024.35	12121.44
0.25	6444.49	4882.3
0.5	11649.68	8185.92
0.75	18010.5	12537.71
1	21482.05	14830.08

Table 15: Sample calibration data for BDP with m/z 521+543

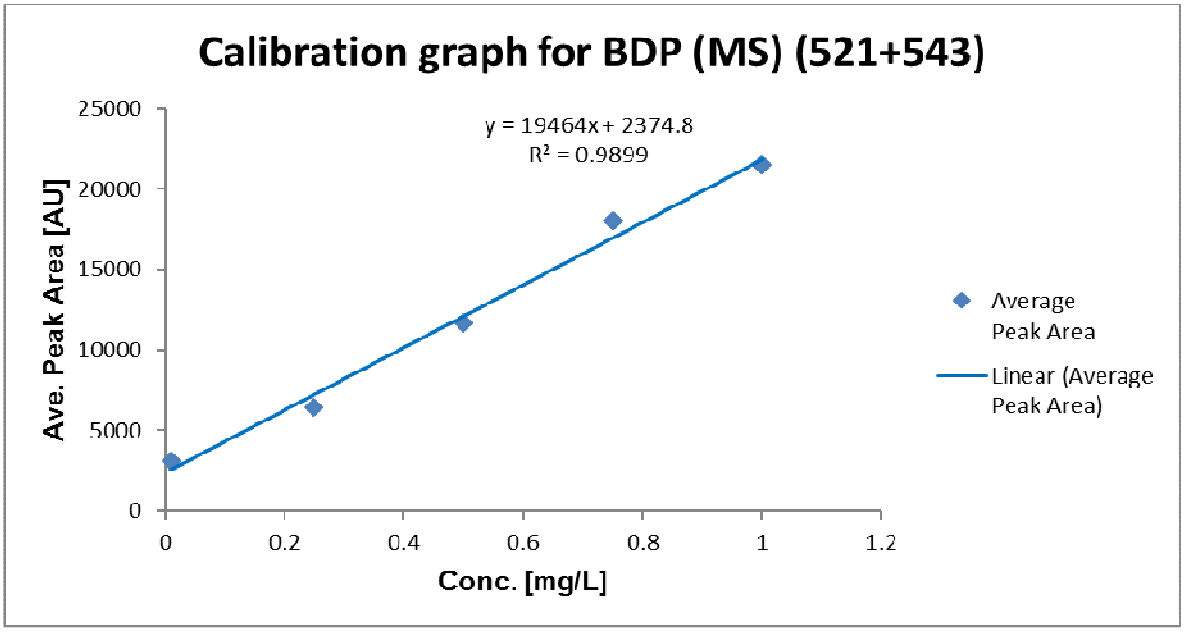

Figure 19: Calibration graph for BDP (MS) (m/z 521+543) (n=2)

Masses	Mol Wt. BDP
	520
$[M+H]^+$	521
$[M+Na]^+$	543
$[2M+H]^+$	1041
$[2M+Na]^+$	1063
$[3M+H]^+$	1561
$[3M+Na]^+$	1583

Table 16: Adducts of BDP used to plot calibration curves

		BDP-521		BDP-543		BDP-1041		BDP-1063		BDP-1561		BDP-1583	
Conc.	Inject.	Reten. Time	Peak Area	Reten. Time	Peak Area	Reten. Time	Peak Area	Reten. Time	Peak Area	Reten. Time	Peak Area	Reten. Time	Peak Area
0.01	1	9.3	316.51	9.5	5283.97	9.5	218.25	9.5	251.67	9.4	794.66	9.4	157.37
	2	9.3	275.66	9.5	6689.36	9.3	340.57	9.5	121.26	6.5	678.6	9.4	128.57
	Ave	**9.30**	**296.09**	**9.50**	**5986.67**	**9.4**	**279.41**	**9.5**	**186.47**	**7.95**	**736.63**	**9.4**	**142.97**
	S.D	**0.00**	**20.42**	**0.00**	**702.70**	**0.14**	**86.49**	**0**	**92.21**	**2.05**	**82.07**	**0**	**20.36**
	Preci	**0.00**	**6.90**	**0.00**	**11.74**	**1.50**	**30.96**	**0**	**49.45**	**25.79**	**11.14**	**0**	**14.24**
0.1	1	9.5	13307.9	9.5	32708	9.5	390.37	9.5	1234.64	9.5	337.88	9.5	105.52
	2	9.5	11598.5	9.5	26483	9.4	282.1	9.5	1231.5	9.5	436.35	9.5	151.41
	Ave	**9.50**	**12453.2**	**9.50**	**29595.5**	**9.45**	**336.24**	**9.5**	**1233.07**	**9.5**	**387.12**	**9.5**	**128.47**
	S.D	**0.00**	**854.70**	**0.00**	**3112.50**	**0.07**	**76.56**	**0**	**2.22**	**0**	**69.63**	**0**	**32.45**
	Preci	**0.00**	**6.86**	**0.00**	**10.52**	**0.75**	**22.77**	**0**	**0.18**	**0**	**17.99**	**0**	**25.26**
0.25	1	9.5	2137.17	9.5	9796.9	9.7	303.45	9.6	150.66	9.5	186.2	9.8	337.34
	2	9.5	3847.18	9.4	9996.7	9.6	304.57	9.6	252.69	9.4	130.27	9.3	348.23
	Ave	**9.50**	**2992.18**	**9.45**	**9896.8**	**9.65**	**304.01**	**9.6**	**201.68**	**9.45**	**158.24**	**9.55**	**342.79**
	S.D	**0.00**	**855.00**	**0.07**	**99.90**	**0.07**	**0.79**	**0**	**72.15**	**0.07**	**39.55**	**0.35**	**7.70**
	Preci	**0.00**	**28.57**	**0.75**	**1.01**	**0.73**	**0.26**	**0**	**35.77**	**0.75**	**24.99**	**3.70**	**2.25**
0.5	1	9.5	8074.9	9.5	19199	9.6	110.44	9.5	591.84	9.5	109.41	9.6	163.71
	2	9.4	3647.81	9.5	15677	9.3	468.04	9.5	274.38	9.4	195.45	9.3	415.16
	Ave	**9.45**	**5861.36**	**9.50**	**17438**	**9.45**	**289.24**	**9.5**	**433.11**	**9.45**	**152.43**	**9.45**	**289.44**
	S.D	**0.07**	**2213.55**	**0.00**	**1761.00**	**0.21**	**252.86**	**0**	**224.48**	**0.07**	**60.84**	**0.21**	**177.80**
	Preci	**0.75**	**37.77**	**0.00**	**10.10**	**2.24**	**87.42**	**0**	**51.83**	**0.75**	**39.91**	**2.24**	**61.43**
0.75	1	9.4	8391.7	9.4	26071	9.4	359.11	9.5	230.97	9.7	186.57	9.5	299.63
	2	9.5	9898.3	9.4	27681	9.5	254.67	9.5	213.043	9.5	189.13	9.6	73.65
	Ave	**9.45**	**9145**	**9.40**	**26876**	**9.45**	**306.89**	**9.5**	**222.01**	**9.6**	**187.85**	**9.55**	**186.64**
	S.D	**0.07**	**753.30**	**0.00**	**805.00**	**0.07**	**73.85**	**0**	**12.68**	**0.14**	**1.81**	**0.07**	**159.79**
	Preci	**0.75**	**8.24**	**0.00**	**3.00**	**0.75**	**24.06**	**0**	**5.71**	**1.47**	**0.96**	**0.74**	**85.62**
1	1	9.5	10938	9.4	30613	9.5	246.44	9.5	744.18	9.6	113.07	9.5	81.99
	2	9.5	11053.1	9.4	33324	9.5	249.32	9.4	503.52	9.4	335.34	9.4	201.15
	Ave	**9.50**	**10995.6**	**9.40**	**31968.5**	**9.5**	**247.88**	**9.45**	**623.85**	**9.5**	**224.21**	**9.45**	**141.57**
	S.D	**0.00**	**57.55**	**0.00**	**1355.50**	**0**	**2.04**	**0.07**	**170.17**	**0.14**	**157.17**	**0.07**	**84.26**
	Preci	**0.00**	**0.52**	**0.00**	**4.24**	**0**	**0.82**	**0.75**	**27.28**	**1.49**	**70.10**	**0.75**	**59.52**

Table 17: m/z Data for BDP

Conc. [mg/L]	Ave. Peak Area [AU]	Standard Deviation [S.D]
0.01	1271.37	2319.72
0.25	2315.95	3872.82
0.5	4077.26	6914.81
0.75	6154.07	10760.83
1	7366.94	12788.89

Table 18: A typical set of calibration data of BDP (MS) (overall)

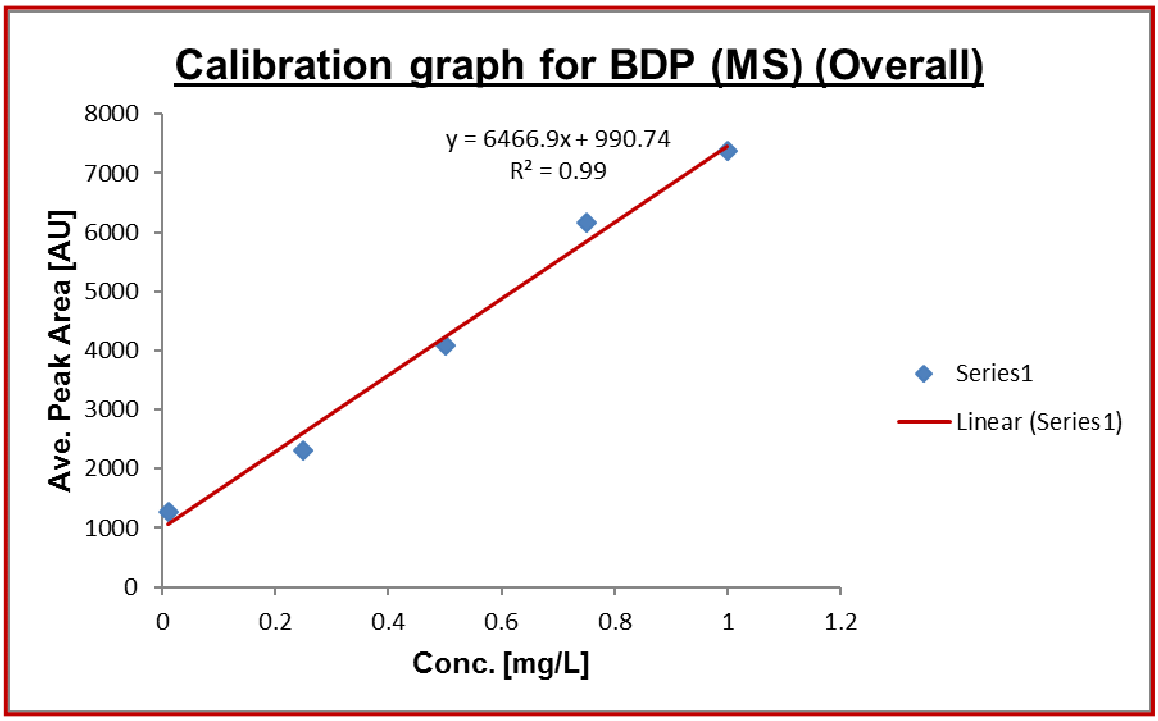

Figure 20: Calibration graph for BDP (MS) (overall) (n=2)

As before, the linearity was greatly improved by taking multiple adducts into account.

1.7.2.5 Limit Of Detection (LOD) of BDP and BOH

For determination of the LOD, a previously prepared stock solution of the two analytes was used. The solution was serially diluted each time *i.e.* 100 to 0.001 ppm. The limit of detection (LOD) was found to be 0.01 ppm both for BDP (Fig. 21) and BOH (Fig. 22).

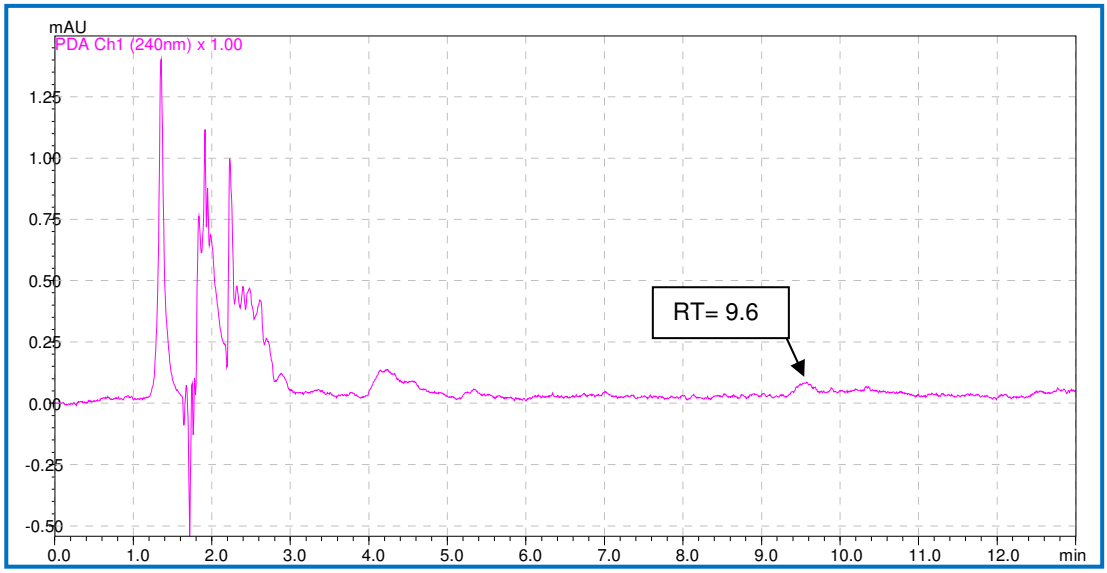

Figure 21: Chromatogram shows LOD for BDP at 0.01 ppm (n=2)

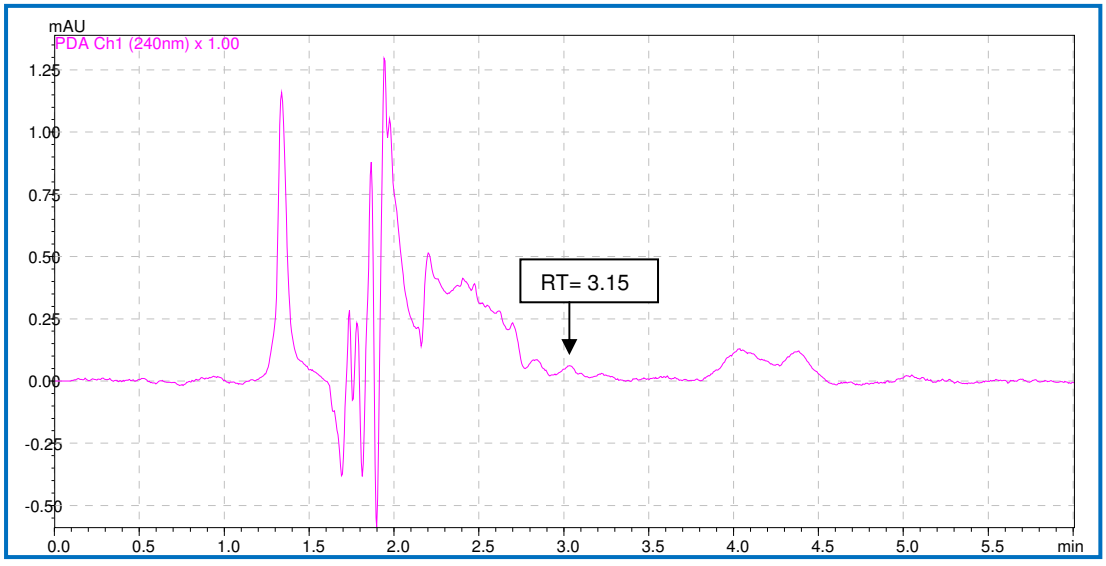

Figure 22: Chromatogram shows LOD for BOH at 0.01 ppm (n=2)

1.7.2.6 Stability - BDP

Two standard solutions of 2.5 and 80 ppm were analysed using HPLC with the same method used to identify the peak. Stability was expressed as the ratio of measured concentration against days. The results showed that both analytes were quite stable under normal room temperature.

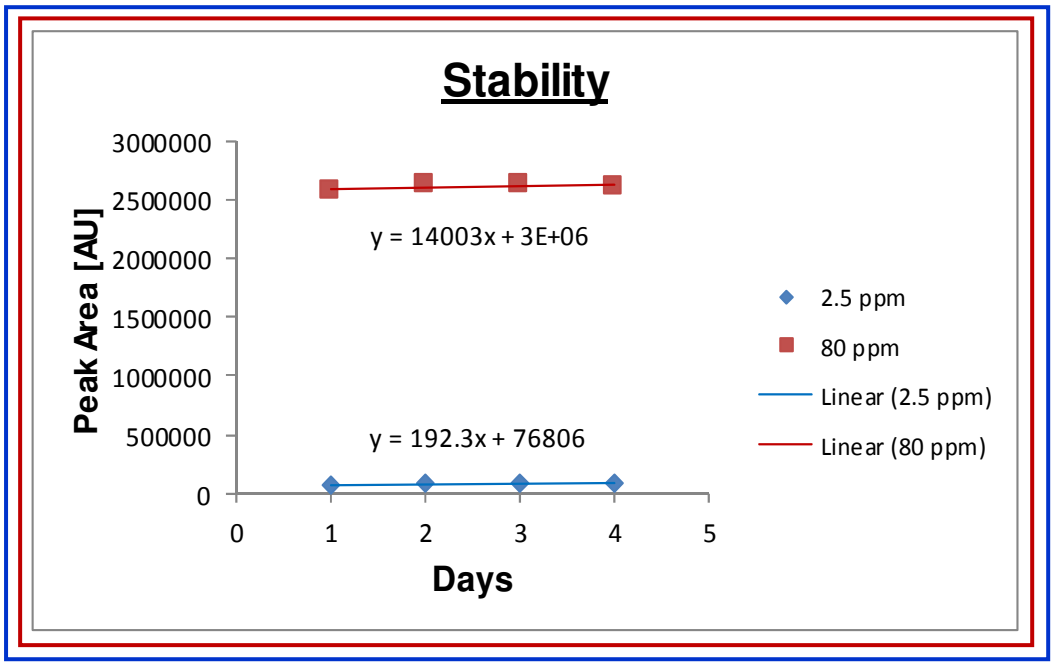

Figure 23: Stability graph for BDP at two different concentrations (2.5 and 80 ppm) (n=4)

Both analytes were found to be stable in solution at both concentrations over 4 days as shown in Fig. 23.

1.7.2.7 Repeatability - BDP

The precision of the work was determined by injecting two concentrations of BDP (low 2.5 ppm and high 80 ppm) which were analysed using HPLC four times at regular time intervals over the course of the day to determine the intra-day variation. The intra-day variations, expressed as the coefficient of variation in peak area ratios, were calculated by dividing the standard deviation of the calculated concentrations by the mean concentration and multiplying by 100.

For intra-day (same day) quality check, the working solutions of 2.5 ppm and 80 ppm were analysed at regular time intervals; Table 18 shows peak areas and RSD % values over the course of the day. The resulting RSD percentages were less than

1%. The intra-day variability, determined for the two standard concentrations of BDP on four occasions, is shown in Table 19, below.

Time ⟶ Conc.[mg/L] ↓	11:00 AM	1300 pm	15 pm	17 pm	Mean	STDEV	RSD %
2.5	77746	77573	77428	77376	77530.75	165.95	0.21
80	2829645	2836445	2855501	2855568	2844290	13277.8	0.46

Table 19: Intra-day repeatability-peak areas for BDP (n=4)

1.7.2.8 Reproducibility - BDP

Any analytical method must give reliable data. Reproducibility of the repeated identical measurements (replicates) for the 2.5 ppm and 80 ppm solutions was calculated on four different days, in order to find out any differences between the repeats. The present method has very good reproducibility. The inter-day variability determined at the same two concentrations and repeated on four different days is illustrated in Table 20 showing the average peak areas for BDP along with S.D and RSD%.

Days ⟶ Conc. [mg/L] ↓	1	2	3	4	Mean	STDEV	RSD %
2.5	76806	77426	77489	77426	77286.8	321.87	0.41
80	2565999	2637022	2636011	2613011	2613011	33244.8	1.27

Table 20: Inter-day reproducibility-peak areas for BDP (n=4)

1.7.3 Enzyme hydrolysis and Size exclusion chromatography

BDP is a widely used inhaled corticosteroid for the inhalation therapy of asthma in both adults and children. Owing to the presence of the dipropionate ester functional group in its side chain, it is easily hydrolysed *via* esterases in the human lung, liver and other parts of the body to the more polar products 17-BMP, 21-BMP

and BOH. 17-BMP is the active metabolite, whereas both 21-BMP and BOH have very low binding affinity to the glucocorticoid receptor. In this experiment, *in-vitro* hydrolysis of BDP using esterase enzyme as well as the isolation and characterisation of its degradation product was reported. Enzyme hydrolysis was performed for 20 hrs. The results were encouraging as product formation was observed (Table 21).

Time/Min	Retention Time (RT)	Peak Area [AU]
0	8.043	845997.1
30	7.274	693241.2
60	6.617	831772.3
120	6.093	896331.3
1060	5.409	1082674.3
1200	5.006	1091303.1

Table 21: Enzyme hydrolysis [50:1ratio] time analysis for 20 hrs with RT and peak areas

The retention time of the major product 17-BMP was not constant. So, it was decided to perform enzyme hydrolysis again and this time data would be collected from the LC (Fig. 24 and 25).

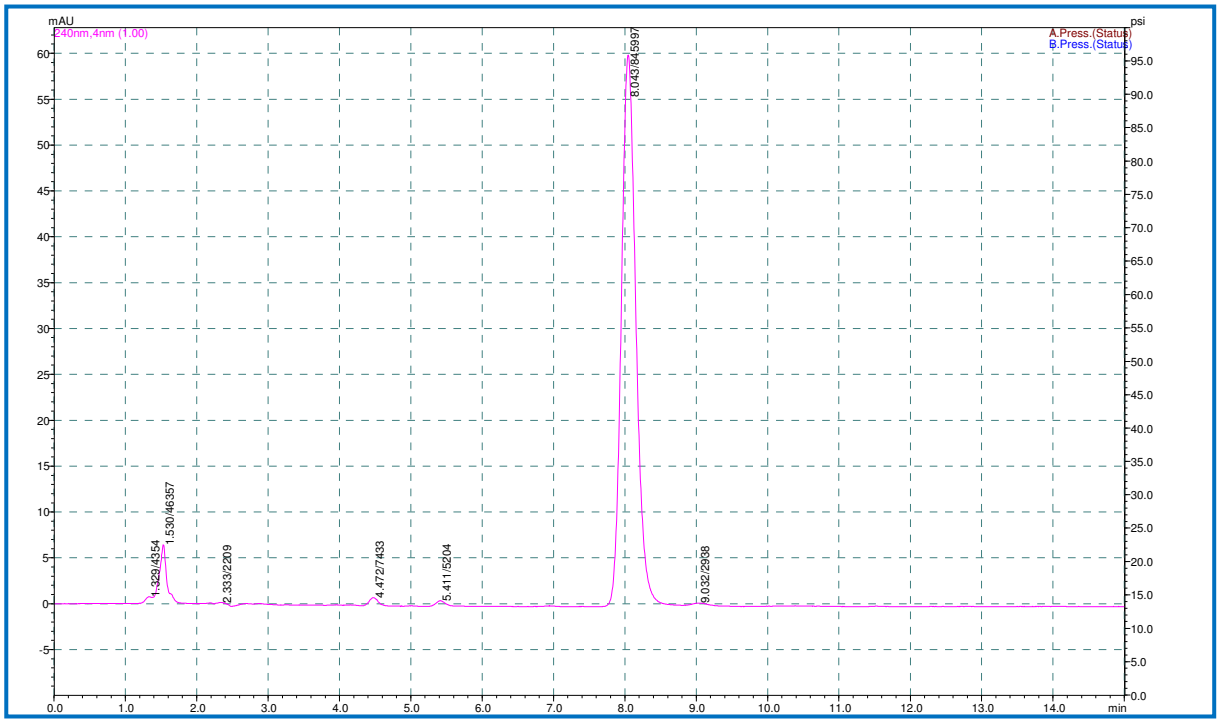

Figure 24: Chromatogram at 0 min, BDP is seen at 8.04 min

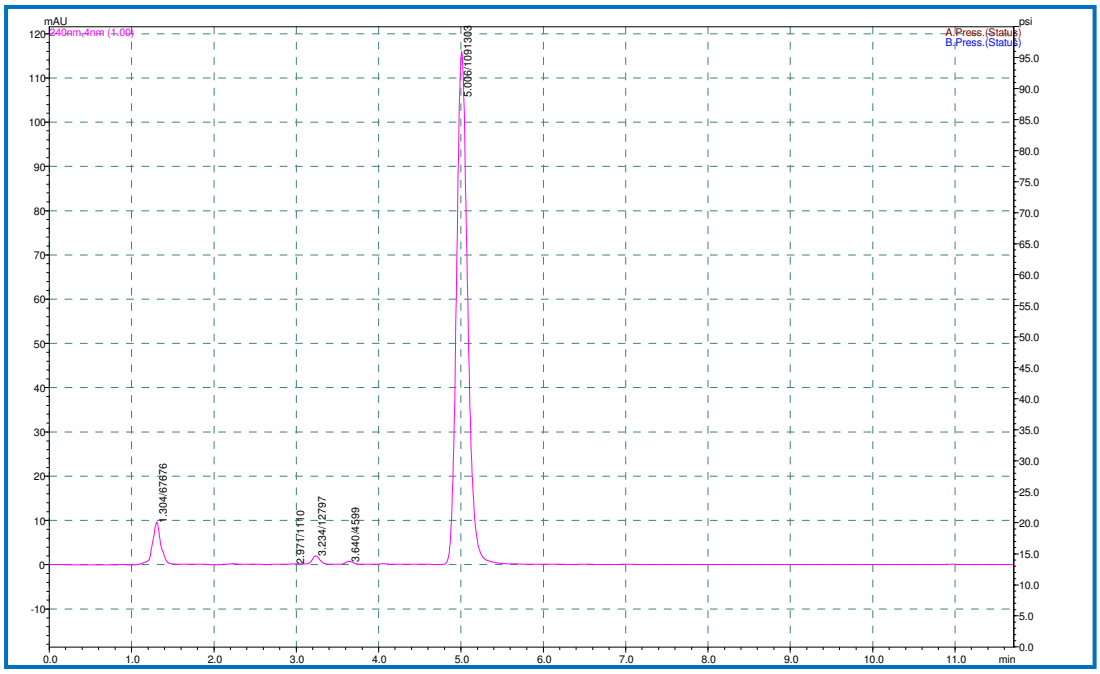

Figure 25: Chromatogram at 120 min, BMP is shown at 5 min

The above chromatograms showed the clear conversion of BDP to BMP. Then it was decided to monitor the reaction for 6 hrs only. Again the conversion of BDP to BMP was seen. Next it was decided to monitor the reaction for 2 hrs only, in order to obtain more data points, as summarized in Table 22, below.

Time/Min	Retention Time	Peak Area [AU]
0	6.386	3985.3
5	6.345	3447.4
10	6.496	3224.9
20	6.277	3538.1
30	6.28	3656.5
45	6.251	6577
60	6.265	5097.7
75	6.262	6859.2
90	6.255	5153
120	6.259	7050.3

Table 22: Enzyme hydrolysis [50:1ratio] time analysis for 2 hrs with RT and peak areas

All the samples were run on the LC-MS in the same way as before. Results were not encouraging as new peaks were seen in the chromatogram. After

discussion it was decided to repeat the enzyme hydrolysis reaction with a ratio of 50: 1 (enzyme : BDP). The results are shown in Table 23 and Fig. 26, below.

Time/min	Peak intensity (465.2)
0	23
5	5
10	15
20	62
45	405
60	446
75	565
120	618

Table 23: Enzyme hydrolysis [50:1ratio] time analysis for 2 hrs with peak intensities

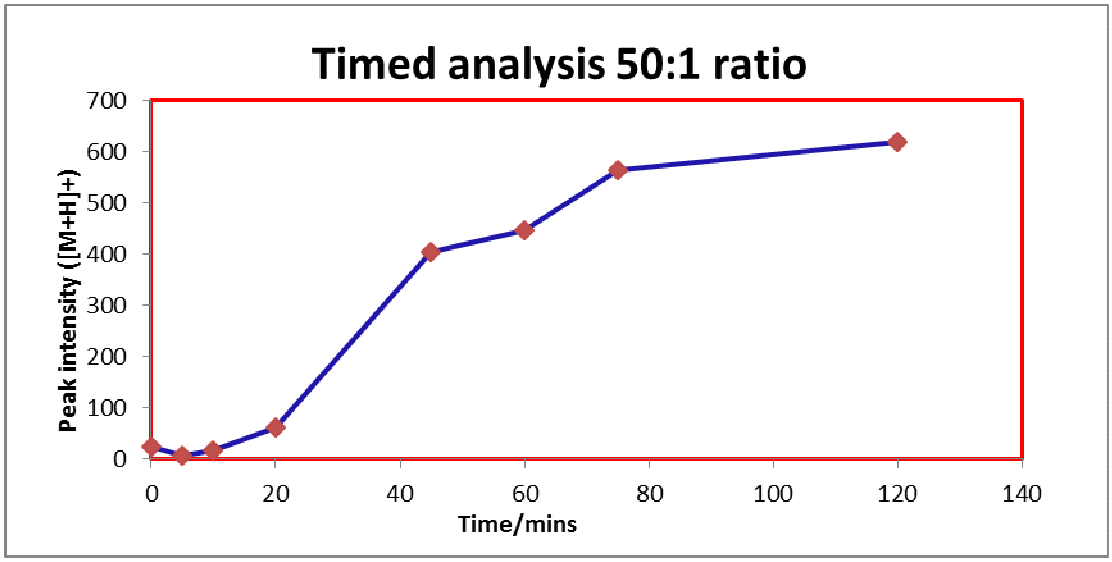

Figure 26: Enzyme hydrolysis [50:1 ratio], timed analysis for 2 hrs

The above LC-MS results showed the formation of the required product *i.e.* BMP. The graph was plotted with time *versus* peak intensity. As expected the graph showed a gradual and steady rise with no reappearance of the parent product. Fig. 27 shows the chromatogram at 0 min and its mass spectrum is shown in Fig. 28. Figs 29 and 30 show the chromatograms and mass spectra for the product. However, it still needs to be determined whether the product is 17-BMP or 21-BMP.

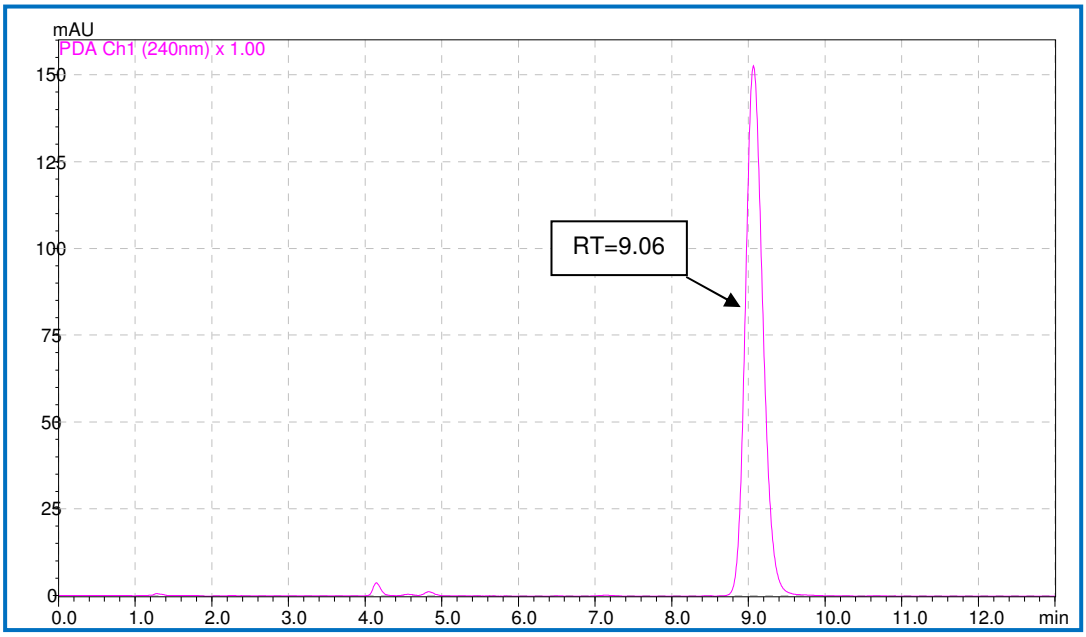

Figure 27: Chromatogram at 0 min, BDP is seen at 9.06 min

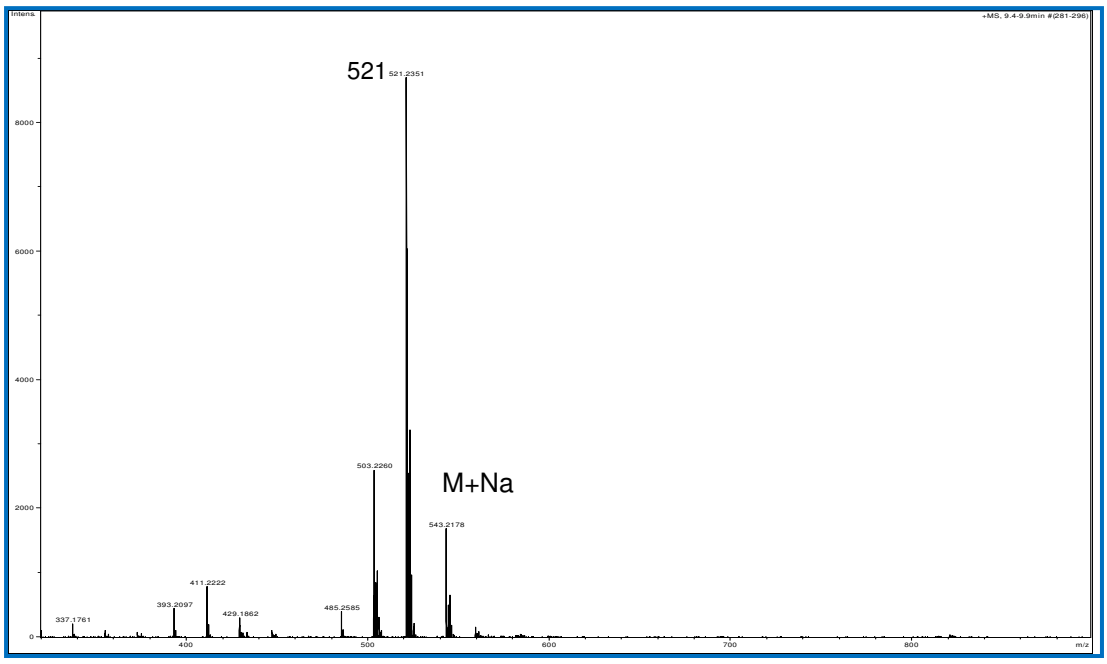

Figure 28: MS of the peak at 9.06 min, BDP is seen at m/z 521

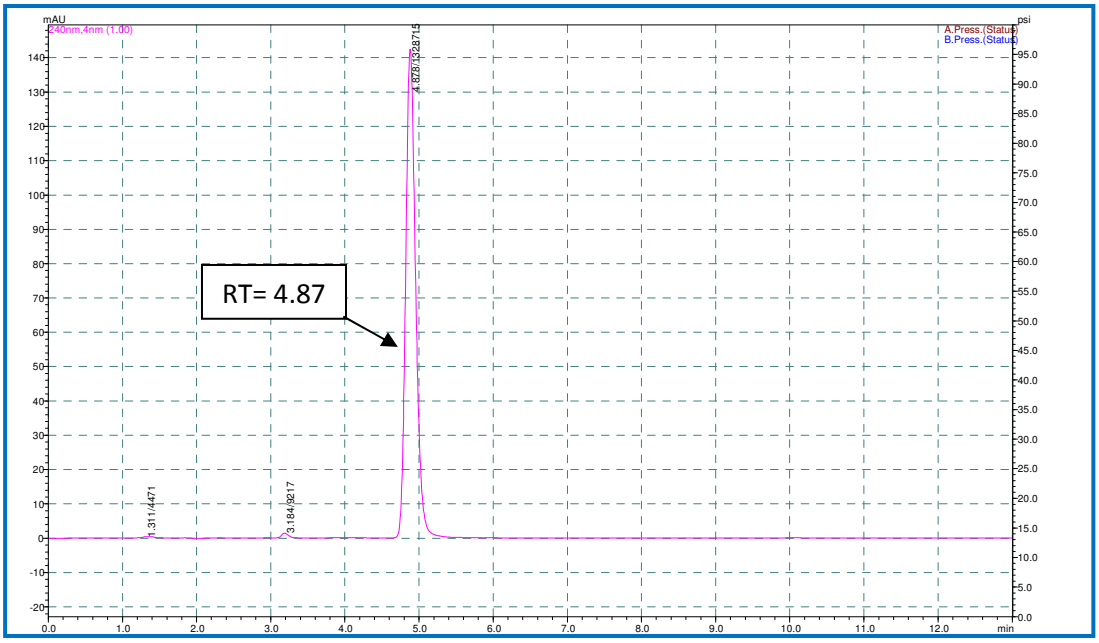

Figure 29: Chromatogram at 120 min, BMP is shown at 4.87 min

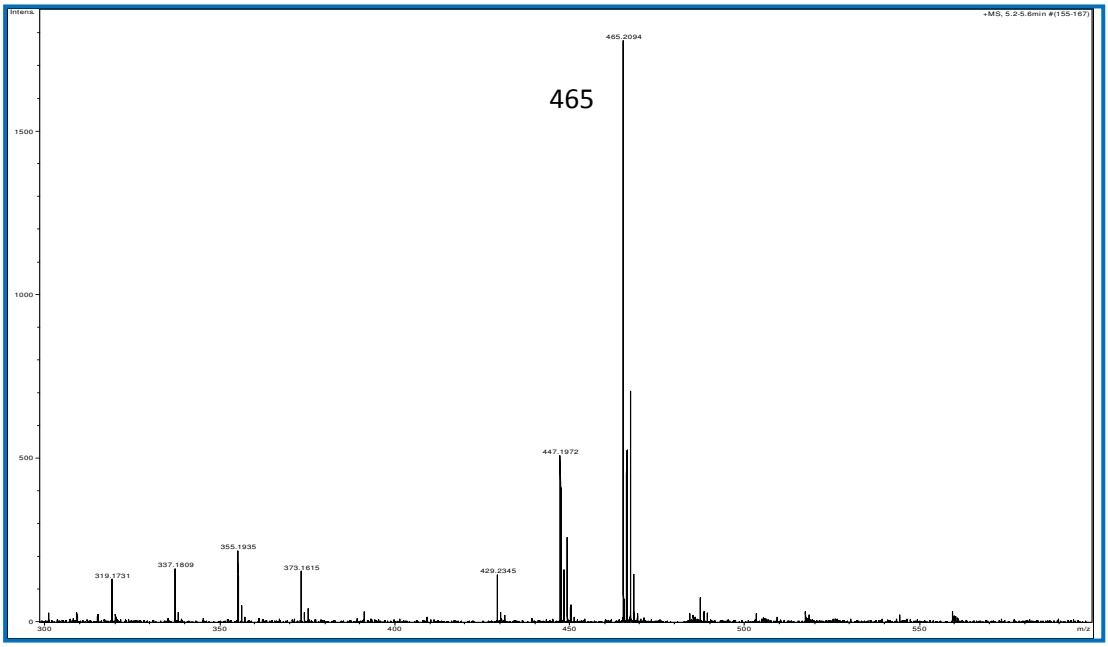

Figure 30: Mass spectrum of the peak at 4.87 min, BMP is seen at m/z 465

Enzyme hydrolysis was conducted in the same way as the above method but this time the amount of enzyme was decreased to half, *i.e.* 1.0 mg, in order to see the effect of decreasing the amount of the enzyme (300: 1; enzyme: BDP ratio). The reaction was monitored for 6 hrs and the results are summarized below in Table 24 and Fig. 31.

Time/Min	Peak Area [AU]
0	18240.7
15	182613.6
30	199795.3
45	1133470.2
60	1612331.4
90	1915128.1
120	2091459.1
150	2082273.2
195	2274796.3
255	2302106
315	2158511.7
375	2310079.1

Table 24: Enzyme hydrolysis [300:1ratio] timed analysis for 6 hrs with peak areas

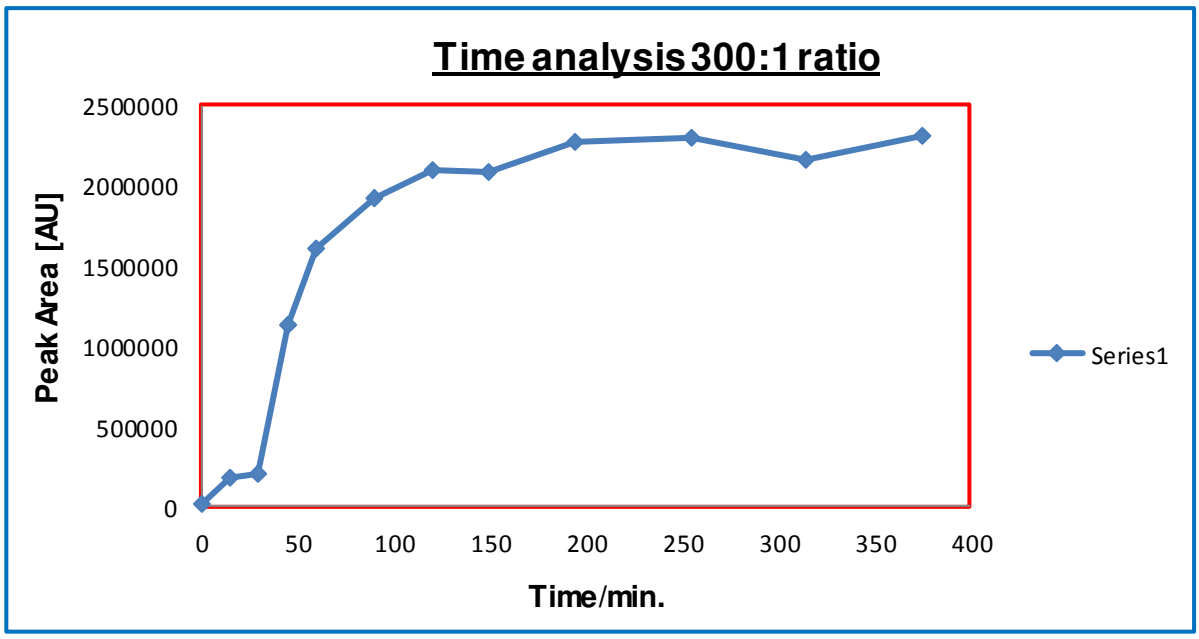

Figure 31: Enzyme hydrolysis [300:1 ratio], timed analysis for 6 hrs

The above graph shows that there was no prominent or drastic change in the reaction as expected. By comparing both the graphs (50:1 and 300:1 ratio), it becomes obvious that after 120 min there was no significant change in the reaction observed. So, if the amount of enzyme was decreased in this specific reaction it would not affect the reaction on a big scale. The method was not only developed but it was also cost effective. Results showed the presence of BDP and this was confirmed with the EIC of BDP at *m/z* 521(Fig. 32) and the mass spectrum (Fig. 33).

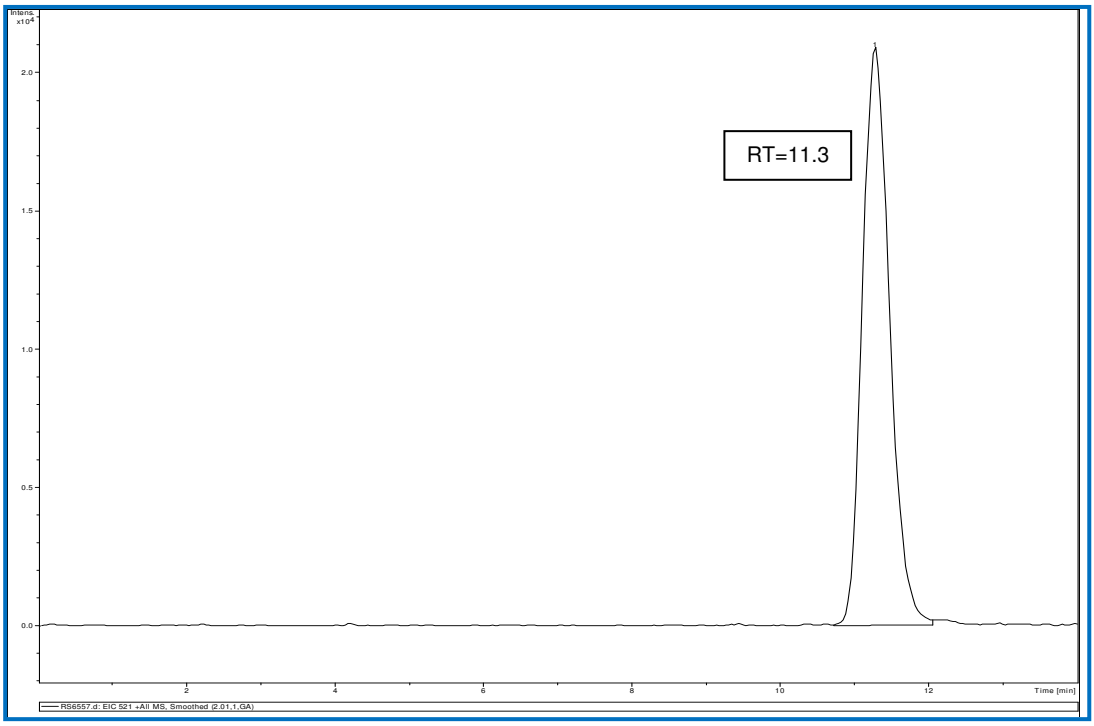

Figure 32: EIC of m/z 521 corresponding to BDP

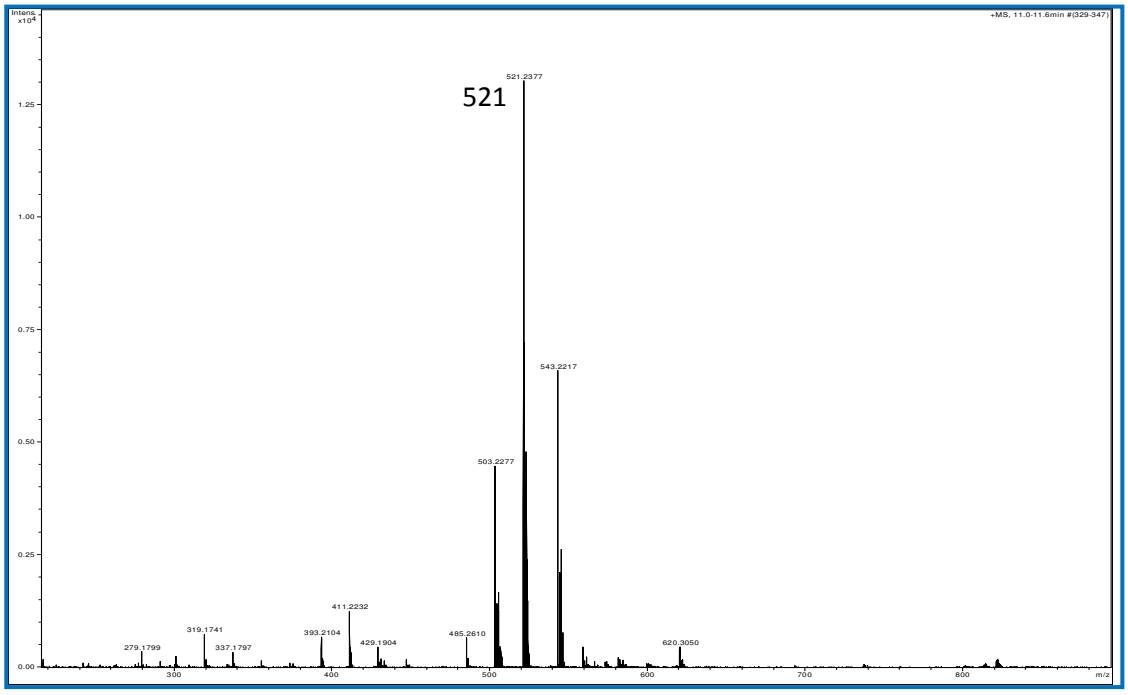

Figure 33: Mass spectrum of the reaction at 0 min, BDP is seen at m/z 521

After 120 min the reaction solution was analysed using LC-MS and the results showed the formation of BMP. Formation of the BMP product was confirmed with the EIC of BMP at *m/z* 465 (Fig. 34) and the mass spectrum (Fig. 35).

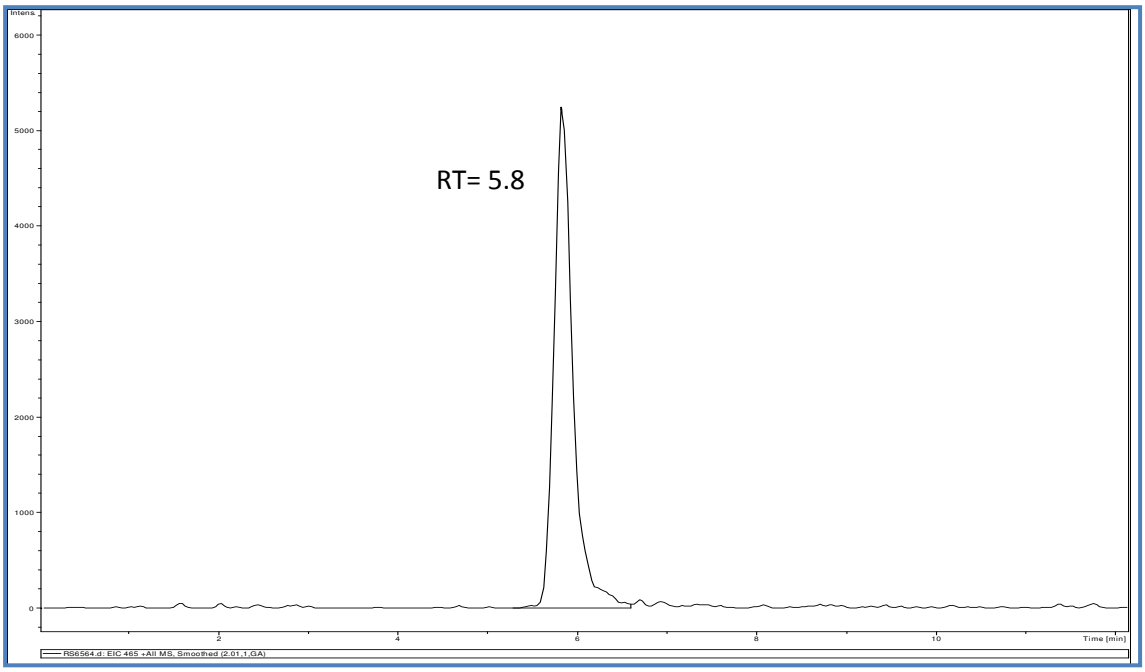

Figure 34: EIC of m/z 465, BMP is seen at RT=5.8 min

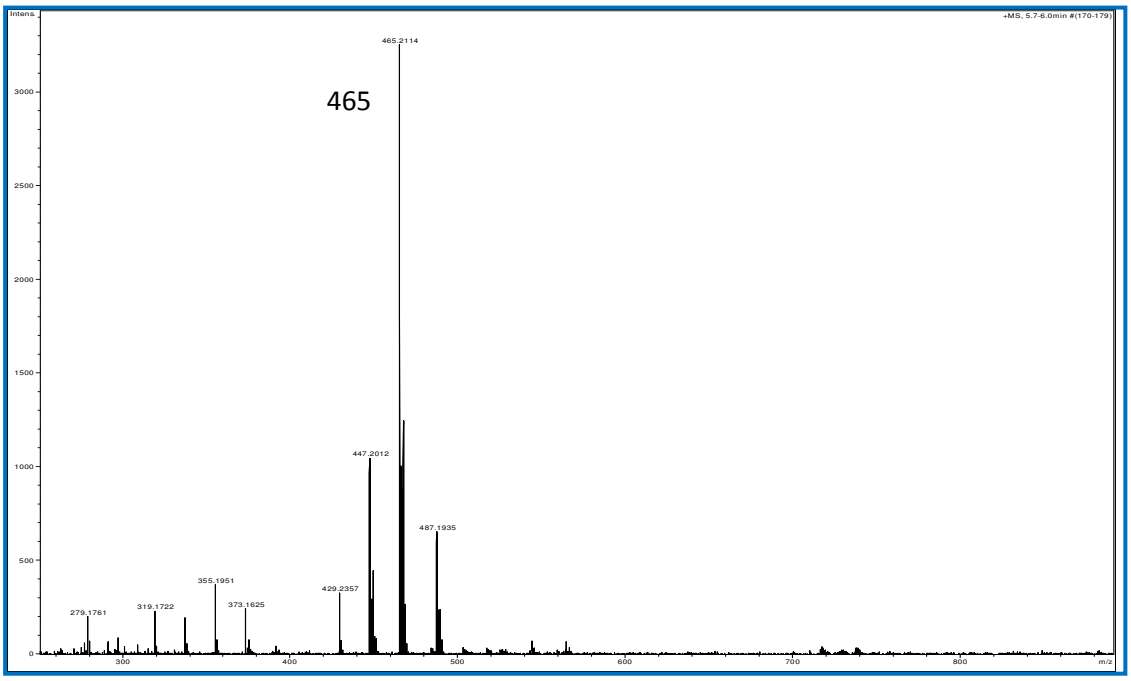

Figure 35: Mass spectrum of the peak at 5.8 min, BMP is seen at m/z 465

BDP is a di-ester compound and both possible mono-ester hydrolysis products may be expected to co-elute. So, the next step was to confirm the formation of the required product (17-BMP).To obtain a usable amount of product for detailed analysis, the reaction was repeated on a large scale.

1.7.3.1 Enzyme hydrolysis of BDP (large scale) using porcine esterase

The reaction was carried on a large scale and was analysed using LC-MS. BMP formation was observed which was shown in the LC chromatogram (Fig. 36). BMP was observed at RT 6.30 min.

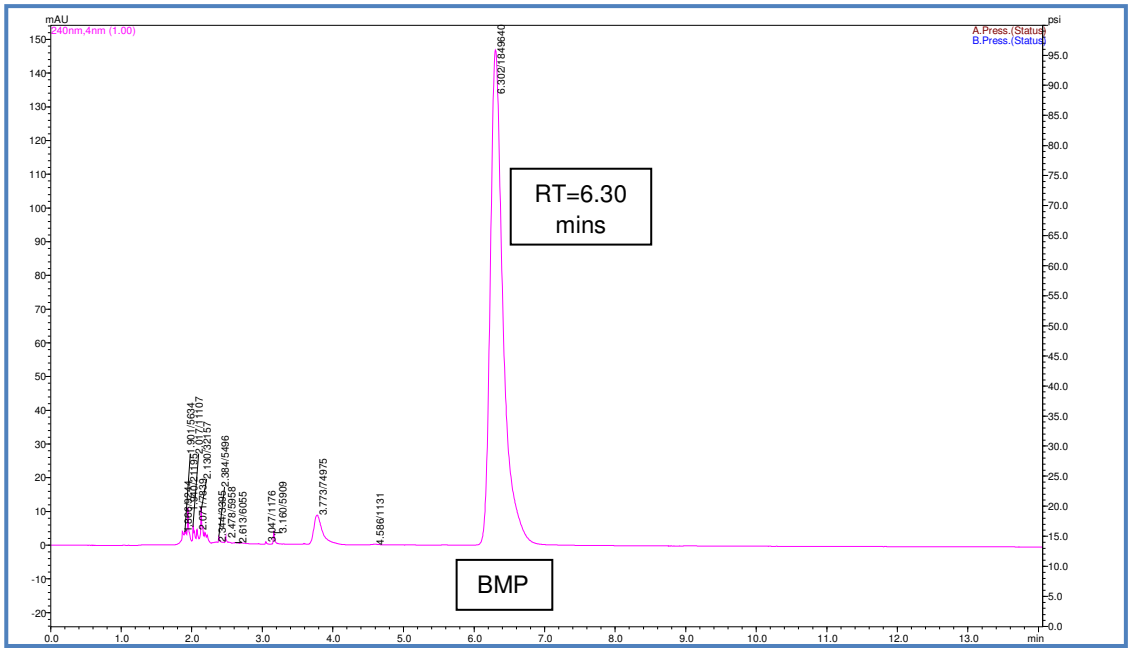

Figure 36: Chromatogram (UV), 180 min, BMP is seen at 6.3 min

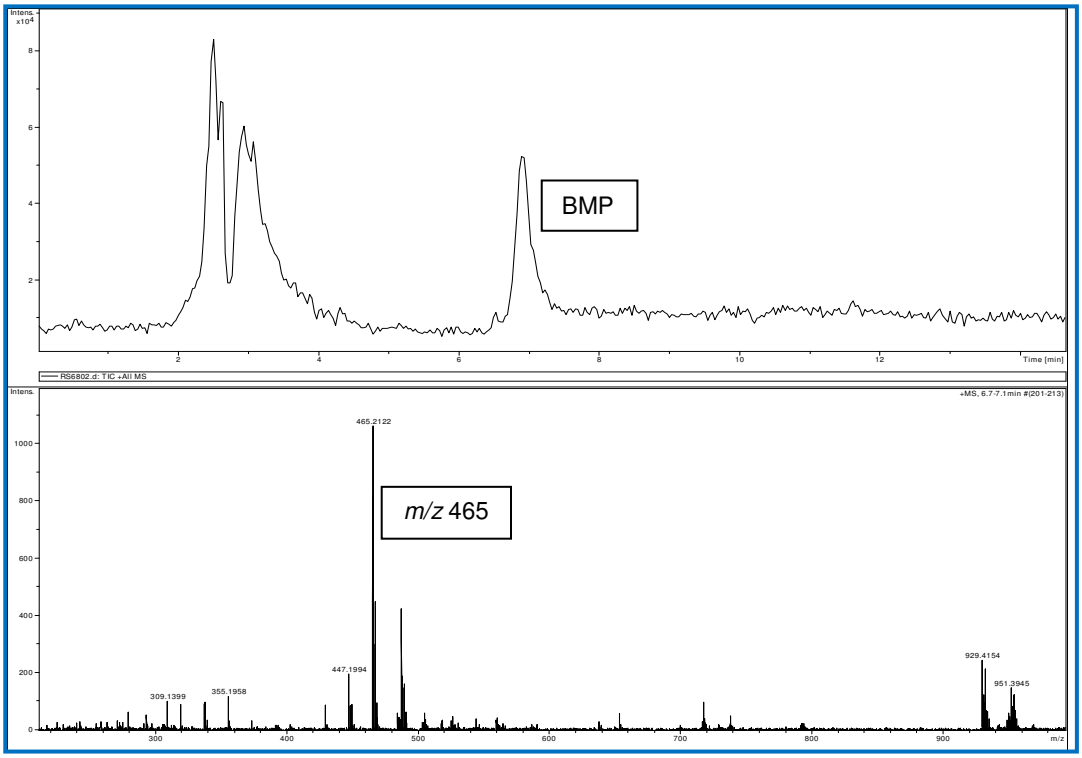

Figure 37: MS chromatogram of the reaction after 180 min (top) and MS of the peak at 6.8 min (bottom). BMP is seen at m/z 465

The results clearly showed formation of BMP, but still some solid was seen in the reaction which may have contained BDP. It was therefore decided to leave the reaction mixture solution for incubation for 5 more hrs. Again, the reaction solution (0.5 mL) was then spun through an Amicon cartridge and analysed using LC-MS.

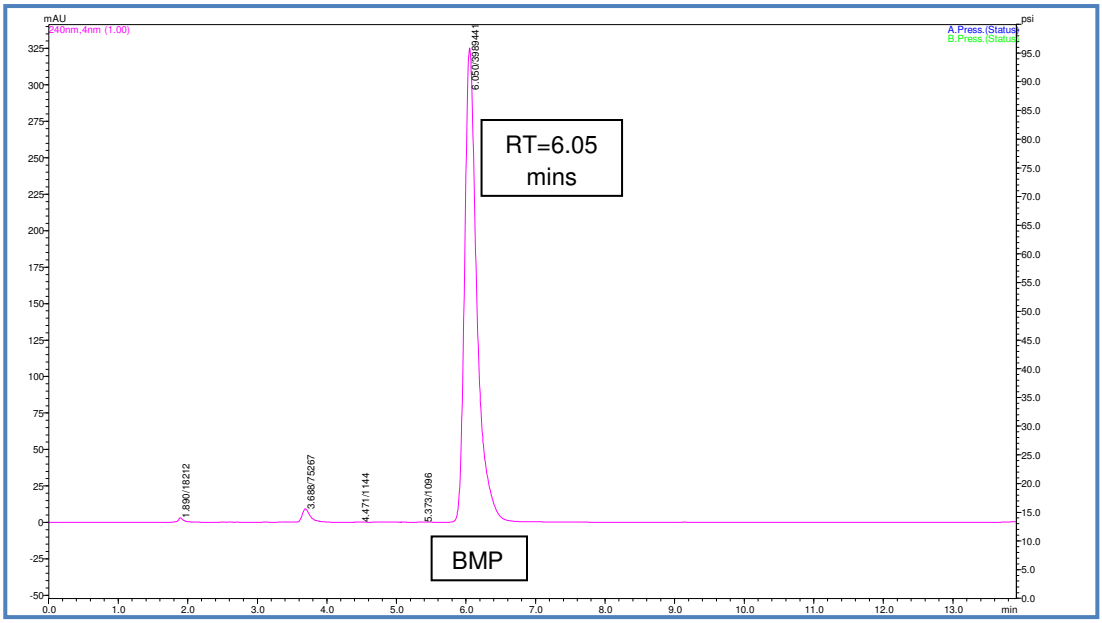

Figure 38: Chromatogram (UV) of the reaction mixture after 8 hrs. BMP is seen at 6.05 min (n=3)

The chromatogram shown in Fig. 38 showed that further conversion of the reactants to product had occurred as the peak area had increased, however some solid was still present in the reaction tube. The reaction was therefore left overnight. After 26 hrs, the reaction solution was analysed using LC-MS and the results showed the formation of BMP at 6.3 min, shown in Fig. 39. This was confirmed with the EIC of BMP at *m/z* 465 (Fig. 40 top) and the mass spectrum (Fig. 40 bottom).

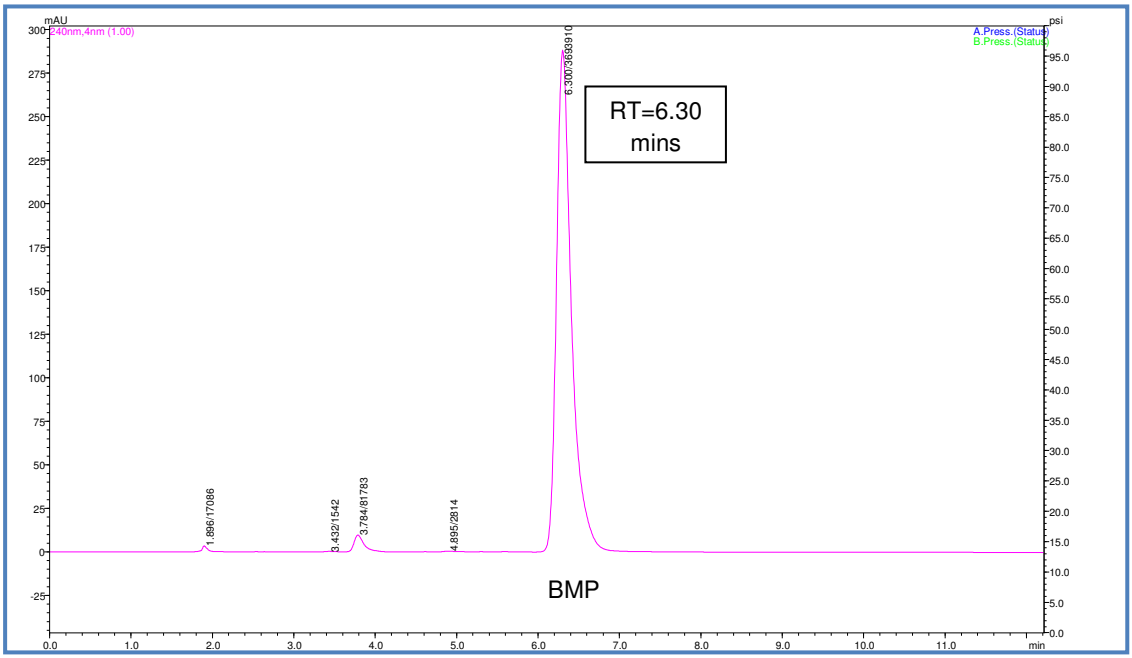

Figure 39: Chromatogram (LC) of the reaction mixture at 26 hrs, BMP is seen at 6.3 min

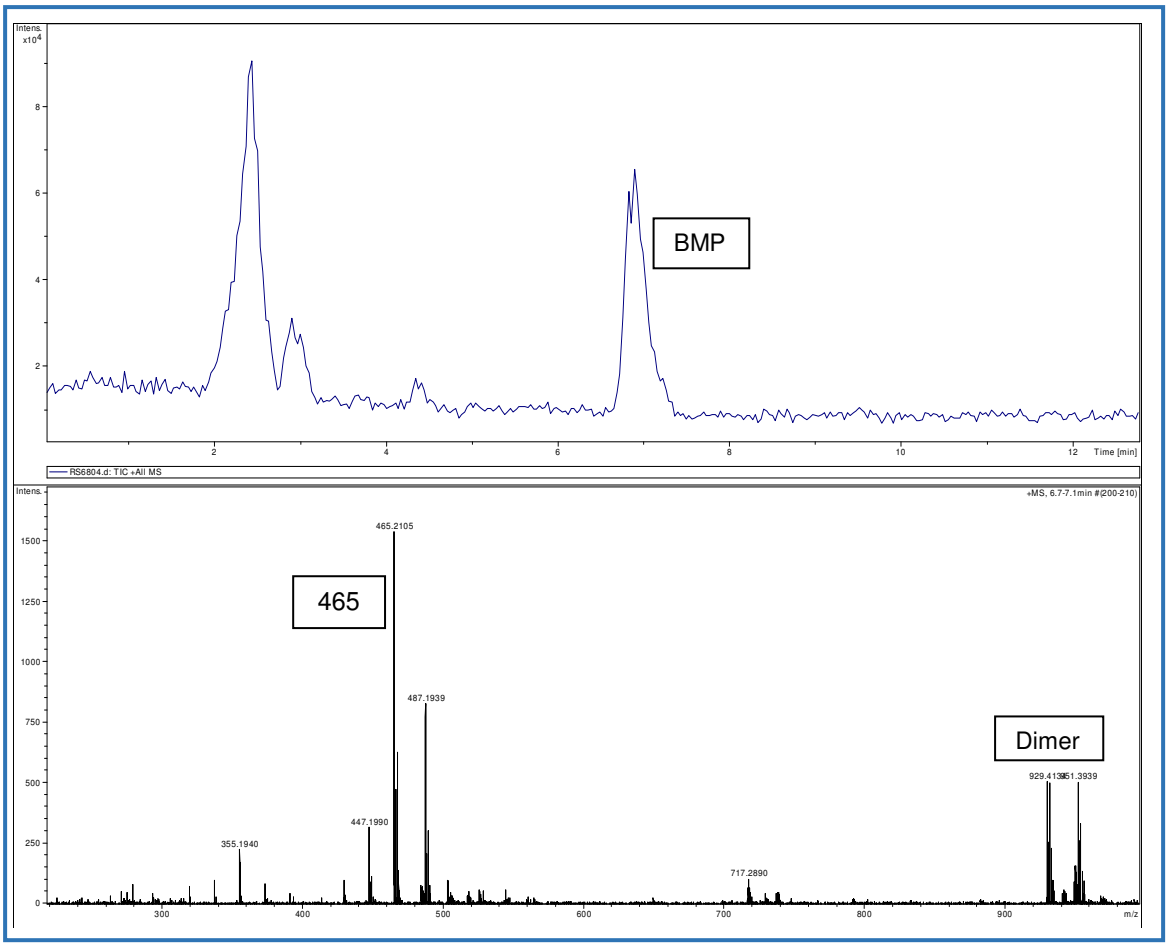

Figure 40: EIC of m/z 465 (top), mass spectrum of the peak at 6.8 min (bottom)

1.7.4 Formation of BMP and BOH using NMR

Over the past fifty years nuclear magnetic resonance spectroscopy has become the well-known technique for determining the structure of organic compounds. Of all the spectroscopic methods, it is the only one for which a complete analysis and interpretation of the entire spectrum is normally expected.

The reaction mixture was filtered under vacuum and then LLE was conducted on the filtrate, with ether (five sequential extractions). The fractions were mixed together, evaporated and dissolved in d_6-ethanol (650 µL) and the sample was analysed using NMR.

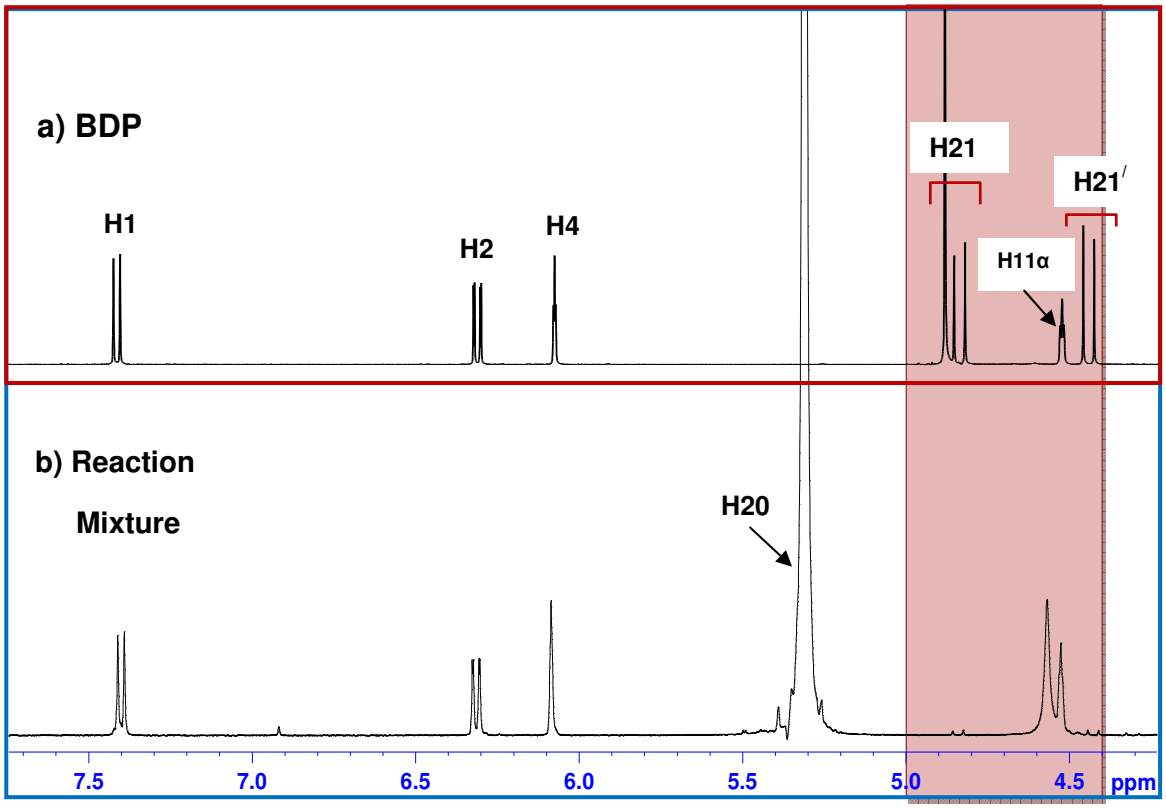

Figure 41: Selected regions of the ^{1}H NMR spectra of BDP (a) and the reaction mixture filtrate after extraction (b)

The reaction showed that the product had been formed and was fairly pure. The ^{1}H NMR spectrum (Fig. 41b) was compared with the spectrum of standard BDP (Fig. 41a). The highlighted portion of Fig. 41 above showed clearly that the signals between 4.4 and 4.5 ppm and between 4.8 and 4.9 ppm, corresponding to the propionate group, has disappeared and new peaks have appeared between 4.5 and 4.6 ppm. However, it was not clear whether the product is 17-BMP or 21-BMP. For further confirmation whether the product is 17-BMP, the above ^{1}H NMR spectrum was compared, at the selected regions, with the spectra from standards of BOH, 17-BMP and 21-BMP and it further confirmed that signals between 4.2 and 5.6 ppm in 17-BMP (2), highlighted in pink, correspond to a steroidal product (Fig. 43).

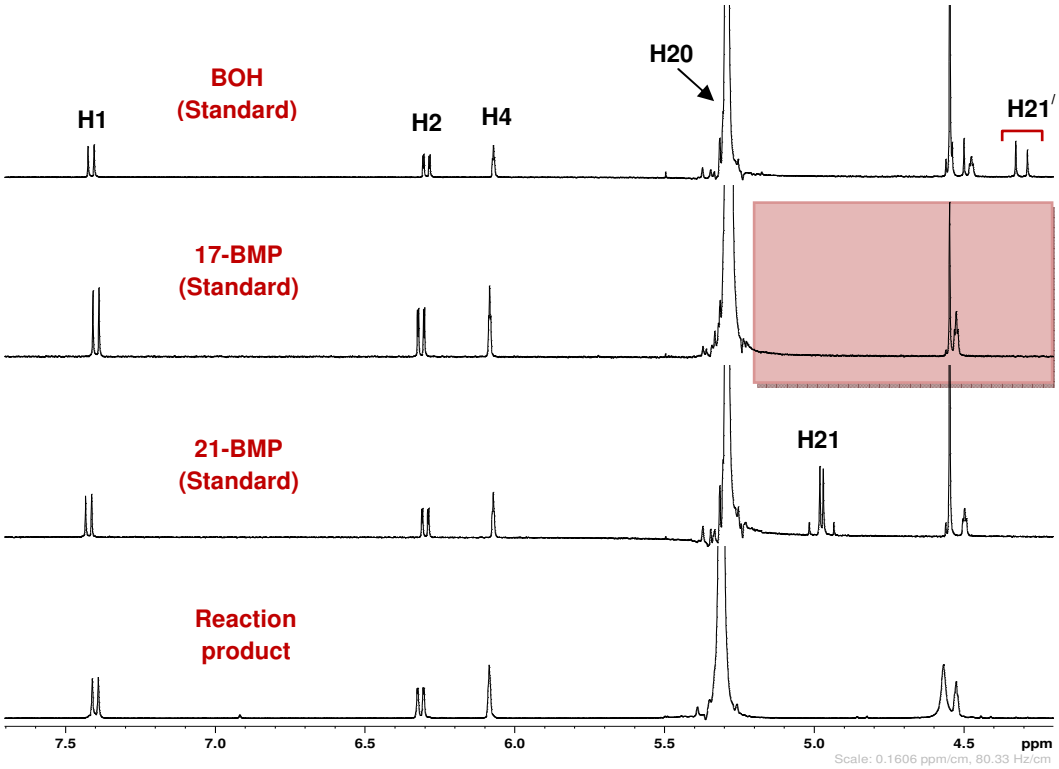

Figure 42: Comparison of selected regions of ^{1}H NMR spectra of BOH (1), 17-BMP (2), 21-BMP (3) and the reaction product (4)

There was some solid residue left on the filter paper which was dissolved in d_6-ethanol (650 µL) and analysed using ^{1}H NMR spectrometry. The spectrum (Fig. 43) showed the presence of BMP, providing evidence that BMP was present both in the liquid sample and the solid.

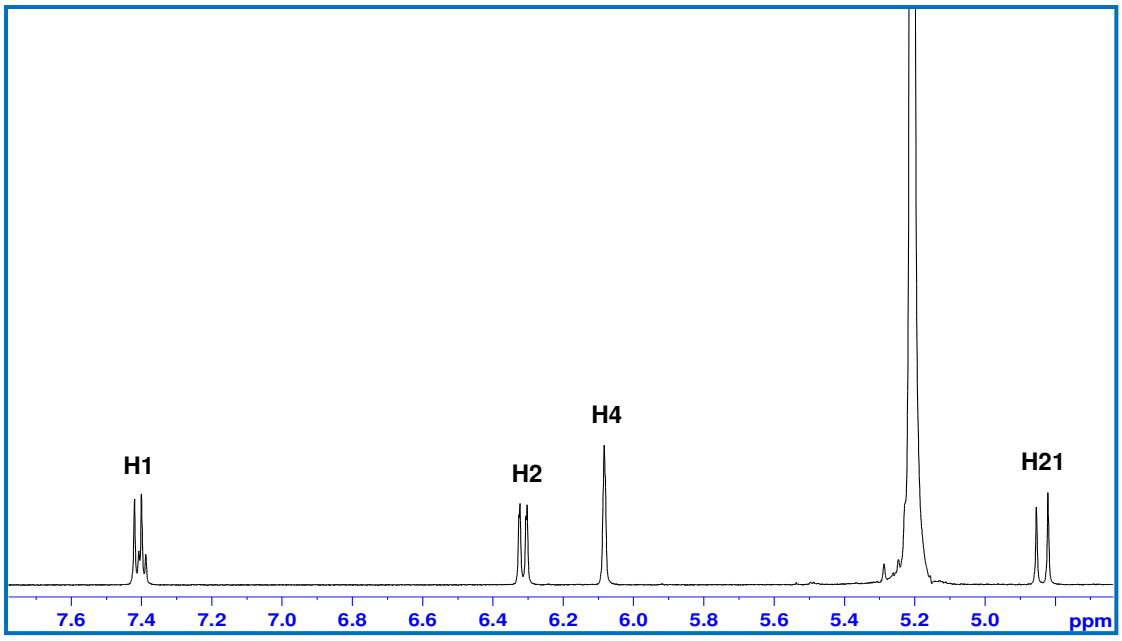

Figure 43: Selected region of the ^{1}H NMR of the residue dissolved in d_6-ethanol from the reaction

The residue was dissolved in ethanol (1-2 mL) and analysed using LC-MS; the resulting chromatogram is shown in Fig. 44.

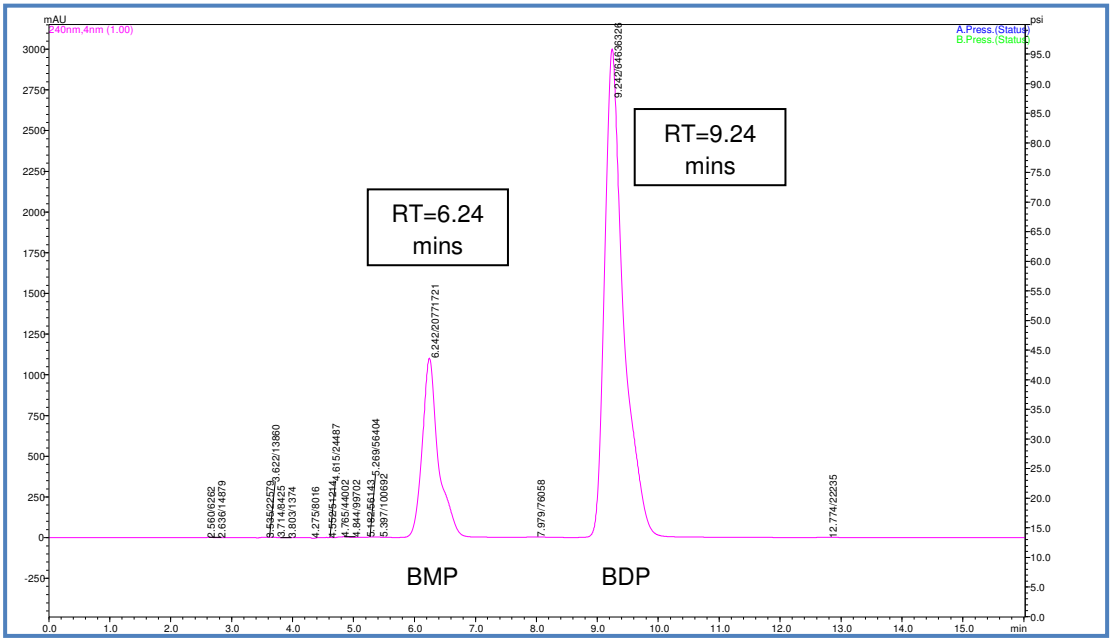

Figure 44: Chromatogram from LC-UV analysis of the residue dissolved in d_6-ethanol

Peaks corresponding to 17-BMP and BDP appeared at 6.24 and 9.24 min., respectively, as expected.

1.7.4.1 Further confirmation of formation of BMP by Nuclear Magnetic Resonance (NMR)

As it was clear that BMP had been formed but not whether it was 17-BMP or 21-BMP, further analysis was carried out using NMR to identify the product.

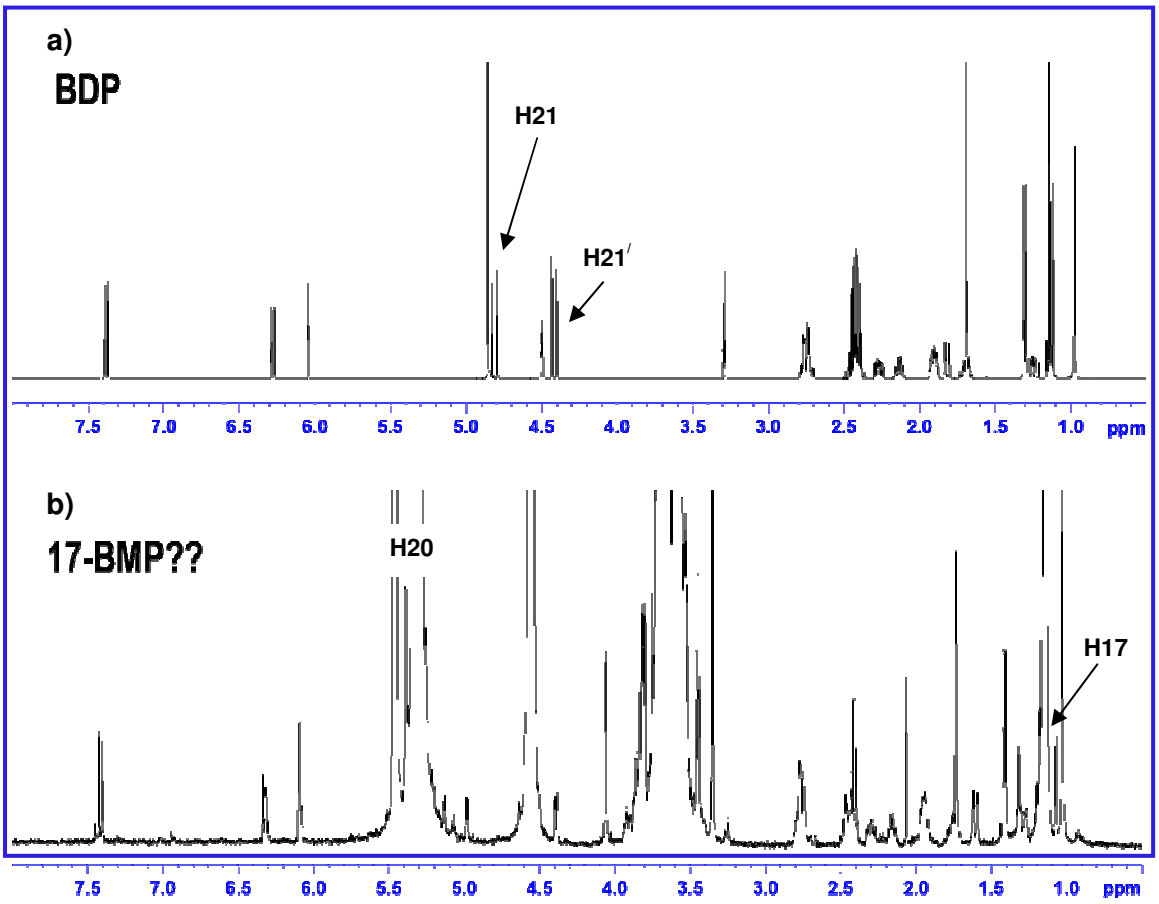

Figure 45: Selected regions of the 1H NMR spectra of BDP standard (a) and the reaction product (b)

Fig. 45 (a) shows the ^{1}H NMR spectrum of the BDP standard and Fig. 45 (b) shows the ^{1}H NMR spectrum of the reaction product. It can be seen that it was not a pure product, but contains many extra peaks; however, the spectrum clearly shows numerous signals corresponding to a steroidal product.

In order to have a clear image, the previous spectrum was expanded from 0.6 ppm to 2.9 ppm, Fig. 46 (a, b). In the spectrum of BDP between 1.1 and 1.2 ppm propionate CH_3- groups are observed. In the reaction mixture those groups were seen at the same shift but are somewhat overlapped by an impurity signal.

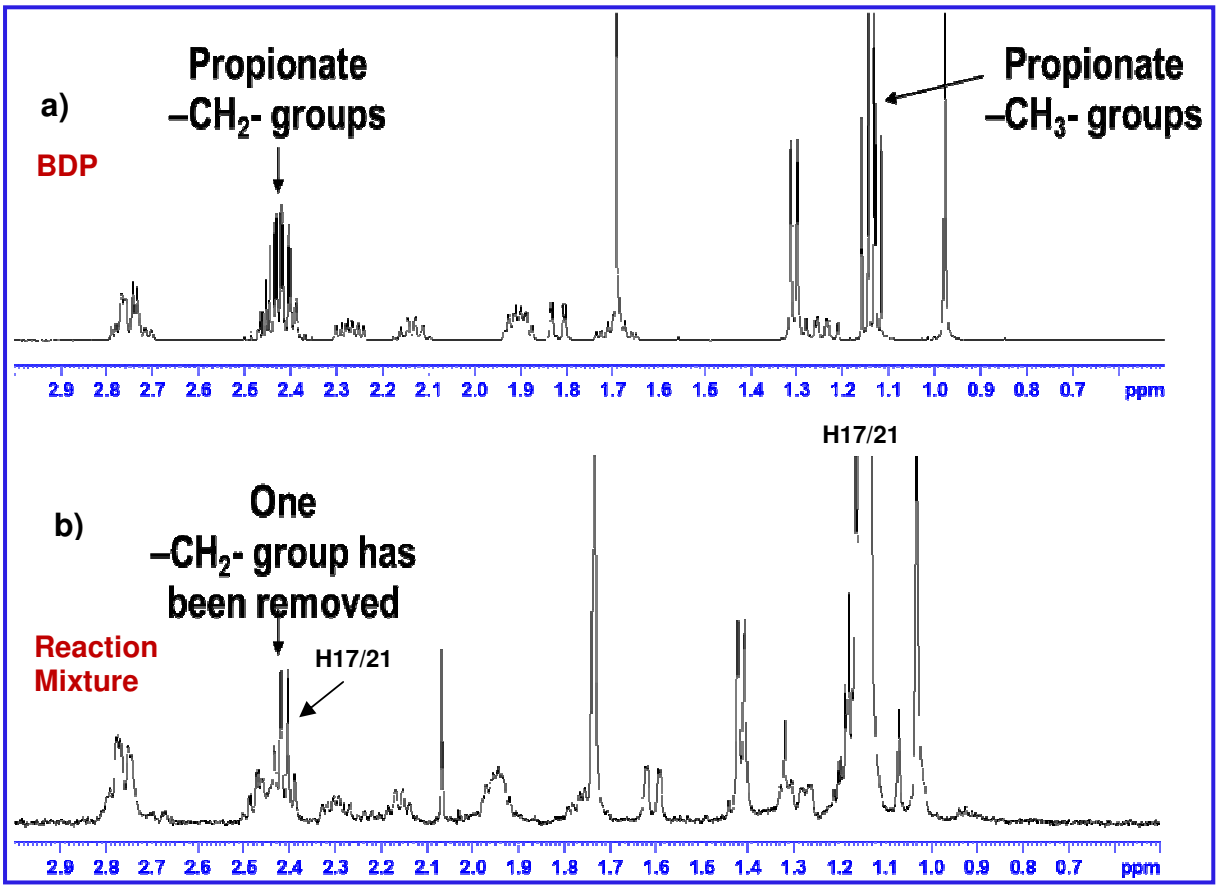

Figure 46: Expansion of the ^{1}H NMR spectra for the BDP standard (a) and the reaction product (b)

However, the signals corresponding to the protons in the 17- and 21-propionate groups of BDP appeared at 2.4 ppm and 1.12 ppm a signal corresponding to 2 x CH_2 groups is present in the spectrum of BDP but in the reaction mixture those signals were decreased (integration = 2H). Inspection of the integrals shows that two protons have been lost from the signal at 2.43 ppm and three from signal at 1.12 ppm, which clearly confirmed that one of the –CH_2 - groups has been cleaved away.

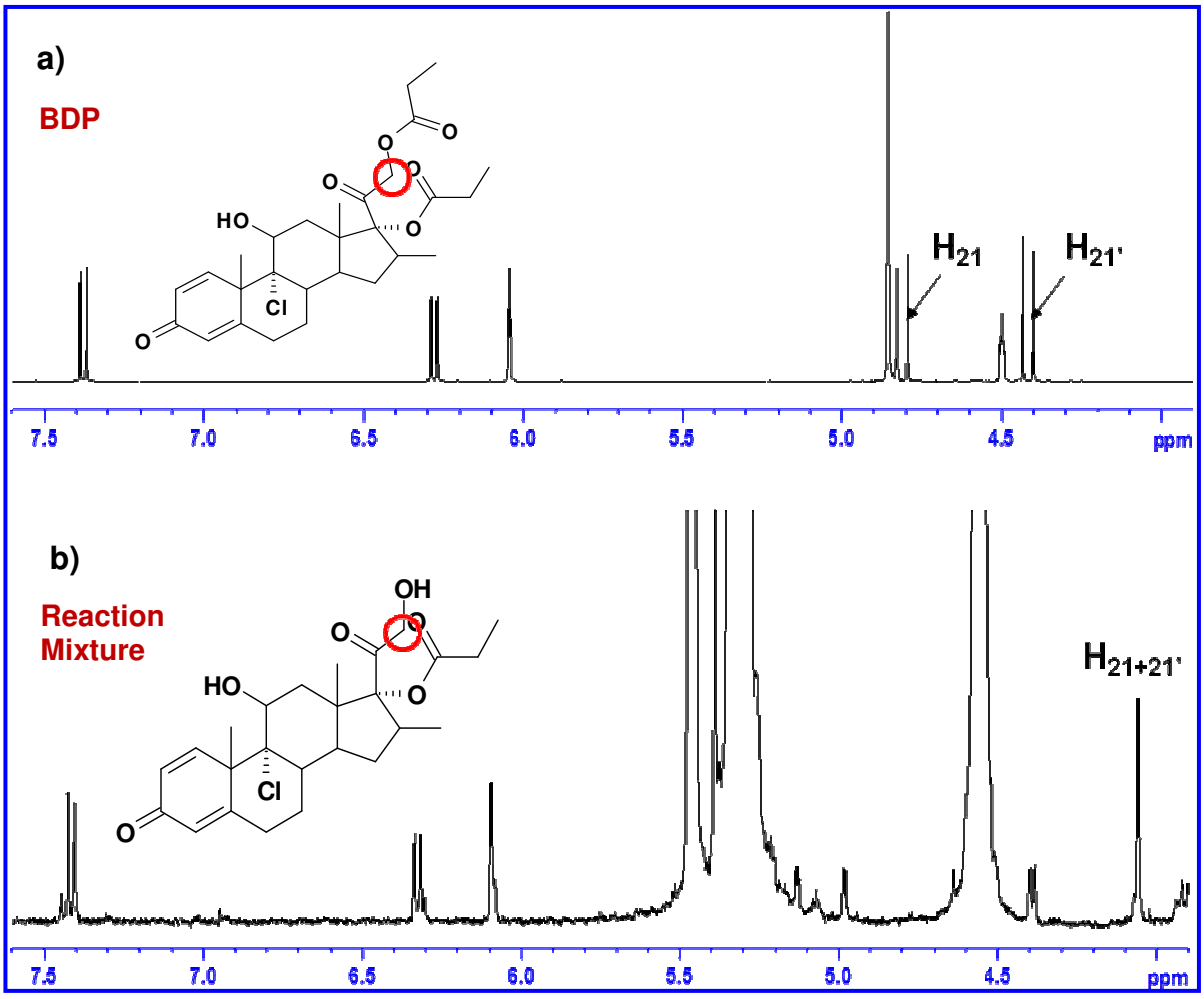

Figure 47: Expansion of the ^{1}H NMR spectra for the BDP standard (a) and the reaction product (b)

Evidence for the formation of 17-BMP (as opposed to 21-BMP) is provided by inpection of the signals for the protons at position 21 in Fig 48 a, where the signals appear as doublets at 4.81 and 4.42 ppm. In the above spectra, Fig. 47 (a, b) it can be seen that the proton signals from H_{21} and $H_{21'}$ have changed dramatically after the hydrolysis reaction.

In the spectrum of the reaction mixture (Fig. 47b), the protons at position H_{21} and $H_{21'}$ were shifted from 4.5 ppm to almost 4.04 ppm (2H) and appeared as a single signal. This is indicative of cleavage of the 21-propionate group from the molecule. In the spectrum of BDP (Fig. 47a) the two protons at 21 and 21'are diastereotopic and their signals appear as doublets with markedly different shift. This is further evidence that the bulky propionate group has been lost, allowing free rotation of the CH_2 protons at C21.[31]

The above results confirms previous findings by Foe *et al* that showed the rapid hydrolysis of BDP via esterase enzyme to 17-BMP which was the major metabolite detected.

1.7.5 Liquid Liquid Extraction (LLE) of BDP and its metabolites

A range of solvents were accessed to see which would be the most efficient for the extraction of BDP metabolites from the reaction solution. Five sequential extractions were carried out with each solvent to attempt complete recovery of the analyte.

1.7.5.1 Liquid Liquid Extraction (LLE) of BDP and its metabolites from aqueous solution with Ether and Cyclohexane

S.No.	BMP	BDP	Ratio	Relative recovery (BMP) (%)	Relative recovery (BDP) (%)
1	4673754	14726	317.38	100	100
2	3402770	30893	110.15	73	210
3	1704314	9552	178.42	36	65
4	572930	18991	30.17	12	129
5	246849	16890	14.62	5	115

Table 25: Peak areas from LC analysis after LLE with a cyclohexane-ether mixture, five sequential extractions

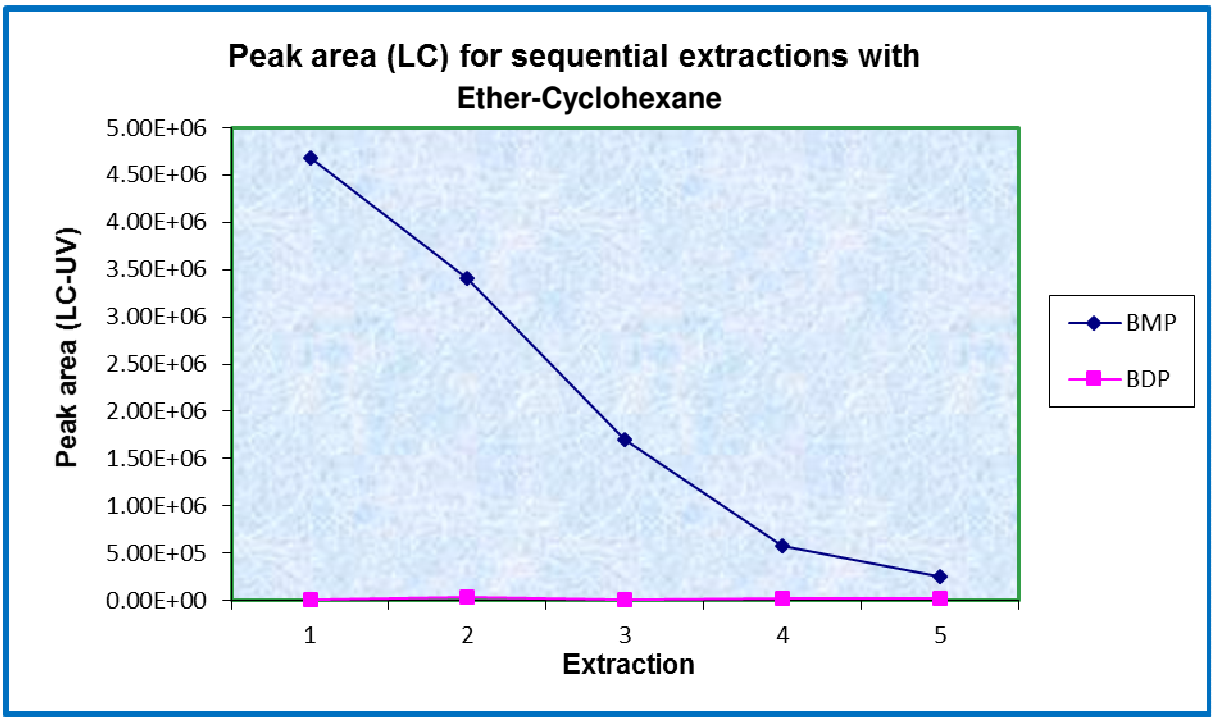

Figure 48: LLE with cyclohexane-ether mixture, five sequential extractions

The above graph shows that almost all BMP was extracted since the amount present in each subsequent extraction decreased until only a small amount was recovered in fraction 5 (5% of the amount in fraction 1). Interestingly, the amount of BDP extracted in each fraction remained broadly constant.

1.7.5.2 Liquid Liquid Extraction (LLE) of BDP and its metabolites from aqueous solution with Ether

S.No.	BMP	BDP	Ratio	Relative recovery (BMP) (%)	Relative recovery (BDP) (%)
1	8333942	3158	2638.66	100	100
2	4724445	67915	69.56	57	2151
3	2064252	94538	21.84	25	2994
4	420671	87027	4.83	5	2756
5	127579	88337	1.44	2	2797

Table 26: LLE with ether, five sequential extractions

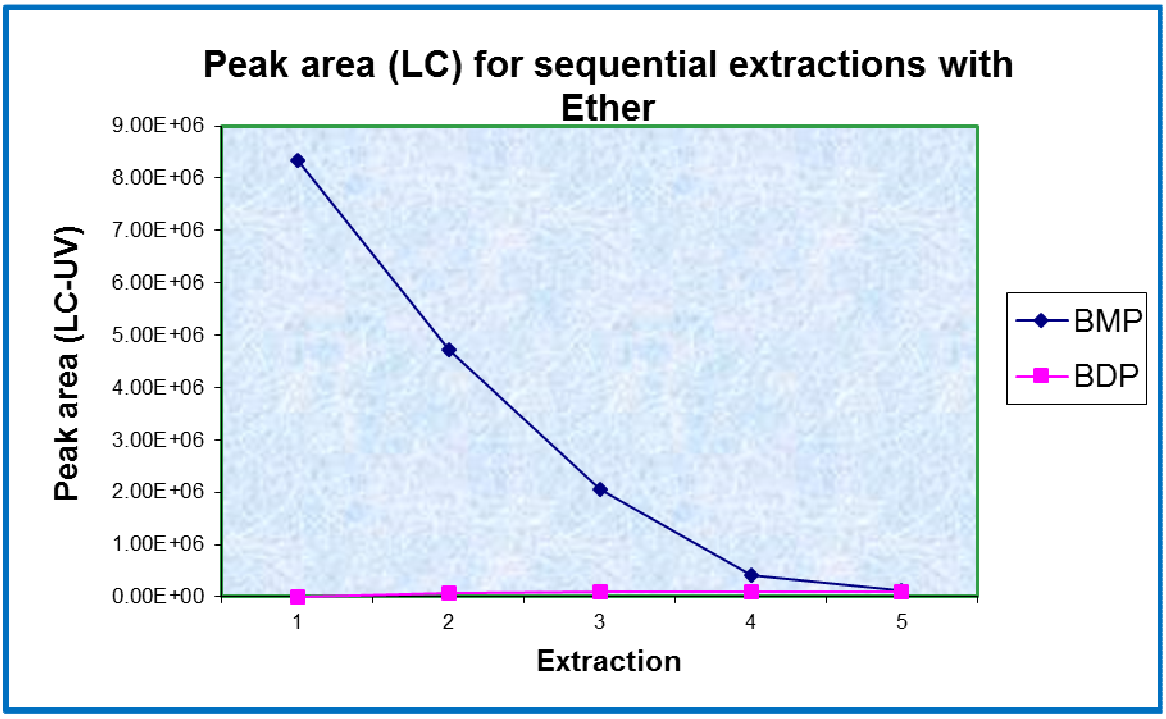

Figure 49: LLE with ether, five sequential extractions

Extraction of the final product was excellent with ether, as can be seen from table 25 and Fig. 49 above. The majority of the product was extracted in fractions 1-3 and by fraction 5 only a small amount of product was still present in the reaction mixture.

1.7.5.3 Liquid Liquid Extraction (LLE) of BDP and its metabolites from aqueous solution with Dichloromethane (DCM)

S.No.	BMP	BDP	Ratio	Relative recovery (BMP) (%)	Relative recovery (BDP) (%)
1	2941309	9649	304.84	100	100
2	2606147	22264	117.06	89	231
3	1082870	13070	82.85	37	135
4	323208	3582	90.23	11	37
5	300781	3531	85.19	10	37

Table 27: LLE with dichloromethane, five sequential extractions

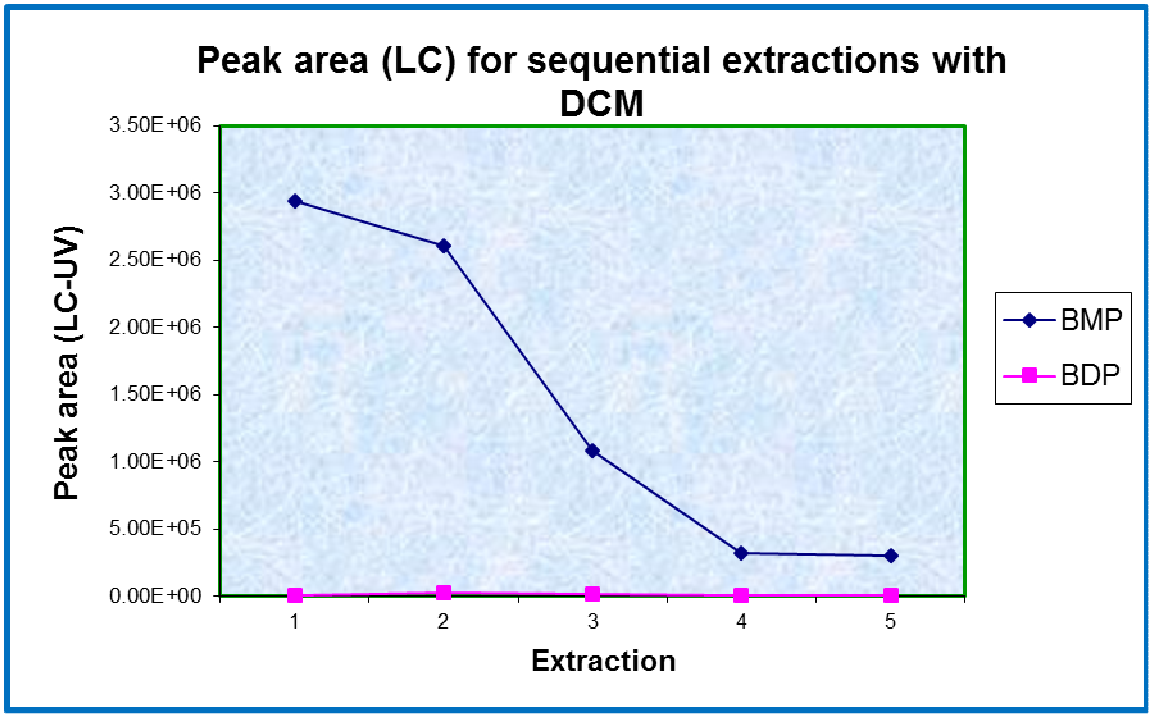

Figure 50: LLE with dichloromethane (DCM), five sequential extractions

The above graph (Fig. 50) shows that after five extractions still some product was left in the reaction mixture; the results were not as good as with the cyclohexane-ether mixture and with ether.

1.7.5.4 Liquid Liquid Extraction (LLE) of BDP and its metabolites from aqueous solution with Tert-butyl methyl ether (TBME)

S.No.	BMP	BDP	Ratio	Relative recovery (BMP) (%)	Relative recovery (BDP) (%)
1	4714836	180245	26.16	100	100
2	1985542	380755	5.21	42	211
3	593007	411464	1.44	13	228
4	158062	375253	0.42	3	208
5	66259	483891	0.14	1	268

Table 28: LLE with *tert*-butyl-methyl ether, five sequential extractions

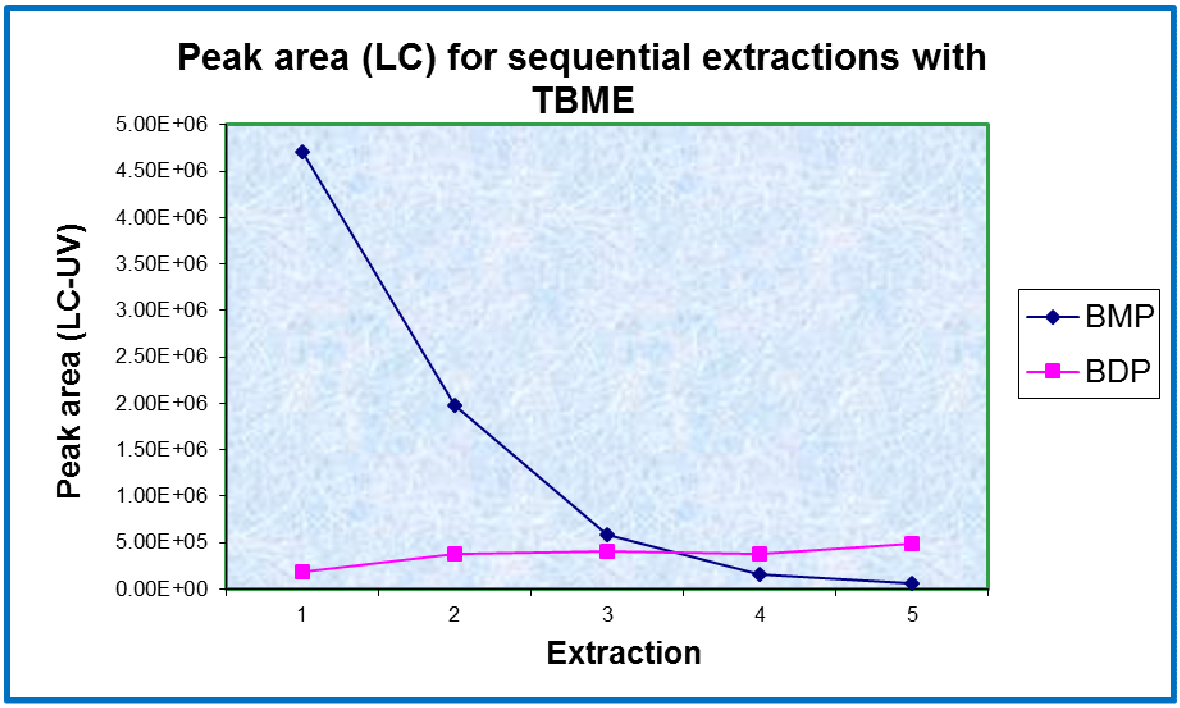

Figure 531: LLE with *tert*-butyl-methyl ether (TBME), five sequential extractions

Extraction of the final product was excellent with TBME as shown in the graph above (Fig. 51). However, a significant amount of the parent compound, BDP, was observed. It was concluded that, from all the solvents used, the best extraction was observed with ether.

1.8 Conclusion

Beclometasone dipropionate (BDP) was the first available inhaled corticosteroid used for the treatment of asthma. BDP is a prodrug that is metabolized by esterases in the human lung, liver and other parts of the body to three different metabolites, beclometasone-17-monopropionate (17-BMP), beclometasone-21-monopropionate (21-BMP) and beclometasone (BOH).

There are few reports in the literature in which pulmonary hydrolysis of esters has been investigated *in vitro*. The method reported here involved *in vitro* metabolism of BDP but using lyophilised porcine esterase instead of lung tissue. Samples of 17-BMP were successfully prepared using selective enzymatic hydrolysis which was in accordance with the literature, for example the investigation conducted by Nave and McCracken[41] in which BDP was hydrolysed to its active metabolite 17-BMP in 2-6 hours using human lung tissue slices. Therefore, the method presented in this chapter was advantageous as the rate of enzyme hydrolysis in this report was faster (the reaction was complete in 2-4 hours) and the requirement for use of lung tissues was removed.

A quick, simple, reproducible and specific LC-MS method for the quantitation of BDP and its metabolites 17-BMP and BOH has been developed and validated in accordance with the ICH guidelines. The accuracy, recovery and precision recovery of the method were within acceptable limits (accuracy and recovery ~100% while precision <10%) and has been successfully used to analyse samples from this study. The calibration curves obtained with this LC-MS method were linear over the concentration range used, 0.001-100 mg/L for BDP and 0.01-10 mg/L for BOH.

The hydrolysis reaction was successfully monitored using LC-MS and further confirmed by recording NMR spectra. The NMR experiments showed evidence for the rapid hydrolysis of BDP to 17-BMP (the major metabolite) *via* the esterase enzyme as expected from previously published studies using lung homogenates.[31,38,39] In addition, it has been found that if the ratio of enzyme to BDP is decreased it does not affect the rate of reaction.

Liquid liquid extraction (LLE) was carried out in an attempt to isolate pure samples of the metabolites of BDP. Four different solvents were compared and the best extraction results were obtained with ether with the recoveries within the

acceptable limits. The recovery of the required products was more than 95%. Previous studies have reported that optimal extraction was achieved with an ether-cyclohexane mixture.[33]

The results of stability tests showed that the three analytes were stable under the conditions investigated in this study.

In conclusion, this work showed that the proposed method has the advantage of rapidity and simplicity over those described in the literature, without using lung tissues.

1.9 Future Work

After development and validation of the LC-MS method for BDP and BMP the next step will be to scale-down these methods, *e.g.* using nano-LC, nano-LC-MS. Additional sensitivity is required to detect drugs at biological concentrations (typically ng/mL); usually samples are concentrated using an off-line SPE step but this can lead to sample losses.

Direct sampling using nano-LC could lead to improved quantitation methods. Furthermore, the applications of the methods to quantify BDP and its metabolites in very low volumes of urine and blood should be investigated. When analysing samples from adult test subjects, it is possible to obtain relatively large volumes of urine and blood for testing. However, in paediatric cases, sample availability is much more limited.

Future studies will aim to develop methods of quantifying BDP and its metabolites in very small volumes of biological fluids and to extend this methodology to analysis of dried blood spots so that finger prick blood testing for these analytes is feasible.

Chapter 2

Electronic *vs.* steric effects in the synthesis of a rhenium complex of progesterone

2.0 Electronic *vs.* steric effects in the synthesis of a rhenium complex of progesterone

2.1 Introduction

2.1.1 Biomolecules

A biomolecule, also called a biogenic substance, is any molecule that is produced by a living organism. This class of molecules includes both large macromolecules such as proteins, polysaccharides, lipids, and nucleic acids, and small molecules such as primary metabolites, secondary metabolites, and natural products.[50] Biomolecules are involved in metabolic processes and maintenance of living organisms, therefore methods for their detection and quantitation are essential. One such method involves "tagging" the biomolecule with a fluorescent label, enabling sensitive and specific detection.[51]

Recent advancements in analytical methods relating to organic chemistry, molecular biology, spectroscopy, engineering, and chemical biology have provided powerful tools to apply different fluorescent labelling techniques for analyzing molecular events in cells.[52] Fluorescence methods involve several unique experimental parameters, for instance excitation and emission wavelength, intensity and fluorescence lifetime.[53]

2.1.2 Luminescence

The word luminescence comes from the Latin *lumen*, meaning light, and was first introduced as "luminescenz" by the physicist and science historian Eilhardt Wiedemann in 1888, to describe 'all those phenomena of light which are not solely conditioned by the rise in temperature', as opposed to incandescence. Many important applications based on photoluminescence have been developed. Fluorescence microscopy, fluorescent tubes and lamps, optical brighteners, plasma screens, fluorescent and phosphorescent paints, phosphorescent labels, safety signs, and counterfeit detection (security documents, bank notes, art works) are a few examples of this. Luminescence occurs when a molecule absorbs energy and an electron is promoted into an excited state. The electron then decays to the ground

state. In any light-emitting process, the sample must absorb an appropriate amount of energy from a suitable source prior to emission of light.[54]

Luminescence is subdivided into a number of categories according to the origin of this energy. Examples include:

- Bioluminescence (emission of light by living animals and plants)
- Chemiluminescence (which may occur during the course of a chemical reaction and consecutive to absorption of energy by the reactant molecules) &
- Electroluminescence (light accompanying an electric discharge, for example in a rarefied gas, or after bombardment by electrons sometimes referred to as cathodoluminescence).

The various types of luminescence are classified according to the mode of emission, including:

- Fluorescence
- Phosphorescence, and
- Delayed fluorescence[54,55]

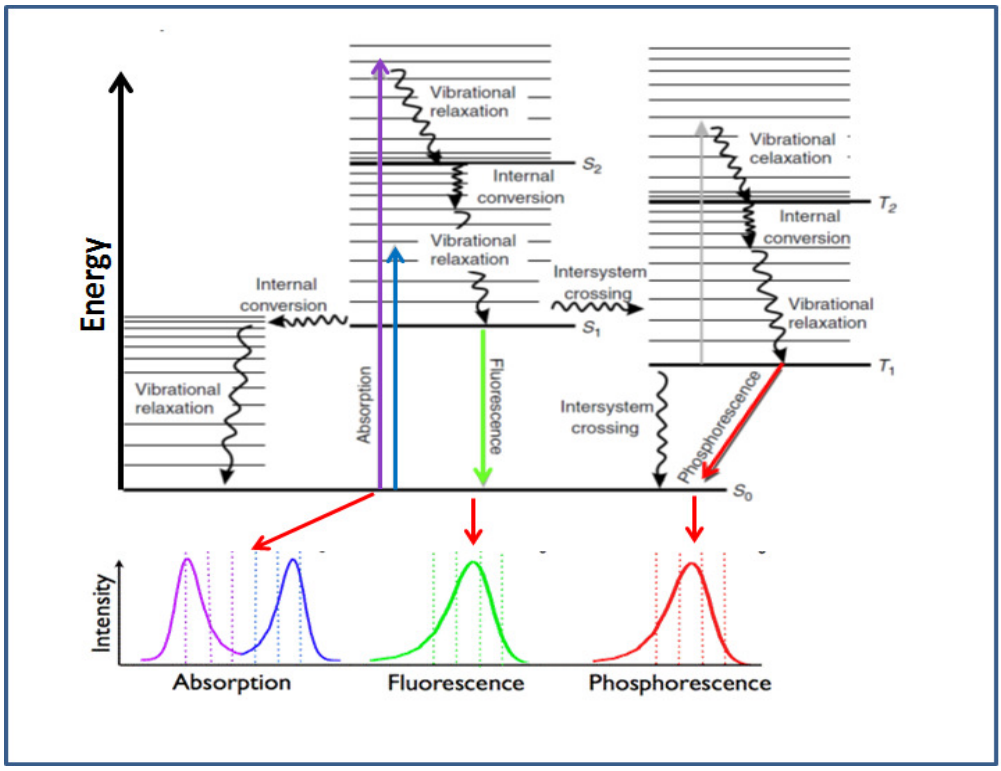

Figure 54: Jablonski diagram showing the electronic states of a molecule and transitions between them.[55]

A Jablonski diagram (Fig. 53) provides a good basic overview of the potential transitions within simple luminescent systems. Light energy is absorbed in order to excite an electron in to one of the singlet excited states from which point relaxation can occur. These principles are used in techniques such as fluorescence spectroscopy which has wide ranges of application in various disciplines of scientific/medical research.[55,56]

Tracking biomolecules (proteins, antibodies, amino acids, and peptides) often requires labelling with a "reporter group", which gives a response in the chosen analytical technique. At present, several labelling methods such as isotope markers, radioactive tracers, colorimetric biosensors, photochromic compounds, electrochemical sensors, and fluorescent labels are available for this purpose.[52] Fluorescence is now used extensively in biotechnology, flow cytometry, medical diagnostics, DNA sequencing, forensic science, and genetic analysis. Fluorescence detection is highly sensitive, and there is no longer the need for the expense and difficulties of handling radioactive tracers for most biochemical measurements. There has been dramatic growth in the use of fluorescence for cellular and molecular imaging. Among the labelling methods, fluorescent labelling has the upper hand due to its non-destructive nature; enhanced performance and simplicity.[57] Two types of fluorescent compounds are often used for bioconjugation: small organic fluorescent compounds, such as fluorescein, and fluorescent proteins that contain a covalently bound chromophore, such as phycobilliprotein. Both types can be used to label antibodies, proteins, and other biomolecules for detection purposes. Most of the common fluorescent compounds are very hydrophobic and not very stable.[58,59]

2.1.3 Luminescent Biological Labels and Probes

A biological label (or a labelling reagent) is a small molecule that can be covalently connected to a biomolecule such as an amino acid, protein or DNA. It contains a signalling group which offers detectable properties and a reactive portion which reacts with a specific functional group of a biomolecule. Luminescent labels and probes can be divided into several types.

Fluorescent organic molecules are the most commonly used. They are designed as chemical and biological probes due to their excellent absorptivity and emission quantum yields which provide remarkable detectability.

Various **lanthanide chelates** have also been employed as luminescent labels due to their extraordinarily long lifetimes and sharp emission bands.

Additionally**, luminescent transition metal complexes** have been widely developed as labelling reagents and probes, because of their intense and long-lived emission; also their emission energy can be tuned by using different ligands.[59,60,61,62]

2.1.4 Labelling of biomolecules with fluorescent compounds

Much work has been done on the labelling of biomolecules with fluorescent groups. Labelling is one of the most common methodologies used for bio-analytical purposes. The use of organic molecules in non-fluorescent labelling, in the ultraviolet and visible regions, is important in several applications. However, in recent years, detection based on fluorescence techniques has received special attention and notable progress has been made in both fluorescence instrumentation and synthesis of new compounds.[63]

The use of metal complexes in therapy and diagnostic imaging is increasing. Throughout history metals and metal compounds have been used in medicine to treat a variety of ailments. In the last century, metal complexes were used to treat diseases ranging from syphilis (organoarsenic compounds) to cancer (platinum anti-tumour drugs) to arthritis (gold compounds). The use of metal complexes as diagnostic agents is a relatively new area of medical research, and has flourished during the last 40 years. An even more recent development is the use of paramagnetic metal complexes for enhancing contrast of magnetic resonance imaging (MRI). In particular, luminescent transition metal complexes of Re(I) and Ru(II) have been recognized as good potential candidates.[64]

2.1.5 Luminescent rhenium(I) polypyridine complexes

Since the first systematic studies of the excited-state properties of luminescent Re(I) polypyridine complexes, their spectroscopic, photophysical, and photochemical properties have been attracting much interest for more than thirty years.[65,66] Re(I) complexes have attracted much attention due to their applications in luminescent biological molecular probes and photocatalysis. For example, Re(I) tricarbonyl polypyridine complexes have been used for luminescent bio-labelling, DNA probes and luminescent materials.[67] The isotopes of rhenium are primarily used as

therapeutic agents that results in the development of therapeutic ^{186}Re and ^{188}Re drugs based on ^{99m}Tc imaging agents. Bone metastasis treatment has been the major use of rhenium complexes to date.[64]

Among the transition metal complexes, rhenium(I) tricarbonyl complexes with a d_6 configuration have interesting photophysical and photochemical behaviour such as high stability and fairly strong emission in the visible region.[68] The advantages of using rhenium(I) complexes over other d_6 transition metal complexes are their ease of emission colour-tuning and longer-lived excited states, which are useful in the development of multicolour probes for time resolved applications such as fluorescence lifetime imaging microscopy (FLIM). Therefore, luminescent labelling reagents are an important addition to the family of Re(I)-based biological probes as they will enable the labelled biomolecules to possess luminescence properties, which could be applied in the design of new bioassays and imaging experiments.[69]

The aim of this project was to investigate new methods of labelling steroids with rhenium-containing luminescent labels, including progesterone and testosterone.

2.1.6 Progesterone

Progesterone (pregn-4-ene-3,20-dione, Fig. 54) is a 21-carbon steroid hormone which possesses ketone groups at carbons 3 and 20. It is synthesized in the ovaries, placenta and adrenal glands and prepares the body for conception and pregnancy and regulates the menstrual cycle. Although progesterone is thought to be a sex hormone of women, it is also synthesized in men.[70]

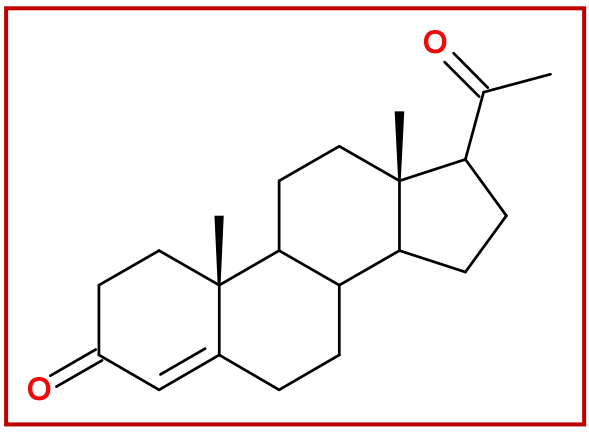

Figure 55: The structure of progesterone

Apart from the primary role of progesterone in women, progesterone derivatives find therapeutic application in men for the treatment of benign prostatic hypertrophy (BPH) and prostate carcinoma. The newer endogenous actions of progesterone in the CNS, including in traumatic brain injury, peripheral nerve injury, Alzheimer's disease and diabetic neuropathy, provide exciting therapeutic opportunities.[70]

2.1.7 Testosterone

Testosterone (4-androsten-17β-ol-3-one, Fig. 55) is one of the important sex hormones produced by the body. It is part of a class of male hormones called androgens. In men, testosterone is produced mainly in the Leydig cells of the testes and production is controlled by the brain's hypothalamus, and also the pituitary gland.[72]

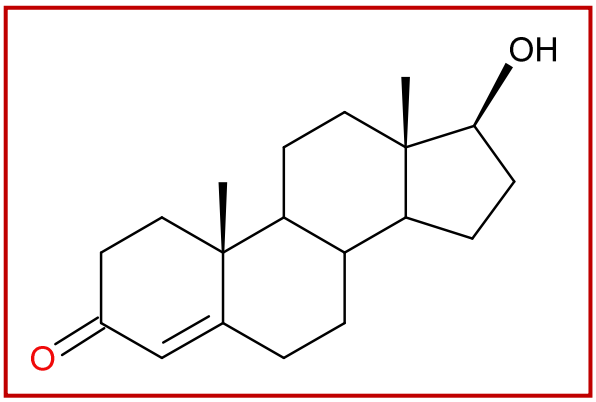

Figure 56: The structure of testosterone

Testosterone is responsible for:

1. promoting male secondary characteristics (*e.g.* increased muscle, hair and bone growth).[73,74]
2. a deep voice and a beard.[73,75]
3. growth of reproductive organs (*e.g.* testes and prostate) and sperm.
4. health and wellbeing as well as the prevention of osteoporosis.[71,72]
5. the maintenance of male reproductive organs and of spermatogenesis.

Testosterone is also metabolised into dihydrotestosterone which regulates the secretion of luteinising hormone and follicle stimulating hormone.[76,77] Circulating

concentrations of testosterone are approximately 15–25 times higher in adult men compared to women. Maintenance of these levels is necessary for development and maintenance of all secondary sexual characteristics described above.[78]

2.2 Steroids and co-ordination chemistry

The Harding group is interested in different areas of research including steroid quantitation and co-ordination chemistry. It was decided to combine both areas for this research project. Tagging of biologically important compounds is done mostly with organic fluorescence, which is mostly short lived and decays very quickly. Also, there are fluorescent compounds present naturally in the body which often exhibit auto-fluorescence. One of the challenges, however, is to differentiate the auto-fluorescence from that of the tagged compound which is applied specifically for study. The possible solution to this problem is perhaps the use of metal-based fluorescence. Luminescent metal complexes tend to exhibit longer-lived emission than organic fluorophores. Therefore, using metal-based fluorescence may enable use of *time-gated* luminescence measurements, which can discriminate fluorescence emissions at certain times. The time-gated luminescence technique has become a useful tool in life science and microbial ecology in recent years. The main advantage of this technique is that it can provide a method for eliminating short-lived, auto-fluorescence if the fluorescence lifetime of the metal-based fluorescent is much longer than the short-lived auto-fluorescence (typically a few ns) and hence the specific long-lived signal can be selected and measured (Fig. 56).[79]

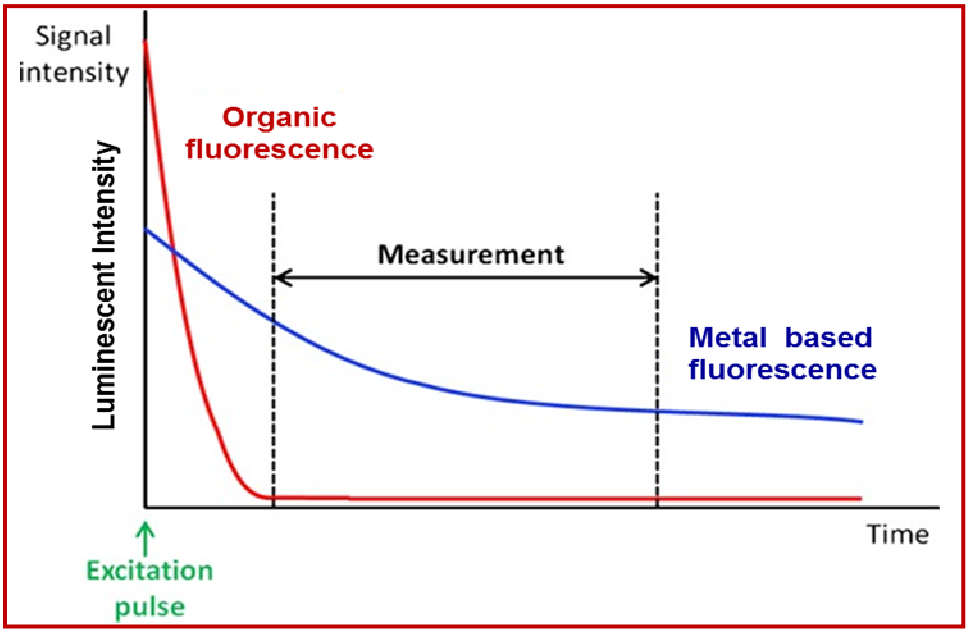

Figure 57: Time-gated fluorescence spectroscopy

2.3 Previous work

Work reported by Harding and co-workers have previously used the rhenium complex of 3,3'-diamino-2,2'-bipyridine (complex 1) as a fluorescent label for various biomolecules.[80] The two amine groups of the complex can react with aldehydes or ketones to form a cyclic aminal product (Fig. 57).

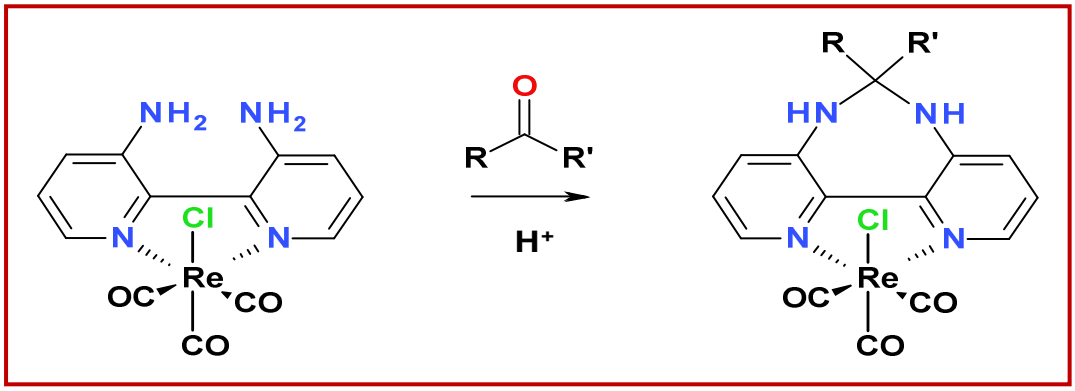

Figure 58: The general reaction of complex 1 with ketones

Previous work includes reaction of complex 1 with dihydrotestosterone (DHT) (Fig. 58).

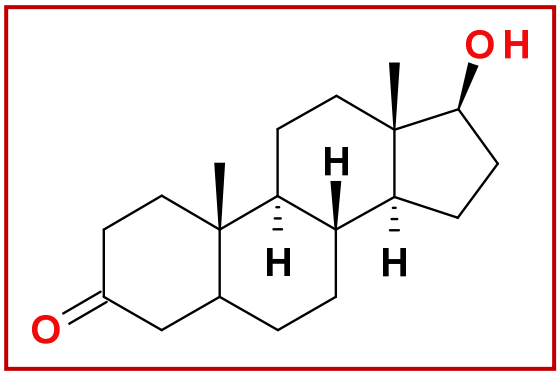

Figure 59: Dihydrotestosterone

DHT is a metabolite of testosterone; the only structural difference is that the double bond between positions 4 and 5 of testosterone (Fig. 57) is absent in DHT. Complex 1 was successfully reacted with DHT, forming two isomers (Fig. 59).

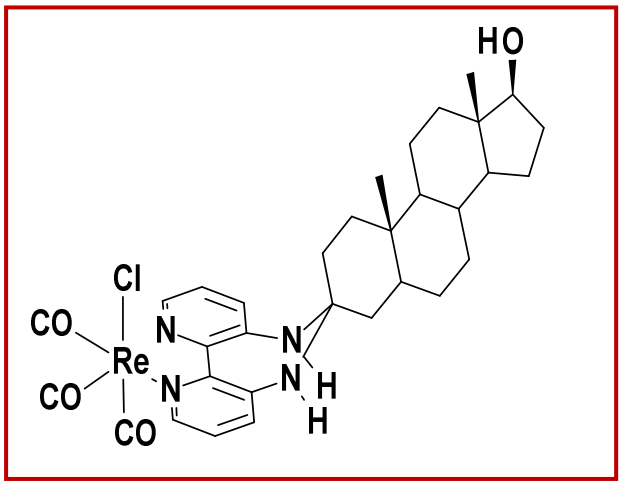

Figure 60 (a): Isomer 1[80]

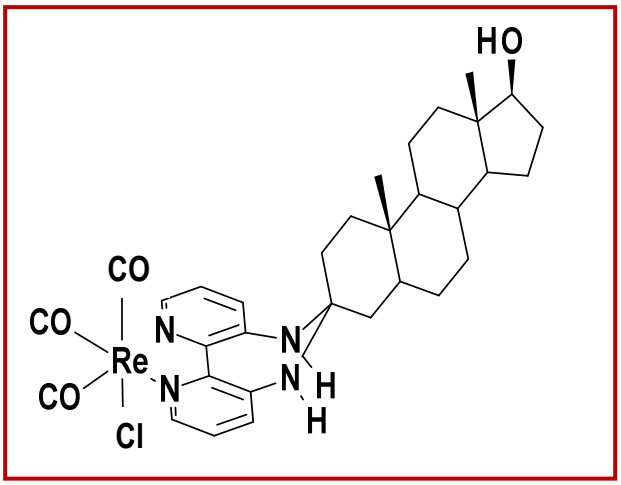

(b): Isomer 3[80]

2.4 Literature Review

The current widespread interest in the coordination chemistry of rhenium is mainly due to the potential therapeutic applications of the radioisotopes ^{186}Re and ^{188}Re in radiopharmacy. Technetium-based radiopharmaceuticals are already well established in diagnostic nuclear medicine. The chemistry of rhenium is characterized by the easily accessible oxidation states from -I to +VII, which readily interconvert under mild conditions. The most easily accessible oxidation state is Re(VII) and it is obtained by the mild oxidation of the metal and its complexes in the presence of oxidizing agents like nitric acid.[81] In recent years the use of complexes containing luminescent transition metal ions for biological interest has gained much attention. Lo *et al*. have reported a range of Re(I)- and Ru(II)-containing complexes which act as biomolecular probes, including biotin-transition metal conjugates as non-covalent probes.[82,83,84,85]

These authors focussed their work on the structural design of the metal complexes, the labelling and photophysical properties of the complexes and the biomolecules, biomolecular interactions, cellular uptake, and intracellular localization properties of luminescent transition metal complexes. The rich photophysical properties of luminescent inorganic and organometallic transition metal complexes made them excellent candidates for biological and cellular studies. They discussed some selected examples of the cellular up-take characteristics and cytotoxicity which can be used in the development of biological probes. The main challenge was the design of probes that were capable of sensing intracellular analytes such as oxygen, proton, ions, and small molecules. The cytotoxicity of transition metal complexes can be substantially reduced by introducing a biocompatible PEG pendant that protects the complexes from interacting non-specifically with extracellular biomolecules. Thus the results showed that the luminescent transition metal–PEG complexes had a strong potential to be applied as non-cytotoxic intracellular probes for various analytes. The formation of covalent adducts with nucleic acids and proteins and the possible inhibition of enzymes by metal complexes have been extensively studied. The possibility of using these complexes as photodynamic therapeutics has received much attention recently. They concluded that with the right choice of metal centres and ligands, as well as a selection of biologically-relevant substrates and reactive

functional groups, luminescent inorganic and organometallic transition metal complexes will continue to contribute to a wide range of biological applications.[86]

L. K. Kam-Wing, C. A. Wing-Tat and L. W. Ho-Tin in 2011 published a micro-review in which they describe the fundamental emission characteristics of luminescent rhenium(I) tricarbonyl polypyridine complexes. They discussed the basic photophysical properties of luminescent rhenium(I) tricarbonyl polypyridine complexes that are used as luminescent probes. They also included and discussed recent reports on the use of these complexes as labels and luminescent probes targeting biomolecules. Great importance was given to the rhenium(I)-labelled biomolecules which gave long-lived emission originating from the metal complexes. Also, the use of various ligands can vary the emission properties of these complexes. This enables them to function as cellular probes and imaging reagents. Furthermore, the addition of various groups and biologically relevant substrates into these complexes has also resulted in the development of new cellular probes for processes with an emphasis on studies of their structure–property relationships, bioconjugation, biomolecular binding, cellular uptake, cytotoxicity, and bioimaging applications.[87]

Harding and colleagues worked mainly upon luminescence from d-block metal ions. Fluorescent labelling of steroids is required for many applications, including immunoassays, receptor binding studies and fluorescence detection (*e.g.* in HPLC). They had discussed many fluorescent labelling reagents in use for derivatisation of steroids but they were mostly organic fluorescents which possessed a short lifetime. In this article a new route to simple, one-step functionalisation of dihydrotestosterone containing a ketone group in the 3- or 17-position has been developed, with a rhenium *fac*-tricarbonyl bipyridyl complex containing a diamino unit. Some examples of rhenium-containing androgen derivatives have also been reported.[80]

D. E. Reichert and colleagues presented a review which summarizes some of the developments of metal complexes and metal-complex bio-conjugates for the diagnosis of disease that have occurred over the past 10 years. They highlighted metal complexes that have been synthesized and evaluated *in vivo* over the last 10 years. This review gave insight to the significant progress made in the field of

coordination chemistry especially metal based radiopharmaceuticals. Radiometals used as labels for biomolecules were used for diseases such as neurological disorders[88] and diagnosing cancer.[89] the discovery of attaching metal complexes to smaller and larger biological molecules[90-92] revolutionized research in the field of bio conjugates. Metal complexes attached to biomolecules allow even more specific biological processes to be studied, including the formation of thrombi[93], the imaging of brain and renal infection[94,95], and the understanding of antigens and receptors found in certain types of cancer.[96] The radiolabeling of antibodies for the detection of cancer in the early 1970s[97,98] marked the beginning of the use of radiolabeled proteins and peptides for targeting antigens and receptors that are up regulated in tumours. Metals and metal compounds were in use in medicine to treat a variety of ailments. In the last century, metal complexes were used to treat diseases ranging from syphilis to cancer to arthritis. The first isotope used in medicine was iodine-131, which in 1946 was used to treat thyroid cancer. Today, there are a wide variety of radiometals and radiometal complexes used in medical practices. An even more recent development was the use of paramagnetic metal complexes for enhancing contrast of MRI. Designing metal complex-based imaging agents require consideration of their redox properties, stability, stereochemistry, charge and lipophilicity of the metal complex. The isotopes of rhenium are primarily used as therapeutic agents, and this has led to the development of therapeutic ^{186}Re and ^{188}Re drugs based on imaging agents.[99]

2.5 Experimental

2.5.1 Materials

The rhenium complex of 3-3'-diamino-2,2'-bipyridine (complex 1) was prepared by other group members according to literature methods.[80]

Progesterone and testosterone were purchased from Fluka chemicals (purity 99 %).

Camphorsulfonic acid (CSA), was purchased from Sigma.

Solvents

Acetonitrile, methanol, ethanol (certified HPLC grade), cyclohexanone, hexane, dichloromethane (DCM), dimethylsulfoxide (DMSO) and diisopropyl ether (DIPE) were purchased from Fisher Scientific (UK).

Deuterated solvents were purchased from Goss Scientific.

Ultrapure water was either purchased from VWR or produced in-house using a Barnstead NanoPure (Thermo scientific).

Stock solutions and working solutions were prepared by successive dilution with MeCN.

2.5.2 Instrumentation

2.5.2.1 Liquid Chromatography Mass Spectroscopy (LC-MS)

Chromatographic separation was developed on a Shimadzu Prominence UFLC system and Lab Solutions v. 5 software was used for the processing of the data (Schimadzu Corporation UK). It is an ultra-high-speed prominence LC-20AD XR that achieves both ultra-high-speed analysis and ultra-high separation, based on high analysis precision and reliability comprising of prominence System Controller, schimadzu Solvent Delivery Unit, prominence AutoSampler (SIL-20A XR), prominence Column Oven (CTO-20A), Schimadzu Fluorescence Detector (RF-10A XL, prominence Diode Array Detector (SPD-M20A) and prominence Degasser (DGU-$20A_3$.

The column used was a Lichrospher 100, RP-18 (250 mm x 4.6 mm, 5 µm), column purchased from VWR (Merck, Germany). The mobile phase (A) was HPLC grade water and mobile phase (B) was acetonitrile. The flow rate was kept constant at 1.00 mL/min. The injection volume was 20 µL. The eluent UV absorbance was monitored using a diode array detector and monitored at a wavelength of 240 nm for the steroids.

The samples were analysed by a Bruker MicrOTOF-Q mass spectrometer coupled to the UFLC system to facilitate the study of BDP standards and metabolite formation. The mass spectrometer was a hybrid quadrupole/orthogonal accelerated Time-of-Flight equipped with an electrospray ionization (ESI) ion source. Positive ion ESI was chosen. Data acquisition and processing was carried out using Bruker's proprietary DataAnalysis software.

For the analysis of complex 1 and its derivatives the mobile phase (A) was HPLC water and mobile phase (B) was MeCN. The flow rate was kept constant at 1.00 mL/min. The injection volume was 20 µL. The eluate UV absorbance was recorded using a diode array detector and monitored at wavelengths of 275 nm and 379 nm (Table 29).

HPLC	Shimadzu UFLC
Mode	Isocratic
Analytical Column	Lichrosphere 100, RP-18 (250 mm x 4.6 mm, 5 µm), column no. 026023 Lot No. 497017
Injection Port Type	Manual
Syringe Volume	50 µL
Injection Volume	20 µL
Mobile Phase A (HPLC water)	40 %
Mobile Phase B (MeCN)	60 %
Column Flow	1.0 mL/min
Detector	UV at 275 and 379 nm
Run Time	30 minutes

Table 29: Instrumental parameters for the analysis of complex 1 and its derivatives

The samples were also analysed by a Bruker MicrOTOF-q mass spectrometer (Bruker daltonics Corporation, Germany) coupled to the UFLC system to facilitate the study. Positive mode electrospray ionisation was chosen. Data acquisition and processing was carried out using Bruker's proprietary DataAnalysis software.

2.5.2.2 Preparative High Performance Liquid Chromatography (HPLC)

Preparative separations were carried out on a Gilson preparative HPLC system Model-803C mono-metric module, using Gilson Piston Pumps Model 303 and 305. The column used was a Dynamax, pre-packed C_{18} column module, 21.4 mm I.D x 250 mm, serial No. B910924. The detector was a Gilson HM Holochrome

UV-VIS using 286 nm wavelength. The data was collected on a chart recorder (Kipp and Zonen BD 40) and integrator. The mobile phase (A) was MeCN, 65 % and mobile phase (B) was HPLC water, 35 %. The flow rate was kept constant at 10.00 mL/min. The run time was 60 min (Table 30).

HPLC	Gilson model 303 & 305 pump,
UV Detector	Gilson HM Holochrome UV/VIS
Chart Recorder	Kipp & Zonen BD 40 (5 mm/min)
Mode	Isocratic
Prep - Column	Dynamax – 60 A
Injection Port Type	Manual
Syringe Volume	1.5 ml
Injection Volume	20 µL
Mobile Phase A (MeCN)	65 %
Mobile Phase B (HPLC water)	35 %
Flow Rate	10 mL/min
Run Time	60 min

Table 30: Instrumental parameters for preparative separations

2.5.2.3 Nuclear Magnetic Resonance (NMR)

NMR spectra were acquired on a Bruker Avance 400 MHz or Bruker Avance 500 MHz NMR spectrometer using Bruker Topspin software. Spectra were recorded at room temperature. Thin-layer chromatography (TLC) was performed on Merek Silica gel 60 F_{254} TLC cards and Aluminium oxide/TLC cards by Fluka (Sigma Aldrich). The samples were dried using a Savant DNA 120 Speed vac Concentrator.

2.5.2.3 X-ray Chrystallography

For this analysis Single crystal X-ray diffraction data was collected on a Bruker APEX II DUO (3-and 4-axis configurations) equipped with a graphite monochromated Mo(Kα) radiation source and a cold stream of N_2 gas and refined using APEX 2 software.

2.6 Methodology

2.6.1 Method development for complex1-cyclohexanone

2.6.1.1 A. complex 1-cyclohexanone, as a method development model

To develop a LC method with cyclohexanone, as a model compound for the steroids, various conditions were tried. A reaction (on small scale) was performed with complex 1 and cyclohexanone to obtain the aminal product. To set a method protocol for the cyclohexanone standards of complex-1 and cyclohexanone was run. It was followed by mixed run of both the compounds at different mobile phase concentrations and flow rates to obtain well separated peaks. Reaction mixture was prepared by dissolving complex 1 (1 mg) in MeCN (1 mL) and to this was added cyclohexanone (1 µL) and few grains of camphor sulfonic acid (CSA) as a catalyst. The mixture was left heating for 2 hrs.

2.6.1.2 B. Reaction of complex 1 with cyclohexanone, as a method development model

To develop a method for the reaction of complex 1 with cyclohexanone, various conditions were optimised to conduct an investigation on large scale.

Reaction mixture was prepared by dissolving complex 1 (20 mg) in MeCN (2 mL) and to this was added cyclohexanone (20 µL) and few grains of camphor sulfonic acid (CSA) as a catalyst. The mixture was left heating for 6 hrs at 60° C in the dark. TLC (5% MeOH in DCM) was done on alumina plate. Separation and collection of the fractions were done on preparative HPLC, dried in DCM and analysed by using NMR and crystallography.

2.6.1.3 Detection Methods (Identification of Analytes)

Firstly, standards of complex 1 and cyclohexanone were run separately to find their retention times. Then, a 100 ppm mixed solution of complex 1 and cyclohexanone was run at different percentages of mobile phase (MeCN) and different flow rates to obtain sharp and well-separated peaks of both the analytes. Table 31 below summarises the methods used.

S.No	Conc. of Solution [mg/L]	B % [HPLC]	Flow Rate [ml/min]
1	100	60	1
2	100	60	1.5
3	100	40	1
4	100	40	2
5	100	70	0.5
6	100	30	2
7	100	40	0.5
8	100	30	0.5
9	100	30	1

Table 31: Method development for the analysis of complex 1 and cyclohexanone

Method 9 was found to give optimum separation. It was decided to use this method for further analysis.

2.6.2 Method optimization and validation for complex1-cyclohexanone

2.6.2.1 Stock solutions

Complex 1

A stock solution of complex 1 was prepared in MeCN at a concentration of 500 ppm equivalent to 1.0 mL of stock solution. Complex 1 (0.5 mg) was weighed on a Mettler analytical balance and put into an eppendorf tube.

The stock solution was made by dissolving the weighed amount in MeCN (1.0 mL) to achieve a clear solution with the final concentration of 500 ppm (0.5 mg/1.0 mL). After preparation the stock solutions were covered in aluminium foil, labelled and stored in the dark for future use.

Cyclohexanone

A stock solution was prepared by dissolving 10 µL cyclohexanone in 1 mL of MeCN to make a 9470 ppm stock solution.

2.6.2.2 Working solutions

Cyclohexanone

From the stock solution, 0.01 mL was measured and added to MeCN (0.99 mL) to give a solution of 94.7 ppm (1.0 mL).

Mixed run of complex 1 and cyclohexanone

A mixed solution of complex 1 and cyclohexanone was prepared as follows; an aliquot (0.2 mL) was pipetted from the 500 ppm stock solution of complex 1. To this solution was added cyclohexanone (0.01 mL) and MeCN (0.79 mL) was added to make the final volume 1.0 mL.

2.6.2.3 Experimental protocol (small scale) of complex 1 and cyclohexanone (small scale)

A reaction solution was made on a small scale to check the method and the data was collected using LC-MS.

2.6.2.3.1 A.Reaction mixture of complex 1 and cyclohexanone

A reaction was performed with complex 1 and cyclohexanone to obtain the aminal product. Complex 1 (1 mg) was dissolved in MeCN (1 mL) and to this was added cyclohexanone (1 µL) and few grains of camphor sulfonic acid (CSA) as a catalyst. The mixture was left heating for 2 hrs and aliquots were removed and analysed after every 20 minutes.

2.6.2.3.2 B. Reaction mixture of Complex 1 and progesterone

Peak identification – Progesterone

To detect the peak of progesterone, a small amount of the steroid (standard) was dissolved in MeCN (1 mL) and analysed using HPLC at 240 nm wavelengths to determine the retention time.

Experimental protocol of progesterone (small scale)

Four experiments were performed with different amount of (equivalence) progesterone in order to obtain the required results.

Experiment - 1

For this reaction, the mixture was prepared as follows: Complex 1 (1 mg) and progesterone (1.28 mg, 2 eq.) were dissolved in MeCN (1 mL) and few grains of CSA were added. The reaction tube was secured with parafilm, incubated in a water bath at 60 °C and incubated for several hrs in the dark; after every 30 min to one hour an aliquot was removed and was analysed using LC-MS**.**

Experiment – 2

The experiment was repeated and the method followed was the same as Experiment 1 above except that the amount of progesterone was increased to 2.56 mg (4 eq.).

Experiment – 3

In this experiment the method followed was same as Experiment 1 above except for the amount of progesterone which was increased to 3.84 mg (6 eq.).

Experiment – 4

The amount of progesterone was increased to 6.4 mg (10 eq.); other parameters were the same as in previous experiments.

2.6.2.3.2.2 Timed NMR experiment for progesterone

The NMR reaction was performed on small scale first using complex 1 (2 mg) and progesterone (12.8 mg) dissolved in d_3-MeCN (650 µL) with a few grains of CSA in an NMR tube. The tube was incubated in a water bath at 60 °C for 2 hrs. in the dark. The reaction mixture was analysed using NMR as shown in Fig. 58.

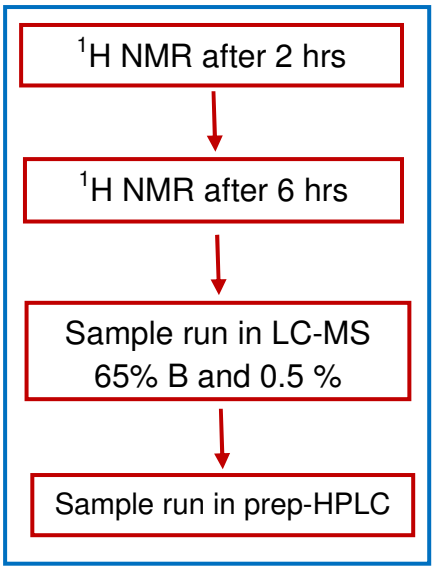

Figure 58: General experimental protocol of NMR timed reaction

Preparative High Performance Liquid Chromatography (HPLC) (large scale)

Complex 1 (50 mg) and progesterone (320 mg) were dissolved in d_3-MeCN (3 mL) and a few grains of CSA were added. The reaction tube was incubated in a water bath for 6 hrs, in the dark, at 60 ℃. After every hr, the ^{1}H NMR spectrum was recorded to observe the changes in the starting materials. That was carried on for six hrs. After 6 hrs heating, another ^{1}H NMR was taken and compared with the ^{1}H NMR of starting material (complex 1). An aliquot (25 µL) was removed from this reaction mixture and MeCN (0.50 mL) was added, the solution mixed thoroughly and then analysed using LC-MS.

The next step was to isolate the pure product. It was decided to use preparative HPLC to collect a workable amount of pure compound and to try to crystallize the product. The sample (in 1 mL aliquots) was run on the preparative HPLC which recorded the graph on a chart recorder. In order to get the pure form, fractions were collected after every 30 sec. from the onset of the progesterone peak, for approximately 24 min in total.

For isomer 1, fractions 99 – 112 were collected, combined, extracted into DCM after removal of MeCN on the rotary evaporator and dried. For isomer 2, fractions 125 – 140 were collected. The same steps were repeated for these fractions. The proton NMR spectra were acquired in d_3-MeCN. After NMR analysis, fraction 2 was purified using column chromatography (SiO_2, 10 % MeOH in DCM). The column showed three bands, one of the bands contained more material than the other two and was

analysed using ^{1}H NMR. The NMR spectrum showed that it was a mixture but it contained more product compared to fraction 1.

Yellow crystals of X-ray quality were obtained by slow evaporation of MeCN. These were analysed on a Bruker APEX II DUO (3-and 4-axis configurations) and refined using APEX 2 software.

Crystal data for {**1**-Progesterone} ($C_{34}H_{38}ClN_4O_4Re_1$): M = 788.33; Monoclinic, $P2_1$, a = 8.2794(4), b = 14.2628(7), c = 13.7207(6) Å, β = 104.9290(10) °; V = 1565.55(13) Å^3, Z = 2; ρ_{calc} = 1.672 Mg m^{-3}, F(000) = 788; dimensions 0.40×0.15×0.01 mm; $\mu(Mo_{K\alpha})$ = 4.012 mm^{-1}, *T* = 150 (2) K. A total of 23647 reflections were measured in the range 1.54 ≤ θ ≤ 33.14 ° (*hkl* range indices: -12≤*h*≤12, -21≤*k*≤18, -21≤*l*≤20), 10735 unique reflections (R_{int} = 0.0369). The structure was refined on F^2 to R_w = 0.0567, R = 0.0305 (9501 reflections with $I > 2\sigma(I)$) and GOF = 0.872 on F^2 for 400 refined parameters, 1 restraint. Largest peak and hole 1.466 and -0.858 eÅ^{-3}.

2.6.2.3.3 C. Reaction mixture of complex 1 and testosterone

2.6.2.3.3.1 Experimental protocol (small scale)

Complex 1 (2 mg) and testosterone (11.71 mg, 10 eq.) were dissolved in d_3-MeCN (0.650 mL) and a few grains of camphor sulfonic acid (CSA) were added. The solution was heated for 1 hr in a water bath at 60 °C and analysed using ^{1}H NMR. Four experiments were performed according to the general experimental protocol as described below in Fig. 60.

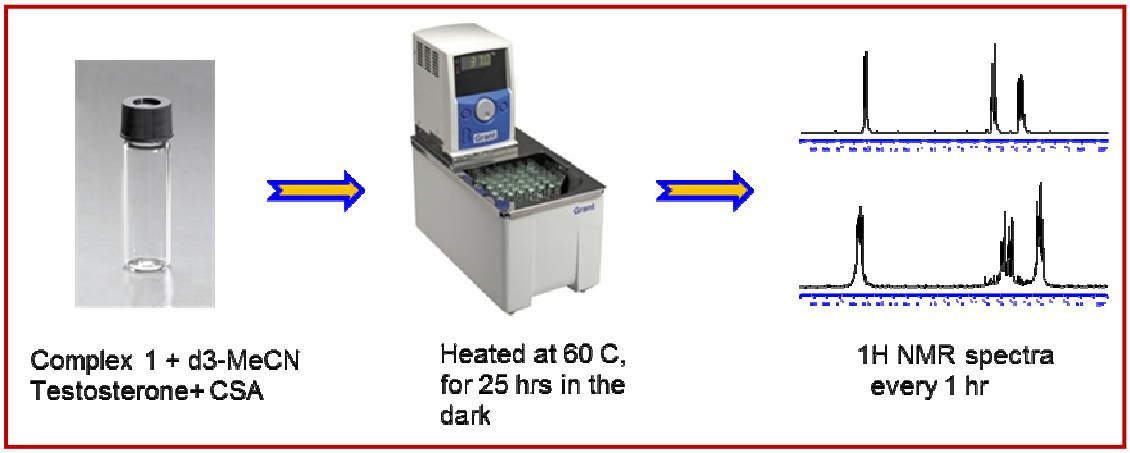

Figure 61: General experimental protocol of complex 1 with testosterone

The reaction mixture was heated for 1 hr in a water bath at 60 ℃ and then analysed using ^{1}H NMR. The sample was heated for further 1 hr period and analysed by NMR until it had been heated for a total of 11 hrs. This was continued the following day when it was heated for 2 hrs period before acquisition of the proton NMR spectrum, to a total of 25 hrs of heating.

2.6.2.3.3.2 Experimental protocol of complex 1 and testosterone (large scale)

The reaction mixture was prepared by dissolving complex 1 (30 mg), and testosterone (176 mg, 10 eq.) in MeCN (3 mL) and adding a few grains of CSA. The reaction tube was heated at 60 $^{\circ}$C in a water bath for 18 hrs in the dark. The reaction was monitored by TLC (SiO_2, 5 % MeOH in DCM) until all of the starting material had been consumed. To confirm the presence of the product, an aliquot of the reaction mixture (25 µL) was mixed with MeCN (0.5 mL) and this sample was analysed using LC-MS at 65% B and 0.5 mL/min flow rate. Also testosterone (0.5 mg) was dissolved in MeCN (0.5 mL) and analysed as a standard to facilitate peak identification. The remaining sample was dried in a Savant DNA 120 Speed vac Concentrator (20 min) and the remaining reaction mixture was put in a freezer.

The purification of the crude product *via* column chromatography (Al_2O_3, MeOH in DCM) gave yellow coloured product. Fractions containing the product were combined, dried, and dissolved in MeCN (1.0 mL); this sample was then diluted approximately. From the above sample, an aliquot (0.25 mL) was removed and mixed with MeCN (0.75 mL - 1.0 mL) and analysed using HPLC at 65% MeCN and 0.5 mL/min flow rate.

Preparative High Performance Liquid Chromatography (HPLC)

It was decided to use preparative HPLC to collect a workable amount of pure compound to try to crystallize the product. The sample (in 1 mL aliquots) was separated on the preparative HPLC. In order to get the optimum separation, fractions were collected after every 30 seconds from the start, *i.e.* T=0. The conditions used on the preparative HPLC were as shown in Table 32.

Method No.	2
Range	1.0 AUFS
Frequency	286 nm
Pressure	88 bar
MeCN (A%)	65%
H_2O (B%)	35%
Flow rate	10 mL/min
Run time	60 min

Table 32: Instrumental parameters for preparative separations

The sample was dissolved in MeCN (3 mL), at which point a small amount of yellow precipitate formed which was removed using vacuum filtration. The filtrate (in 0.5 mL aliquots) was then separated using the preparative HPLC using the conditions shown above. Samples were collected every 30 sec in labelled vials. However, in the initial experiment the peaks recorded were quite small, so it was decided to change the range from 1.0 to 0.5 AUFS.

Two isomers were identified from the chromatogram and selected fractions of each isomer were combined. The acetonitrile was removed by rotary evaporation and the remaining aqueous solution for each isomer was extracted into DCM, dried ($MgSO_4$) and evaporated to dryness under vacuum. The ^1H NMR spectra of both isomers were acquired in CD_3CN. The NMR spectra showed that isomer 2 contained more products. Crystallisation of isomer 2 was attempted in two ways:

(a) By solvent diffusion of DIPE into an acetonitrile solution of isomer 2
(b) A small amount of the sample was dissolved in MeCN and placed in the fridge.

Unfortunately, attempts to crystallise this sample have so far been unsuccessful.

2.7 Results and Discussion

Liquid chromatography is a fundamental separation technique in the life sciences that combines the resolving power of liquid chromatography with the detection specificity of mass spectrometry. Liquid chromatography (LC) separates the sample components and then introduces them to the mass spectrometer (MS). The MS creates and detects charged ions. LC-MS systems facilitate the analysis of samples that traditionally have been difficult to analyze.

Cyclohexanone was used as a method development model for the reaction between complex 1 and steroids (Fig. 61, Scheme 1), and their subsequent analysis by liquid chromatography coupled with mass spectrometry (LC-MS), since it replicates the "A" ring of the steroid but is cheaper and available in larger quantities.

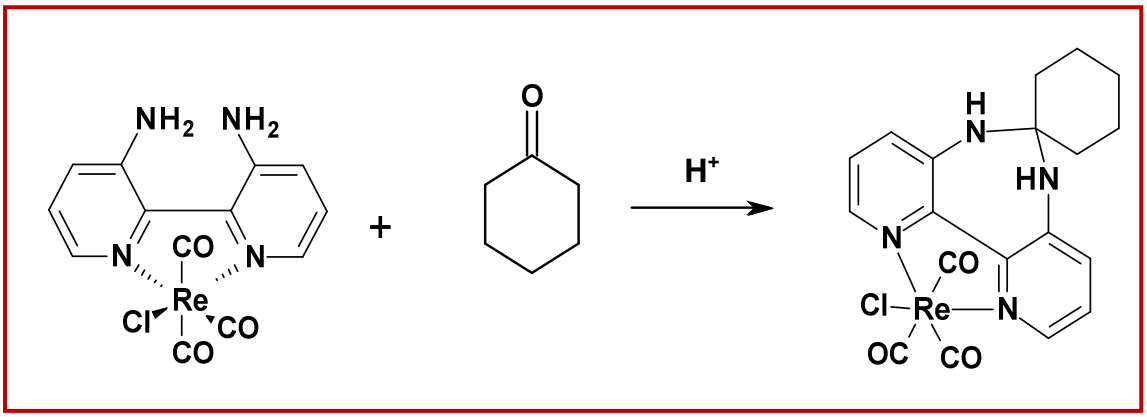

Figure 62: Scheme 1: Reaction between complex 1 and cyclohexanone to form the 1-cyclohexanone product

2.7.1 Determination of retention times of the starting materials

Complex-1

A 100 ppm solution of complex 1 was analysed using LC-UV and the peak from the compound appeared at RT 5.57 min. at 60% B MeCN and 1.0 mL/min flow rate using 379 nm wavelengths (Fig. 62).

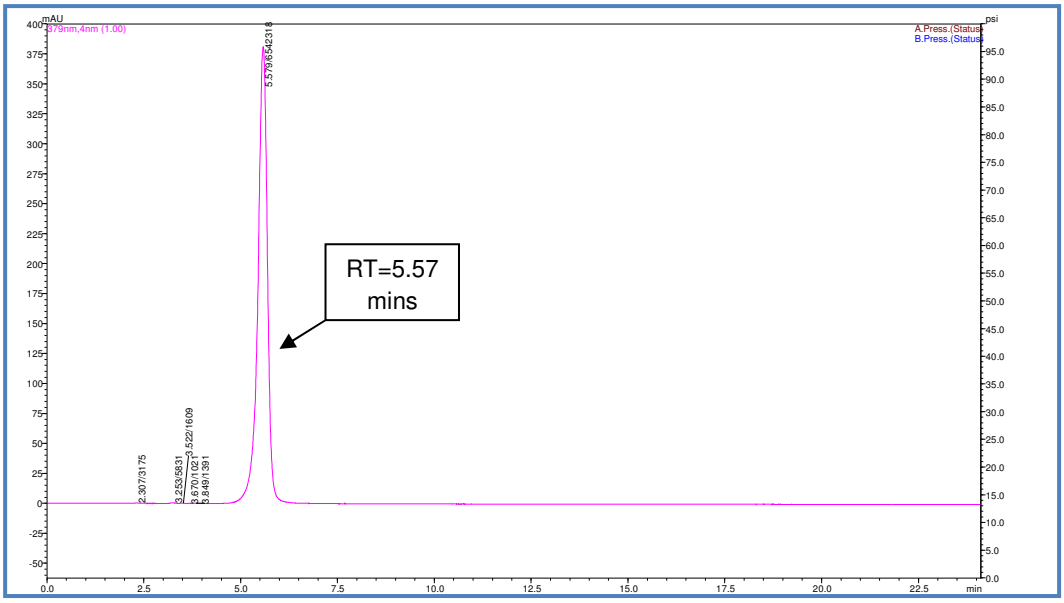

Figure 63: LC-UV chromatogram showing complex1, (100 ppm), 60 % MeCN, 1.0 mL/min flow rate, 379 nm

Cyclohexanone

A 100 ppm solution of cyclohexanone was analysed using LC-UV giving a retention time of 11.26 min. at 60% B MeCN and 1.0 mL/min flow rate using 286nm wavelength (Fig. 63).

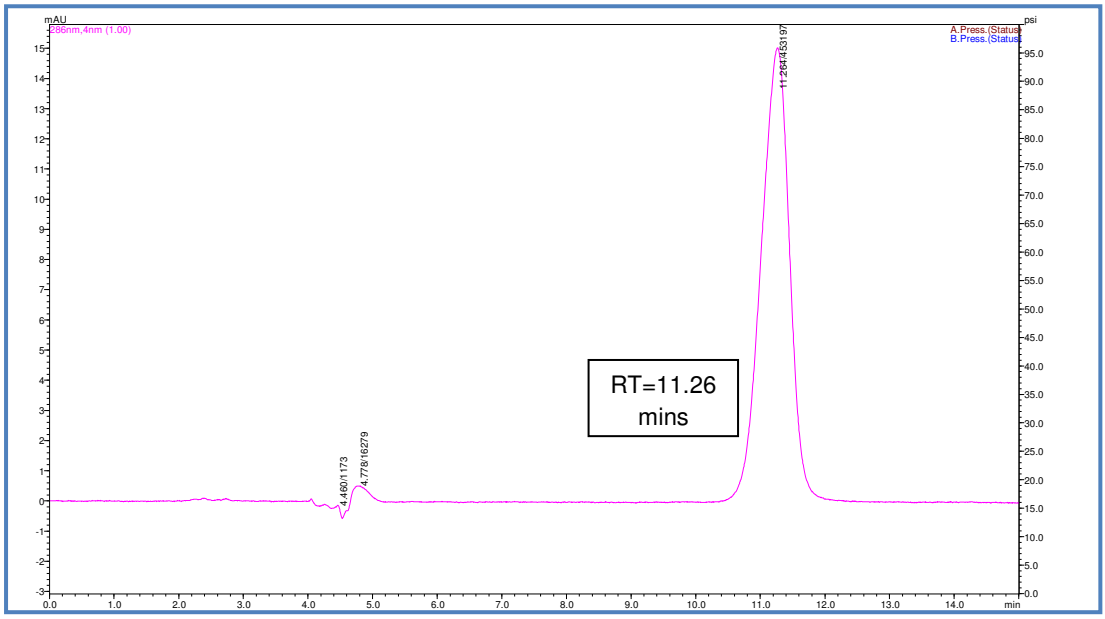

Figure 64: LC-UV chromatogram showing cyclohexanone, (100 ppm), 60 % MeCN, 1.0 mL/min flow rate, 286 nm

Mixture of complex 1 and cyclohexanone

A mixture of complex 1 and cyclohexanone was analysed to optimise separation of the starting materials. Many methods were tried to get the best separation. The best method for separation of complex 1 and cyclohexanone was found to be method 9 (30 % MeCN and 1.0 mL/min flow rate), which gave excellent detection, separation and retention time. It was therefore decided to use this method for further analysis.

2.7.2 A. Method development of complex 1 & cyclohexanone

A timed reaction of complex 1 with cyclohexanone was carried out using the newly developed chromatographic method (30 % MeCN, 1.0 mL/min). A solution of complex 1 (1 mg) and cyclohexanone (1 µL) in MeCN (1mL) with a few grains of CSA was heated in the dark. The reaction was monitored for 2 hrs. Aliquots were removed and analysed using HPLC at 0 min, 20, 60, 90 and 120 min.

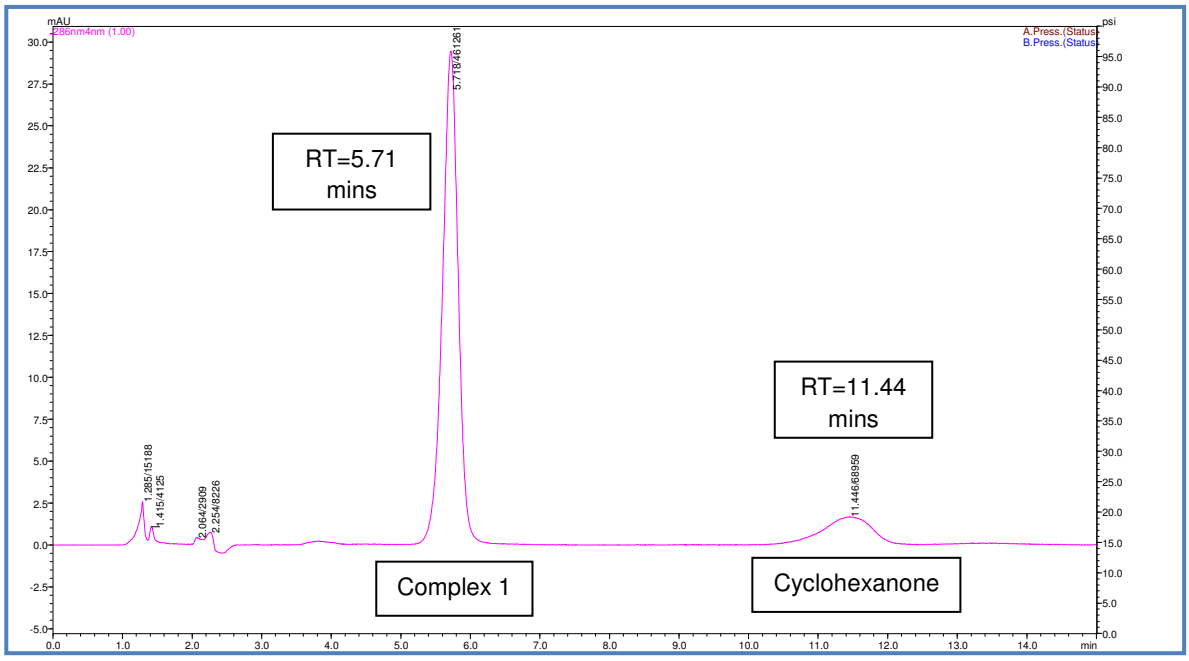

Figure 65: LC-UV chromatogram of the complex 1 and cyclohexanone reaction (100 ppm), 30 % B and 1.0 mL/min flow rate (t=0 min)

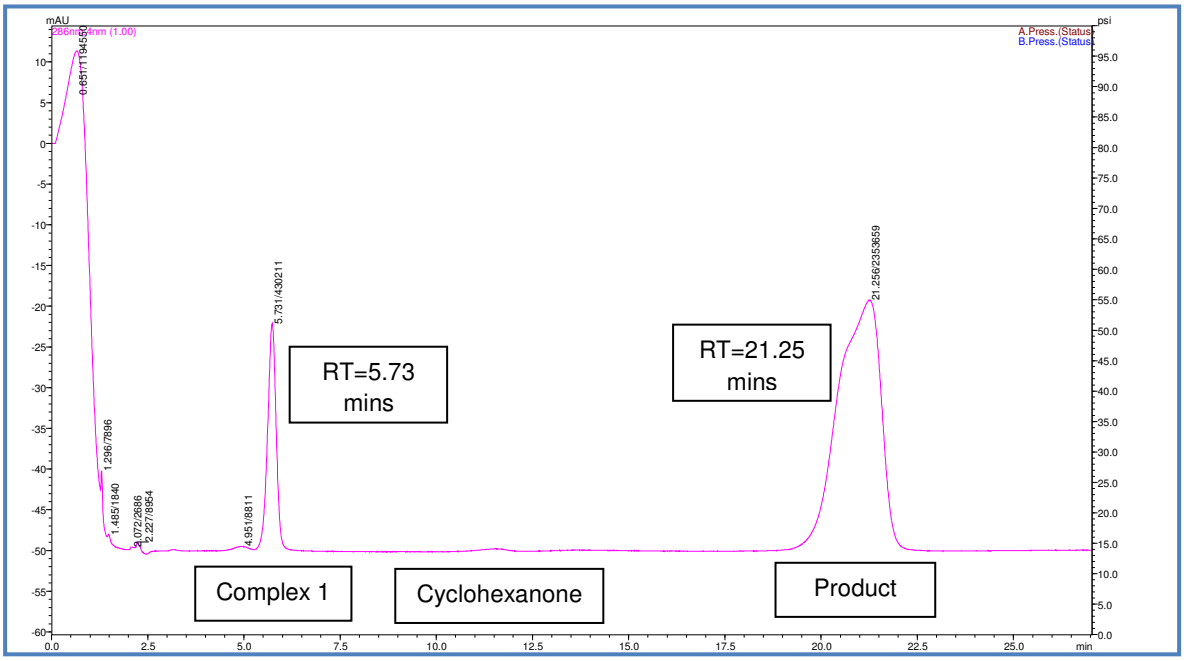

Figure 66: LC-UV chromatogram of the complex 1 and cyclohexanone reaction (100 ppm), 30 % B and 1.0 mL/min flow rate (t=60 min)

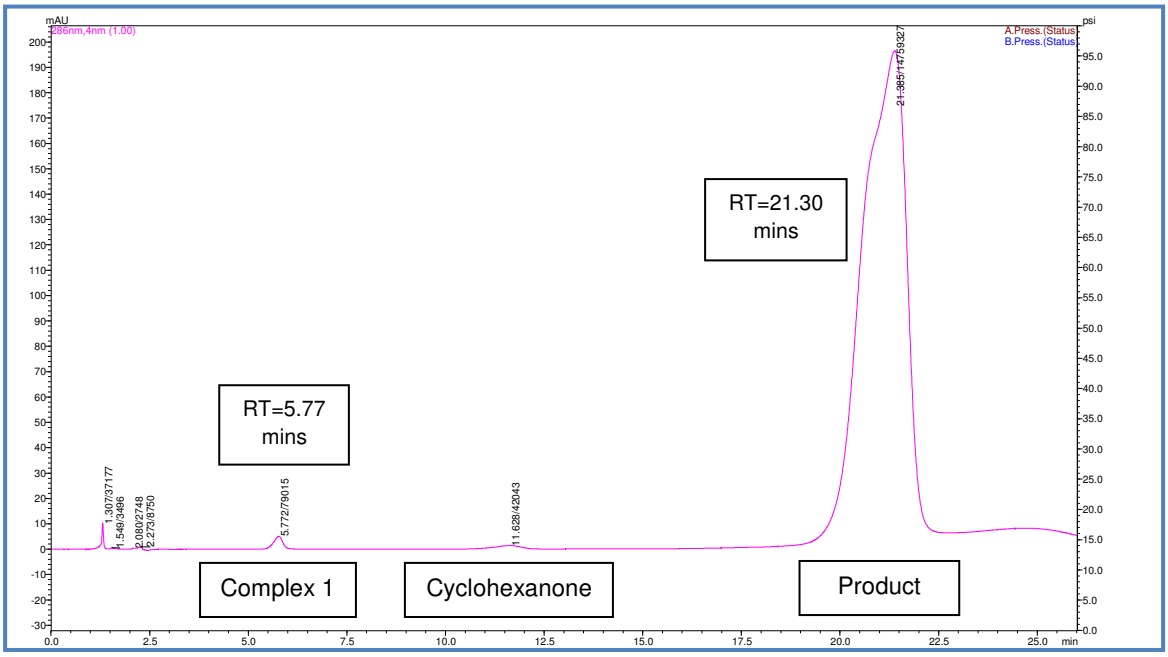

Figure 67: LC-UV chromatogram of the complex 1 and cyclohexanone reaction (100 ppm), 30 % B and 1.0 mL/min flow rate (t=120 min)

The results in Figs. 64, 65 and 66 show that complex 1 reacted well with the cyclohexanone. It seemed that the two expected isomers of the product were

overlapping at around 21 min. However, the retention time of the two peaks was excessively long (more than 15 min). It was therefore decided to reduce the retention time by using different percentages of mobile phase (MeCN) and different flow rates to obtain a shorter analysis time, as shown in Table 33 below.

S.No.	Solvent B (%)	Flow rate (ml/min)
1	40	1
2	50	1
3	50	0.5
4	**55**	**0.5**

Table 33: MeCN compositions and flow-rates of the selected methods

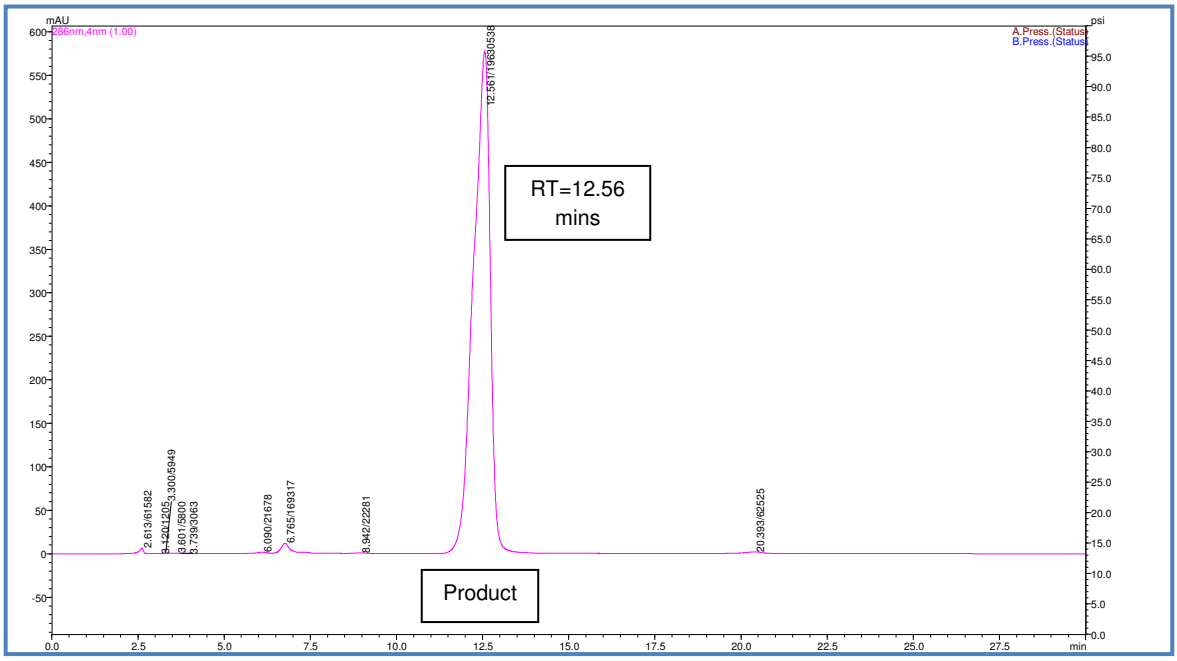

Figure 68: LC-UV chromatogram of the complex 1 and cyclohexanone reaction, 55 % B and 0.5 mL/min flow rate (t=180 min)

Excellent separation of the analytes was observed in the chromatogram (Fig. 67) and the retention time of the product was also reasonable (12.56 min). So within 20 min the reaction can be monitored easily.

2.7.3 B. Method development of complex 1 & Progesterone

2.7.3.1 Timed liquid chromatography mass spectroscopy (LC-MS) experiment

As the reaction of complex 1 with cyclohexanone was successful it was decided to proceed with the steroid of our interest, *i.e.* progesterone. The timed reaction of complex 1 with progesterone was run using the newly developed chromatographic method (55 % MeCN, 0.5 mL/min) (Fig. 68, Scheme 2).

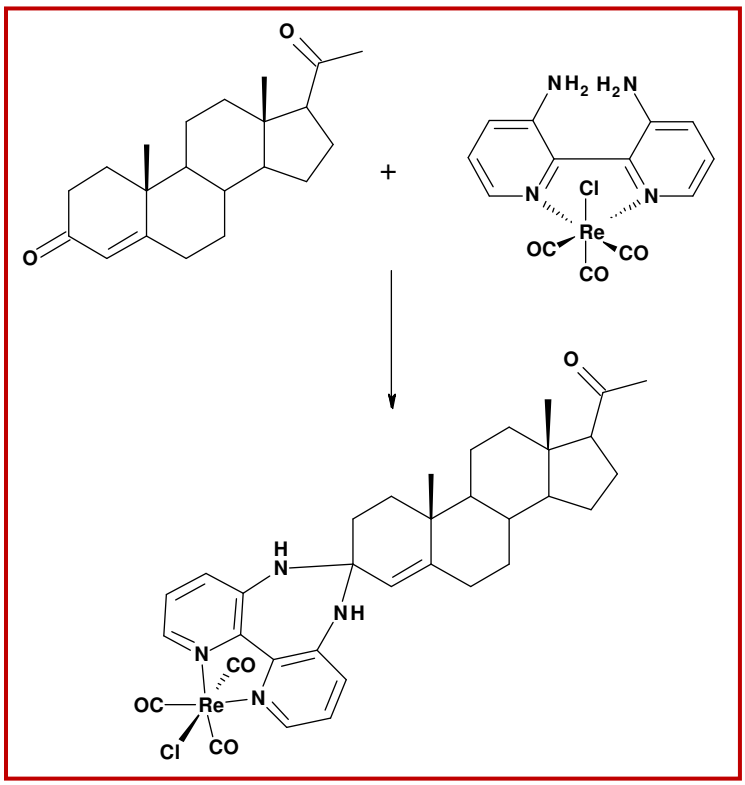

Figure 69: Scheme 2: Reaction between complex 1 and progesterone to form the 1-progesterone product

Initially, a solution of progesterone was prepared in MeCN (1 mL) and analysed using LC to locate its peak and retention time. The chromatogram below, Fig. 69, showed that the peak appeared at RT 25.83 min.

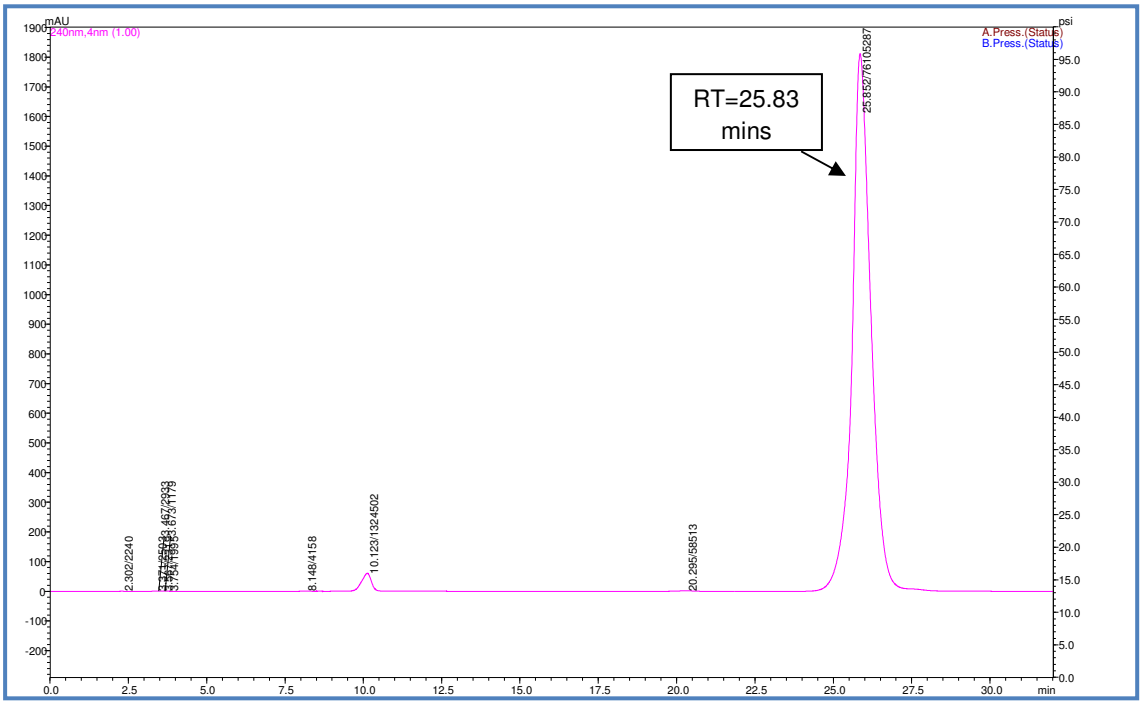

Figure 70: LC-UV chromatogram showing progesterone (100 ppm) in MeCN, 55 % MeCN, 0.5 mL/min flow rate, 240 nm

A solution of complex 1 (1 mg) and progesterone (6.4 mg, 10 eq.) in MeCN (1 mL) and a few grains of CSA was heated in the dark. The reaction was monitored for 3 hours. Aliquots were removed and analysed using LC at 0, 30, 60, 90 and 120 min. Reference chromatograms are shown below (Figs 70-73).

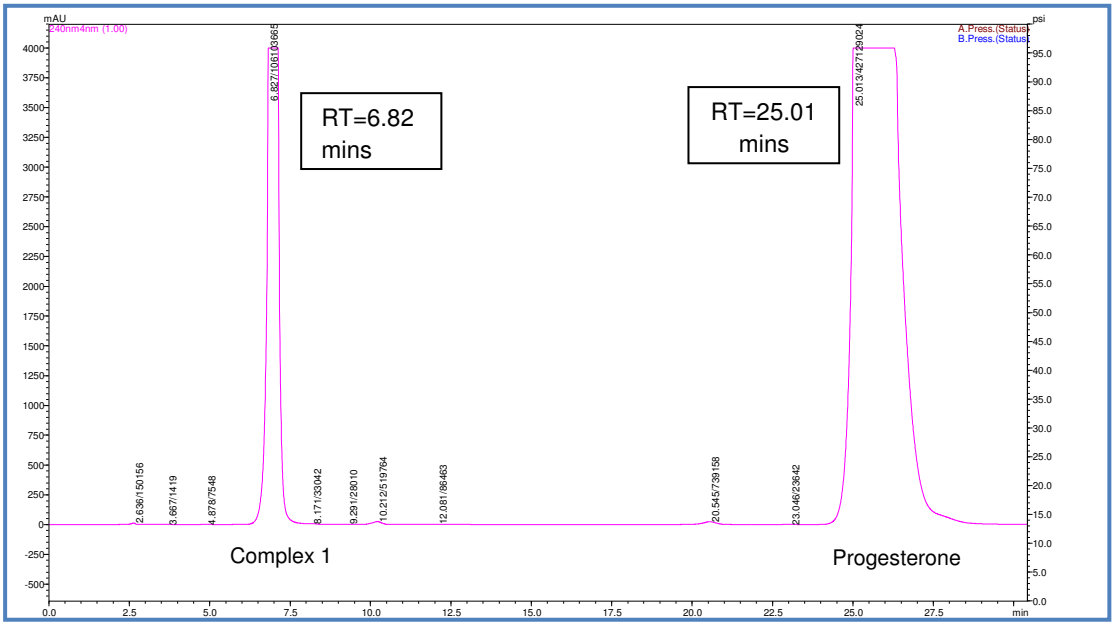

Figure 71: LC-UV chromatogram of the complex 1 and progesterone reaction at 100 ppm, 55 % B and 0.5 mL/min flow rate (t=0 min)

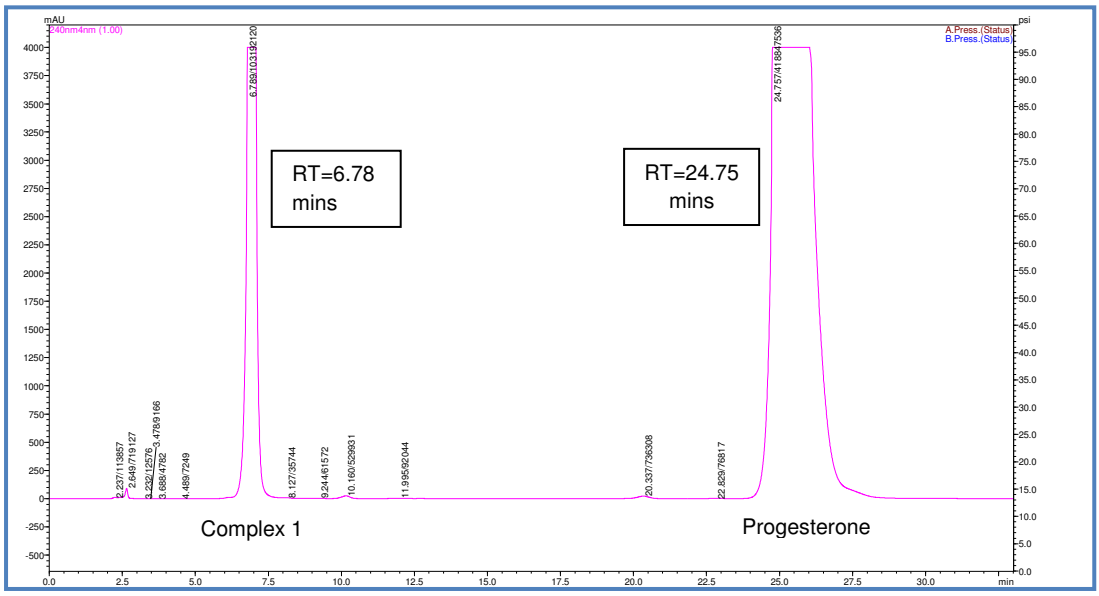

Figure 72: LC-UV chromatogram of the complex 1 and progesterone reaction at 100 ppm, 55 % B and 0.5 mL/min flow rate (t=30 min)

.

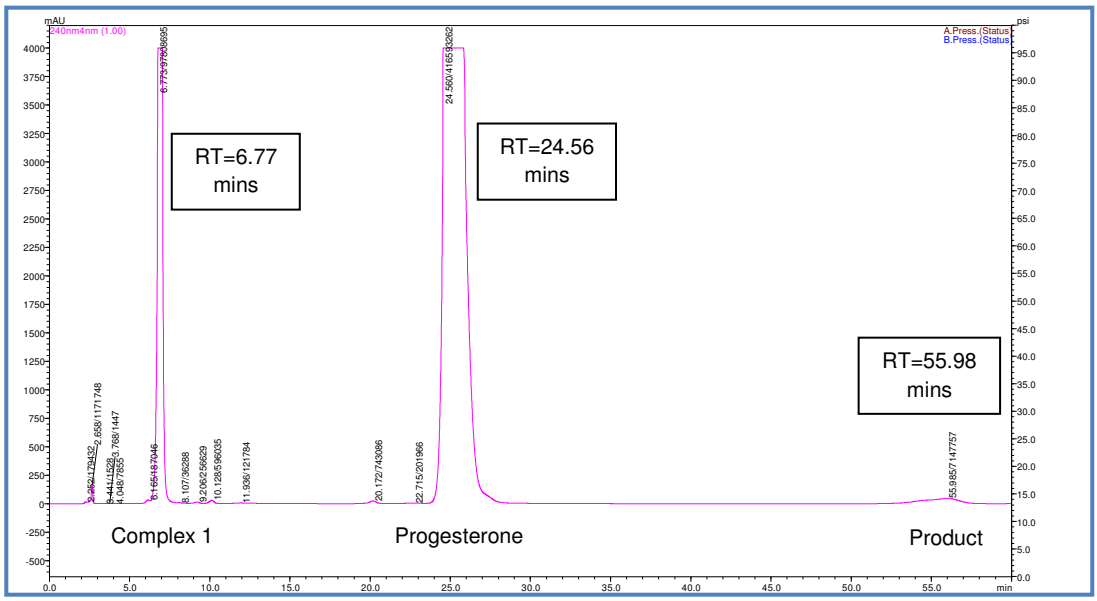

Figure 73: LC-UV chromatogram of the complex 1 and progesterone reaction at 100 ppm, 55 % B and 0.5 mL/min flow rate (t=90 min)

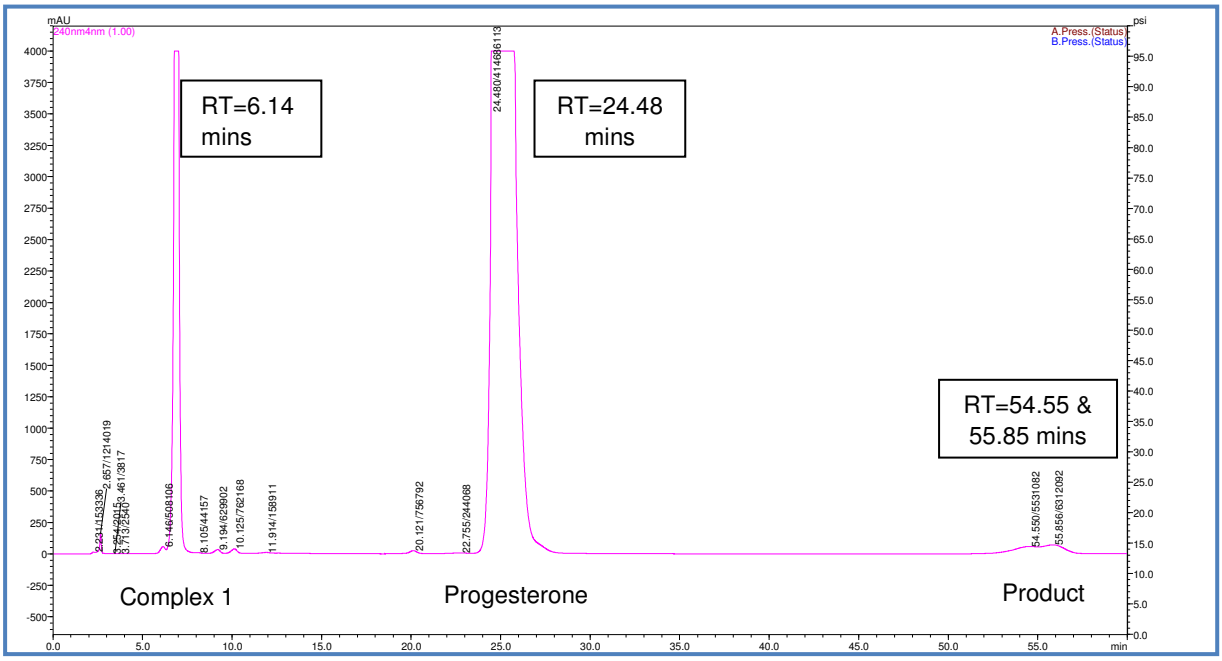

Figure 74: LC-UV chromatogram of the complex 1 and progesterone reaction, 55 % B and 0.5 mL/min flow rate (t=180 min)

Fig. 73 above shows the result at 180 minutes. Two peaks were observed corresponding to two isomers of the product between 53 and 56 min, which was considered to be an excessive retention time. In order to reduce the retention times of the analytes, the mobile phase composition was changed; the amount of acetonitrile in the mobile phase was increased to 65 %, keeping the flow rate the same at 0.5 mL/min.

The results were quite encouraging as the retention time for the products was decreased from 55 minutes to 22.5 min. Fig. 74, below, shows that increasing the acetonitrile concentration from 55% to 65% brought the two isomers and other peaks to reasonable retention times: complex 1 (5.25 min), progesterone (14.62 min) and for the two product peaks isomer 1 appeared at 20.39 min and isomer 2 appeared at 22.71 min. These chromatographic conditions were used for subsequent experiments.

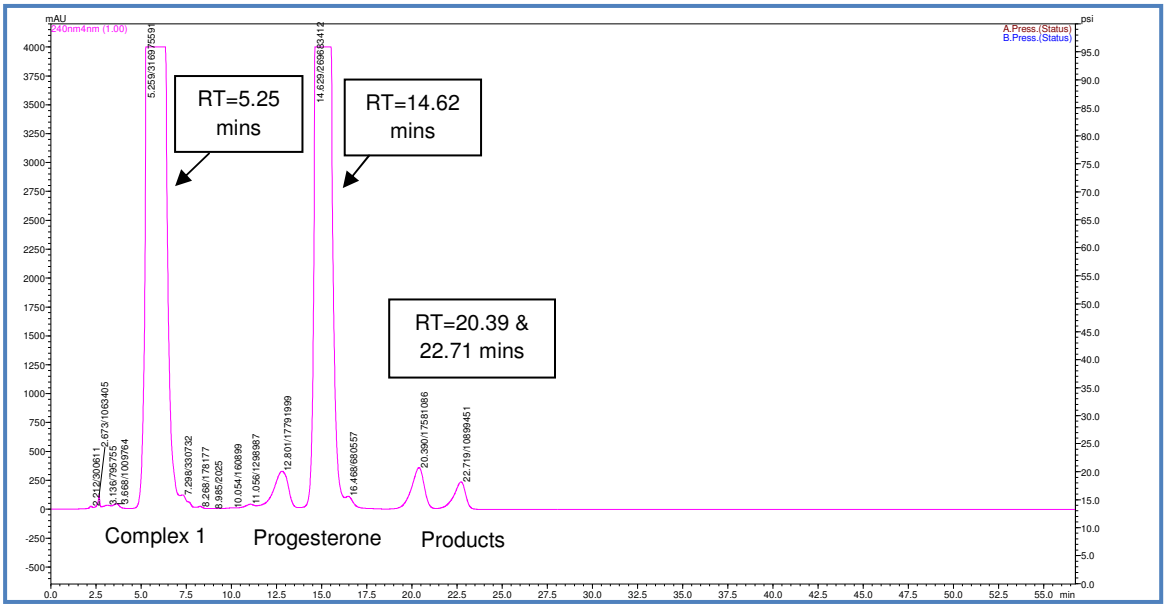

Figure 75: Chromatogram of the complex 1 and progesterone reaction at 100 ppm, 65 % B and 0.5 mL/min flow rate (t=300 min)

Another analysis was carried out after 360 min and it was observed that a significant amount of product had been formed (Fig. 75).

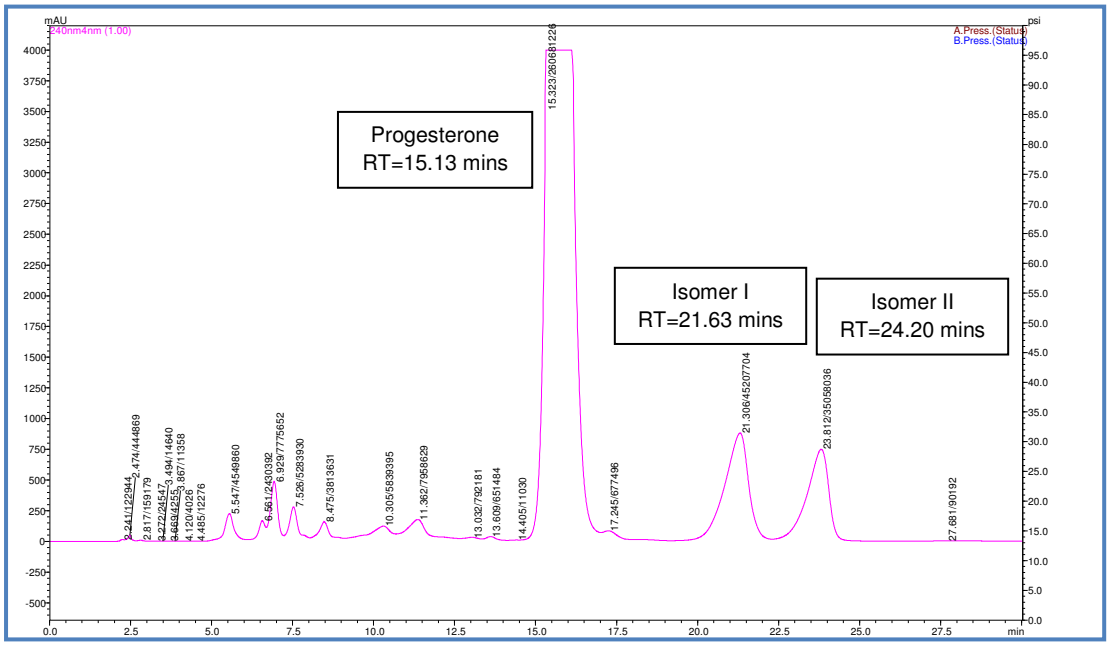

Figure 76: Chromatogram of the complex 1 and progesterone reaction at 100 ppm, 65 % B and 0.5 mL/min flow rate (t=360 min)

2.7.3.2 *Timed NMR experiment for progesterone (large scale)*

To gain more insight into the reaction between complex 1 and progesterone, a timed NMR experiment was carried out. Complex 1 (2 mg) and progesterone (12.8 mg, 20 eq.) were dissolved in CD_3CN (650 µL) and a few grains of CSA were added at t = 0. At t = 2 hrs, the ^1H NMR spectrum of the reaction was acquired; some signals from the product were observed (Fig. 76). Since the steroid region of the spectrum is complex and non-first order, only the aromatic regions of the spectra are shown here.

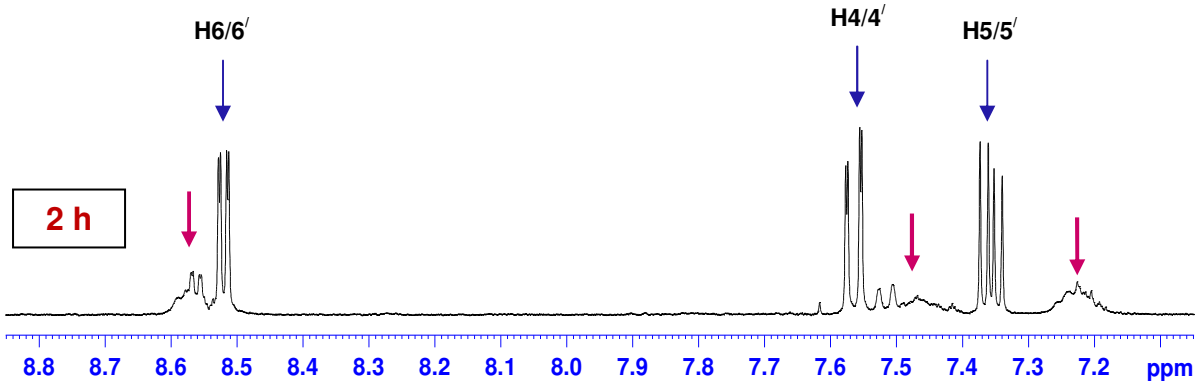

Figure 77: Selected region of the ^1H NMR spectrum of the reaction of complex 1 and progesterone (t=2 hr)

→ Represents the starting material

→ Represents the formation of products

Since the reaction had not gone to completion, the reaction mixture was heated for 4 more hours. The ^1H NMR spectrum was re-recorded (Fig. 77) and showed that all the starting material had been converted to the product.

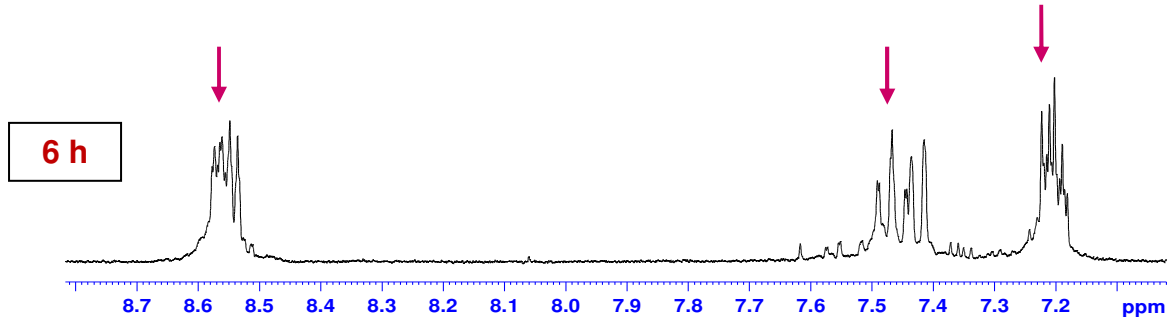

Figure 78: Selected region of the ^1H NMR spectrum of the reaction of complex 1 and progesterone (t=6 hr)

→ Represents the formation of products

The reaction was repeated, recording ^{1}H NMR spectra every hr; the results are shown in Fig. 78.

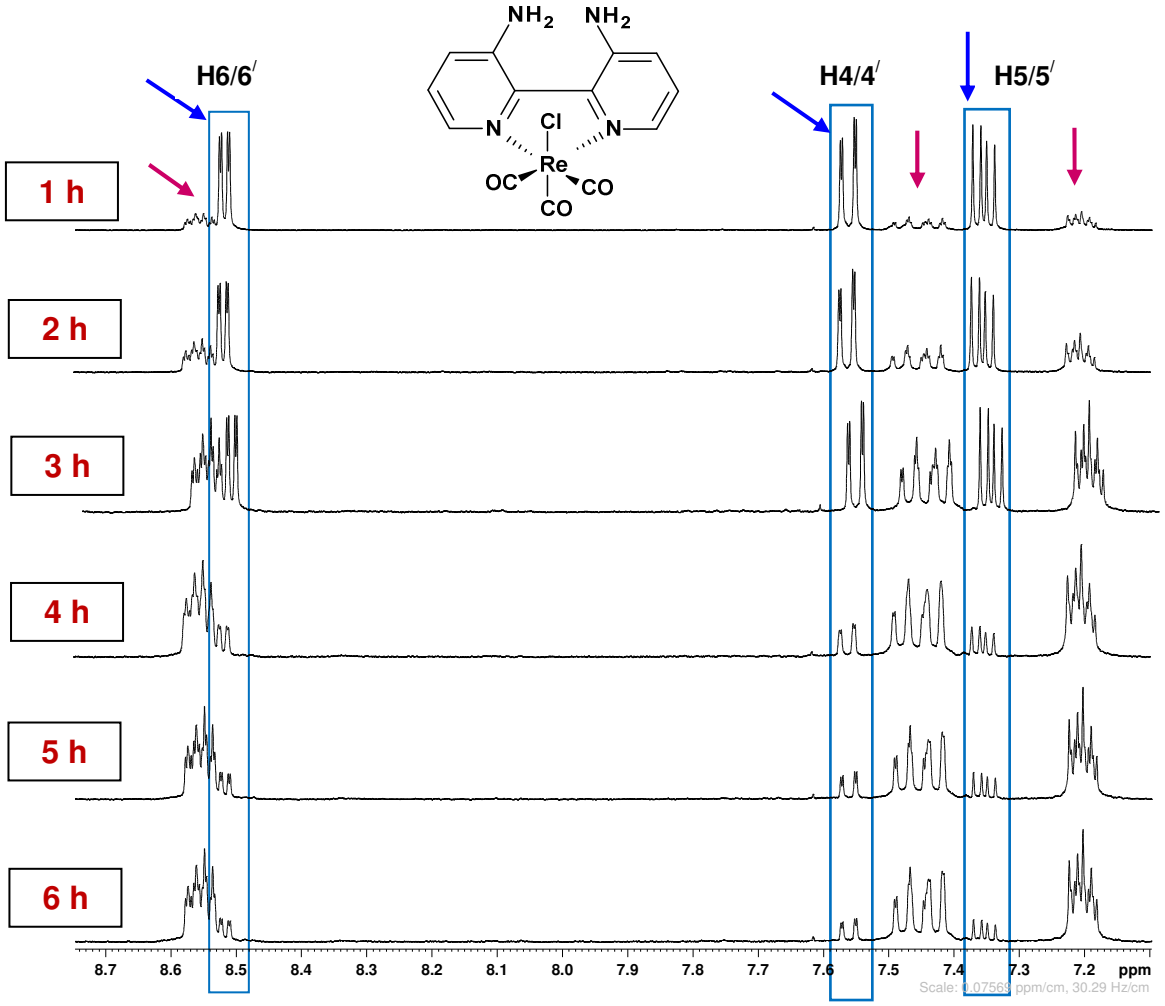

Figure 79: Stacked ^{1}H NMR spectra showing progress of the reaction from 1 hr to 6 hr

Key: → Represents the starting material
→ Represents the formation of products

The above stacked plot shows the aromatic regions of the ^{1}H NMR spectra. In the first spectrum (t=1 hr), the starting materials are indicated by blue arrows. These three signals came from the protons on the bipyridine rings in the starting material *i.e.* complex 1. The above figure shows clearly that the starting material gradually decreased and there was an increase in product formation after every hr**.**

Comparison of the spectra for complex 1 and the product (1-progesterone) shows that two isomers have been formed (Fig. 79). In the spectrum of the starting material (top) signals from the bipyridyl groups were present between 7.3 and 8.6 ppm.

The spectrum of the reaction mixture after 6 hrs of heating (bottom) showed that these signals shifted upon reaction of complex 1 with progesterone and also became more complicated; in fact, there are two sets of bipyridyl signals, confirming the formation of the two isomers.

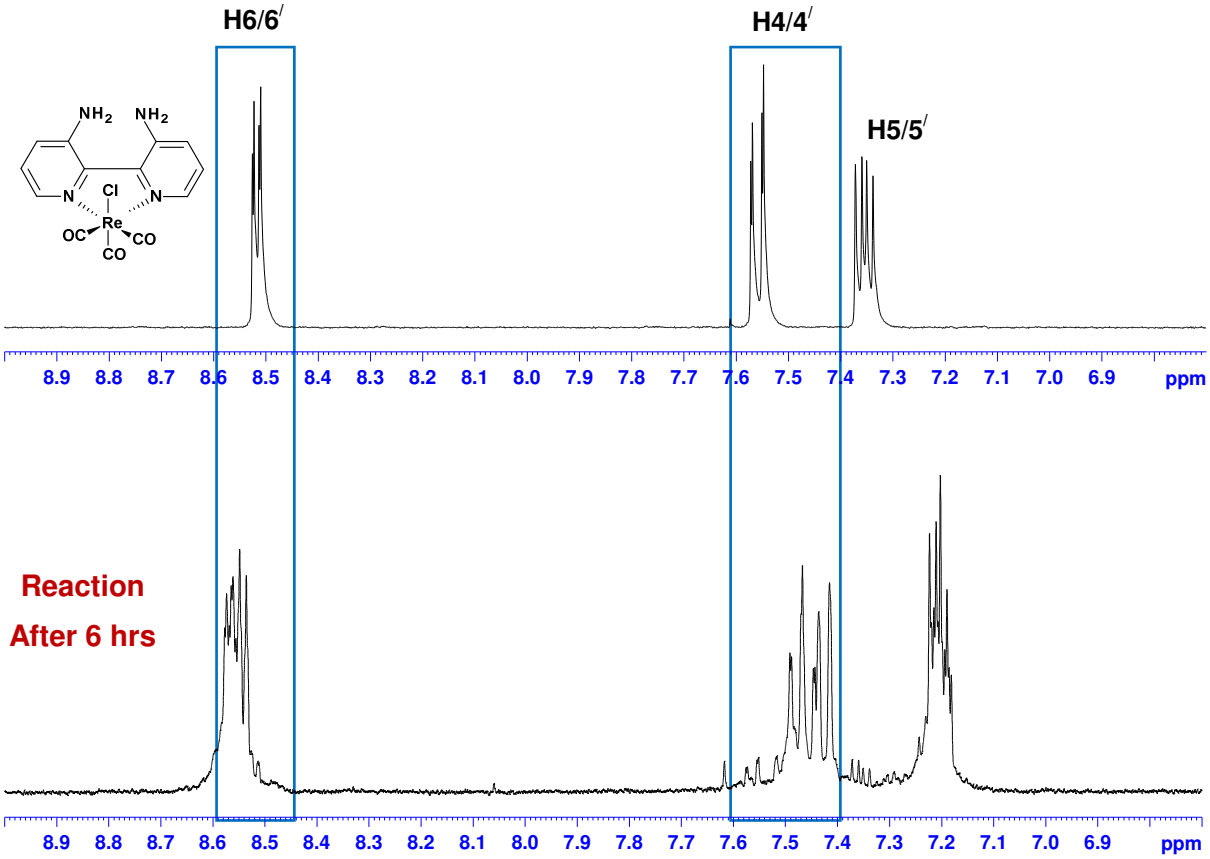

Figure 80: Selected regions of the ^{1}H NMR spectra of complex 1 (top) and the 1-progesterone product (bottom)

2.7.3.3 Preparative Chromatography to produce the metabolites of BDP

Beclometasone dipropionate is a widely used inhaled corticosteroid for the inhalation therapy of asthma in both adults and children. Owing to the presence of the dipropionate ester functional group in its side chain, it is easily hydrolysed via esterases in the human lung, liver and other parts of the body to the more polar products 17-beclometasone monopropionate (17-BMP), 21-beclometasone monopropionate (21-BMP) and beclometasone (BOH). 17-beclometasone monopropionate is the active metabolite, whereas both 21-BMP and BOH have very low binding affinity to the glucocorticoid receptor. In this experiment, we reported the

in-vitro hydrolysis of BDP using esterase enzyme as well as the isolation and characterisation of its degradation product.

The reaction mixture was prepared by dissolving complex 1 (50 mg) and progesterone (320 mg, 10 eq.) in MeCN (3 mL) with addition of a few grains of CSA. The solution was heated at 60 ºC for 6 hrs before analysis using LC-UV to develop a method suitable for a preparative separation (Fig. 80).

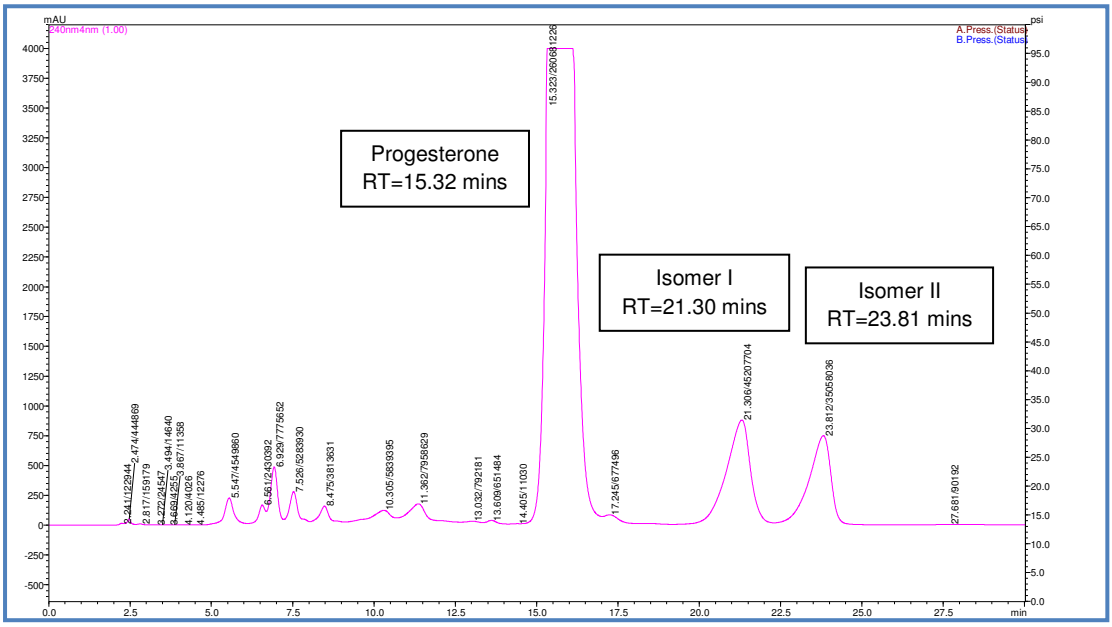

Figure 81: LC-UV chromatogram for the complex 1/progesterone reaction, after 6 hrs of heating

The sample (in 1 mL aliquots) was separated using the preparative HPLC. The chromatogram showed some side products, a prominent peak due to progesterone at 24 min and two unresolved peaks for the product isomers (since the resolution of preparative HPLC was not as high as analytical scale HPLC). The chromatogram obtained is shown in Fig. 81 below.

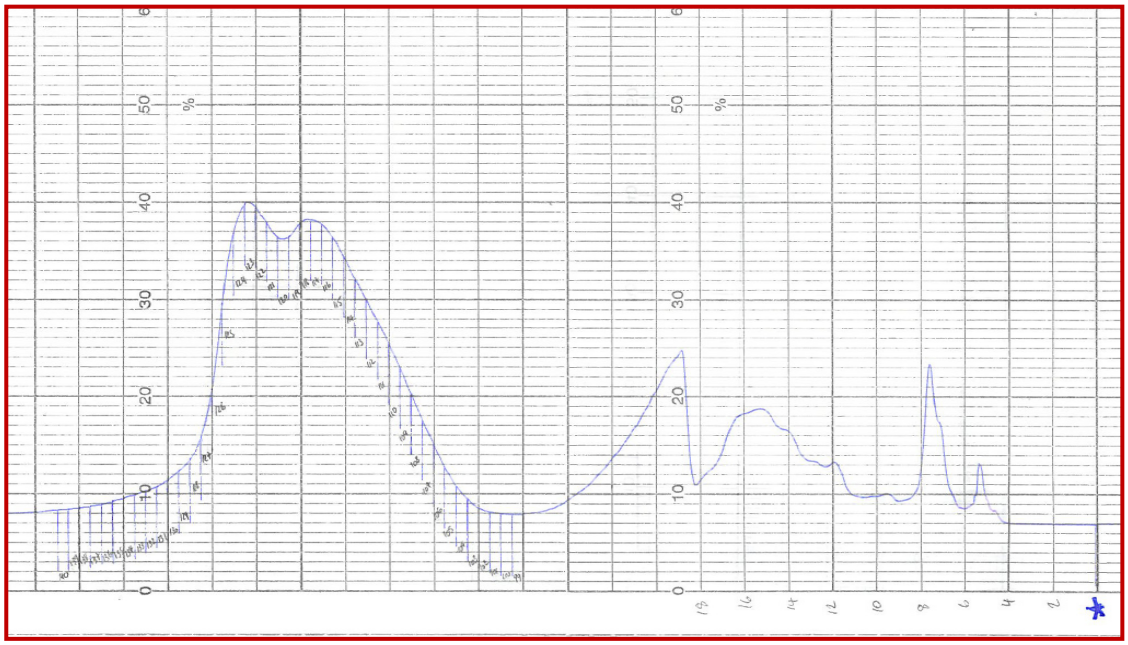

Figure 82: Preparative HPLC chromatogram of the complex 1/progesterone product (65 % MeCN, 10 mL/min, run time 60 min)

For each isomer, fractions were collected (Fig. 82), combined and the acetonitrile removed *in vacuo*. The remaining aqueous sample was extracted into DCM and dried ($MgSO_4$), giving a yellow solid.

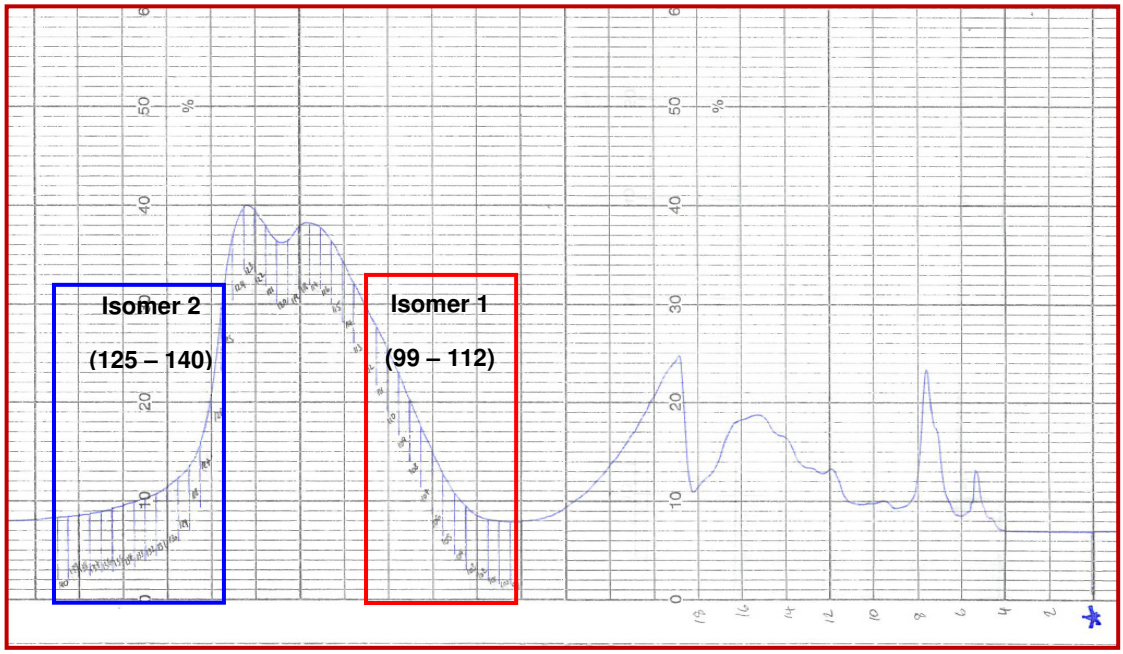

Figure 83: A preparative HPLC chromatogram showing collection of fractions for the two isomers of 1-progesterone

2.7.3.4 Solid state characterisation for 1-progesterone

Single crystal X-ray Diffractometer can determine crystal structure with detailed information about bond lengths and bond angles, of small molecules and macromolecules, and also provides accurate and precise measurements of molecular dimensions.

Yellow crystals of 1-progesterone were formed by slow evaporation of MeCN. These were analysed using single-crystal X-ray diffraction, and the structure is shown below in Fig. 83.

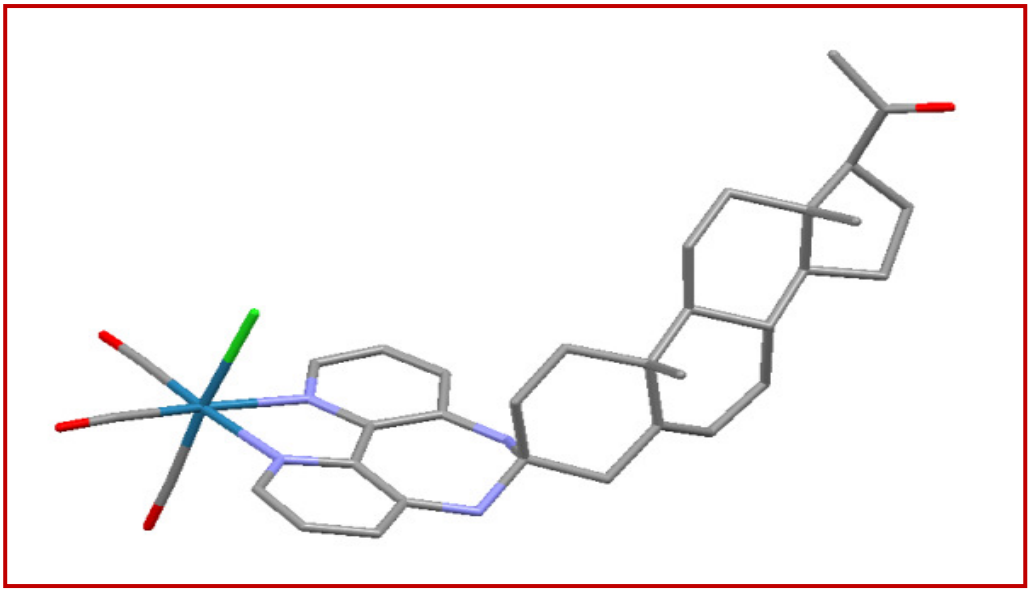

Figure 84: Single-crystal X-ray structure of 1-progesterone

The rhenium centre adopts a distorted octahedral geometry and is coordinated by two pyridyl nitrogen atoms and two carbon monoxide ligands in the equatorial positions, with another carbon monoxide ligand and a chloride ion occupying the axial coordination sites.

Fig. 84 shows that complex 1 reacted with the carbonyl group at carbon 3, which was not expected; it had been thought that as this is a conjugated ketone the rhenium complex would be more likely to react at the acetyl carbonyl at position 20. Examination of the space-filling model for this molecule, however, shows that C20 is sterically hindered by the methyl group at position 18.

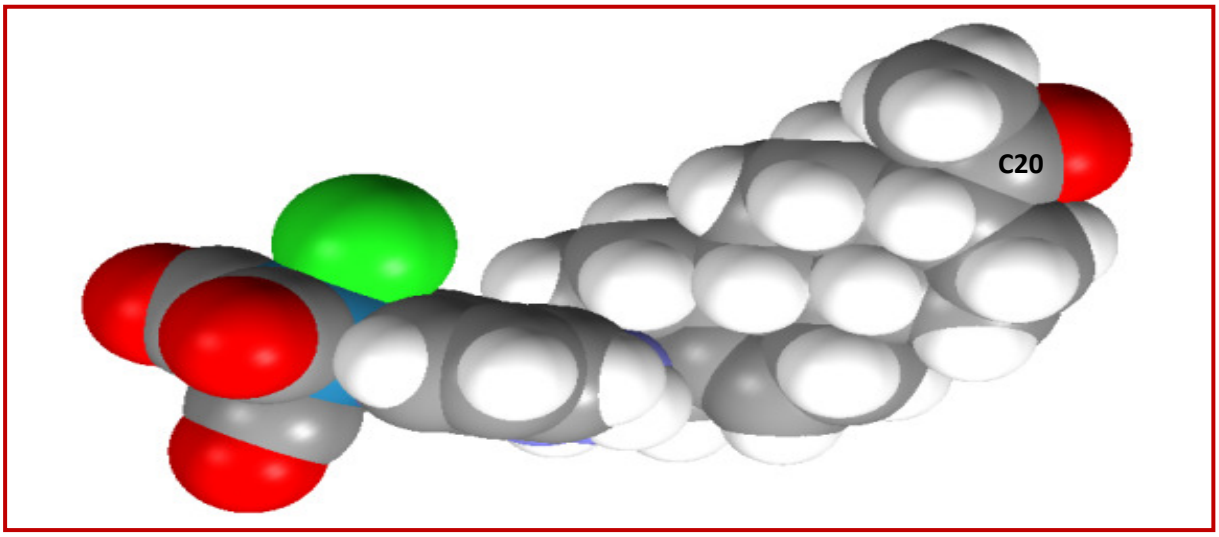

Figure 85: Single-crystal X-ray structure of 1-progesterone as a space-filling model, showing the steric hindrance around C20

Selected bond lengths were measured using Mercury software and showed a surprising result - a rearrangement of the double bond between C4 and C5 had occurred at the conjugated end of the progesterone; interestingly, the double bond was now found between C5 and C6 (Fig. 85).

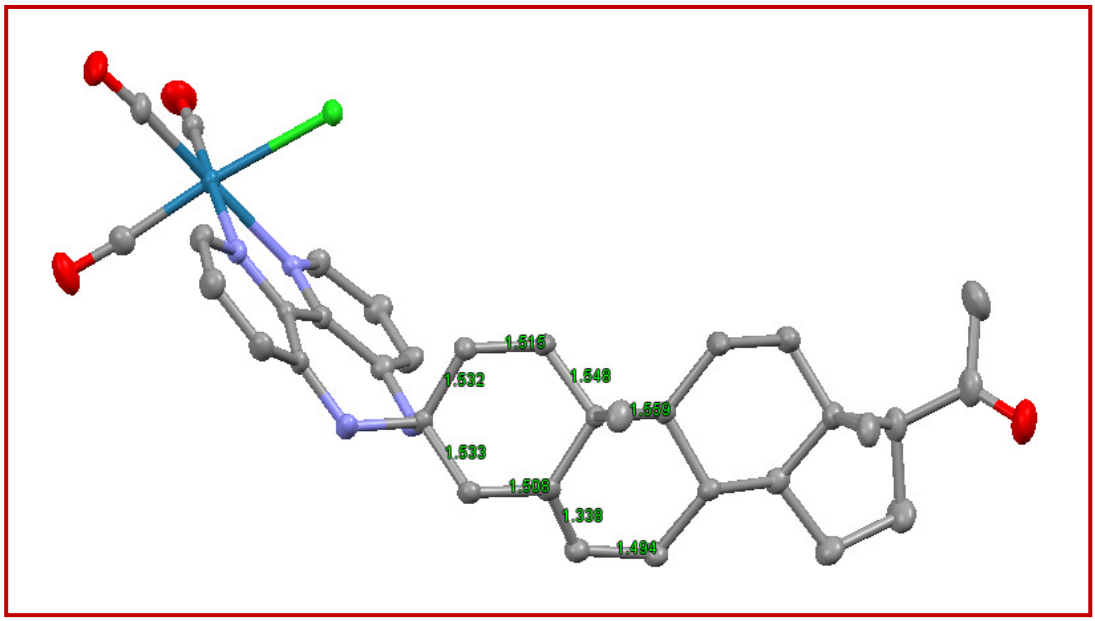

Figure 86: Single-crystal X-ray structure of 1-progesterne with bond length (Å)

The structure of the progesterone standard with bond measurements is shown below in Fig. 86.

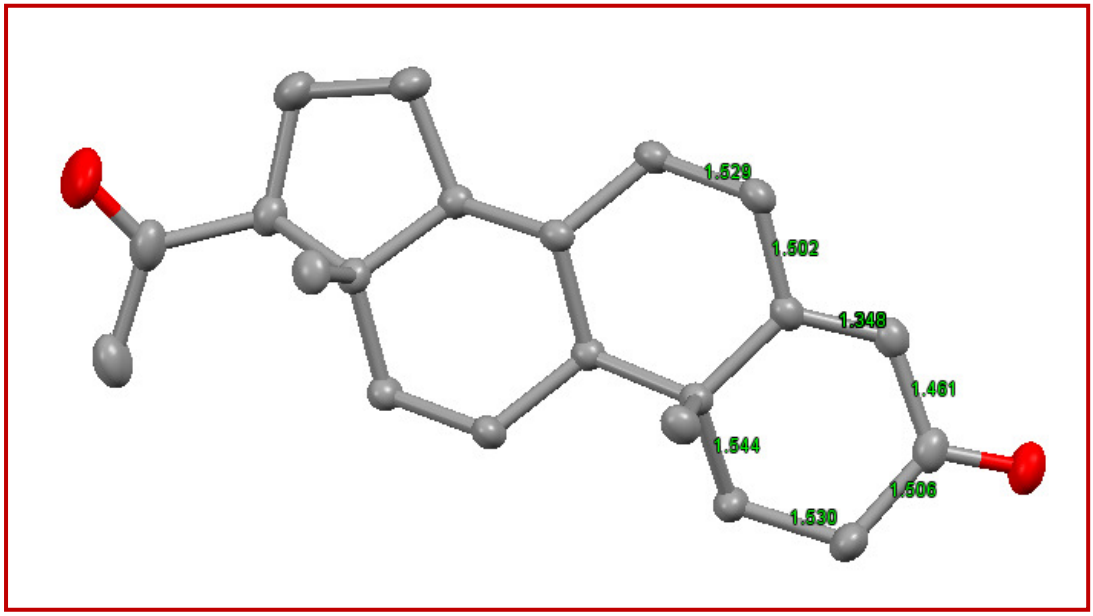

Figure 87: Single-crystal X-ray structure of the progesterone standard with bond lengths (Å)

The measurements of the relevant bond lengths are shown in Table 34 below, along with the analogous measurements for the progesterone standard.

	1-Progesterone	Progesterone
C3-4	1.533	1.461
C4-5	1.508	1.348
C5-6	1.338	1.502
C6-7	1.494	1.529

Table 34: Selected bond lengths for 1-progesterone and progesterone (Å)

To obtain further evidence for the shift in the double bond, the structure was refined without modelling the hydrogen atoms on the alkene and methylene groups in question. The software located three Q peaks (*i.e.* unassigned peaks of electron density of ~ 1 eÅ^{-3}); two Q peaks were located on C4 and one Q peak was found on C6. This confirmed the shifting of the double bond (Fig. 87).

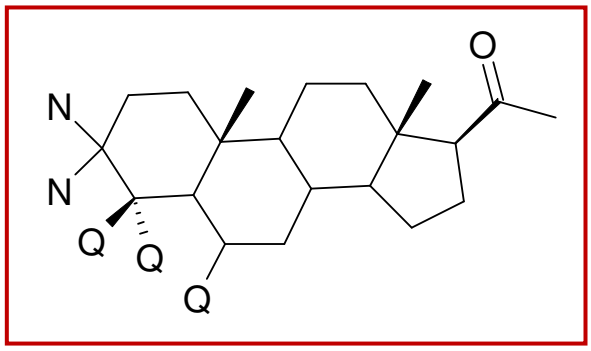

Figure 88: Partial structure of 1-progesterone showing the location of the Q peaks

A similar bond rearrangement is seen on formation of ketals from Δ^4-3-ketosteroids with ethylene glycol, in which Δ^5-steroids are formed (Fig. 88).

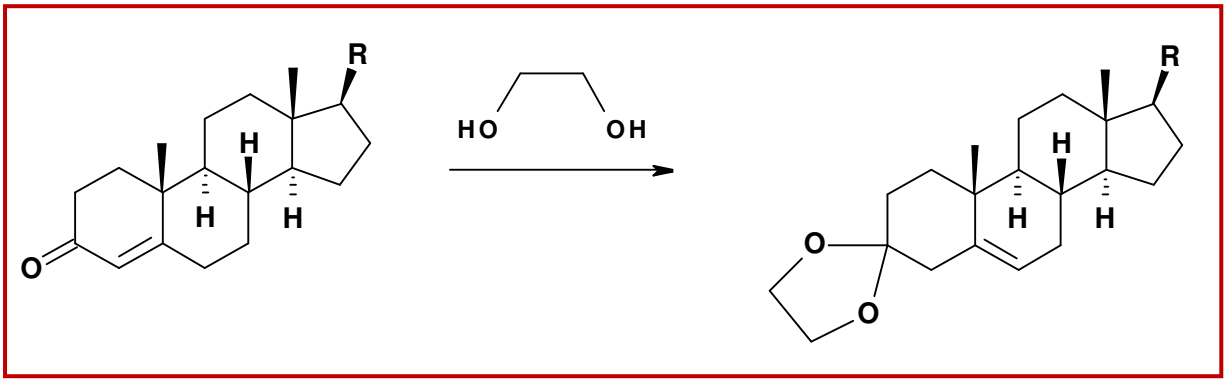

Figure 89: Ketal formation with 3-ketosteroids

This has been demonstrated with a number of steroids[100,101] including progesterone.[102] In this latter paper ketal moieties were formed at both C3 and C20 of progesterone; however this was not observed in the work reported here, probably because progesterone was used in large excess in the aminal formation.

2.7.4 C. Reaction of complex 1 and testosterone

2.7.4.1 Analysis using NMR

Having successfully prepared 1-progesterone, it was decided to investigate whether a similar product could be prepared with testosterone, an androgenic steroid which contains the same conjugated ketone moiety in the A ring (Fig. 89 and 90 Scheme 3).

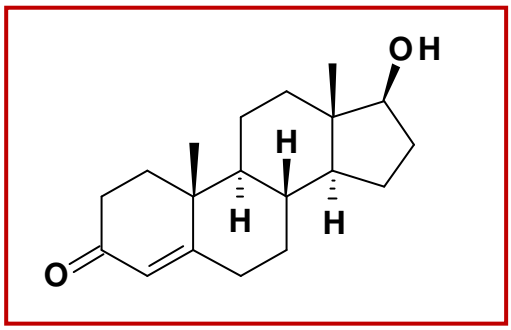

Figure 90: Testosterone

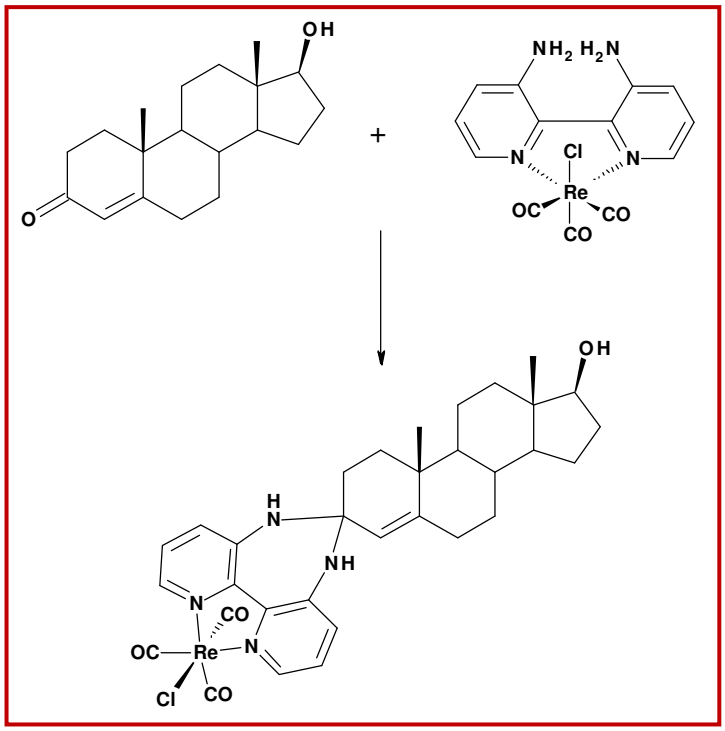

Figure 91: Scheme 3: Reaction between complex 1 and testosterone to form the 1-testosterone product

Firstly, an experiment was carried out in an NMR tube to see whether a product could be formed on a small scale. Complex 1 (2 mg) and testosterone (11.7 mg, 10 eq.) were dissolved in CD_3CN. A small amount of camphor sulfonic acid was added and the solution was heated at 60 ºC in a water bath. The reaction was monitored using ^1H NMR. By looking at the results (Fig. 91) it becomes clear that the reactants were converted to products after 10 hrs as no obvious changes were observed after that. Therefore, the experiment was repeated on a larger scale to enable isolation and characterisation of the product.

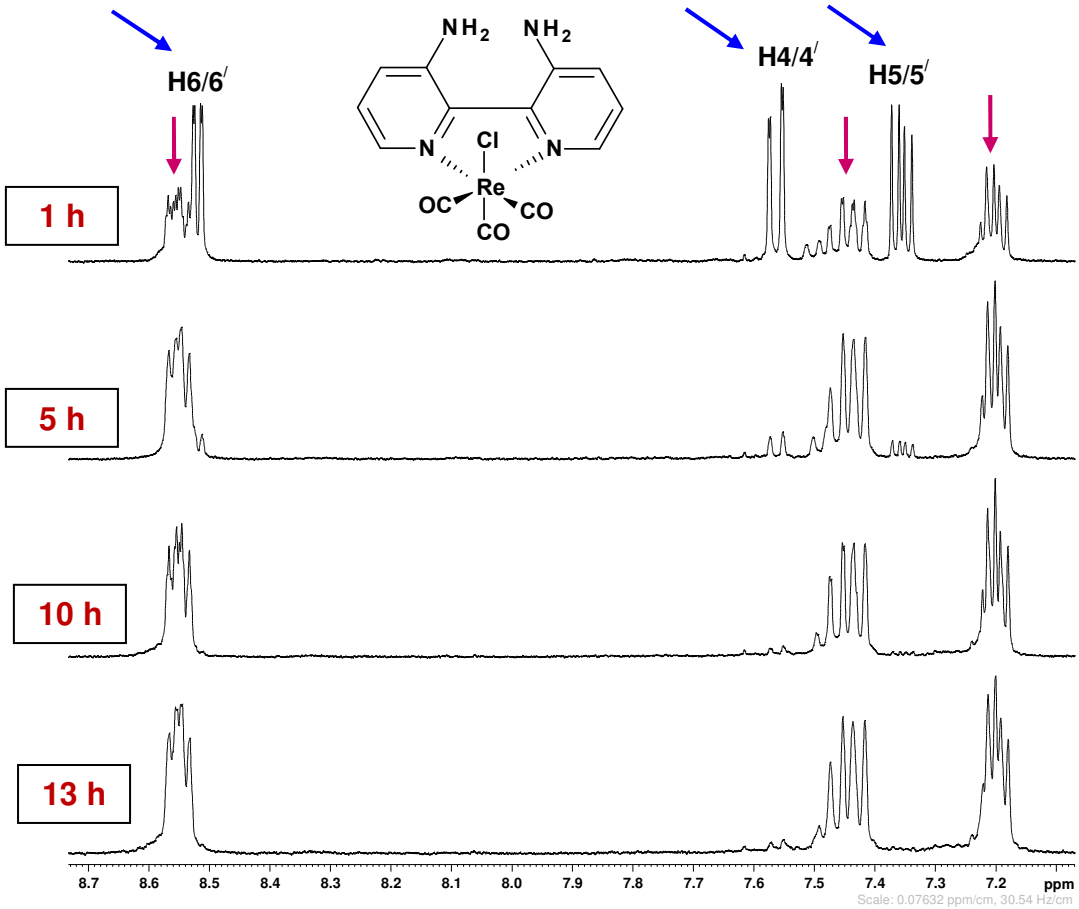

Figure 92: Selected regions of the ^{1}H NMR spectra of the reaction between complex 1 and testosterone (CD_3CN) after 1, 5, 10 and 13 hrs

Key: → Represents the starting material
→ Represents the formation of products

2.7.4.2 *Reaction of testosterone and complex 1 (large scale)*

Complex 1 (30 mg) and testosterone (176 mg, 10 eq.) were dissolved in MeCN (3 mL) and a few grains of camphor sulfonic acid were added. The reaction was stirred for 3 hrs at 60 ºC and monitored using TLC (Al_2O_3, 5% MeOH in DCM) until all of the starting material had been consumed (after approximately 24 hr). An aliquot (0.25 mL) was removed from the reaction solution and diluted with MeCN (0.5 mL) and analysed using HPLC. Fig. 92 shows the chromatogram obtained at 286 nm. A sample of testosterone was analysed under the same conditions for comparison (Fig. 93).

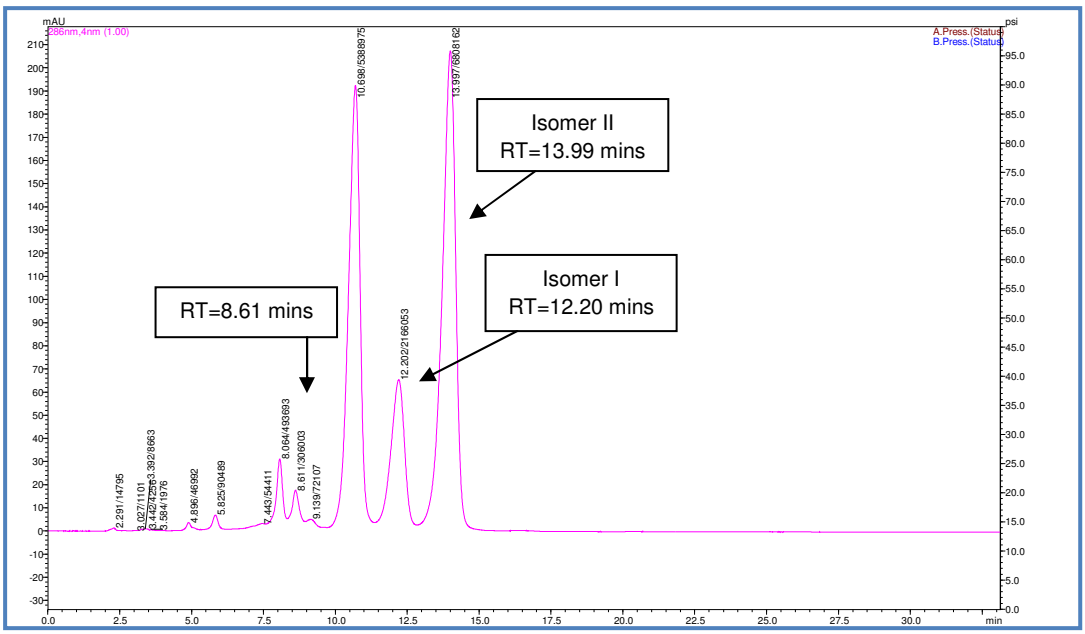

Figure 93: LC chromatogram of the reaction mixture after 24 hrs, at 65 % B, 1.0 mL/min flow rate and 286 nm

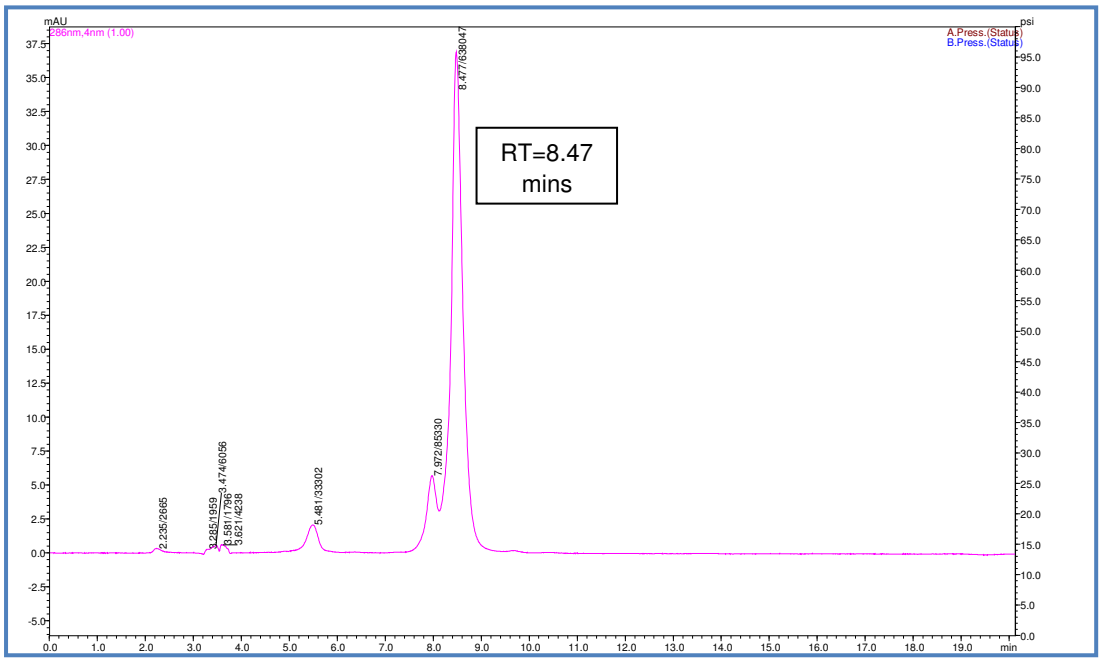

Figure 94: Chromatogram of testosterone at 65 % B and 1.0 mL/min flow rate

The chromatogram (Fig. 92) showed some side products, a very small peak of the starting material testosterone at 8.61 min and two peaks from the two product isomers (RT=12.20 and 13.99) for isomer I and 2 respectively. Once it was

confirmed that the product isomers were formed, it was decided to separate them using preparative HPLC. The reaction solution was then separated (in 1 mL aliquots) by preparative HPLC; the chromatogram is shown in Fig. 94 below. The chromatogram showed a very small peak due to testosterone and unresolved peaks for the product isomers (since the resolution of preparative HPLC was not as high as analytical scale HPLC).

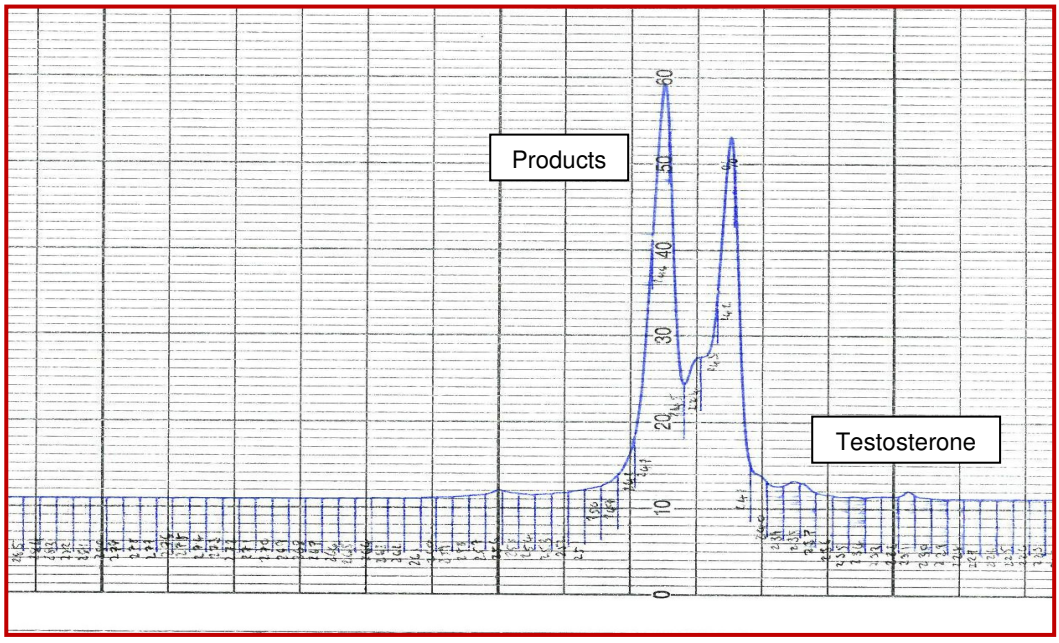

Figure 95: Preparative HPLC chromatogram showing collection of fractions for the two isomers of 1-testosterone

For each isomer, fractions were collected (Fig. 95), (isomer 1: 21-23, 110-113, 175-178, 241-242 and for isomer 2: 27-30,116-122, 181-188, 245-251) combined and the MeCN was removed under vacuum. The fractions were extracted into DCM, dried ($MgSO_4$), filtered and evaporated *in vacuo*. The proton NMR spectrum of each fraction was acquired in CD_3CN (Fig. 96).

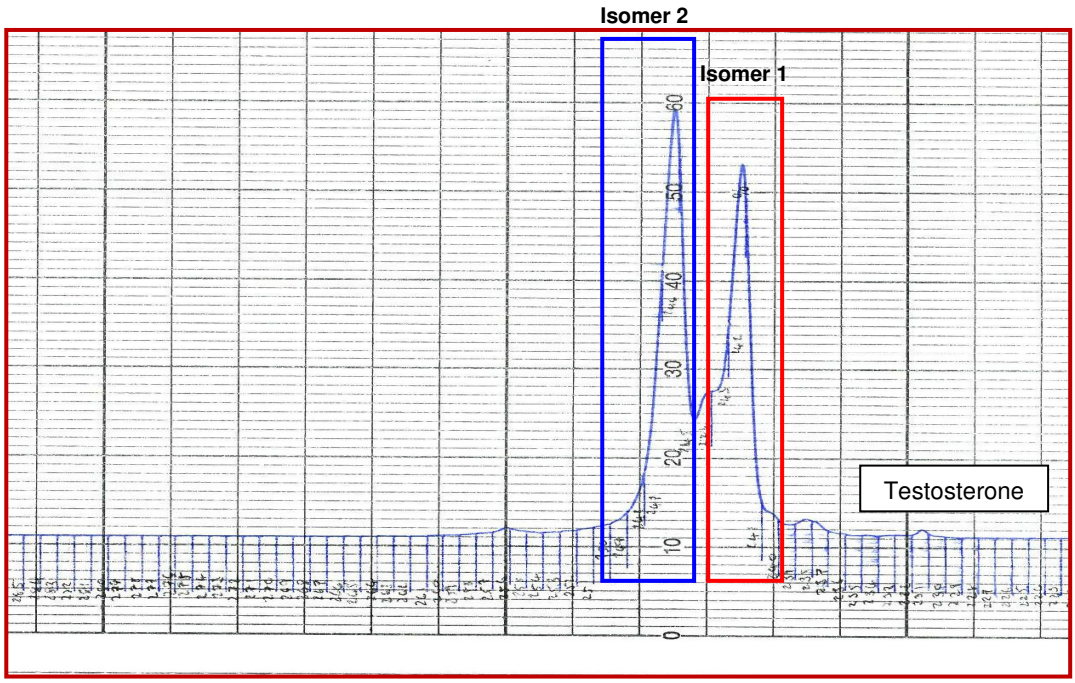

Figure 96: Preparative HPLC chromatogram showing collection of fractions for the two isomers of 1-testosterone

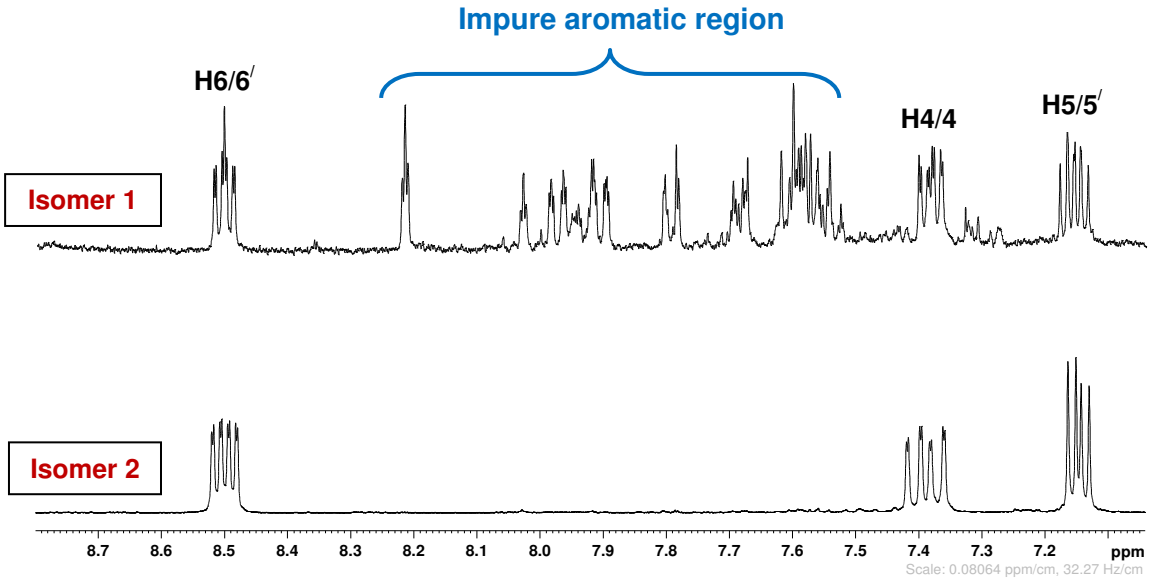

Figure 97: Selected regions of the ^{1}H NMR spectra of 1-testosterone fraction 1 (top) and fraction 2 (bottom)

Examination of the aromatic region of the spectrum of isomer 1 (Fig. 96) showed many signals and the sample was clearly impure. However, the spectrum of isomer 2 shows a clean sample of the product has been isolated.

Attempts were made to crystallise the product both by solvent diffusion and by refrigeration of an acetonitrile solution of fraction 2. Unfortunately to date these attempts have been unsuccessful.

2.8 Conclusion

The main aim of the work presented here was to attach a steroid, progesterone, to a rhenium-containing fluorescent group (the rhenium complex of 3,3'-diamino-2,2'-bipyridine, complex **1**, section 2.3); this aim was achieved with formation of the desired product and full characterisation obtained. Much of the work reported previously in the literature on metal complexes of steroids uses androgens but few studies have used female hormones such as progesterone. This is one of the first examples of a luminescent metal complex of this steroid.

The method was developed using the model compound cyclohexanone which mimics the A-ring of progesterone (section 2.6.1.1). The product **1**-progesterone was successfully characterized by using a HPLC method (which was developed for this research), preparative HPLC, column chromatography, 1D-NMR and X-ray crystallography. The co-ordination chemistry of **1**-progesterone revealed some interesting results. After reaction between complex **1** and progesterone rearrangement of the double bond from positions 4-5 to 5-6 was observed from the single-crystal X-ray structure which, as far as we can tell, has not previously been reported for diamine derivatives of ketosteroids, although is well-precedented during derivatisation of ketosteroids using diols.[91,92]

After successful reaction of progesterone with complex **1**, the same method was applied for the synthesis of the **1**-testosterone product which was characterised using the LC method, preparative HPLC, column chromatography, and 1D-NMR. The formation of **1**-testosterone was confirmed using 1D-NMR. Despite meticulous attempts to grow crystals under different conditions both by solvent diffusion and by refrigeration of an acetonitrile solution unfortunately production of crystals for X-ray analysis has so far been unsuccessful due to the limited amount of the product obtained after column chromatography.

2.9 Future Work

This project and the results displayed in this thesis could be developed in various ways, for example by attaching other metals which possess fluorescent properties, such as ruthenium, or by exploring the addition of steroid groups in the axial position of the $Re(CO)_3Cl(L_2)$ core with the aim of enhancing the luminescence lifetime of the metals. The methods developed could also be used with other steroidal compounds such as corticosteroids.

Further work is required to complete the structural determination of **1**-testosterone produced by X-ray crystallography. Detailed 2D-NMR experiments are required.

Chapter 3

Enzymatic oxidation of galactose

3.0 Enzymatic oxidation of galactose

3.1 Introduction

The four major classes of organic molecules in living systems are:

- proteins;
- lipids;
- nucleic acids and;
- carbohydrates.

Carbohydrates are the most abundant organic molecules found in nature.[103] Nearly all organisms synthesize and metabolize carbohydrates. Plants and animals combine numerous glucose molecules to form large energy-storing molecules such as starch and glycogen and a variety of other macromolecules.[104,105]

Carbohydrates are always challenging targets for analytical chemists as there are difficulties in both their separation and detection. Due to the chirality, branching structures and cross-linking the number of isomers of carbohydrates is huge.[106] For over a century, nucleic acids, proteins and lipids have been extensively studied worldwide. Carbohydrates have only more recently received close attention through the expanding field of glycobiology. Glycobiology is advancing at increasing rates due to advanced developments in new technologies and in genomics. Glycobiology is the study of the roles of carbohydrates in cellular life. Carbohydrates are the primary products of plant photosynthesis and the metabolic precursors of all other organic compounds. Often they are covalently bound to proteins (glycoproteins) and lipids (glycolipids) to form glycoconjugates.[107]

Carbohydrates are composed of polyhydroxyl units known as monosaccharides, of which some of the more common monosaccharides are glucose, galactose, mannose, fucose and N-acetylgalactosamine. These units are joined together by a glycosidic bond between the hydroxyl group of one monosaccharide and the hydroxyl functions of the second monosaccharide, with loss of a molecule of water. Oligosaccharides and polysaccharides are composed of the different monosaccharide unit repeated over and over such as in cellulose and starch. Complex carbohydrates act as receptors for binding proteins, typically lectins (carbohydrate-binding proteins). Carbohydrate–protein interactions occur through

glycoproteins, glycolipids, or polysaccharides present on cell surfaces.[108-110] Carbohydrates interact with lectins through hydrogen bonds, metal coordination, van der Waals and hydrophobic interactions.[111,112]

So, it is incomplete to discuss carbohydrates without discussing lectins.

3.1.1 Lectins

Lectins, derived from the Latin word *legers* meaning ‘‘to choose ’’or ‘‘select’’, are defined as proteins that preferentially recognize and bind carbohydrate complexes protruding from glycolipids and glycoproteins.[113-117]

Lectins are a class of proteins that bind mono- and oligosaccharides of eukaryote glycoconjugates reversibly, do not possess catalytic activity[104], agglutinate cells and precipitate complex carbohydrates or polysaccharides. Their interaction with polysaccharides resembles the antibody–antigen and enzyme–substrate reactions. In contrast to antibodies, lectins are not the products of the immune system, their structures are diverse, and their specificity is restricted to binding to carbohydrates.[97,98,99] Lectins interact with carbohydrates through binding sites to create complexes. Such complex formation is dependent on the particular lectin and its specificity for certain carbohydrate structures.[118-120]

High resolution X-ray crystallography of lectins in complex with their ligands showed the types of bonds formed and identified the chemical groups on the protein and the carbohydrate that interact with each other.[120,121] Multiple lectins were isolated from microorganisms and also from animals.[122] Hydrophobicity is the main force of binding lectins with carbohydrates.[120]

Carbohydrate-binding sites are often shallow depressions on the surface of the protein.[123] The carbohydrate-binding sites of lectins recognise and fit to the ligand carbohydrate through a lock and key-type mechanism, involving complex networks of hydrogen bonds which result in the displacement of water molecules with the establishment of new hydrogen bonds. These hydrogen bonds and van der Waals contacts are the dominant forces in binding stability.[120,124]

Applications of lectins

The availability of lectins with distinct and different carbohydrate specificities has resulted in the use of these proteins:

- as tools in medical and biological research;
- for red blood cell typing, structural studies of blood group substances and identification of new blood groups;
- for investigation of complex carbohydrate functions on surfaces of animal cells, bacteria and viruses;
- for isolation, purification and structural studies of carbohydrate-containing polymers.[125]
- Lectins have applications in many fields, including cancer research, immunology and cell identification.[126]

3.1.2 Galactose Oxidase (GO)

In recent years use of galactose oxidase (GO) has gained much attention. The enzyme GO contains a metalloradical complex consisting of a type 2 copper site and a protein derived cofactor covalently attached to the sulphur of a cystein,[126] which permit the oxidation of primary alcohols to the corresponding aldehyde with reduction of dioxygen to hydrogen peroxide (Fig. 97).

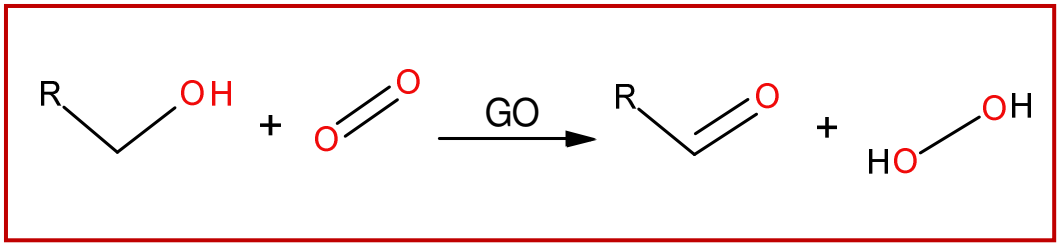

Figure 98: Oxidation of alcohols to aldehyde using galactose oxidase (GO)

GO was first reported in the growth medium of *Polyporus circinatus*[127] although the organism was later identified as the filamentous fungus *Dactylium dendroides*[128] and then *Fusarium.*[129] It catalyses a wide range of primary alcohols (RCH_2OH), including sugars and polysaccharides, to the corresponding aldehydes under aerobic conditions while reducing oxygen to hydrogen peroxide,[124,130,131] as shown in Equation 3.1 and Fig. 98.[132]

$$RCH_2\,OH + O_2 \longrightarrow RCHO + H_2O_2 \qquad (3.1)$$

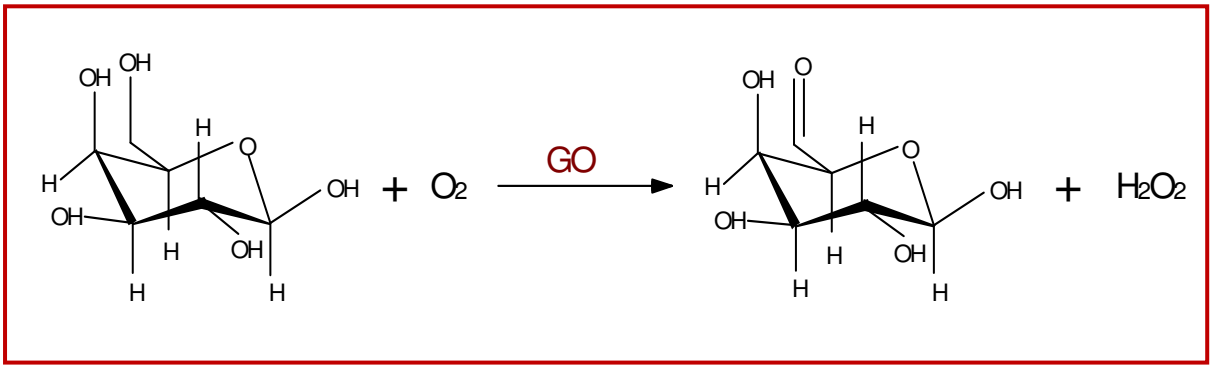

Figure 99: A reaction catalysed by galactose oxidase (GO).[130,131]

It is thought that hydrogen peroxide produced is then used for either antibiotic defence or for use by peroxidases in lignin degradation. GO is strictly regioselective, and no secondary alcohol or other reducing group is oxidized. However, the enzyme exhibits a broad substrate spectrum ranging from monosaccharides and polysaccharides to aliphatic and aromatic alcohols and polyalcohols.[131,133,134]

3.1.2.1 Structure of GO

The enzyme is monomeric, made up of 639 amino acids[136] and has a relative molecular mass of 68.5 kDa.[135]

Substrate specificity and binding

GO displays broad substrate specificity with activity towards a wide range of primary alcohols. This is a desirable trait in an industrial biocatalyst.[136] GO activity has also been reported towards polysaccharides where D-galactose occurs on the non-reducing end.[137,138]

Applications of Galactose Oxidase (GO)

GO is used for various biomedical applications, including clinical assays for galactose in blood and other fluids, histochemical studies and early detection of cancer. GO is a promising enzyme for the production of biosensors because of its ability for direct electron transfer (DET) to the electrode and could thus be attractive for applications in biofuel cells, especially if the substrate specificity of GO could be

broadened to other sugars, especially glucose.[131,133,134] There are numerous examples of the use of GO in biotechnological applications:

- Detection and quantification of D-galactose is important in a number of different situations. For example, the condition galactosaemia, where one of the enzymes required for D-galactose metabolism is absent, requires the patient to closely monitor their D-galactose intake and blood and urine levels.[139] It is necessary to monitor the levels of D-galactose and other GO substrates in the food industry, for example in processing of sugar beet[140] and in the dairy industry[141,142]

- Labelling of D-galactose-terminating glycans on cell surfaces has been used by several groups in characterising and quantifying different cell types, such as in brain tissue.[143] GO is also used in characterising changes upon virus infection of fibroblasts.[144]

- Labelling of cell surface glycans is also used in cancer diagnosis as the disaccharide D-galactose-β-(1-3)-*N*-acetyl-D-galactosamine (Gal-GalNAc) is expressed on the surface of colon cells in the early stages of carcinogenesis.[145-148] The same method has also been used for detection of breast carcinoma.[148]

- Modification of polysaccharides by GO provides access to oxidation of the natural plant-based polymer guar which has uses in paper strengthening.[149] Derivatives of galactoxyloglucan have potential uses in abrasion resistant clothing or diagnostic strips.[150]

- Generation of chemicals such as unnatural sugars,[151] sugar-based polymers used in hydrogels, adsorbents and biorecognition agents[152] and 5-*C*-(hydroxymethyl hexoses), a potential group of artificial sweeteners[153] can all be carried out using GO as a catalyst.

Parikka and Tenkanen studied GO catalyzed oxidation.[154] Their main aim was to control the degree of reaction, optimizing aldehyde (methyl-α-D-galacto-hexodialdo-1,5-pyranoside) production, and minimizing the formation of side products from the reactive aldehydes. The reaction conditions chosen for preliminary experiments were combined as reported earlier. GO, produced in transgenic *Pichia pastoris* carrying

the galactose oxidase gene from *Fusarium* spp. was used as a catalyst, methyl-α-D-galactopyranoside as substrate, reaction temperatures were between 4 and 40 ℃, combinations of galactose oxidase, catalase, and horseradish peroxidase were varied. Phosphate buffer (pH 6 to pH 7.3), and H_2O have been used as reaction media in GO-catalyzed reactions. The reactions were first followed with thin-layer chromatography (TLC) and then analysed by ^1H NMR spectroscopy and GC-MS and the main products were isolated, characterized, and identified. The preliminary experiments showed one main product and several secondary products in the reaction mixture. The three most stable products were isolated by preparative TLC, and characterized by NMR and mass spectrometry. The main product of GO-catalyzed oxidation of methyl-α-D-galactopyranoside **1** was an aldehyde **2,** shown below in Fig. 99.[154]

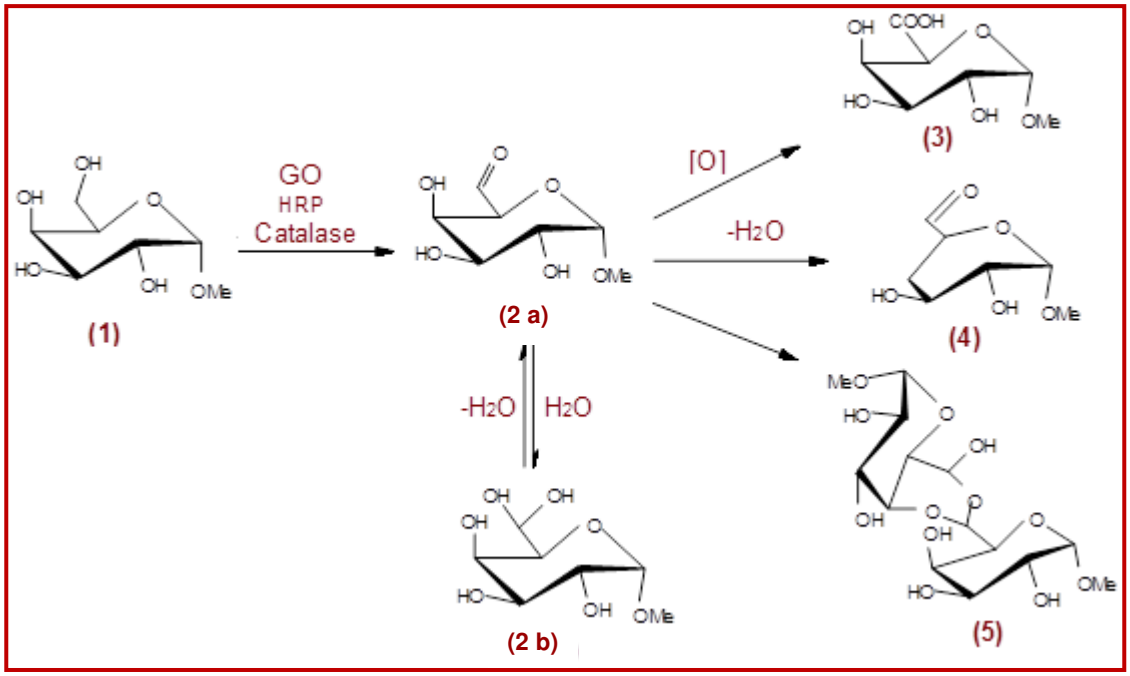

Figure 100: Oxidation of methyl-α-D-galactopyranoside and the formation of secondary products.[154]

The product **2** existed as a hydrate in D_2O, Fig 99, 2b above with an intermediate 2a, and NMR analysis confirmed the structure. The main side products were found to be uronic acid **3** and α, β unsaturated aldehyde **4**. An optimal combination of all the three enzymes gave aldehyde (methyl-α-D-galacto-

hexodialdo-1,5-pyranoside) in approximately 90% yield. The main secondary product, uronic acid (3), and an unsaturated aldehyde (4), were observed for the first time to form in parallel. ^{1}H and ^{13}C NMR data of the products were reported for the α, β unsaturated aldehyde for the first time.[154]

The reaction conditions in oxidations of other galactose derivatives were optimised with a trisaccharide, D-raffinose, and the reaction was followed by NMR spectrometry. Substrate **6,** D-raffinose, was converted to the corresponding aldehyde **7**, using all the three enzymes and water as a solvent (Fig. 100). Oxidation of D-raffinose resulted in approximately 90% yield of the corresponding aldehyde.

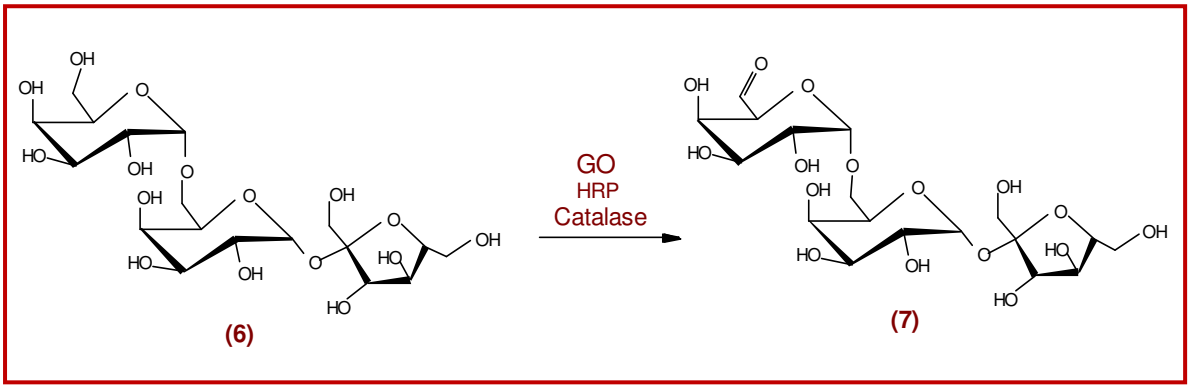

Figure 101: Oxidation of D-raffinose using three types of enzymes.[156]

Parikka, Tenkanen and colleagues published further work in which they used GO as a catalyst to oxidize selectively the C-6 hydroxyls of terminal galactose to carbonyl groups.[155] The polysaccharides studied included spruce galactoglucomannan (GGM), guar galactomannan (guar gum, GM), larch arabinogalactan (AG), corn fibre arabinoxylan (corn fibre gum, AX), and tamarind seed xyloglucan (XG) with terminal galactose contents varying from 6% to 40%. A combination of two enzymes was used to enhance the action of galactose oxidase. The oxidation conditions optimized earlier with methyl-α-D-galactopyranoside and raffinose were applied here for the oxidation of the polysaccharides (Fig. 101) and spruce galactoglucomannan was used in the preliminary experiments to confirm the reaction conditions and enzyme dosages suitable for the polymers. An analysis technique was developed for the quantification of the reactive aldehydes with GC-MS, utilizing reduction with $NaBD_4$ and acidic methanolysis. Results were varied

between the polysaccharides. The best degrees of oxidation of terminal galactosyls were obtained with xyloglucan (85%) and spruce galactoglucomannan (65%). The highest oxidation degree based on total carbohydrates was achieved with guar gum (28%), which had the highest galactose content. Some other alcohols with a primary hydroxyl group, such as glycerol, salicyl alcohol, and xylitol, are reported to be substrates for GO.[155]

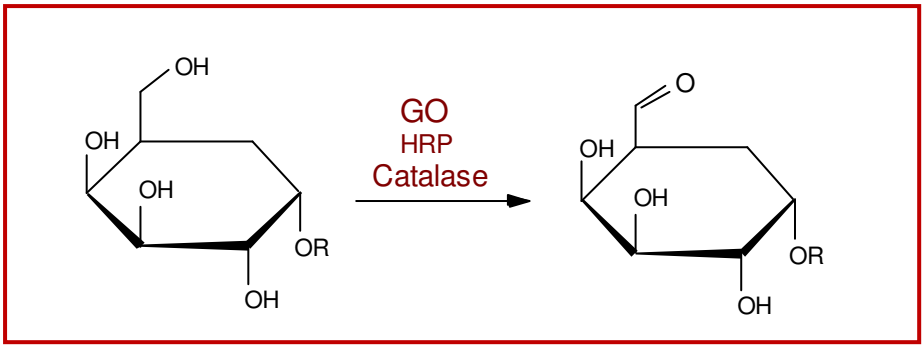

Figure 102: GO-Catalysed oxidation of the galactose units of polysaccharides.[155]

Leppanen, Parikka, Eklund *et al*. presented the first ever report on the utilization of MALDI-TOF-MS in the analysis of enzymatically and chemically modified GGM, and GM derivatives.[156] Galactose units of spruce GGM, guar GM and tamarind (XG) were selectively allylated. Aldehyde groups formed enzymatically in the above-mentioned galactose-containing polysaccharides were chemically derivatized by indium mediated allylation. Aldehyde functionalities were formed at the C-6 position *via* enzymatic oxidation by galactose oxidase along with catalase and horse radish peroxidase (HRP). Polysaccharides that were selectively oxidized by GO were spruce O-acetyl GGM, guar GM, and (galacto) XG. They were modified in a one-pot reaction as all reaction steps were done in water. The formation of the allylated or propargylated product was identified by MALDI-TOF–MS. All polysaccharide products were isolated and further characterized by GC–MS or NMR spectroscopy on Bruker AV 600 instrument. As a solvent a mixture of d_6-DMSO and D_2O (1:2) was used. These experiments were successful in adding allyl functionalities onto different polysaccharides.[156]

Siebum and colleagues investigated the utility of both galactose oxidase and alcohol oxidase for use in alcohol-to-aldehyde oxidations. Alcohol oxidase has been successfully used in combination with the aldolase DERA in a two-step, one-pot reaction.[157] These authors investigated the preparative scope and limitations of the enzymes on the basis of 30 different alcohol substrates. Galactose oxidase (*D. dendroides*) and alcohol oxidase (*P. pastoris*) were used as biocatalysts. Both enzymes were oxidases that use molecular oxygen as an electron acceptor in the oxidation of alcohols to aldehydes (Fig. 102). It was discovered that the reaction does not require a cofactor like NADPH which makes oxidases more suitable for biocatalytic oxidations than the cofactor-dependent dehydrogenases. To test the synthetic utility of the oxidizing enzymes, 30 different (highly) functionalized primary alcohols were treated with GO and AO. Overall conversions were determined by NMR after 48 hrs of reaction. GO remained largely selective to galactose-derived substrates. AO had a clear preference for unbranched, aliphatic, primary alcohols. They had proved that both GO and AO can be used for the preparation of functionalized aldehydes, under mild aqueous conditions, on a synthetically useful scale.[157]

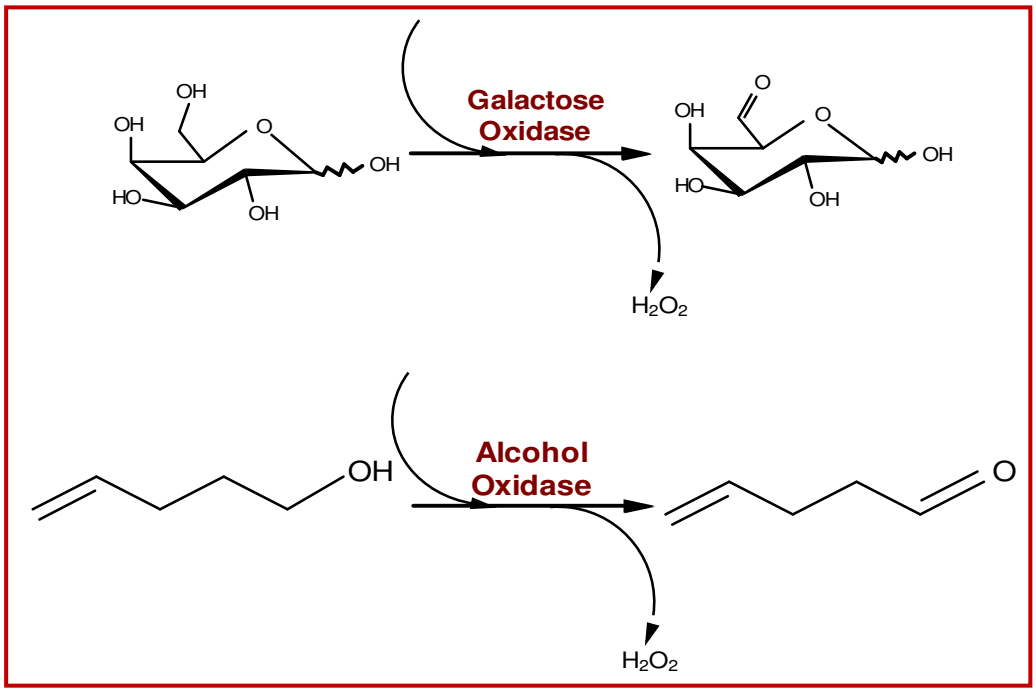

Figure 103: The galactose oxidase (GO) and alcohol oxidase (AO) catalytic systems.[157]

Kinoshita, Inagake and co-workers carried out fluorimetric determination of mucin-type glycoproteins using galactose oxidase and peroxidase.[160] Galactose oxidase oxidizes galactose and/or *N*-acetylgalactosamine in solution (Fig. 103) and produces hydrogen peroxide which reacts with the fluorogenic substrate, 3-(*p*-hydroxyphenyl) propionic acid (HPPA), in the presence of HRP; the oxidized substrate emits fluorescence at 405 nm after excitation at 320 nm.

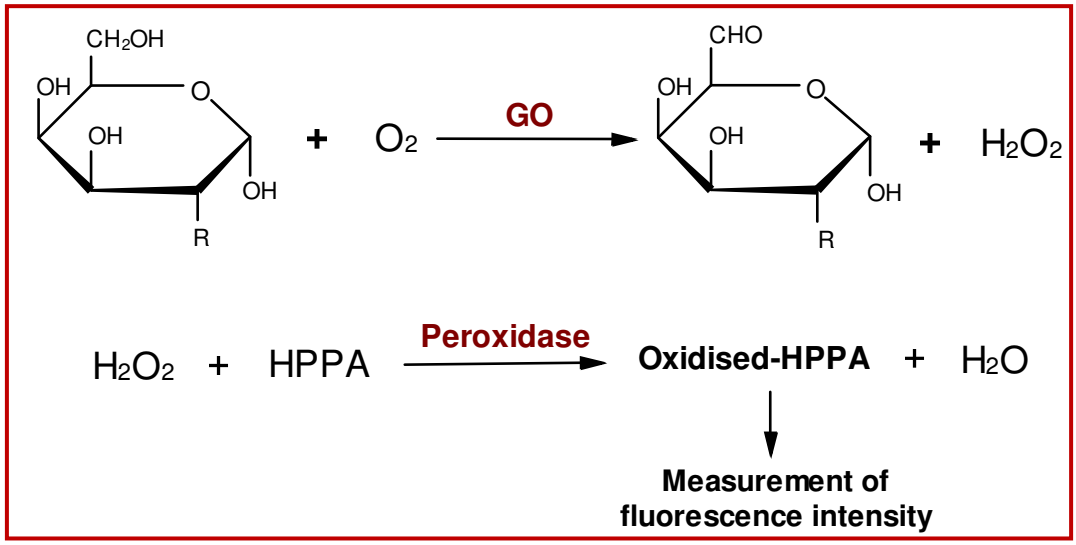

Figure 104: The galactose oxidase (GO) and alcohol oxidase (AO) catalytic systems.[158]

Although the fluorimetric determination of carbohydrates using glucose oxidase and galactose oxidase has been reported, the optimal conditions for quantitative determination were not described before. Using acid-hydrolysates of bovine submaxillary mucin (BSM, 50 mg) as a model, conditions for fluorimetric determination by the galactose oxidase-HRP method were optimized. Tris-HCl buffer (0.1 M, pH 8.0) was employed for the enzyme reaction and both enzyme reactions proceeded sufficiently at pH 8.0. With the change in concentration of galactose oxidase and peroxidase, the fluorescent yields became constant. Galactose oxidase (D-galactose: oxygen 6-oxidoreductase) specifically oxidizes the C-6 hydroxymethyl group of galactose and *N*-acetylgalactosamine. Previous studies evaluated fluorogenic substrates for the fluorometric assay of hydrogen peroxide based on the HRP-catalyzed reaction and demonstrated that 3-(*p*-hydroxyphenyl propionic acid) (HPPA) was one of the best substrates. They described a specific method for the determination of galactose/*N*-acetylgalactosamine in some glycoprotein samples.[158]

3.2 Aim of research

This project aims are;

- To evaluate different methods for enzyme oxidation of galactose to produce galactose with an aldehyde group on.
- To react that compound with complex-1 (as mentioned in section 2.3 at page 76) to make a luminescent sugar complex.

3.3 Experimental

Materials

Galactose, methyl-β-D-galactopyranoside and horse radish peroxidase were purchased from Fluka chemicals (purity 99 %).

Galactose oxidase, camphorsulfonic acid (CSA), catalase (solid) and catalase suspension were purchased from Sigma (purity 99 %).

Solvents

Acetonitrile (99.6 +%) certified HPLC grade, methanol (99.8 +%) certified HPLC grade and phosphate buffer (potassium dihydrogen phosphate 50 mM) were purchased from Fisher Scientific (UK).

DCM, DMSO, DIPE, glacial acetic acid, potassium permanganate, acetic acid, petroleum ether and 2-propanol were all purchased from Fisher Scientific (UK).

Chloroform-d and D_2O were purchased from Goss Scientific Ltd.

Stock solutions and working solutions were prepared by successive dilution with acetonitrile or DMSO.

Instrumentation

- Chromatographic separation was developed on a Shimadzu Prominence UFLC system running LabSolutions software (v. 5). The column used was a Lichrospher 100, RP-18 (250 mm x 4.6 mm, 5 µm), column no. 026023, Lot. No. 497017 purchased from VWR (Merck, Germany).
- Samples were analysed on a Bruker MicrOToF-q mass spectrometer coupled to the Shimadzu UFLC system. Positive mode electrospray ionisation was chosen.

MS data acquisition and processing were carried out using Bruker's proprietary software, DataAnalysis.

- Sample purification was carried out using a Gilson prep-HPLC, Model-803C mono-metric module, using Gilson Piston Pumps Model 303 and 305. The column used was a Dynamax, pre-packed C_{18} column module, 21.4 mm I.D x 250 mm, serial No. B910924. The detector was a Gilson HM Holochrome UV-VIS using 286 nm wavelength. The data was collected on a chart recorder (Kipp and Zonen BD 40) and integrator. The mobile phase (A) was MeCN, 65 % and mobile phase (B) was HPLC water, 35 %. The flow rate was kept constant at 10.00 mL/min. The run time was 60 mins.
- NMR experiments were carried out using a Bruker Avance 500 MHz NMR spectrometer at room temperature. The software used was Topspin 1.3.
- Removal of the enzyme from reaction mixtures was performed using Amicon cartridges (Millipore) and an MSE Microcentaur centrifuge at 13,000 rpm.
- TLC was performed on silica and alumina plates, as appropriate.
- Where samples required drying they were frozen under liquid nitrogen and freeze-dried overnight using a Modulyo Edwards Model RV 3 freeze dryer. The parameters used are tabulated below:

Temperature	-45^0 C
Pressure	10^{-3} Torr
Capacity of round-bottom flask	250 ml
Sample volume	3-4 ml

Table 35: Instrumental parameters used for the freeze dryer

3.4 Methodology

3.4.1 NMR Timed experiment for oxidation reaction

Galactose powder (2 mg) and galactose oxidase enzyme (2.56 mg) were dissolved in D_2O (0.650 mL).

Experimental protocol - On small scale

Experiment – 1

Galactose powder (2 mg) was dissolved in D_2O (0.650 mL) and the ^1H NMR spectrum was recorded. Galactose oxidase (2.56 mg) was then added and the solution heated for 4 hrs in a water bath at 37 $^{\circ}C$. The ^1H NMR spectrum was then re-recorded.

Experiment – 2

Experiment 1 was repeated keeping all the conditions constant. Galactose powder (2 mg) was dissolved in D_2O (0.650 mL) and the ^1H NMR spectrum was recorded. The reaction mixture was heated for 1 hr only, instead of 4 hrs, in a water bath at 37 $^{\circ}C$ and the ^1H NMR spectrum was re-recorded.

3.4.2 Comparison of Methodologies for oxidation reaction

Four different methodologies were tested, and compared to see which one was the best one for the enzyme oxidation of galactose and that method can be used to attach complex 1 to obtain a luminescent sugar complex.

3.4.2.1 Method 1

The first experimental protocol followed was the enzymatic assay of galactose oxidase.[159]

NMR Timed experiment for oxidation reaction

Galactose powder (99.3 mg) was dissolved in D_2O (1.0 mL) and galactose oxidase enzyme (0.135 mg) was added. The reaction mixture was incubated for 2 hrs in a water bath at 37 $^{\circ}C$. An aliquot (0.650 mL) was removed and analysed by ^1H NMR spectrometry.

3.4.2.2 Method 2

Next method of enzymatic oxidation was used according to the paper of Parikka and Tenkanan .[154] The reaction mixture was prepared as follows:

Experiment (1)

Enzymatic assay of galactose oxidase

Galactose oxidase (1.41 mg), horse radish peroxidase (0.39 mg), methyl-β-D-galactopyranoside (100 mg) and catalase (56 mg) were combined and dissolved in deionized water (7.5 mL) in a large vial, without a lid. The reaction was stirred for 24 hrs at 4 °C. After 4.5 hrs an aliquot (0.5 mL) of the reaction mixture was removed and spun through an Amicon filter (10,000 MWCO) for 30 min. to remove the enzymes. The filtrate containing the small molecules was collected, dried in a speed dryer for 1 hour then reconstituted with D_2O (0.650 mL) and the ^1H NMR spectrum was recorded. Then, after 24 hrs the reaction was stopped, another aliquot (0.5 mL) was removed, the enzymes were removed and the sample was dried and reconstituted with D_2O (0.650 mL) and its ^1H NMR spectrum was recorded.

Experiment (2)

With catalase suspension

Galactose oxidase (1.41 mg), horse radish peroxidase (0.39 mg), methyl-β-D-galactopyranoside (100 mg) and catalase suspension (0.03 mL) were dissolved in deionised water (7.5 mL). An aliquot (0.5 mL) was removed, spun through an Amicon filter (10,000 MWCO) to remove the enzymes and set aside for subsequent analysis (t = 0). The reaction solution was transferred into a large vial, without a lid, which was stirred for 24 hrs at 4 °C. Aliquots were removed after 1, 2, 3, 4 and 24 hrs and processed as the t = 0 sample. All samples were dried, reconstituted with D_2O (0.650 mL) and their ^1H NMR spectra recorded. An additional sample was removed at t = 24 hrs and processed as before except that the ^1H NMR spectrum was recorded in d_6-DMSO rather than D_2O.

Experiment (3)

The above experiment was repeated. Galactose oxidase (1.41 mg), horse radish peroxidase (0.23 mg), methyl-β-D-galactopyranoside (100 mg) and catalase suspension (0.03 mL) were dissolved in deionised water (7.5 mL). A small portion of the reaction mixture (0.5 mL) was removed, spun down through an Amicon filter to remove the enzymes and set aside (t = 0). Further aliquots were removed over 4 hrs and the ^{1}H NMR spectra of all aliquots were recorded. The reaction mixture was left overnight. After 24 hrs a further aliquot (0.5 mL) was removed, the enzyme removed, the sample dried and d_6-DMSO added (0.650 mL). The ^{1}H NMR spectrum was recorded.

3.4.2.3 Method 3

Another method of enzymatic oxidation was used according to the paper of Siebum *et al.*[157] The reaction mixture was prepared as follows:

Experiment (1)

TLC

Methyl-β–D-galactopyranoside (30 mg) was dissolved in deionised water (1 mL) and the solution was analysed using TLC (SiO_2, MeOH, chloroform, acetic acid and deionized water (30:60:4:4 v/v). The TLC plate was dipped in potassium permanganate to allow visualisation of the spots.

Experiment (2)

To a conical flask (20 mL capacity) was added phosphate buffer (5.0 mL, 50 mM, pH 7.0). Methyl-β–D-galactopyranoside (194 mg), galactose oxidase (8.1 mg, 30 units), and catalase (14.4 µL, 4880 units) were dissolved in deionised water (7.5 mL). The aqueous solution was then added to the buffer. This reaction mixture was placed under an oxygen atmosphere and stirred at 4 ºC for six days, during which time the reaction was monitored by TLC (SiO_2, MeOH, chloroform, acetic acid and deionised water (30:60:4:4 v/v). The TLC plate was dipped in either potassium permanganate or DNP to aid visualisation of the spots. The sample was separated using column chromatography using the same mobile phase used for TLC. The fractions were collected, combined and freeze dried in a round bottom flask,

separately, overnight. Then a small part of the sample was removed and its ^{1}H NMR spectrum was recorded in d_6- DMSO.

3.4.2.4 *Method 4*

A different method of enzymatic oxidation was used according to the paper of Osuga *et al.*[160] The reaction mixture was prepared as follows:
Methyl-β-D-galactospyranoside (40 mg), galactose oxidase (122 mg, 450 U) and catalase (4 mg) were dissolved in phosphate buffer (1 mL, pH 6.0). The mixture was stirred on a hot plate at 25 ºC for 24 hrs and the reaction was monitored by TLC (SiO_2, n-propanol/ethanol/water (3:2:1 v/v). The aldehyde product was visualised using 0.4 % DNP in HCl (2 N). After 24 hrs the reaction mixture was heated to 95 ºC for 5 min (to denature the enzyme) and the protein precipitated was removed by centrifugation. The product obtained was freeze dried. Two samples of the product were scratched from the side and the base of the flask. The ^{1}H NMR spectra of both samples were recorded in d_6- DMSO and D_2O.

3.4.2.5 *Best oxidation method to use with rhenium complex*

Four different methodologies were investigated for the oxidation of methyl-β-D-galactopyranoside using galactose oxidase and the best results were achieved using method 2. The aldehyde product of methyl-β-D-galactopyranoside obtained in method 2, was then reacted with complex 1 (as mentioned in section 2.3 at page 76).

A) Reaction of oxidation product with rhenium complex (Complex 1) experiment using Method 2

TLC analysis of the reaction mixture (without complex-1)

The mobile phase for TLC was made by mixing MeOH (10 mL), DCM (20 mL), glacial acetic acid (1 mL) and deionised water (1 mL). The reaction mixture was spotted onto the silica plate and the plate was eluted. The plate was dried and dipped in a solution of potassium permanganate, ($KMnO_4$, in 5% NaOH) dried and observed under a UV lamp.

Column chromatography of the reaction mixture

The reaction mixture was separated on a silica column using the same mobile phase as the TLC separation and fractions were collected. Fractions 1-23, 24-45 and 46-70 were combined (separately) and dried. The ^{1}H NMR spectra of the samples were acquired in DMSO-d_6 which showed that fractions 24-45 contained more material than other two fractions 1-23 and 46-70.

Reaction mixture (with complex-1)

Next, MeCN (5 mL) was added to a flask containing fractions 24-45. Complex 1(10 mg) and few grains of CSA were added to it. The reaction mixture was left overnight. An aliquot (1.0 mL) was removed after 24 hrs, dried under vacuum and the ^{1}H NMR spectrum of the sample was acquired in d_6- DMSO.

TLC of fraction 24-45

TLC separation of the reaction mixture was attempted using a silica plate and 1% MeOH in DCM as the mobile phase. This experiment was then repeated using 3 %, 5 % and 10 % MeOH in separate experiments to find out which percentage separated the reaction mixture best. The result showed that 10 % MeOH in DCM separated the reaction mixture best.

Column chromatography of the reaction mixture

After optimisation of the separation conditions, the sample was then separated by column chromatography using 10% MeOH solution in DCM as the mobile phase. Two prominent bands were visible. Any yellow fractions were collected as these would correspond to rhenium-containing species. Fractions 1 (18-23) and fractions 2 (26-39) were combined, dried under vacuum and dissolved in d_3-MeCN and analysed using ^{1}H NMR spectrometry.

Liquid chromatography

Fraction 1 was dissolved in MeCN (1 mL) and analysed using LC at 65% MeCN and 0.5 mL/min flow rate. The separation achieved was insufficient so the experiment was repeated using different percentages of MeCN (50%, 45% and 35%)

to obtain adequate separation. Separation with 35% MeCN, 0.5 mL/min gave optimum separation. Fraction 2 was then analysed using this method.

Preparative high performance liquid chromatography (HPLC)

It was decided to use preparative HPLC to collect a workable amount of pure compound for subsequent analysis. The remainder of the LC-MS sample was divided into two aliquots (2 x 0.45 mL) and run through the preparative HPLC. In order to get the pure product, fractions were collected after every 30 sec from the start, *i.e.* t = 0, for both aliquots. The fractions were collected and stored in labelled vials. The conditions used on prep-HPLC were as shown in Table 36.

Method No.	**2**
Range	1.0, 0.2 AUFS
Frequency	286 nm
Pressure	116 bars
ACN (A%)	65%
H_2O (B%)	35%
Flow rate	10 mL/min
Run time	50 min

Table 36: Conditions used for preparative HPLC separation of fractions

Two isomers were observed which were designated isomer 1 and isomer 2 in order of elution. For isomer 1, fractions 32-36 and 125-129 were collected, combined and the MeCN removed under vacuum. The remaining aqueous solution was extracted into DCM, dried ($MgSO_4$) and the solvent removed under vacuum. The ^1H NMR spectrum was acquired in CD_3CN. For isomer 2, fractions 43-48 and 137-142 were collected, combined and isolated as described above.

B) Reaction of oxidation product with rhenium complex (Complex 1) using Method 3

It was decided to separate the sample (section 3.4.2.3, method 3 and experiment 2) using column chromatography prior to analysis.

Column chromatography

The reaction mixture was separated on a silica column using the same mobile phase as the TLC separation (SiO_2, MeOH, chloroform, acetic acid and deionised water (30:60:4:4 v/v) Fractions 21-24 and 28-33 were collected, after column chromatography, and combined to give two samples for further analysis. The ^1H NMR spectra of the samples were acquired in d_6- DMSO and the fractions were freeze dried.

Next, MeCN (5 mL) was added to a flask containing fractions 28-33. Complex 1(10 mg) and few grains of CSA were added to it. The reaction mixture was left overnight. An aliquot (1.0 mL) was removed after 24 hrs, dried under vacuum and the ^1H NMR spectrum of the sample was acquired in d_6-DMSO.

3.5 Results and discussion

3.5.1 NMR Timed experiment for oxidation reaction

To determine whether the desired product had been formed in the reaction mixture a series of 1D NMR experiments were carried out.

Experimental protocol - On a small scale

Experiment – 1

Galactose powder (2 mg) was weighed and dissolved in D_2O (0.650 mL) and the ^1H NMR spectrum was recorded as a reference. Galactose oxidase (2.56 mg) was then added and the solution was heated for 4 hours in a water bath at 37 $^{\circ}C$. The ^1H NMR spectrum was then re-recorded. Fig.104 shows the ^1H NMR spectrum of the reaction mixture at t=4 hrs (In the spectra, below, α-s and β-s represents the peaks for starting materials and α-p and β-p represents the peaks for the product/s).

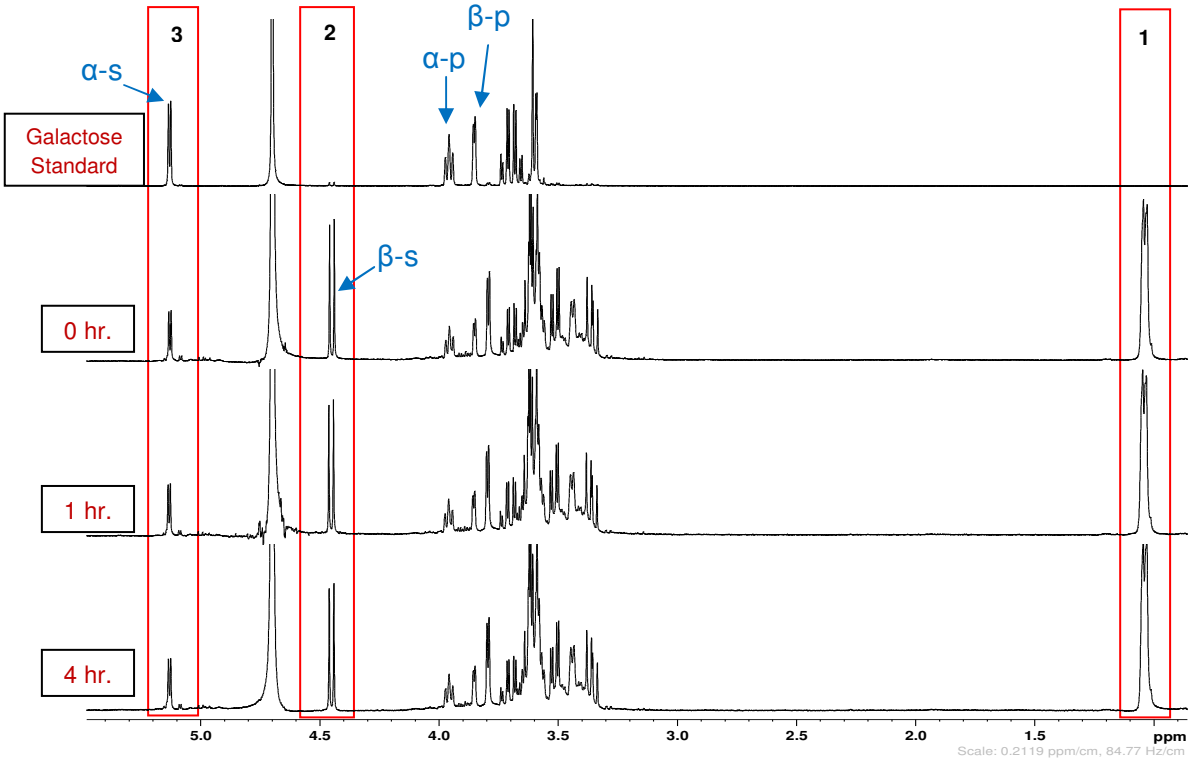

Figure 105: Comparison of selected regions of the ^{1}H NMR spectra of the reaction mixture with the galactose standard over time (t=0, 1 and 4 hr)

Comparison of a reaction mixture, run for up to 4 hrs with the standard of galactose suggested that subtle changes were observed between 3-4 ppm. A new signal arose at 1.0 ppm (1) and it persists there throughout the reaction run time. From the starting material (galactose) in Fig. 104, a reduction in the peak size was observed between 3.6 ppm to 4.0 ppm. There was an increase in the signals between 3.3-3.5 ppm. Signals become complex after 4 hrs in the reaction mixture. A doublet was seen to increase from minimal value as seen in the starting material between 4.4-4.5 ppm (2) which suggested that α-galactose was converted to β-galactose whose anomeric proton signal appeared between 4.4-4.5 ppm.

Experiment – 2

A spectrum was recorded for the galactose reaction mixture after 1 hr (Fig. 105, B) (B) compared with the standard (A) under identical conditions as above.

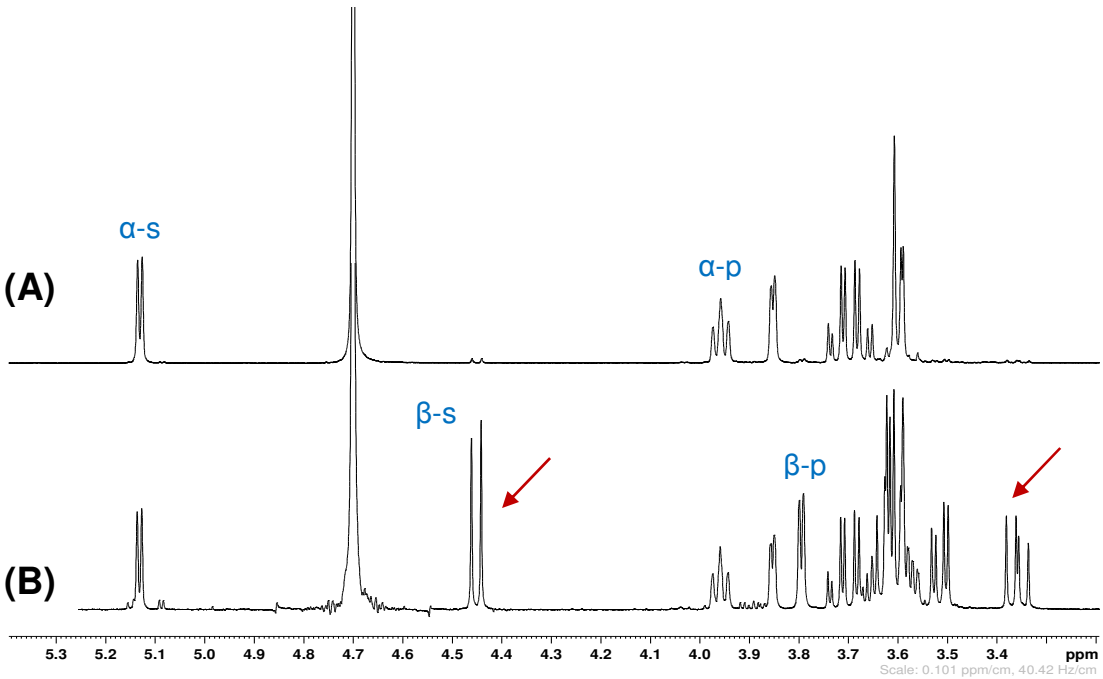

Figure 106: Selected regions of the ^{1}H NMR spectrum of the galactose reaction mixture after 1 hr (B) compared with the standard (A)

When the spectrum of the galactose standard (Fig. 105, A) was compared with the reaction mixture after 1 hr of heating in the water bath changes in the spectrum were seen between 4.4 and 4.5 ppm. Many changes were also observed when the part of the spectra between 3.30 – 4.06 ppm was expanded.

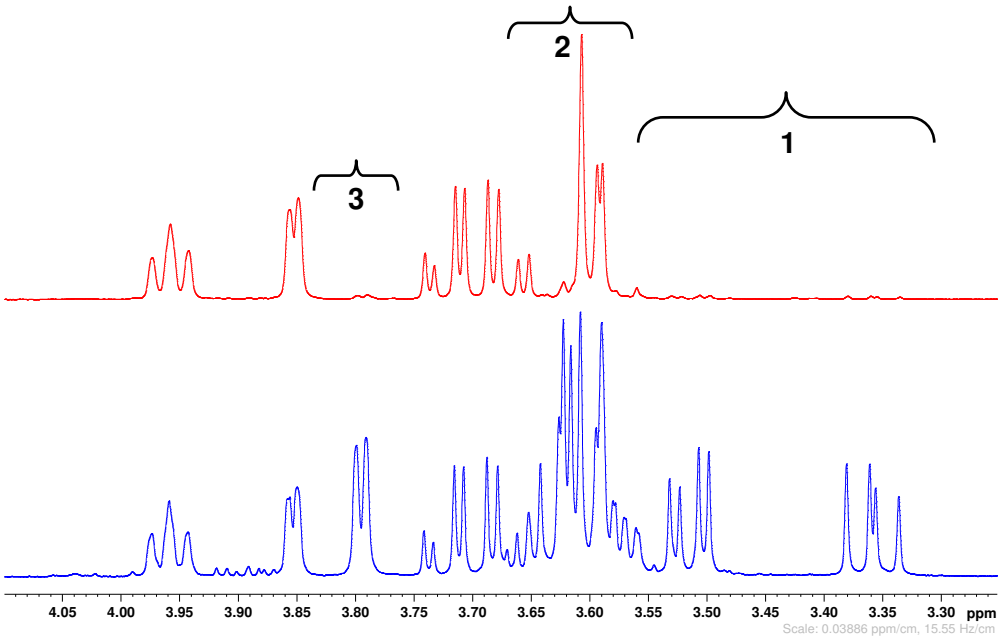

Figure 107: Selected regions of the ^{1}H NMR spectra of the galactose reaction mixture (bottom) compared with galactose (above)

Regions 1 and 3, above, showed that new signals appeared between these parts of the spectra, while in region 2 the signals became much complex.

3.5.2 Comparison of Methodologies for oxidation reaction

Four different methodologies were tested, and compared to see which one was the best one for the enzyme oxidation of methyl-β-D-galactopyranoside.

3.5.2.1 Method 1

The first experimental protocol followed was the enzymatic assay of galactose oxidase.[159]The basic principle is given below:

$$\text{D-Galactose} + O_2 \xrightarrow{\text{GO}} \text{D-Galacto-hexodialdose} + H_2O_2$$

NMR Timed experiment for oxidation reaction

Two ^{1}H NMR experiments were performed. For experiment A the reaction mixture was prepared with galactose powder (99.3 mg) in D_2O (1.0 mL) and galactose oxidase enzyme (0.135 mg) was added and incubated for 2 hrs. An aliquot (0.650 mL) was removed and analysed by ^{1}H NMR spectrometry. For experiment B the reaction mixture was prepared with methyl-β-D-galactopyranoside (99.3 mg) keeping all other conditions the same as experiment A.

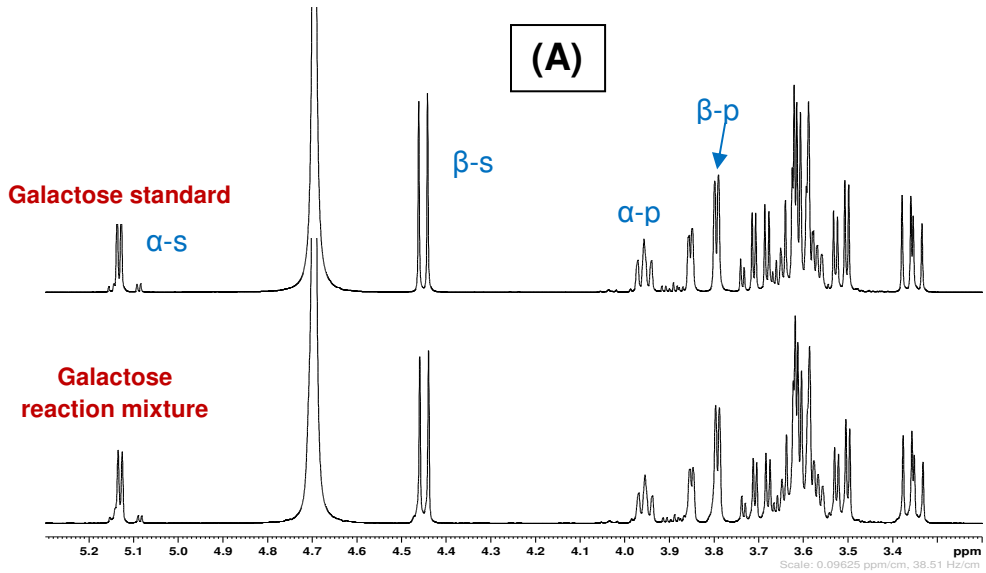

Figure 108: Selected regions of the ^{1}H NMR spectra of the galactose reaction mixture showing progress in the reaction (after 2 hrs)

The galactose reaction mixture was run for two hrs and when the ^{1}H NMR spectra of the selected regions (Fig. 107) were compared with the standard of galactose no significant change in the reaction mixture was observed (Fig. 108).

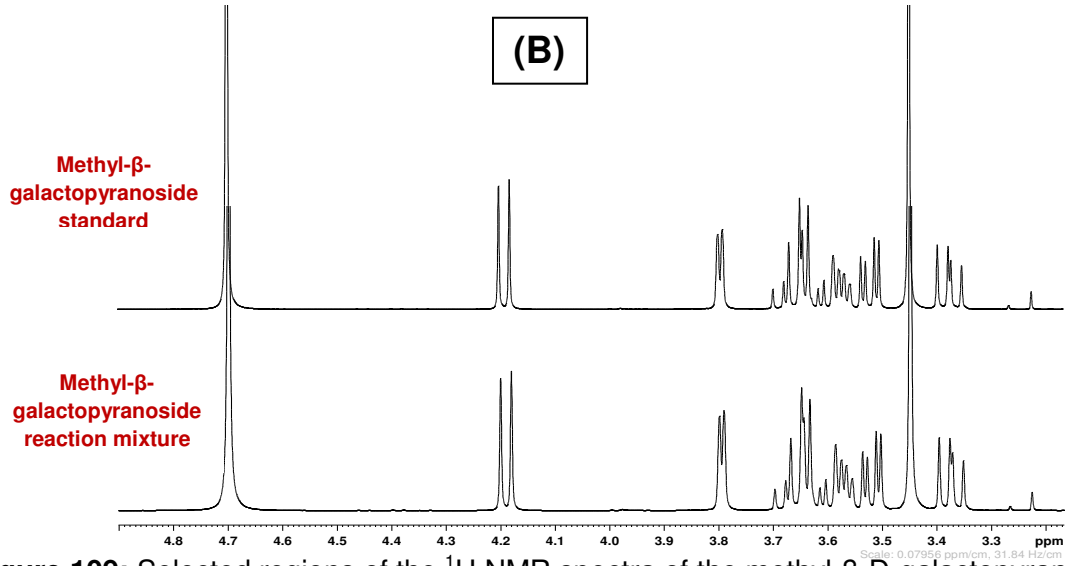

Figure 109: Selected regions of the ^{1}H NMR spectra of the methyl-β-D-galactopyranoside reaction mixture showing progress in the reaction (after 2 hrs)

3.5.2.2 *Method 2*

The experimental protocol followed was the oxidation of methyl-α-galactopyranoside by galactose oxidase described by Parrikka *et al.*[154] The main secondary products, a uronic acid (methyl-β-D-galactopyranosiduronic acid) and an unsaturated aldehyde, were observed for the first time to form in parallel.

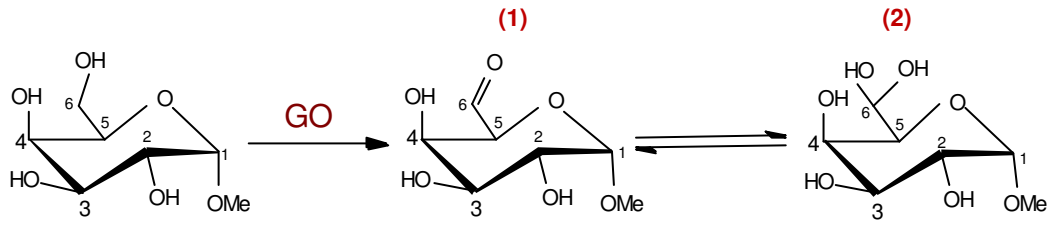

Figure 110: Conversion of methyl--D-galactopyranoside in to its oxidation products.[154]

Experiment (1)

Enzymatic assay of galactose oxidase

The reaction mixture was prepared with three types of enzymes: galactose oxidase (1.41 mg), horse radish peroxidase (0.39 mg) and catalase (56 mg). Methyl-β-D- galactopyranoside (100 mg) was used as a substrate and was dissolved in deionized water (7.5 mL). The reaction was stirred for 24 hrs at 4 °C. After 4.5 hrs an aliquot (0.5 mL) was removed and the enzymes removed using an Amicon filter (10,000 MWCO). The filtrate was collected, dried *in vacuo* then reconstituted with D_2O (0.650 mL) and the ^1H NMR spectrum was recorded.

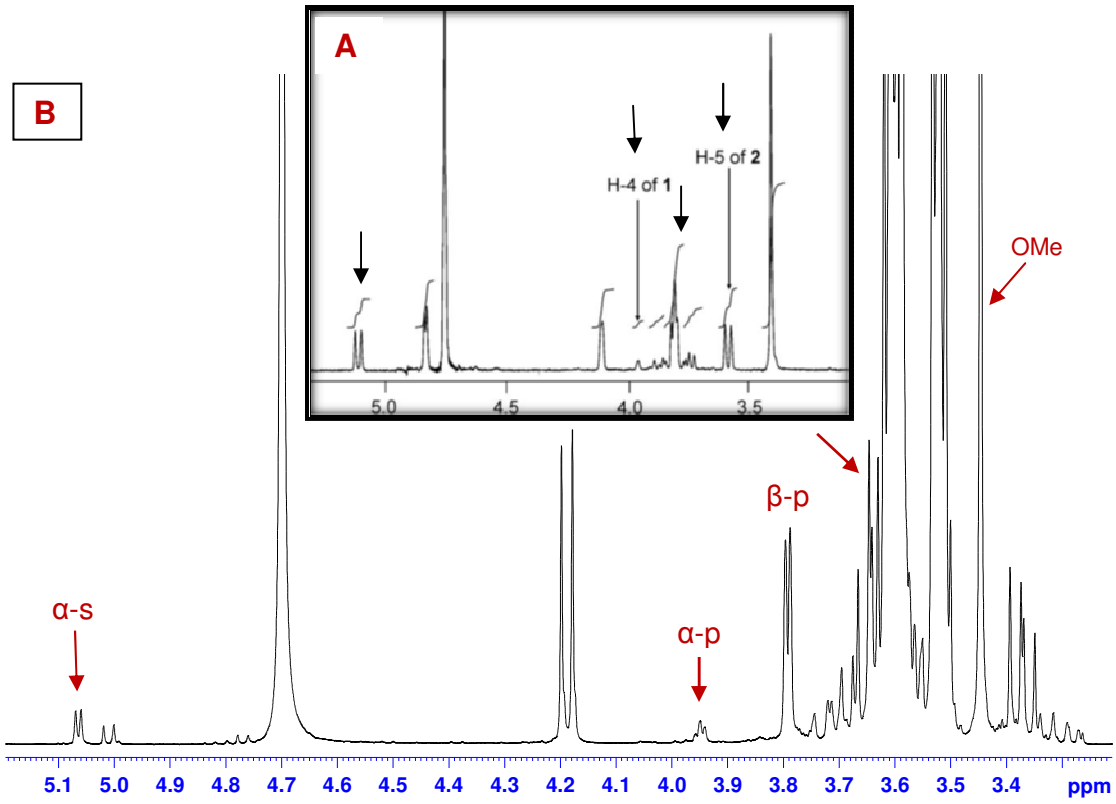

Figure 111: Selected regions of the ^1H NMR spectrum of the galactose oxidase reaction mixture (in D_2O) showing progress in the reaction after 5 hrs (B) compared with the reference ^1H NMR spectrum from K. Parikka and M. Tenkanen.[154]

The ^{1}H NMR spectrum (Fig. 110) shown in inset (A) was obtained by Parikka and co-workers after 5 hrs of reaction. It was clear from the above figure (B) that after 5 hrs changes were observed in the reaction mixture, especially at 3.6 ppm which shows that second product was formed. Between 3.9-4.0 ppm a very small peak showed that the first product was there but less abundant than was depicted in the literature.

After 24 hrs the reaction was stopped, another aliquot (0.5 mL) was removed, dried and reconstituted with D_2O (0.650 mL) and its ^{1}H NMR spectrum was recorded (Fig. 111, A) and compared with the reference spectrum from the literature (Fig. 111, B, inset). Some changes were observed in the spectrum; Fig. 112 shows the comparison of the ^{1}H NMR spectra after 5 and 24 hrs. A new signal was observed at 9.0 ppm (Fig. 113).

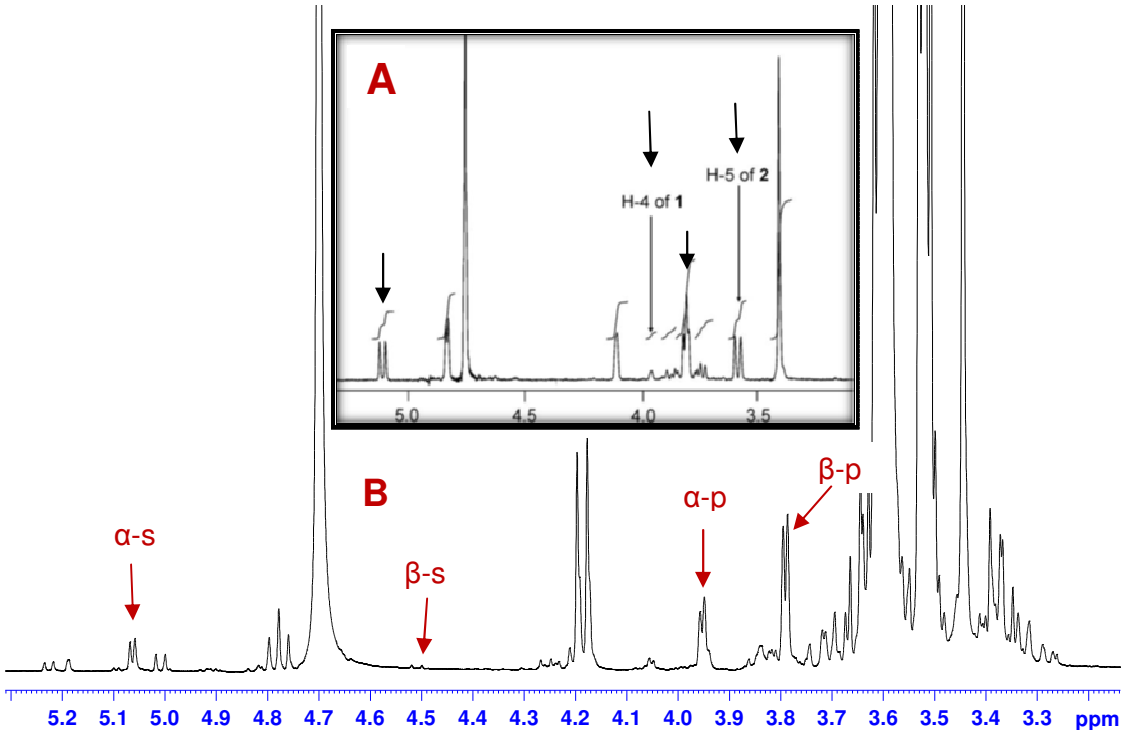

Figure 112: Selected regions of the ^{1}H NMR spectrum of the galactose reaction mixture (in D_2O) showing progress in the reaction after 24 hrs.[154]

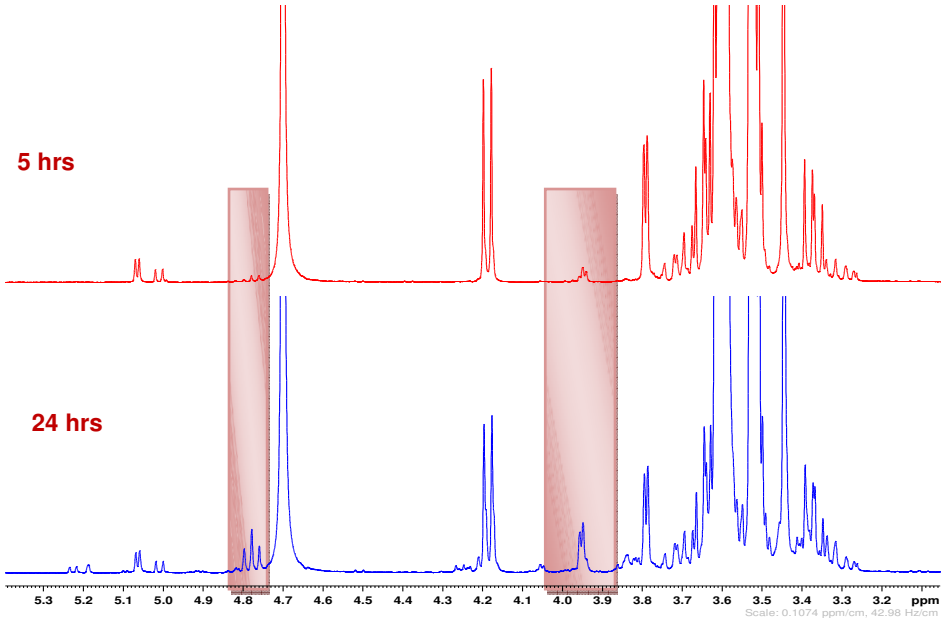

Figure 113: Selected regions of the ^{1}H NMR spectra of the galactose oxidase reaction mixture showing progress in the reaction after 5 hr and 24 hrs

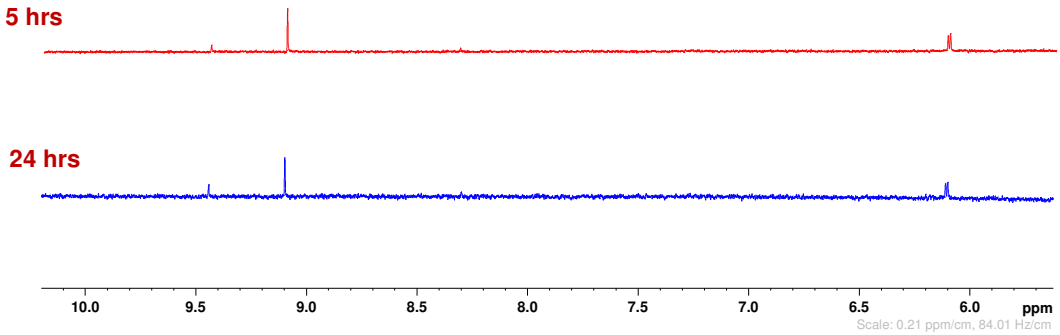

Figure 114: Expansion of the ^{1}H NMR spectra of the galactose oxidase reaction mixture showing formation of the aldehyde product after 5 hr and 24 hrs

Experiment (2)

With catalase suspension

The same reaction mixture was repeated but with the catalase suspension instead of the solid enzyme, to see whether it will give the products of our choice. The reaction mixture was prepared as follows: galactose oxidase (1.41 mg), horse radish peroxidase (0.39 mg), methyl-β-D-galactopyranoside (100 mg) and catalase suspension (0.03 mL) were dissolved in deionized water (7.5 mL). An aliquot (0.5

mL) was removed, ultrafiltered through an Amicon cartridge (10,000 MWCO) to remove the enzymes and set aside for subsequent analysis (t = 0).

The reaction solution was stirred for 24 hrs at 4 °C. Aliquots were removed after 1, 2, 3, 4 and 24 hrs and processed as the t = 0 sample. All samples were dried, reconstituted with D_2O (0.650 mL) and their ^1H NMR spectra recorded (Fig. 114). An additional sample was removed at t = 24 hrs and processed as before except that the ^1H NMR spectrum was recorded in d_6- DMSO rather than D_2O.

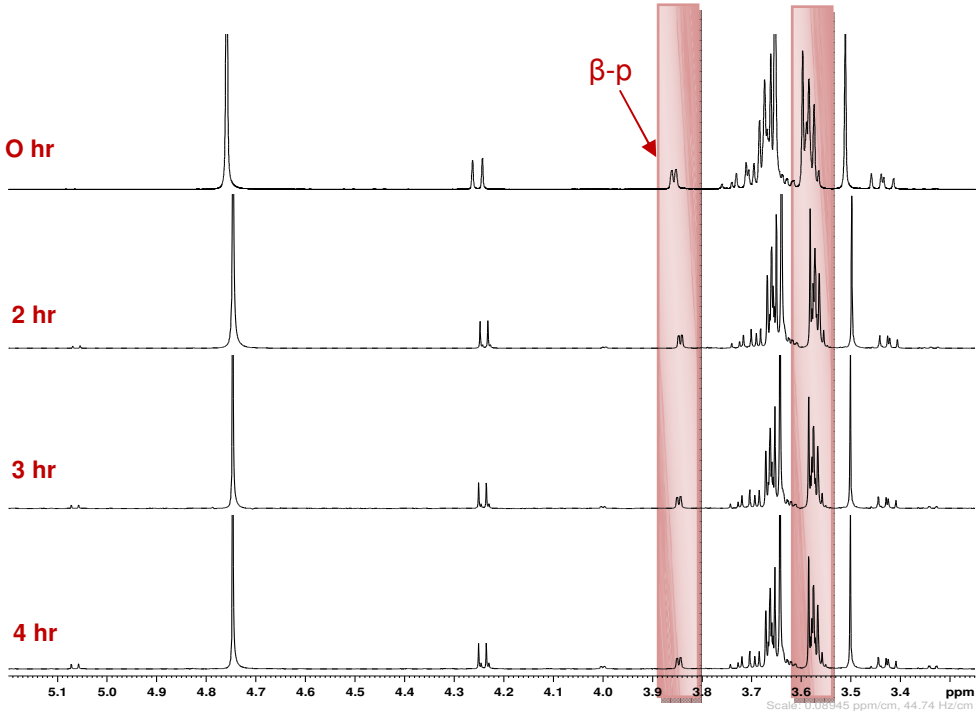

Figure 115: Stacked ^1H NMR spectra of above reaction (t=2 hr and 4 hr) compared with t=0

After comparing results, at different time intervals, it was found out that the results were encouraging but not as clear. The ^1H NMR spectra of the reaction mixture (t=0 and t=4 hrs) were compared with the reference ^1H NMR spectrum from Parikka *et al*[154] which indicated that a number of peaks were in accordance with the reference spectrum showing that partial oxidation had occurred. The signals for the formation of the product were present between 3.5 ppm and 3.6 ppm (Fig. 115). The signals present between 3.8-3.9 ppm clearly showed that the proton signals from product 1, which were expected and a peak appeared at 9.1-9.2 ppm (Fig. 116, below) corresponding to formation of an aldehyde although there was also a new signal at 9.5 ppm which could not be identified.

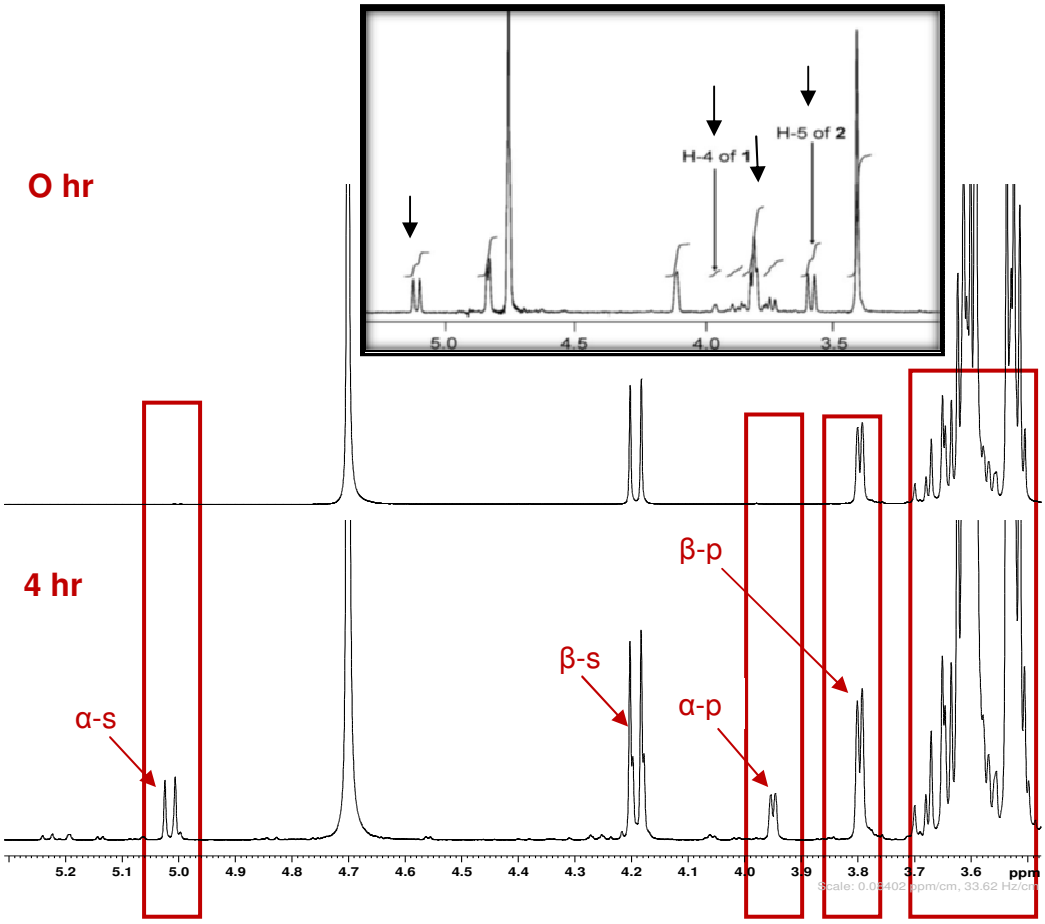

Figure 116: ^{1}H NMR spectra of the reaction mixture (t=0) and after (t=4 hr) along with the reference ^{1}H NMR spectrum from Parikka *et al.*[154]

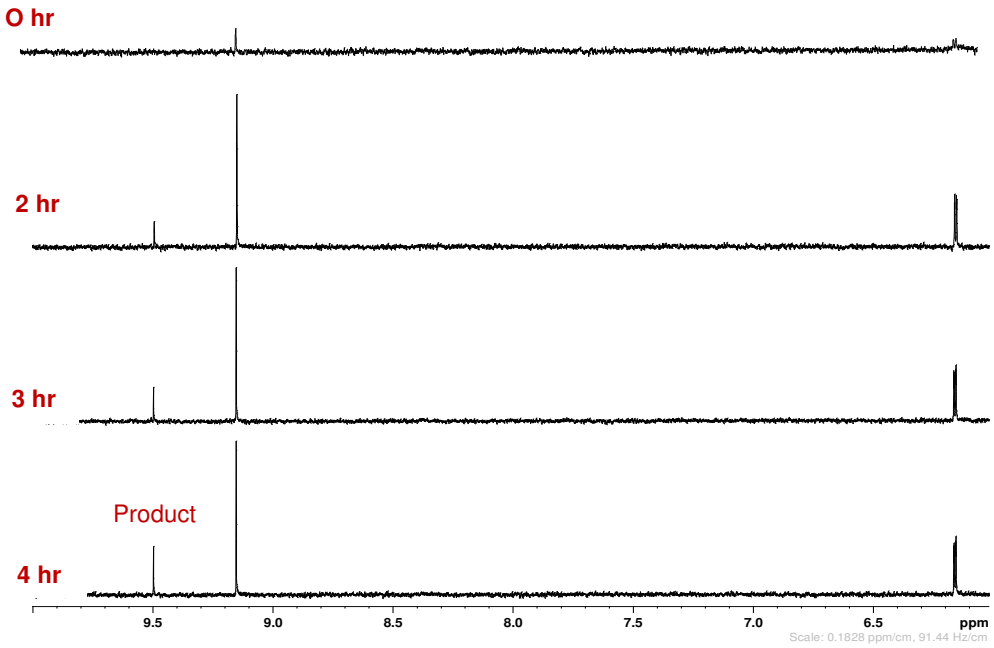

Figure 117: Selected regions of the ^{1}H NMR of the reaction (t=2 hr to 4 hr) compared with t=0 showing formation of the aldehyde product

The reaction mixture was allowed to run for 24 hrs. After that, the ^{1}H NMR spectra were run in d_6-DMSO and D_2O and the result with D_2O showed that the oxidation reaction brought changes in the proton NMR as the signals become quite complex in the region between 3.6-4.1 ppm (Fig. 117).

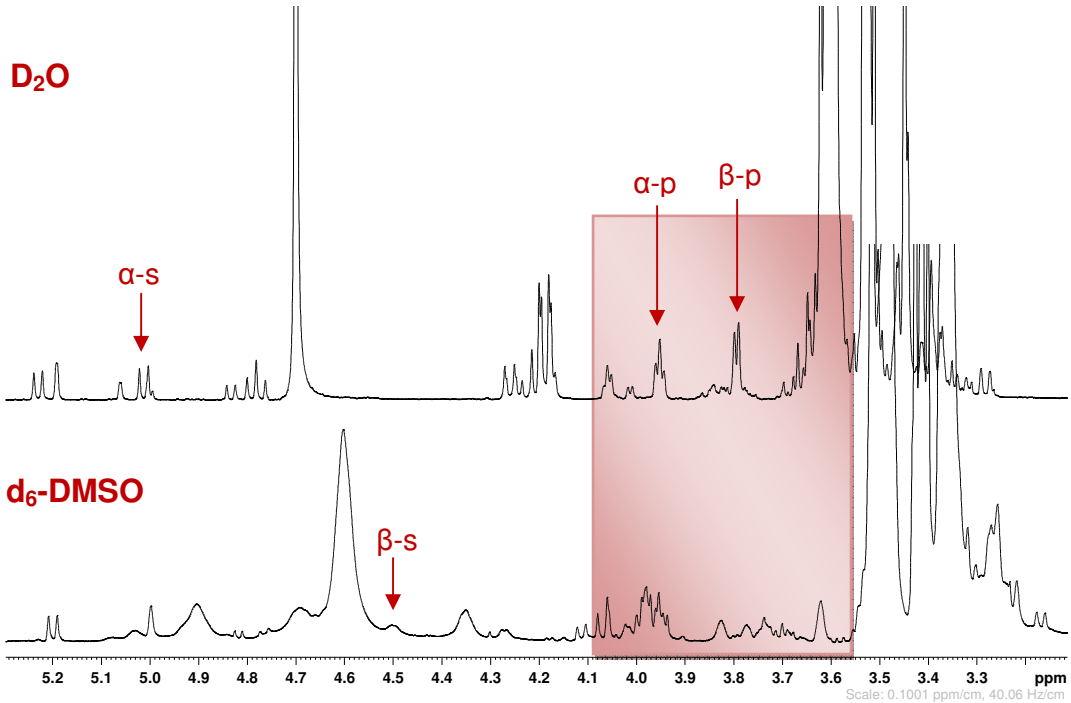

Figure 118: Selected regions of the ^{1}H NMR spectra of the galactose oxidase reaction mixture showing progress in the reaction after 24 hr in D_2O and d_6-DMSO

When the selected regions of the reaction mixture after t=24 hrs (D_2O) were compared with t=0, the spectra clearly indicated that oxidation had occurred and this brought changes in the spectrum after 24 hrs (Fig. 118). However, when the spectrum of t=24 hrs (D_2O) was compared with the reference spectrum t=0 (Fig. 117) it was concluded that reaction did occur but was not as efficient as had been expected.

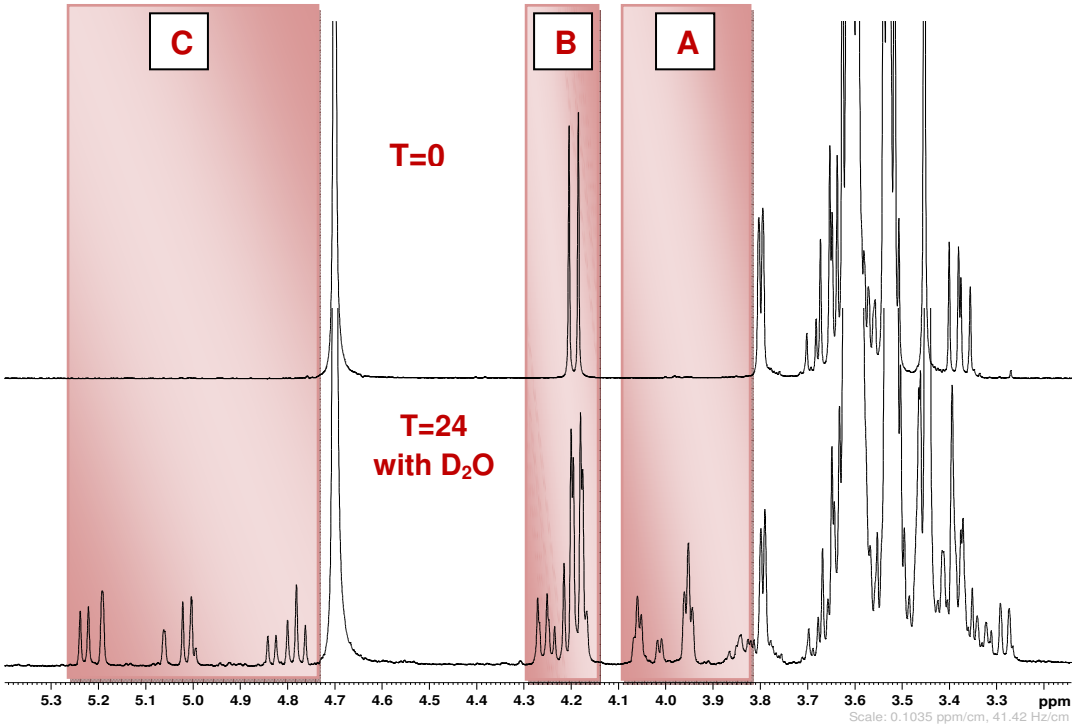

Figure 119: Selected regions of the ^{1}H NMR spectrum of the galactose oxidase reaction mixture showing progress in the reaction after 24 hrs in D_2O and compared with t=0

The above proton NMR clearly showed that after 24 hrs most of the features not observed at t=0 in Fig. 118 appeared in the post reaction, especially in the region labelled as A. New signals appeared in two regions of the proton NMR spectrum, between 3.8-4.1 ppm and 4.7-5.2 ppm. The peaks corresponding to the reaction mixture became complex (B).

Experiment (3)

With all fresh compounds

Galactose oxidase (1.41 mg), horse radish peroxidase (0.23 mg), methyl-β-D galactopyranoside (100 mg) and catalase suspension (0.03 mL) were dissolved in deionised water (7.5 mL) and the reaction was followed for 4 hrs. An aliquot (0.5 mL) was removed (t=0), ultra filtered to remove the enzymes and set aside for subsequent analysis (t = 0). Further aliquots were removed over 4 hrs and the ^{1}H NMR spectra (in D_2O) were recorded.

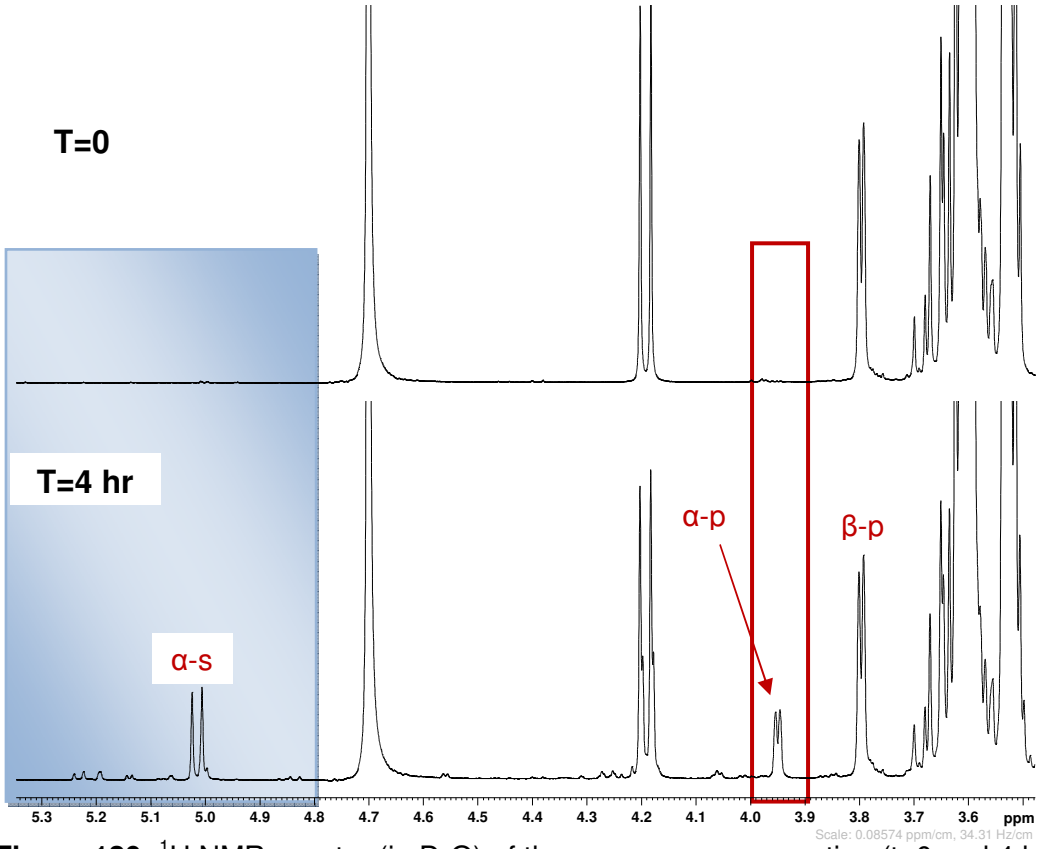

Figure 120: ^{1}H NMR spectra (in D_2O) of the enzyme assay reaction (t=0 and 4 hr)

Comparing the spectra of t=0 hr and 4 hrs, it was found that after 4 hrs (Fig. 119) there was an increase of the signals seen in the reaction mixture as compared to t=0. Also two additional signals appeared between 3.9-4.0 ppm, and at 4.1-4.2 ppm which could indicate the presence of oxidation products or degradation of the product before NMR. From the literature reference[154] (Fig. 121), it was indicated that the reactants were converted to the products of interest. When the region between 4.8– 5.3 ppm was expanded further, it showed that new signals had appeared in this region.

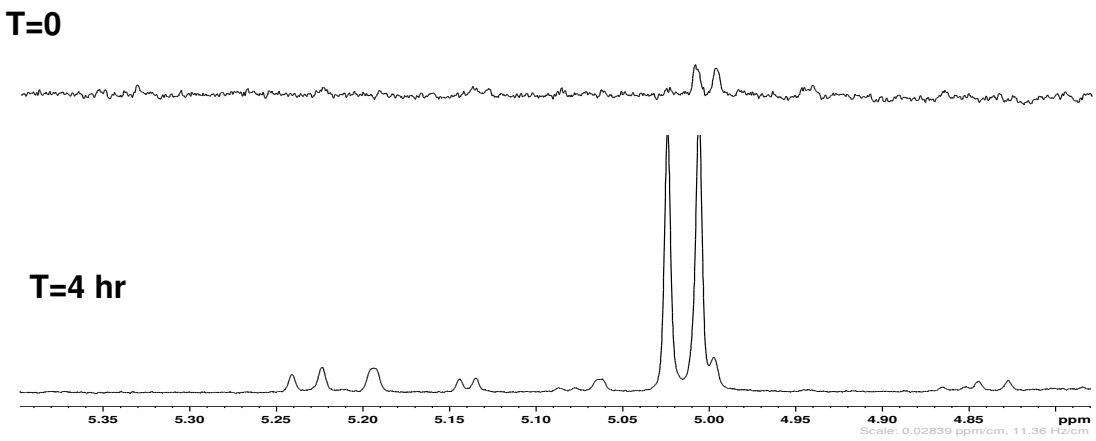

Figure 121: Selected regions of the ^{1}H NMR spectra (in D_2O) of the enzyme assay reaction (t=0 and 4 hr)

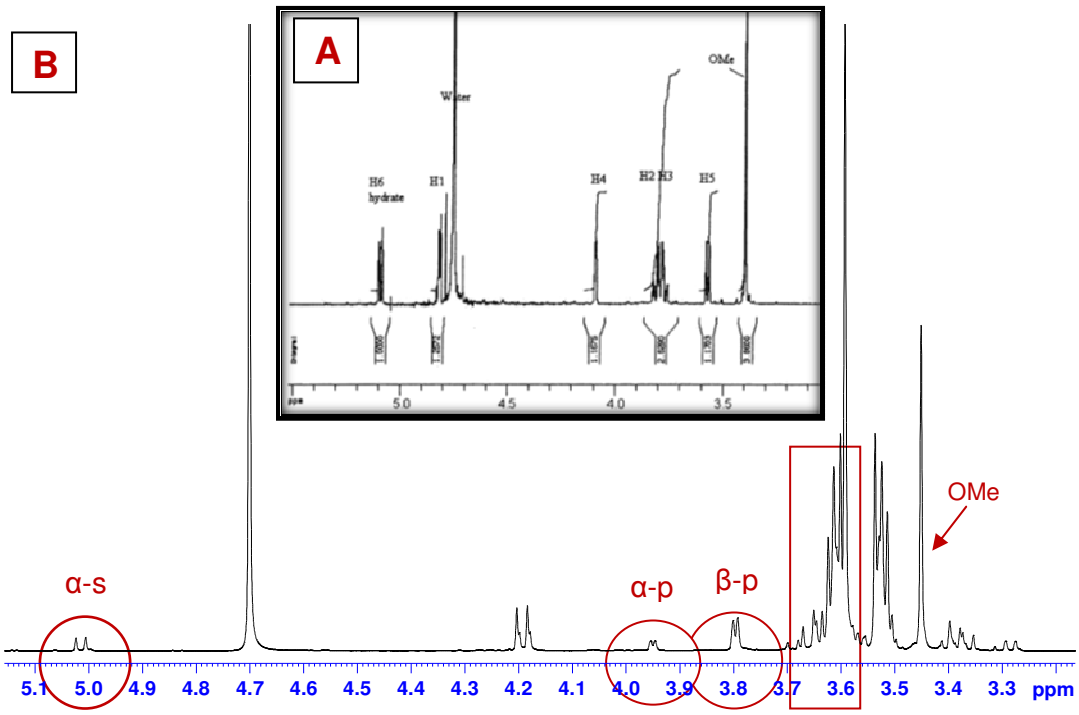

Figure 122: ^{1}H NMR spectra (B, in D_2O) of the enzyme assay reaction (t=4 hr) compared with the reference ^{1}H NMR spectrum (A) from the literature.[134]

New signals had appeared in the downfield region of the proton NMR at 6.0, 9.1 and 9.4 ppm (Fig. 122).

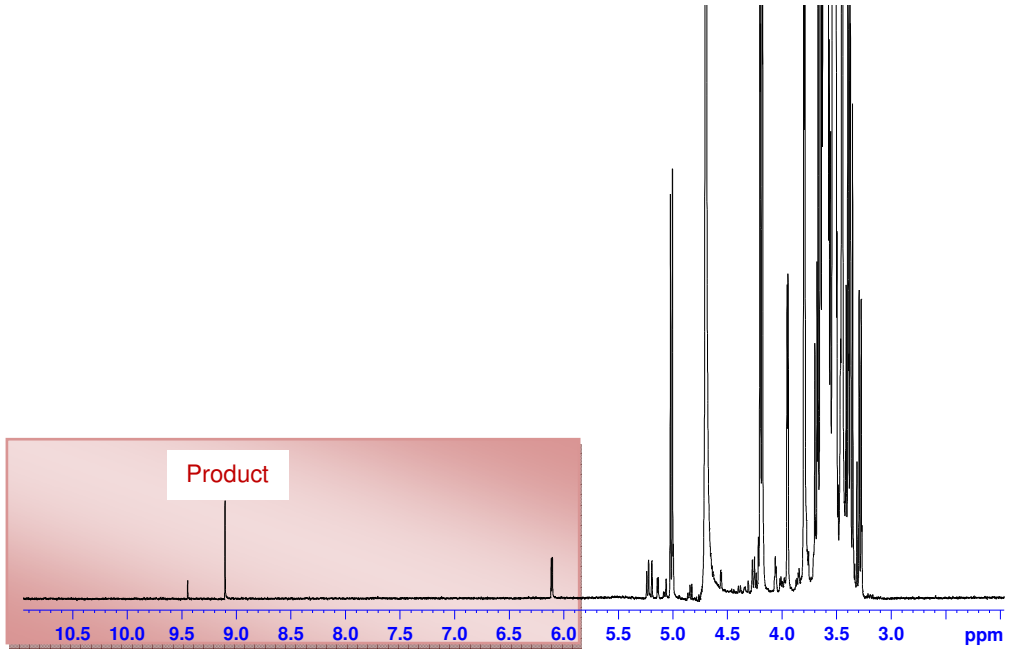

Figure 123: ^{1}H NMR spectrum of the enzyme assay reaction (t=4 hr) highlighting the formation of an aldehyde product

The reaction mixture was left overnight. After 24 hrs a further aliquot (0.5 mL) was removed, the enzymes removed, the sample dried and reconstituted in d_6-DMSO (0.650 mL). The ^{1}H NMR spectrum was recorded (Fig.124).

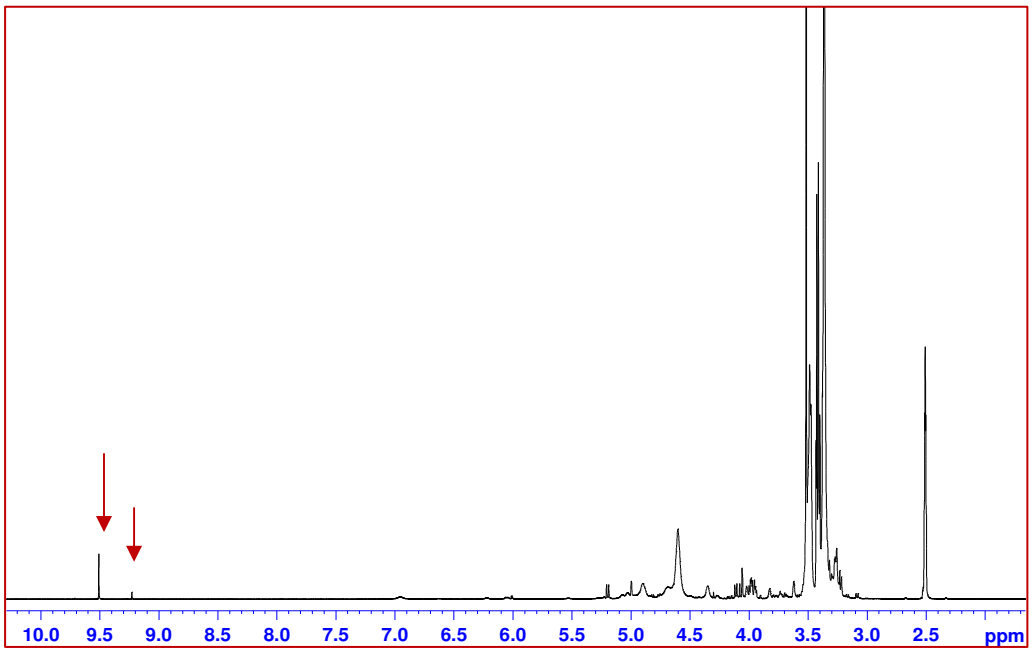

Figure 124: ^{1}H NMR spectrum (in d_6-DMSO) of the enzyme assay reaction (t=4 hr)

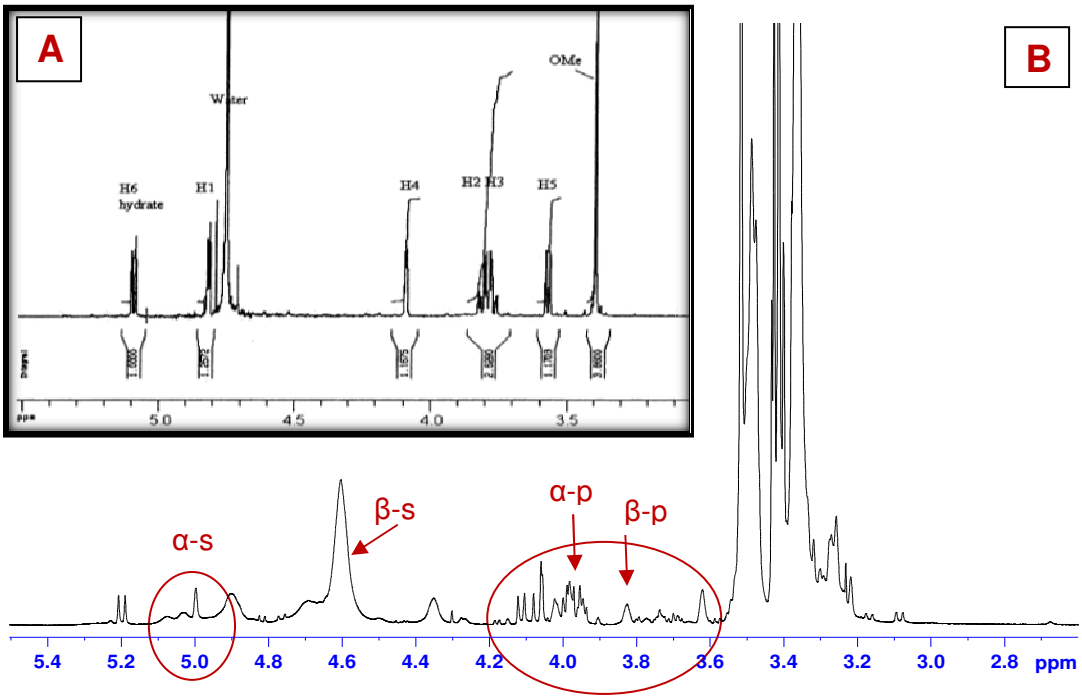

Figure 125: Expanded anomeric region of ^{1}H NMR spectra (B, in d_6-DMSO) of the enzyme assay reaction (t=24 hr) compared with the reference NMR spectrum (A) from the literature.[134]

The proton NMR spectrum clearly showed that the signals became more abundant after 24 hrs. It was therefore decided to analyse the sample using thin layer chromatography.

3.5.2.3 Method 3

It was reported by Siebum *et al*[157] that galactose oxidase could transform a range of primary alcohols into the corresponding aldehydes by using molecular oxygen as an electron acceptor in the oxidation of alcohols to aldehydes (p: 157, section 3.4.2.3)

Experiment (1)

TLC

An experiment was done on a small scale to prepare for separation of the reaction mixture using TLC. Analysis of methyl-β-D-galactopyranoside (30 mg) in deionised water (1 mL) was attempted using a silica TLC plate with a mobile phase of MeOH, chloroform, acetic acid and deionised water (30:60:4:4 v/v). The TLC plate was dipped in potassium permanganate to allow visualisation of the spot.

Experiment (2)

With all fresh compounds

A mixture of methyl-β-D-galactopyranoside (194 mg) galactose oxidase (8.1 mg, 30 units), and catalase (14.4 µL, 4880 units) were dissolved in deionised water (7.5 mL). The aqueous solution was then added to the phosphate buffer (5.0 mL, 50 mM, pH 7.0). This reaction mixture was placed under an oxygen atmosphere and stirred at 4 ºC for 6 days. During this time the reaction was monitored by TLC (SiO_2, MeOH, chloroform, acetic acid and deionised water (30:60:4:4 v/v). On completion of the reaction the sample was freeze dried. The ^{1}H NMR spectrum was acquired by dissolving a small part of the dried sample in d_6-DMSO (Fig. 125).

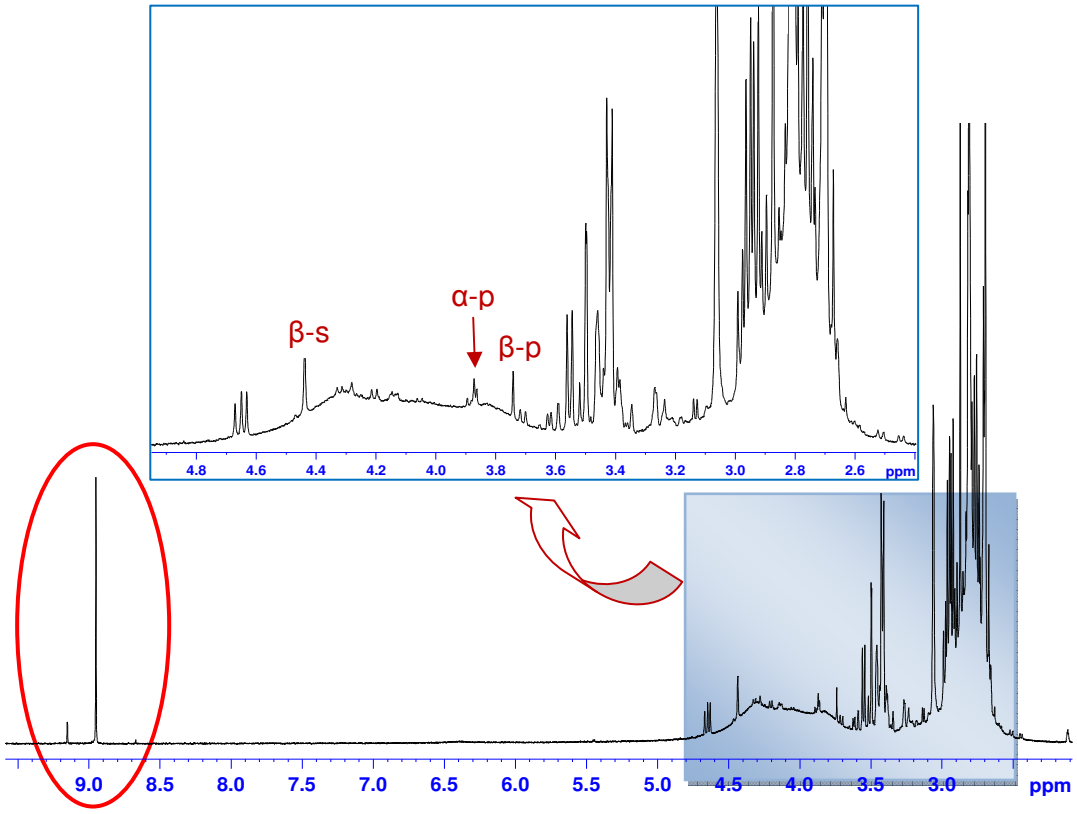

Figure 126: ^{1}H NMR spectrum of the reaction product

The ^{1}H NMR spectrum exhibited many peaks along with the formation of a prominent peak at 9.0 ppm. The resultant ^{1}H NMR showed the presence of many signals probably arising from impurities or side-products.

3.5.2.4 *Method 4*

A different kind of enzymatic oxidation was used according to the paper of Osuga *et al.,*[160] who proposed this protocol to attach amino acids and peptides to the C-6 hydroxyls of galactose and N-acetylgalactosamine by first oxidizing the C-6 hydroxyls to aldehydes using galactose oxidase in the presence of small amounts of catalase. The method was highly specific as enzymes were used rather than chemicals.

The reaction mixture was prepared as follows; methyl-β-D-galactose (40 mg), galactose oxidase (122 mg, 450 U) and catalase (4 mg) were dissolved in phosphate buffer (1 mL, pH 6.0). The mixture was stirred on a hot plate at 25 ºC for 24 hrs and the reaction was monitored by TLC (SiO_2, n-propanol/ethanol/water (3:2:1 v/v).

On completion of the reaction, TLC analysis was carried out using a silica plate. The aldehyde product was visualized using 0.4 % DNP in HCl. The product was observed clearly. After 24 hrs the reaction mixture was heated to 95 ºC for 5 min (to denature the enzyme) and the protein precipitated was removed by centrifugation. The product obtained was freeze dried. The ^{1}H NMR spectra of both samples were recorded in d_6-DMSO and D_2O, Fig. 126 (a) and (b).

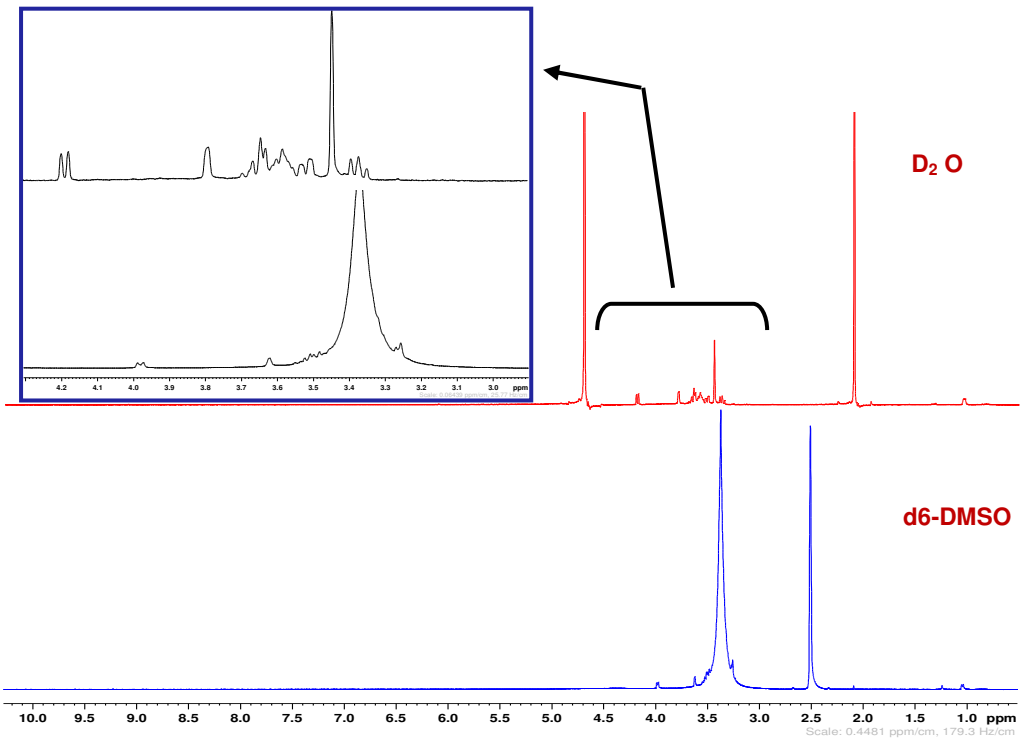

Figure 127: ^{1}H NMR spectra of the oxidation reaction with methyl-β-D-galactopyranoside in d_6-DMSO (a) and D_2O (b)

3.5.2.5 *Best oxidation method to use with rhenium complex (Complex-1)*

Four different methodologies were investigated for the oxidation of methyl-β-D-galactopyranoside using galactose oxidase. The best method was found to be method 2 as results obtained were in accordance with the results given in literature Parikka and Tenkanen[154] which confirmed that the oxidation reaction has occurred. The same experiment protocol (as method 2) was used further to make samples to react with complex 1. The reaction scheme is given below in Fig. 127. The aim was to attach a rhenium complex to the galactose containing the aldehyde group to obtain a luminescent compound.

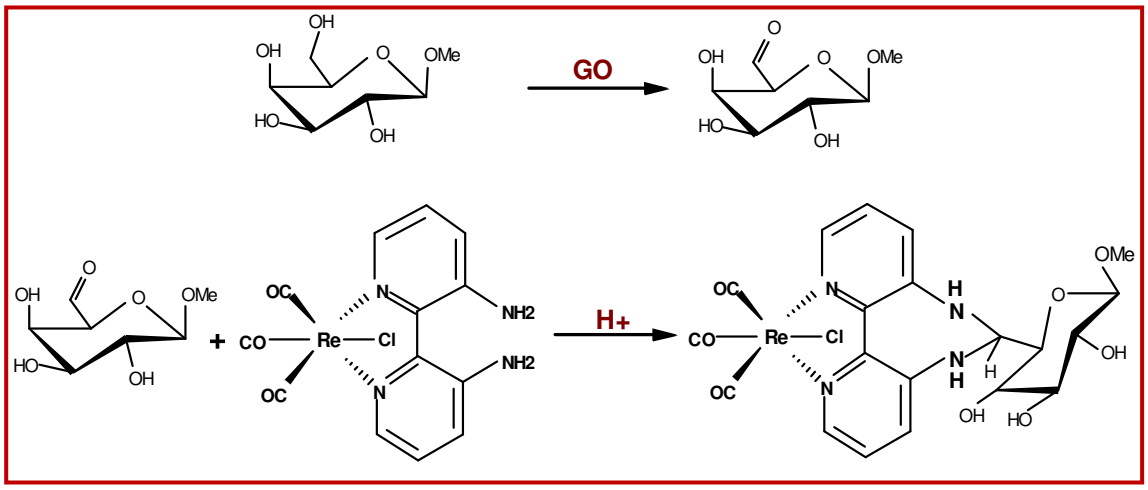

Figure 128: Oxidation of methyl-β-D-galactopyranoside to form the product and subsequent reaction with complex 1

A) Reaction of oxidation product with Rhenium complex (complex-1) using Method 2

TLC analysis

The reaction mixture was analysed by TLC on a silica plate which gave clearly separated spots. It was decided to attempt purification using column chromatography. The reaction mixture was separated and fractions were collected; fractions 24-45 were combined, dried and dissolved in d_6-DMSO and analysed using ^{1}H NMR (Fig. 128).

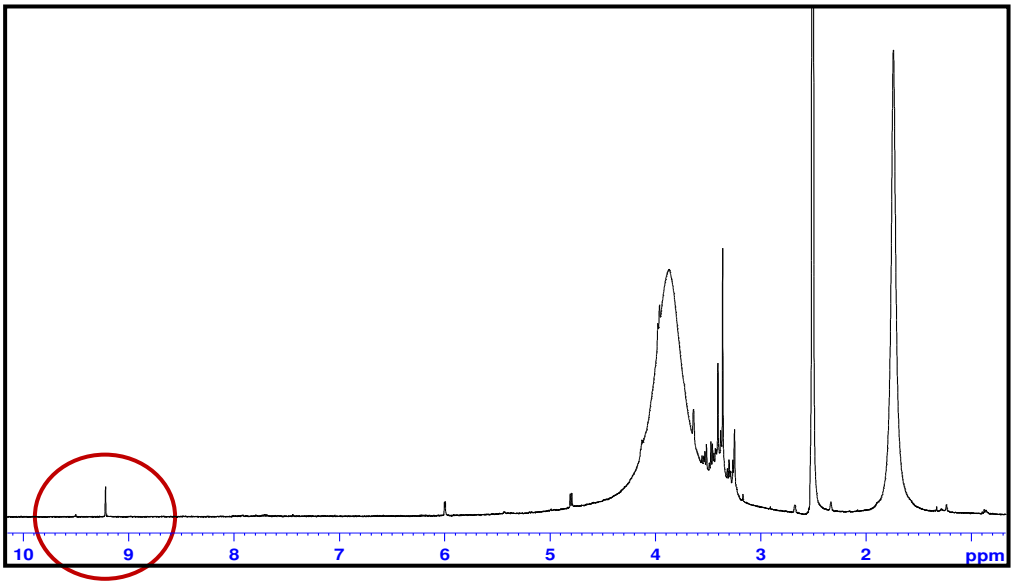

Figure 129: ^{1}H NMR spectrum of fractions 24-45 dissolved in d_6-DMSO

The results showed the appearance of a peak at 9.2 ppm which was also observed during the oxidation reaction corresponding to the product. The sample was freeze dried for future use. Fractions 1-23 and fractions 46-70 were also analysed in d_6- DMSO but only a small amount of product was observed in both fractions (Fig. 129 A and B).

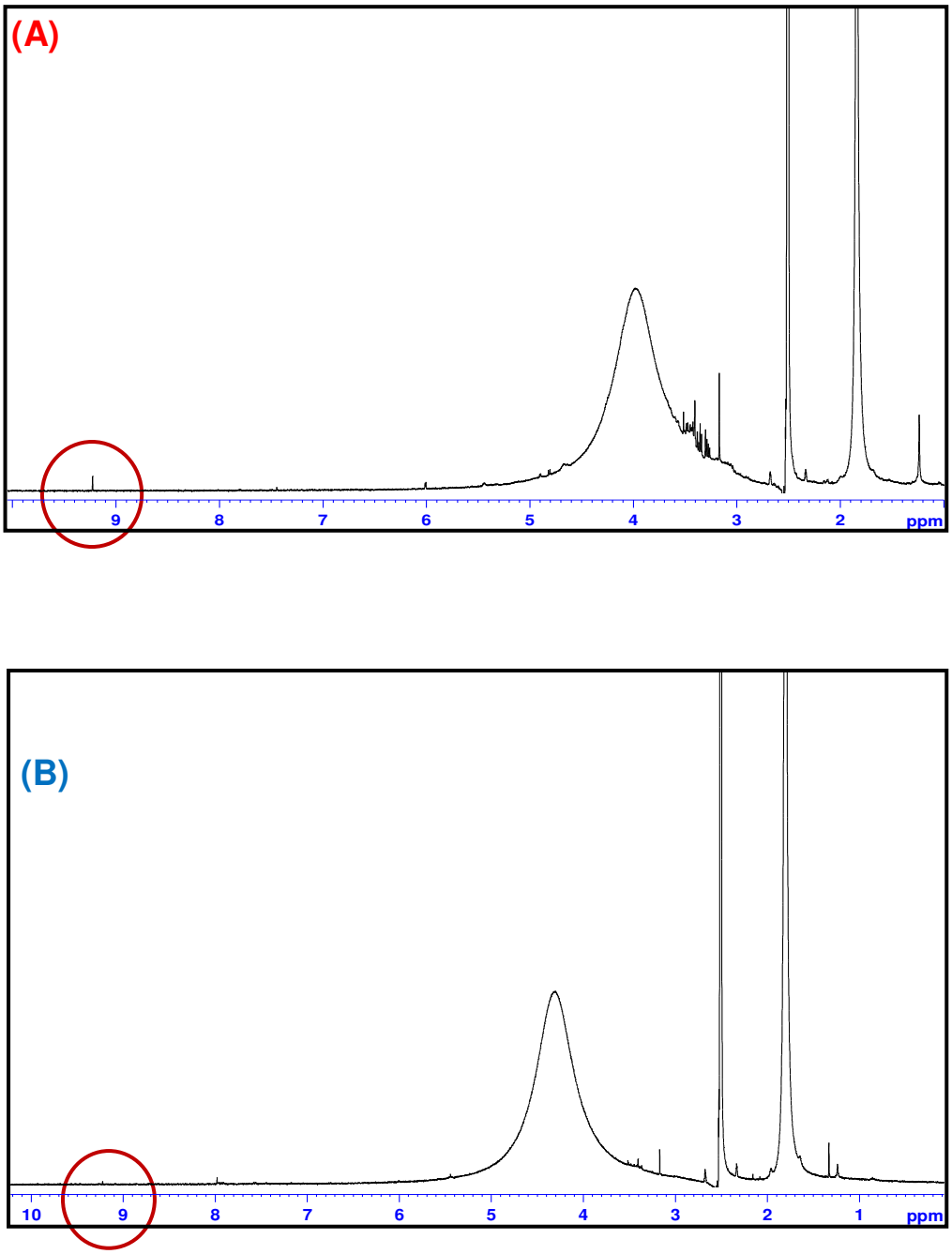

Figure 130: ^{1}H NMR spectra of fractions 1-23 (A) and fractions 46-70 (B) in d_6-DMSO

From method 2 (section 3.5.2.2, experiment 3) the ^{1}H NMR spectrum of fractions 24-45 gave more peaks of interest compared to the other fractions. For this purpose the reaction mixture was prepared as follows: complex 1 (10 mg) was dissolved in MeCN (5mL) and a few granules of CSA were added. This solution was added to fractions 24-45 and the reaction was left overnight. An aliquot (1 mL) was removed, dried and the ^{1}H NMR spectrum was acquired in d_6-DMSO (Fig. 130).

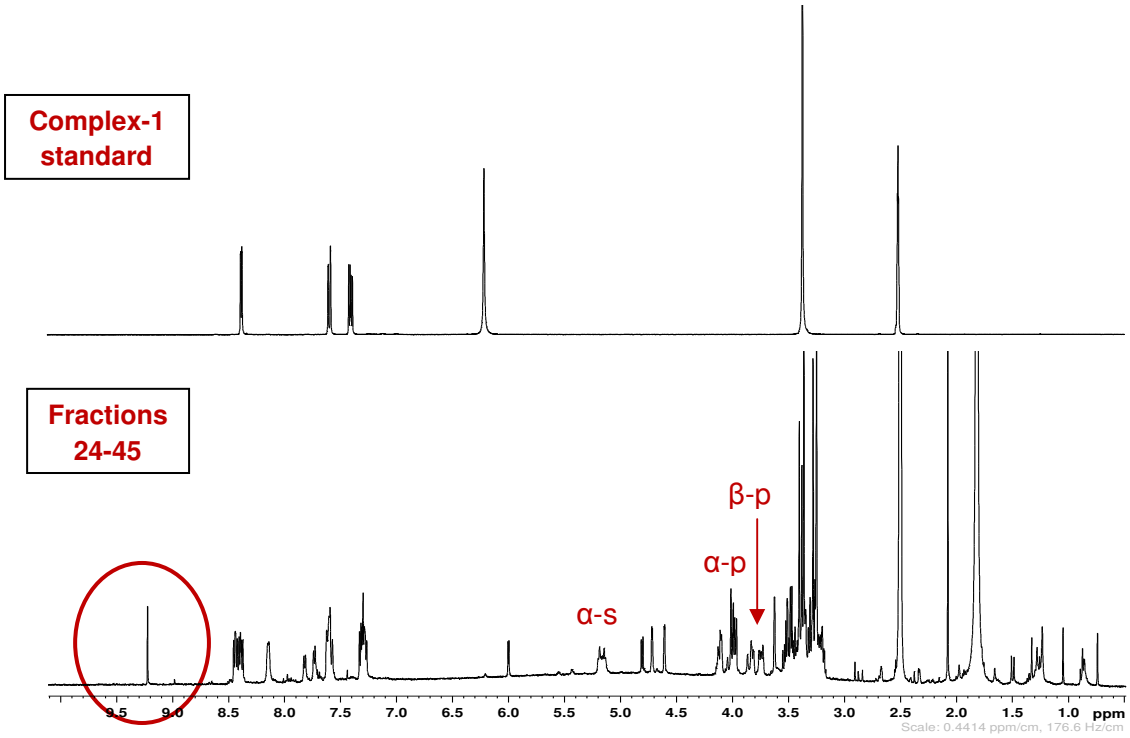

Figure 131: Stacked ^{1}H NMR spectra of complex 1 plus fractions 24-45 (bottom) with complex 1 standard (top) in d_6-DMSO

Fig. 130 clearly revealed the formation of many peaks and the signal at 9.2 ppm is common to other ^{1}H NMR spectra previously described. At 7.6-8.6 ppm the signals became complex and a doublet was seen at 8.4-8.5 ppm. The result was encouraging so TLC analysis of the sample was carried out with 10% MeOH in DCM which showed fairly good results with good separation. The fractions were then separated using column chromatography. Two prominent bands were obtained which were dried and dissolved separately in CD_3CN and analysed using NMR. It was found by comparison of both the fractions (1 and 2) that signals at 9.2-9.3 ppm were present in Fig 130 fraction 1. When the selected region between 7.0-10.5 ppm was expanded, it became clear that the proton NMR became complex and new peaks were seen (Fig. 131).

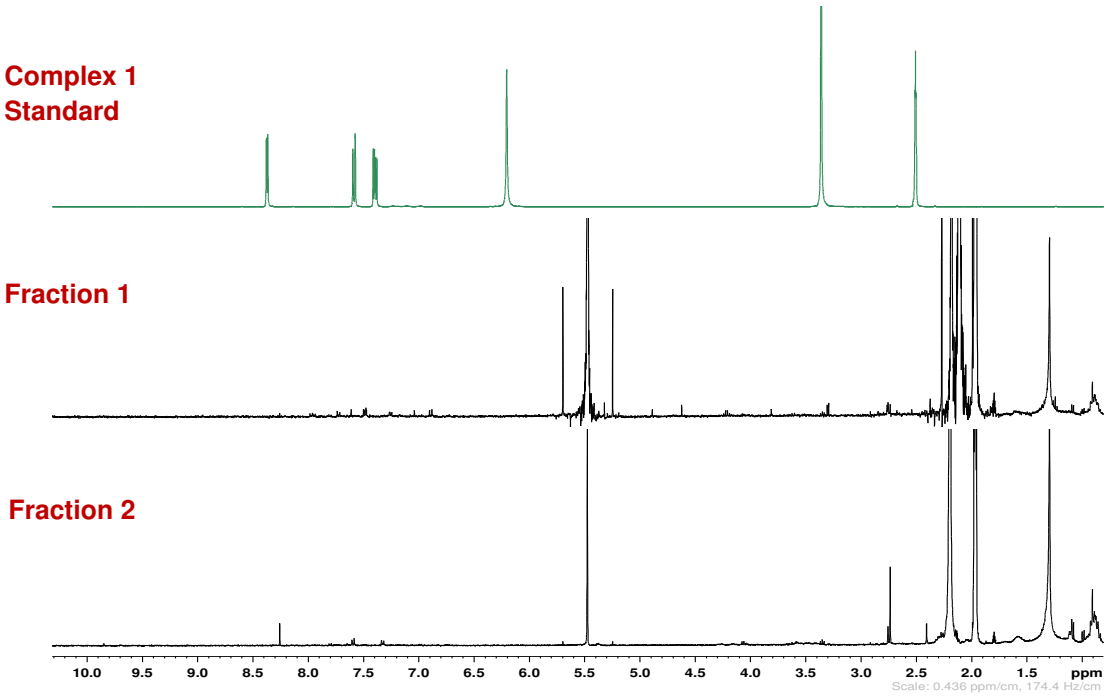

Figure 132: Comparison of ^{1}H NMR in CD_3CN, showing fraction 1 (centre) and fraction 2 (bottom) with complex 1 (top)

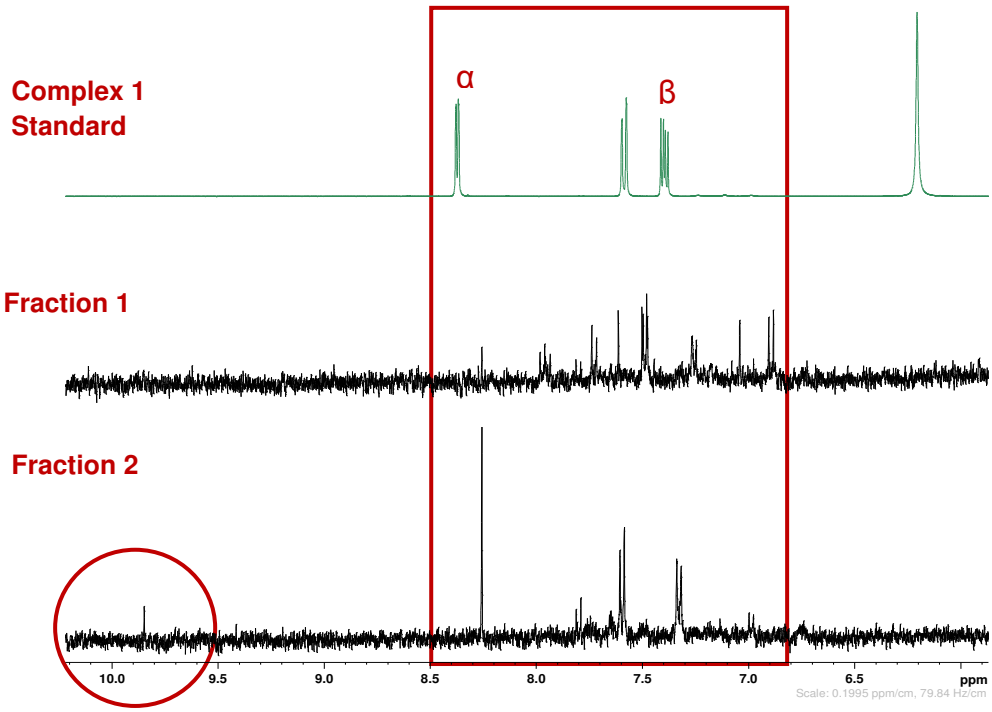

Figure 133: Comparison of selected regions of the ^{1}H NMR spectra, in CD_3CN, showing fraction 1 (centre) and fraction 2 (bottom) with complex 1 (top)

When compared with the complex 1 standard it was observed that in the region between 6.8-8.0 ppm there was an increase in the peaks in fraction 1 but in fraction 2, the peaks became less complex and a lone peak appeared at 9.8 ppm. It appears that fraction 2 contains mostly complex 1.

Next the sample was dissolved in MeCN (1 mL) and analysed using LC at 65% B and 0.5 mL/min flow rate. The chromatogram (Fig. 133) gave three peaks but the separation was not good. Different percentages of MeCN (B%) were tried to obtain a better separation. With 35% B and 0.5 mL/min flow rate very good separation was obtained (Fig.134).

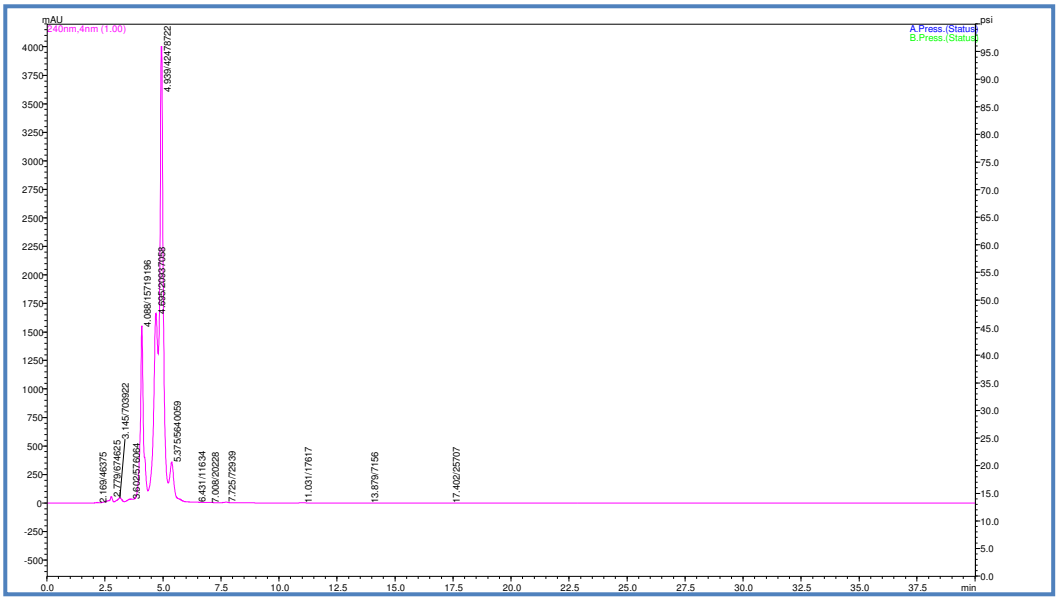

Figure 134: LC chromatogram of fraction 1 run at 65 % B, 0.5 mL/min flow rate, at 379 nm

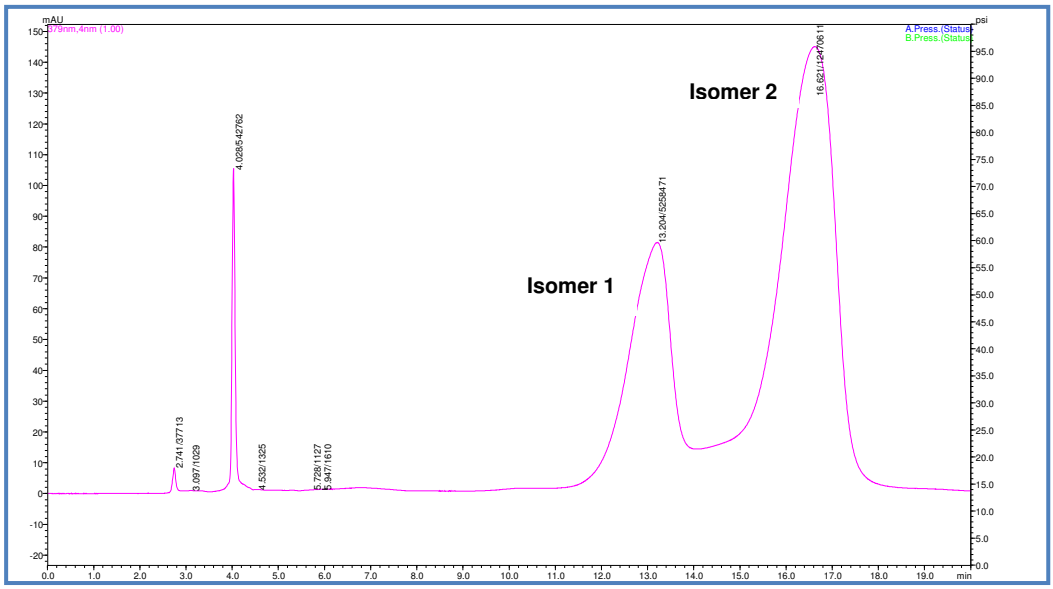

Figure 135: Chromatogram of fraction 1 at 35 % B, 0.5 mL/min flow rate

The results were good with 35% B and 0.5 mL flow rate. This method was successful in separating peaks between 11-19 min. It was decided to try the same conditions for fraction 2 (Fig. 135).

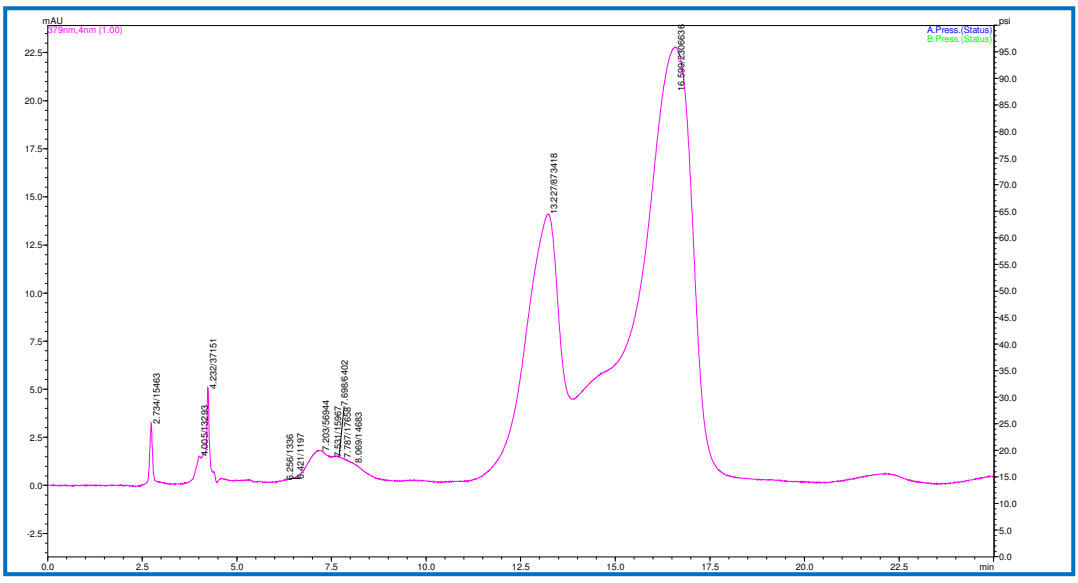

Figure 136: Chromatogram of fraction 2 at 35 % B, 0.5 mL/min flow rate

It was decided to use preparative HPLC to collect a workable amount of pure compound to attempt crystallization of the product. The LC sample was divided into two parts and was separated using preparative HPLC which recorded the chromatogram on a chart recorder. In order to get the pure form, fractions were collected after every 30 sec from the start *i.e.* t=0, for all 1.5 mL. Samples were collected and stored in labelled vials.

Two isomers were observed which were designated isomer 1 and isomer 2 in order of elution. For each isomer, fractions were collected. For isomer 1, fractions 32 – 36 and 125-129 (Fig. 136) and for isomer 2, fractions 43 – 48 and 137 - 142 were collected combined and the MeCN removed under vacuum.

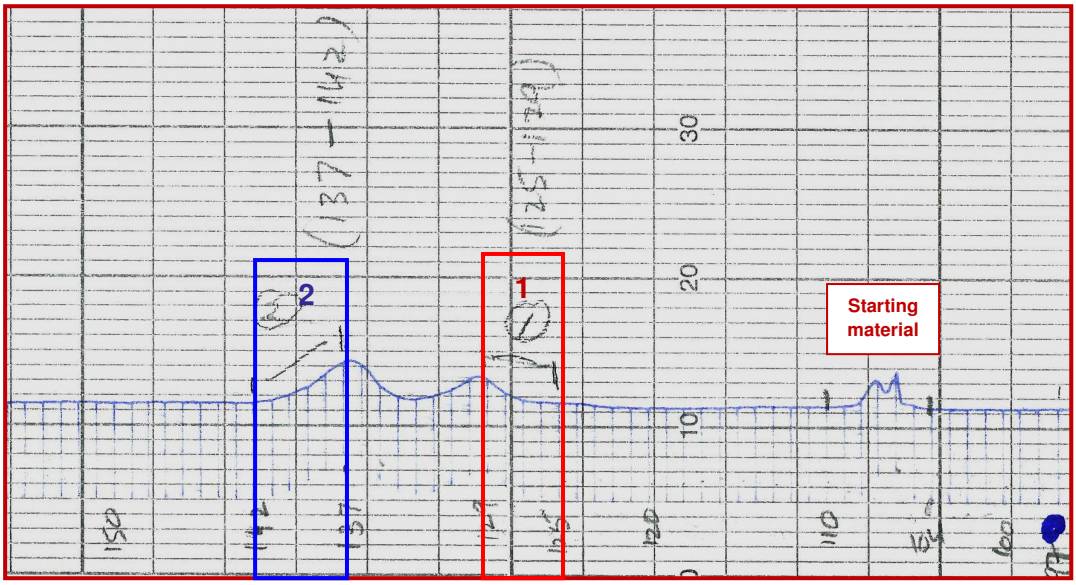

Figure 137: Preparative HPLC chromatogram of the complex 1 and dialdehyde reaction product (65 % MeCN, 10 mL/min, run time 50 min) showing collection of fractions for the two isomers

The samples were extracted with DCM, dried ($MgSO_4$) and evaporated *in vacuo* and their ^1H NMR spectra were acquired in CD_3CN (Fig. 137).

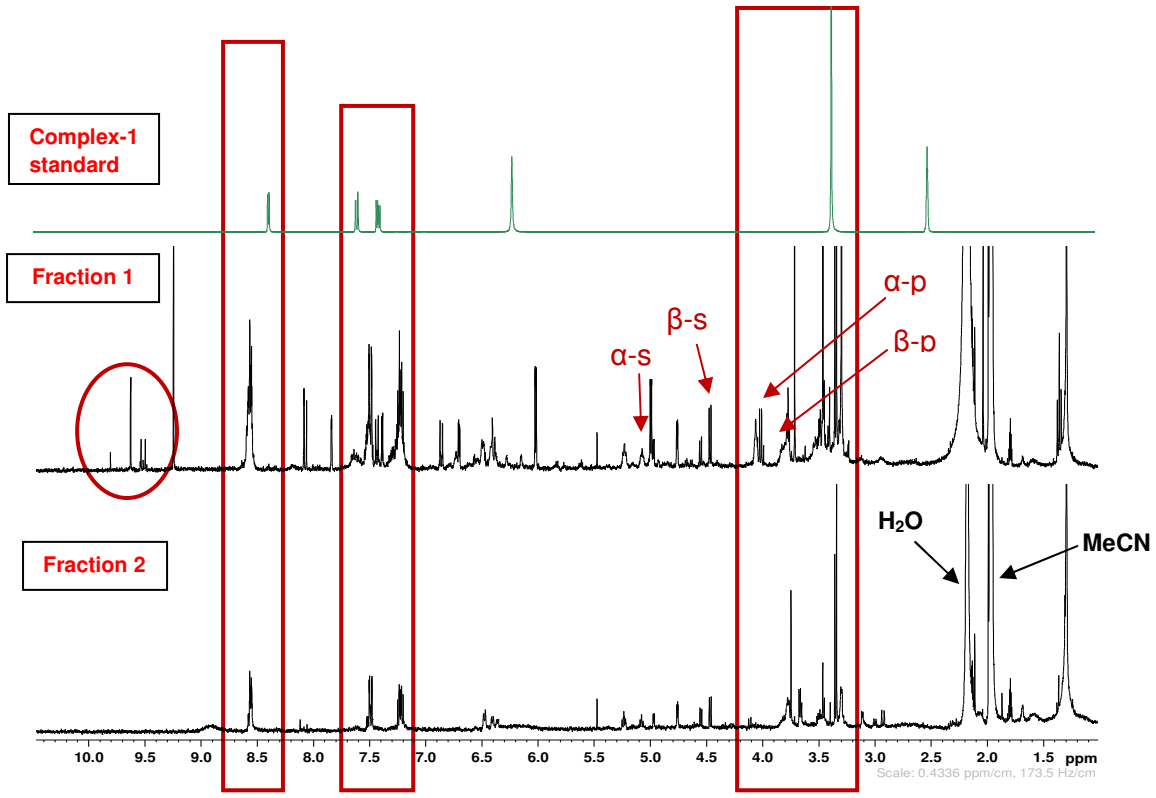

Figure 138: ^{1}H NMR spectra of fraction 1 (above) and fraction 2 (bottom) in CD_3CN

Through comparison of the above spectra it becomes clear that there was a significant amount of starting material remaining in fraction 1 and 2. In fraction 1 the appearance of new signals around 8.0 and between 9.6 and 10 ppm were seen. The signals became very complex in the region from 3.2 to 4.2 ppm as compared to fraction 2. The region was expanded between 6.0-10.0 ppm (Fig. 138) which clearly indicated that in the region between 7.1-8.2 ppm the signals became more complex as compared to fraction 2 (bottom) and a group of signals were present around 9.5-9.9 ppm.

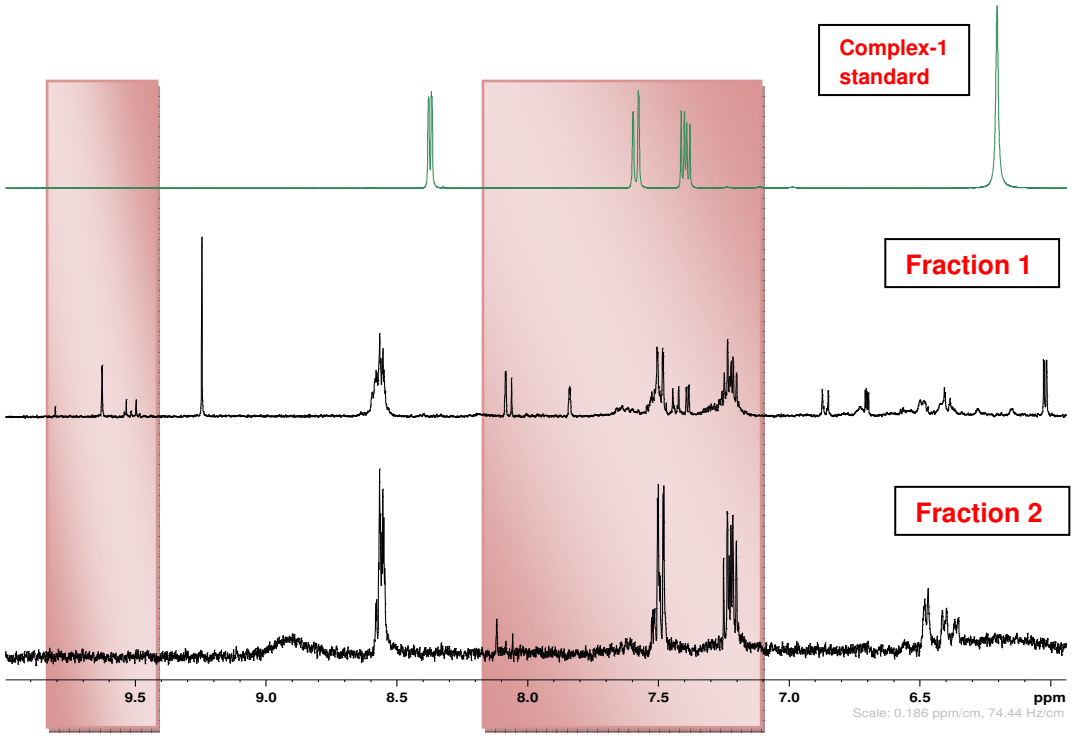

Figure 139: Selected regions of the ^{1}H NMR spectra of fraction 1 (top) and fraction 2 (bottom) in CN_3CN

B) Reaction of oxidation product with rhenium complex (complex-1) using Method 3

On the basis of the ^{1}H NMR results the reaction mixture was separated using column chromatography and fractions 21-24 and 28-33 were combined and analysed using ^{1}H NMR for fractions 21-24 and 28-33 (Fig. 139).

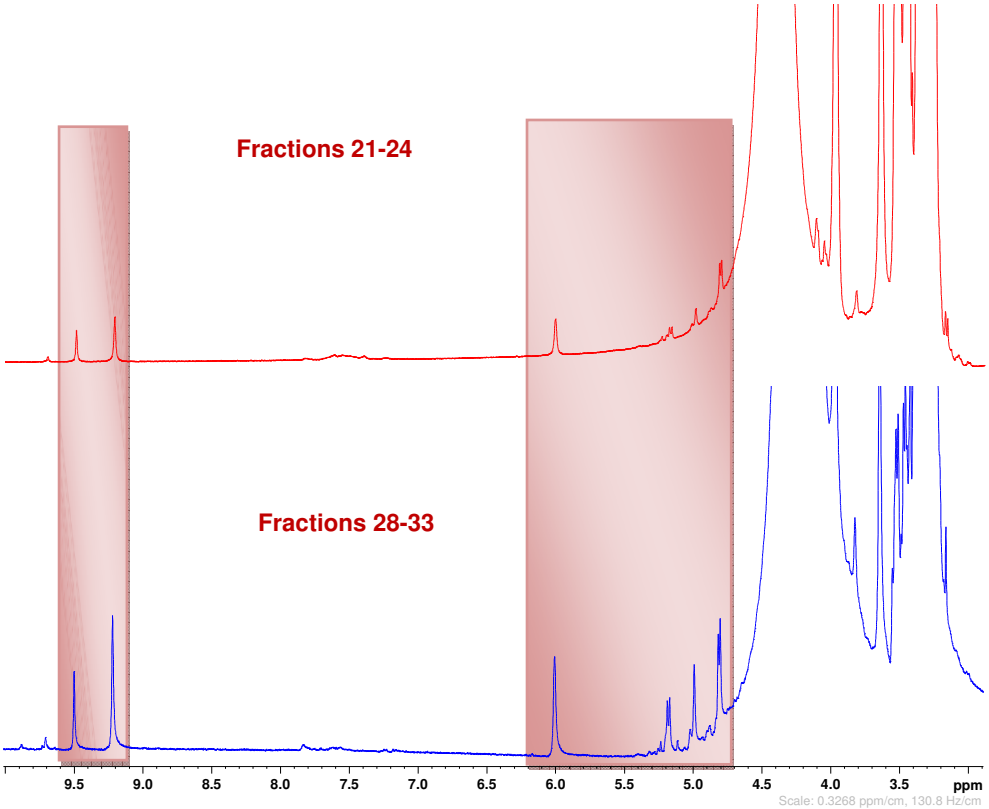

Figure 140: ^{1}H NMR spectra of fractions 21-24 and 28-33

Comparing the proton NMR spectra of both the fractions clearly showed that a peak was present at 9.2 and 9.5 ppm in both fractions. Fractions 28-33 contained more material as the sizes of the signals were double in fractions 28-33 than fractions 21-24 (Fig. 139). The proton NMR spectrum was also recorded in d_6-DMSO and compared with that of complex 1. The proton NMR spectrum obtained showed that no change in the aromatic region was observed and a significant peak for the aldehyde starting material was still present (Fig. 140).

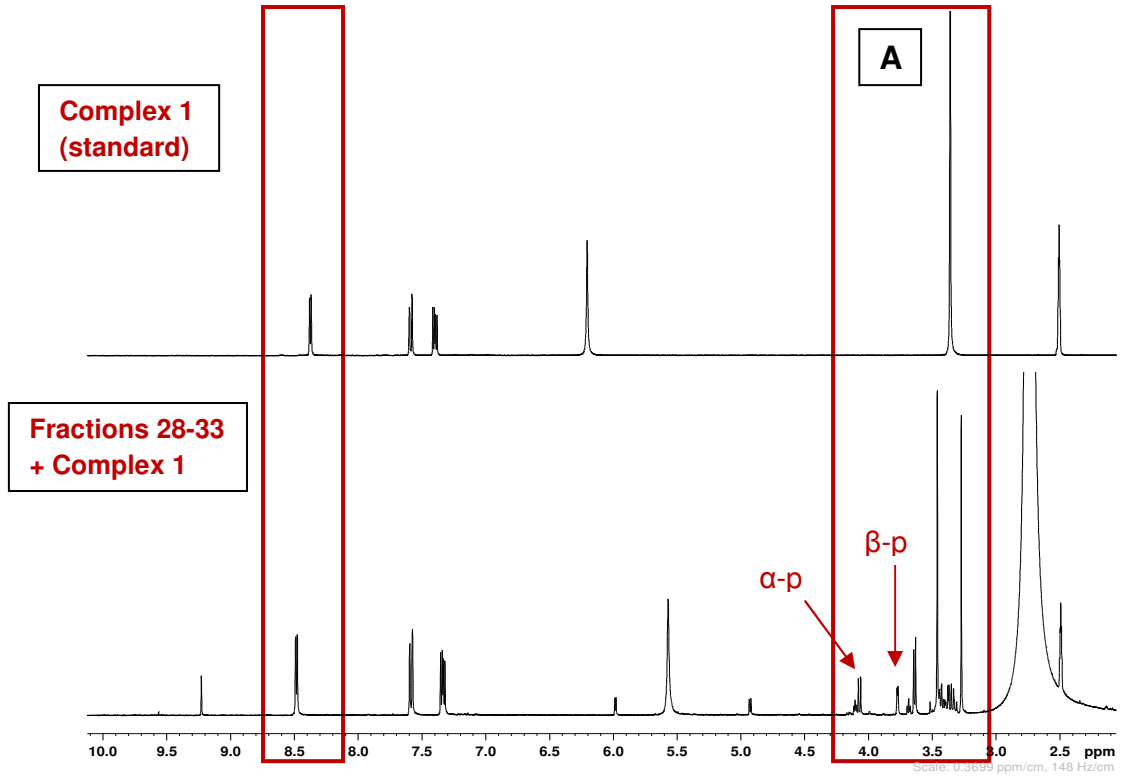

Figure 141: ^{1}H NMR spectra of complex 1 (standard) and reaction mixture of fractions 28-33 with complex 1

3.6 Conclusion

Research presented in this thesis evaluates different methodologies using galactose oxidase for the enzymatic oxidation of methyl-β-D-galactopyranoside to form an aldehyde group at position 6 of the sugar. The best method for the enzymatic oxidation of the sugar was found to be method 2 (section 3.4.2.2) and the aldehyde product was successfully characterized by TLC, LC, column chromatography and 1D-NMR. The product was further reacted with complex **1** to obtain a luminescent sugar complex. The product was characterized using LC, preparative HPLC and NMR although the product could not be isolated in sufficient yield or purity for complete characterisation.

3.7 Future Work

This research can be enhanced by extending it towards a range of alternative substrates with the aim of expanding the potential of galactose oxidase as a tool to prepare ligands for use in coordination chemistry. Enzymatic oxidation of other disaccharides and monosaccharides seems a good starting point.

Further work is required to complete the structural determination of the **1**-galactose product by using X-ray crystallography and more detailed 2D-NMR experiments are also required.

In many ways GO represents an ideal enzyme for use in these applications as it is a stable enzyme, easily purified in high quantities and does not require expensive cofactors in order to function. Parikka and Tenkanen[145] demonstrated that oxidation of D-galactose by GO can lead to formation of multiple products and demonstrated that reaction conditions can be optimised to reduce formation of unwanted by-products which would be important in developing an efficient process for use on larger scales.

Chapter 4

References

Chapter 4: References

1. *Hormones - Anatomy & Physiology* [online] Available at: <http://en.wikivet.net/Hormones_-_Anatomy_%26_Physiology> [Accessed 16th March 2011].

2. Tulane University, *e.hormone: your gateway to the environment and hormones,* [online] <http://e.hormone.tulane.edu/learning/types-of hormones.html> [Accessed 16th March 2011].

3. King M. W. (1996) *The Medical Biochemistry page.org, LLC* [online] Available at: < http://themedicalbiochemistrypage.org/peptide-hormones.php > [Accessed 16th March 2011].

4. Mandal, A, MD. (2010), *Chemical classes of hormones*, [online] Available at: < http://www.news-medical.net/health/Chemical-Classes-Of-Hormones.aspx > [Acessed 25th march 2011].

5. J.R. Murray, *The history of corticosteroids*, (1989), **151,** 4-6, discussion 47-52.

6. NHS Choices, *Corticosteroids* [online] Available at: <http://www.nhs.uk/conditions/corticosteroid-(drugs)/pages/introduction.aspx > [Accessed 05th March 2011].

7. H.J.Vander Velden, *Mediators of Inflammation*, (1998), 7, 229-237.

8. Polosa, R. & Holgate, S.T. (2007) *Therapeutic Strategies, Asthma: Current treatments*, 1st ed. Oxford: Clinical publishing Oxford.

9. P.J. Barnes, S. Pedersen, W.W. Busse, *Am J Respi Crit Care Med*, (1998), 157, S1-S53.

10. J.B. Wilcox, G.S. Avery, *Drugs*, (1973), 6, 84-93.

11. K. Lexmuller et al., (2007), *Drug Metabolism and Disposition*, (2007), 35(10), 1788-1796.

12. E. Mutch, R. Nave, N. McCracken, K. Zech, F. M. Williams, *Biochemical Pharmacology,* (2007), 73, 1675-1664.

13. J.L. Malo, A. Cartier. H. Ghezzo, S. Mark, J. Brown, M. Laviolette, L. P. Boulet, *Eur Respir J.*, (1999), 993±998.

14. J.P. Barnes, *Clinical Science,*(1998), 94, 557-572.

15. Desai, U.R. (2000), *Steroids Introduction* [online] Available at: < http://www.people.vcu.edu/~urdesai/intro.htm > [Accessed 13th May 2011].

16. Lodish H & Zipursky S. L. et al. (2000), *Molecular Cell Biology*, 4th ed. New York: W. H. Freeman and Company.

17. G.P. Moss, *Pure Applied Chem.*, (1989), 61(10),1783-1822.

18. Lewis, D.V. (2011) *Topical corticosteroids* [online] Available at: < http://www.netdoctor.co.uk/skin_hair/eczema_corticosteroids_003762.htm. > [Accessed 05th March 2011].

19. K. Biggadike, L. Uings, S.N. Farrow, Proc Am Thorac Soc, (2004), (1), 352–355.

20. J. P. Barnes, *Pharmaceuticals*, (2010), 3, 514-540.

21. A. Othman, R. K. Harris, P. Hodgkinson, E. A. Christopher and R. W. Lancaster, *New J. Chem.*, (2008), 32, 1796-1806.

22. TAPI, T. (2011), *Beclomethasone dipropionate* [online] Available at: < http://www.tapi.com/tapiteva/productPages/Beclomethasone_Dipropionate > [Accessed 11th June 2011].

23. Drugs.com, (2009), *Beclomethasone Dipropionate* [online] Available at: < http://www.drugs.com/ppa/beclomethasone-dipropionate.html > [Accessed 15th June 2011].

24. Rowland M. & Tozer T. N. (2011), *Clinical Pharmacokinetics: Concepts and Applications,* 4th ed. Philadelphia: Lippincott Williams & Wilkins.

25. Z. Wang, J. F. Chen , Y. Le and Z. G. Shen, *Ind. Eng. Chem. Res.*, (2007), 46 (14), 4839-4845.

26. Chemicalland 21, (2011), *Beclometasone Dipropionate* [online] Available at: <http://www.chemicalland21.com/lifescience/phar/BECLOMETHASONE %20DIPROPIONATE.html> [Accessed 11th March 2011].

27. GP notebook, (2011), *Beclometasone (beclomethasone) dipropionate* [online] Available at: < http://www.gpnotebook.co.uk/simplepage.cfm?ID=859111426 > [Accessed 11th May 2011].

28. Teva Specialty Pharmaceuticals LLC: Clinical Pharmacology, (2011), *Pro., D. Drug Information for product information QVAR 40mcg Inhalation Aerosole For Oral Inhalation Only, QVAR 80mcg* [online] Available at: <http://en.diagnosispro.com/drug_information-for/product-information-qvar-40mcg-beclomethasone-dipropionate-hfa-40-mcg-inhalation-aerosolfor-oral/6751-491983.html> [Accessed 11th May 2011].

29. Busse et al., *J Allergy Clin. Immunol.,* (2007), **120**(5), S94-*S138*.

30. K. Foe, H.T. A. Cheung, B. N. Tattam, K. F. Brown and J. P. Seale, *Drug Metabolism and Disposition*, (1998), **26**(2), 132-137.

31. K. Foe, K.F. Brown, and J.P. Seale*, Biopharmaceutics and Drug Disposition*, (1998), **19**, 1-8.

32. P. T. Daley-Yates, A. C. Price, J. R. Sisson, A. Pereira and N. Dallow, *Br J Clin Pharmacol*, (2001), **51**(5), 400-409.

33. J. J. Zou *et al., Journal of Chromatography B.*, (2008), **873**(2),159-164.

34. K. Foe. D. J. Cutler, K. F. Brown and J. P. Seale*, Pharmaceutical Research*, (2000), **17**(8), 1007-1012.

35. P. A. Dickinson, G. Taylor, *International Journal of Pharmaceutics,* (1995),**116**, 231-236.

36. F. Guan, C. Uboh, L. Soma, A. Hess, Y. Luo and D. S. Tsang, *Journal of Mass Spectrometry, J. Mass Spectrum*, (2003), **38**, 823-838.

37. Inc., G.S. (2011), *Budesonid,* [online] Available at: < http://druginfo.goldstandard.com> [Accessed 18th February 2011].

38. B. A. Kostenbauder, *J. Pharm. Sci.,* (1982), **11**, 12784-1281.

39. GlaxoSmithKline LLC, (2010), *Beconase (beclomethasone dipropionate monohydrate) spray, suspension* [online] Available at:

< http://dailymed.nlm.nih.gov/dailymed/drugInfo.cfm?setid=6e8f7981-f2ca 4b56-8759-4f18cf9706c8 > [Accessed 15th June 2011].

40. R. Nave, R. Fisher, N. McCracken, *Respiratory Research*, (2007), **8**(65), 1-9.

41. L. D. Bowers, *Clinical Chemistry,* (1997), **43**(7), 1299-1304.

42. P. Volin, *Journal of Chromatography* B, (1995), **671**, 319-340.

43. M. Blanco, D. Serrano, J.L. Bernal*, Talanta*, (1999), **50**(3), 527-532.

44. R. Batavia, K. M. G. Taylor,D. K. M. Craig, M. Thomas, *Int. J. Pharm.,* (2001), **212**, 109–119.

45. J. L. Bernal, M. J. Nozal, M. T. Martin, J. C. Diez-Masa, A. Cifuentes, *J. Chromatogr. A*, (1998), **823**, 423–431.

46. O. Holz, I. Zuhlke *et al., Pulm. Pharmacol. Ther.*, (2004), **17**, 233–238.

47. M. Shou, W. A. Galinada, Y. C. Wei, Q. Tang, R. J. Markovich, A. M. Rustum, *J. Pharm. Biomed. Anal.,* (2009), **50**, 356-361.

48. A. R. Boobis, *Respiratory Medicine,*(1998), **92,** (Suppl B), 2-6.

49. A. Helle, S. Hirsjärvi, L. Peltonen, J. Hirvonen, S.K. Wiedmer, *J. Chromatogr. A*, (2008), **1178**(1-2), 248-255.

50. Slabaugh M. R. & Seager S.L. (2007), *Organic and Biochemistry for Today,* 6th ed. Pacific Grove: Published by Brooks Cole, ISBN 0-495-11280-1.

51. Vaithianathan S., (2011), *Fluorescent labelling of biomolecules with organic probes*, [online] Available at:< http://www.biobasics.gc.ca/english/View.asp?mid=411&x=696 > [Accessed 07th April 2013].

52. H. Sahoo, *RSC Adv.*, (2012), **2**, 7017–7029.

53. U. Resch-Genger, M. Grabolle, S.C. Jaricot, R. Nitschke, T. Nann, *Nature Methods*, (2008), **5**(9), 763-775.

54. B. Valeur, M. N. Berberan-Santos, *J. Chem. Educ.* , (2011), **88**, 731–738.

55. Albani J. R. (2007), *Principles and Applications of Fluorescence Spectroscopy*, 1st ed. Blackwell Science, a Blackwell Publishing company.

56. Dr. T. Chakraborty**, (2013),** *Fluorescence Spectroscopy: History, Principle and Application – Part-III* [online] Available at **<** http://blog.reseapro.com/2013/09/fluorescence-spectroscopy-history-principle-and-application-part-iii/ > [Accessed 07th April 2013].

57. Lakowicz J. R. (2006), *Principles of Fluorescence Spectroscopy*, 3th ed. Maryland, USA: *Springer Science,* ISBN-10: 0-387-31278-1.

58. Life technologies, Thermo Fisher Scientific Inc, (2014), *Labeling Chemistry* [online] Available at: < http://www.lifetechnologies.com/uk/en/home/life-science/cell-analysis/labeling-chemistry.html > [Accessed 30th March 2014].

59. W. Liana, S. A. Litherland *et al., Analytical Biochemistry,* (2004), **334**, 135–144.

60. R. Hiramoto, K. Engel, D. Pressman, *Proc. Soc. Exp. Biol. Med.*, (1958), **97**, 611-614.

61. L. M. Smith, J. Z. Sanders, R. J. Kaiser, P. Hughes, C. Dodd, C. R. Connell, C. Heiner, S. B. H. Kent, L. E. Hood, *Nature,* (1986), **321**, 674-679.

62. H. Du, C. M. Strohsahl, J. Camera, B. L. Miller, T. D. Krauss, *J. Am. Chem. Soc., (* 2005), **127**, 7932-7940.

63. M. Sameiro, T. Gonçalves, (2009), *Chem. Rev.*, (2009), **109**, 190–212.

64. D. E. Reichert, J. S. Lewis, C. J. Anderson, *Coordination Chemistry Reviews*, (1999), **184**, 3–66.

65. M. S. Wrighton, D. L. Morse, *J. Am. Chem. Soc.,* (1974), **96**, 998-1003.

66. S. M. Fredericks, J. C. Luong, M. S. Wrighton, *J. Am. Chem. Soc.*, (1979), **101**, 7415-7417.

67. X. Yi, J. Zhao, W. Wu, D. Huang, S. Ji, J. S. Dalton, *Dalton Trans.*, (2012), **41**, 8931-8940.

68. A. Ramdass, V. Sathish. M. Velayudham. P. Thanasekaran, K. L. Lu, S. Rajagopal, *Inorganic Chemistry Communications,* (2013), **35**, 186–191.

69. M. W. Louie, F. T. Tsz-Him, L. Kam-Wing, *Inorg. Chem.,* (2011), **50**, 9465–9471.

70. N. S. Kaore, D. K. Langade, V. K. Yadav, P. Sharma, V. R. Thawani, R. Sharma, *Journal of Pharmacy and Pharmacology,* (2012), **64**, pp. 1040–1062.

71. A. Mazur, A. Booth, *Brain Sci.,* (1998), **21**, 353–363.

72. R. Rettner, (2014), *Reference: What is Testosterone*? [online] Available at: <http://www.livescience.com/38963-testosterone.html > [Accessed 07th Oct. 2014].

73. Medicine Net.com, (no date), *Definition of Testosterone* [online] Available at: < http://www.medterms.com/script/main/art.asp?articlekey=5747 > [Accessed 17th Sep. 2013].

74. S. M. Dehm, D. J. Tindall, *Mol. Endocrinol.* (2007), **21**(12), 2855-2883.

75. C. Eisenegger, J. Haushofer, E. Fehr, *Trends in Cognitive Sciences*, (2011), **15(**6), 263-271.

76. A. D. Mooradian, J. E. Morley and S. G. Korenman, (1987), *Endocr. Rev.*, **8** (1), pp 1–28

77. F. Rahman, H. C. Christian, (2007), *Trends in Endocrinology and Metabolism,* (2007), **18**(10), 371-378

78. J. L. Shea, P. Y. Wong, Y. Chen, *Elsevier Ltd., (2014),* **63,** 59-84.

79. A. J. Amoroso, M. P. Coogan *et al., Chem. Commun*., (2007), (29), 3066–3068.

80. S. Bullock, L.P. Harding, J. J. Higginson, S. A. F. Piela, S. J. A. Pope, C. R. Rice, *Dalton Trans*.,(2012), **41**, 14690–14696.

81. J. C. Vites, M. L. Lynan, *Coord. Chem. Rev*., (1998), **172**, 357.

82. K. K.-W. Lo, W.-K. Hui, D. C.-M. Ng, *J. Am. Chem. Soc*., (2002), **124,** 9344–9345

83. K. K.-W. Lo, T. K.-M. Lee, *Inorg. Chem*., (2004), **43**, 5275–5282.

84. K. K.-W. Lo, W.-K. Hui, *Inorg. Chem*., (2005), **44**, 1992–2002.

85. K. K.-W. Lo, M.-W. Louie, K.-S. Sze, J. S.-Y. Lau, *Inorg. Chem*.,(2008), **47**, 602–611.

86. K.K.W. Lo, A.W.T Choi, W.H.T Law, *Dalton Trans*.,(2012), **41**(20), 6021-6047.

87. K. K. W. Lo, K. Y. Zhang, S. P. Y. Li, *Eur. J. Inorg. Chem.,* (2011), **2011**(24),3551–3568.

88. S. Jurrison, D. Berning, W. Jia, D. Ma, *Chem. Rev*., (1993), **93**, 1137.

89. C.N. Coleman, *J. Natl. Cancer Inst*., (1988), **80**, 137.

90. A.J. Fischman, J.W. Babich, R.H. Rubin*, Sem. Nucl. Med.,* (1994), **24**, 154.

91. M.L. Thakur, *Nucl. Med. Commun*., (1995), **16**, 724.

92. J. Lister-James, B.R. Moyer, T. Dean, Quart. *J. Nucl. Med*., (1996), **40**, 221.

93. D. Som, Z.H. Oster, *J. Nucl. Med*., (1994), **35**, 202.

94. D.A. Goodwin, C.H. Song, R. Finston, P. Matin, *Radiology*, (1973), **108**, 91.

95. D.A. Goodwin, M.W. Sundberg, C.I. Diamanti, C.F. Meares, *Radiopharmaceuticals*, *Society of Nuclear Medicine, New York*, (1975).

96. A.J. Fischman, M.C. Pike, D. Kroon, A.J. Fucello, D. Rexinger, C. ten Kate, et al., *J. Nucl. Med*., (1991), **32**, 483.

97. J. Quinomones, G. Mizejewski, W.M. Beierwaltes, *J. Nucl. Med.,* (1971), **12**, 69.

98. F.J. Primus, R.H. Wang, D.M. Goldenberg, H.J. Hansen, *Cancer Res.,* (1973), **33**, 2977.

99. D. E. Reichert, J. S. Lewis, C. J. Anderson, 'Metal complexes as diagnostic tools', *Coordination Chemistry Reviews*, (1999), **184**, 3–66.

100. R. Antonucci, S. Bernstein, R. Littell, K. J. Sax, J. H. Williams, *J. Org. Chem*., 1952, **17**, 70.

101. R. Antonucci, S. Bernstein, R. Littell, K. J. Sax, J. H. Williams, *J. Org. Chem*., 1952, **17**, 1341-1350

102. R. Antonucci , S. Bernstein , R. Lenhard , K. J. Sax , J. H. Williams, *J. Org. Chem*., (1952), **17** (10), 1369-1374

103. Puri, D., (2006), *Textbook of Medical Biochemistry*,2th ed. Elsvier-A division of Reed Elsvier India Private Limited.

104. H. Ghazarian, B. Idoni, S.B. Oppen heimer, *acta histochemica,* (2011), **113,** 236-247.

105. H. Namazi and R. Sharifzadeh, *Molecules, (*2005), ***10***, 772–782

106. T. Ikegami & K. Horie, N. Saad, K. Hosoya, O. Fiehn, & N. Tanaka, *Anal Bioanal Chem*., (2008)**, 391**(7), 2533-42.

107. N. Kresge, R. D. Simoni, R. L. Hill, *Journal of Biological Chemistry,(* 2010), by The American Society for Biochemistry and Molecular Biology, Inc.

108. H. Kogelberg, D. Solis, J. Jimenez-Barbero, Curr Opin Struct Biol., (2003), **13**,646-653.

109. H. J Gilbert, *et al*., *Royal Soc Chem.,* (2002) , **275**, 89–98.

110. N. Sharon, H. Lis, *Adv Exp Med Biol*., (2001), **491**, 1–16.

111. D. R. Bundle, N. M. Young, *Curr Opin Struct Bio*., (1992), **2**, 666–673.

112. D. Spillmann, M. M. Burger, *J Cell Biochem.,* (1996), **61**, 562–568.

113. R. Mody, S. Joshi, W. Chaney, *J Pharmacol Toxicol Methods*, (1995), **33**, 1–10.

114. E. Gorelik, U. Galili, A. Raz, *Cancer Metastasis Rev, (*2001), **20**, 245–77.

115. T. Minko, *Adv Drug Deliv Rev., (*2004), **56**, 491–509.

116. C. Bies, C. M. Lehr, J. F. Woodley, *Adv Drug Deliv Rev*., (2004), **56**, 425–435.

117. R. Loris, D. Tielker, K. E. Jaeger, L. Wyns, *J. Mol. Biol.,* (2003), **331**, 861–870.

118. P.M.G. Palva, M.T.S. Corella, M.S.M. Cavalcanti, L.C.B.B. Coelho, *Carbohydrate Polymers,* (1995), **26**, 219-230.

119. A. Surolia, N. Sharon, F. P. Schwarz, *The Journal of Biological Chemistry*, (1996), 271, (30), 17697–17703.

120. S. Nathan, H. Lis., (2001), Chapter-The Structural Basis for Carbohydrate Recognition By Lectins, *The Molecular Immunology of Complex Carbohydrates - 2*, **491**, pp 1-16, Springer US.

121. K. C. David, *Biochimica et Biophysica Acta.,* (2002), **1572**, 187– 197.

122. R.J. Stockert, A.G. Morell, I.H. Scheinberg, *Science,* (1974), **186**, 365– 366.)

123. M. Ambrosi, N. R. Cameron, B. G. Davis, *Org. Biomol. Chem.*, (2005), **3**, 1593-1608.

124. C. D. Borman, C. G. Saysell, A. Sokolowski, M. B. Twitchett, C. Wright and A.G. Sykes, *Coordination Chemistry Reviews*, (1999), **190-192**, 771–779

125. E. L. Irvin, S. Nathan, J. G. Irwin, The Lectins: Properties, Functions, and Applications in Biology and Medicine, (1986), Academic press Inc., London, 294-357.

126. F. Z. Paola, D. C. Richard, *Biochemical Education*, (1992), **20** (1), 2-9.

127. J. A. D. Cooper, W. Smith, M. Bacila, H. Medina, *Journal of Biological Chemistry,* (1959), **234,** 445-448.

128. M. K. Nobles, C. Madhosingh, *Biochemical and Biophysical Research Communications,* (1963), **12,** 146-147.

129. Z. B. Ogel, D. Brayford, M. J. Mcpherson, *Mycological Research,*(1998), **98,** 474-480.

130. J. W. Whittaker, *Archives of Biochemistry and Biophysics*, (2005), **433**, 227–239.

131. M. M. Whittaker, D. P. Ballou, J. W. Whittaker, *Biochemistry*, (1998), **37**, 8426-8436.

132. J. W. Whittaker, M. M. Whittaker, *Pure and Applied Chemistry*, (1998), **70,** 903-910.

133. W. Choosri, R. Paukner, P. Wuhrer, D. Haltrich, C. Leitner, *World J Microbiol Biotechnol*, (2011), **27,** 1349–1353.

134. V. Bonnet, R. Duval, C. Rabiller, *Journal of Molecular Catalysis B: Enzymatic,* (2003), **24–25** (9–16).

135. M. J. Mcpherson *et al., Journal of Biological Chemistry, (*1992). **267,** 8146-8152.

136. M. Breuer, K. Ditrich, T. Habicher, B. Hauer, M. Kesseler, R. Sturmer, T. Zelinski, *Angewandte Chemie-International Edition*, (2004), **43,** 788-824.

137. H. Bretting, G. Jacobs, *Biochimica Et Biophysica Acta,,* (1987), **913,** 342-348.

138. G. Avigad, *Archives of Biochemistry and Biophysics,*(1985), **239,** 531-537.

139. J. B. Holton, *Journal of Inherited Metabolic Disease,* (1990), **13,** 476-486.

140. E. S. Rorem, J. C. Lewis, *Analytical Biochemistry,*(1962), **3,** 230-235.

141. N. Adanyi, E. E. Szabo, m. Varadi, *European Food Research and Technology,* (1999), **209,** 220-226.

142. S. Mannino, M. S. Cosio, S. Buratti, *Italian Journal of Food Science,*(1999), **11,** 57-65.

143. H. Singh, J. N. Kanfer, *Analytical Biochemistry,* (1980), **109,** 27-31.

144. D. R. Critchley, *Cell,* (1974), **3,** 121-125.

145. Shamsuddin, A. M. & Elsayed, A. M. *Human Pathology,* (1988), **19,** 7-10.

146. J. H. Carter, J. A. Deddens, J. L. Pullman, B. M. Colligan, L. O. Whiteley, H. W. Carter, *Clinical Cancer Research*, (1997), **3,** 1479-1489.

147. G. Y. Yang, A. M. Shamsuddin, *Histology and Histopathology,*(1996), **11,** 801-806.

148. A. Chagpar, M. Evelegh, H. A. Fritsche, S. Krishnamurthy, K. K. Hunt, H. M. Kuerer, *Cancer,* (2004), **100,** 2549-2554.

149. S. Delagrave, R. E. Hawtin, C. M. Silva, M. M. Yang and D. C. Youvan*, Protein Engineering,* (2001), **14** (4) **,** 261-267.

150. K. Parikka, A. S. Leppanen *et al., Biomacromolecules,* (2012), **13,** 2418-2428.

151. R. L. Root, J. R. Durrwachter, C. H. Wong, *Journal of the American Chemical Society,* (1985), **107,** 2997-2999.

152. X. C. Liu, J. S. Dordick, *Journal of the American Chemical Society,* (1999), **121,** 466-467.

153. A. W. Mazur, G. D. Hiler, *Journal of Organic Chemistry,* (1997), **62,** 4471-4475.

154. K. Parikka, M. Tenkanen, *Carbohydrate Research*, (2009), **344,** 14–20.

155. K. Parikka, L. A. Sofie, P. Leena, R. Markku, W. Stefan, T. Maija*, J. Agric. FoodChem.*, (2010), **58**, 262–271.

156. A. S. Leppanen and K. Parikka et al., *Carbohydrate Polymers*, (2014), **100***,* 46– 54.

157. A. Siebum, A. V. Wijk, R. Schoevaart, T. Kieboom, *Journal of Molecular Catalysis B: Enzymatic*, (2006), **41**, 141–145.

158. M. Kinoshita, K. Inagake, A. Kawabata, R. Kuroda, Y. Oda, K. Kakehi, *Anal Biochemistry*, (2000), **284,** 87–92.

159. K. Yamamoto, Y. Kondo, H. Kumagai, T. Tochikura, (1985), *Agric. Biol. Chem.* **49**, 2463 - 2464.

160. D. T. Osuga, M. S. Feather, M. J. Shah, and R. E. Feeney*, J. Protein Chem.*, (1989), **8**(4), 519-528.